

Aus der I. Medizinische Klinik und Poliklinik
Der Universitätsmedizin der Johannes Gutenberg-Universität Mainz

Investigation of blood-based biomarkers as prognostic and predictive
factors in patients with neuroendocrine neoplasms

Inauguraldissertation
Zur Erlangung des Doktorgrades
der physiologischen Wissenschaften
der Universitätsmedizin
der Johannes Gutenberg-Universität Mainz

Vorgelegt von

Neda Bakhshandeh

Mainz, 2021

Wissenschaftlicher Vorstand: Univ.-Prof. Dr. Ulrich Förstermann

1. Gutachter: Univ.-Prof. Dr. Matthias M. Weber
2. Gutachter: Univ.-Prof. Dr. med. Stephan Gehring
3. Gutachter: PD Dr. med. Olaf Beck

Tag der Promotion: 24.01.2023

In memoriam, my father

Content

| | |
|--|-----|
| List of abbreviations | I |
| List of Figures..... | III |
| List of Tables..... | VI |
| 1. Introduction | 1 |
| 1.1 Neuroendocrine neoplasia | 1 |
| 1.2 Circulating biomarkers for neuroendocrine neoplasms (NENs) | 2 |
| 1.3 Biopsy..... | 5 |
| 1.4 cfDNA | 7 |
| 1.5 cfDNA integrity index as a tumor marker | 8 |
| 1.5.1 Non-coding genomic DNA repetitive elements: <i>ALU</i> and <i>LINE-1</i> | 8 |
| 1.6 cfDNA epigenetic modifications as a tumor marker (hypomethylation) | 10 |
| 1.7 Aim of the work | 13 |
| 2. Material and Methods..... | 14 |
| 2.1 Material..... | 14 |
| 2.1.1 Devices | 14 |
| 2.1.2 Laboratory materials..... | 15 |
| 2.1.3 Chemicals..... | 16 |
| 2.1.4 Kits with manufacturer information..... | 16 |
| 2.1.5 Enzymes with manufacturer information | 16 |
| 2.1.6 Software with manufacturer information..... | 17 |
| 2.1.7 Adaptor and primer sequences..... | 17 |
| 2.1.8 Clinical sample (Human Participants) | 18 |
| 2.1.9 Media and Cell line | 19 |
| 2.2 Methods..... | 19 |
| 2.2.1 Sample collection | 19 |
| 2.2.2 cfDNA purification and isolation | 19 |
| 2.2.3 cfDNA measurement | 20 |
| 2.2.4 Isolation of the genomic DNA from <i>BON-1</i> cell culture..... | 20 |
| 2.2.5 Measurement of the <i>BON-1</i> genomic DNA | 21 |
| 2.2.6 Quantitative polymerase chain reaction | 21 |
| 2.2.7 cfDNA hypomethylation test | 24 |
| 2.2.8 Determination of established tumor marker | 26 |
| 2.2.9 Statistical analysis | 26 |
| 3. Results | 29 |
| 3.1 Real-time PCR assay performance | 29 |

| | |
|--|-----|
| 3.1.1 Efficiency and standard curves | 31 |
| 3.2 The study population characteristics | 34 |
| 3.3. Assessment of biomarkers | 35 |
| 3.3.1 Plasma cfDNA quantification | 35 |
| 3.3.2 Evaluation of cfDNA fragment size distribution | 42 |
| 3.3.3 Analysis of cfDNA integrity indexes | 56 |
| 3.3.4 Analysis of <i>ALU</i> hypomethylation percentage | 64 |
| 3.3.5 Biomarkers correlation analysis | 70 |
| 3.3.6 Prognostic value evaluation | 74 |
| 4. Discussion | 80 |
| 4.1. cfDNA Isolation | 80 |
| 4.2 cfDNA concentration as a biomarker for NEN patients | 81 |
| 4.3 cfDNA Fragmentation as a biomarker for NEN patients | 83 |
| 4.4 cfDNA Integrity as a biomarker for NEN patients | 86 |
| 4.5 cf DNA Hypomethylation as a biomarker for NEN patients | 88 |
| 5. Challenges and future perspectives | 93 |
| 6. Conclusion | 95 |
| 7. Summary | 97 |
| 7.1 Summary | 97 |
| 7.2 Zusammenfassung | 99 |
| 8. References | 101 |
| 9. Appendix | 113 |
| 10. Acknowledge | 119 |
| 11. Curriculum Vitae | 120 |

Abbreviations

List of abbreviations

| Term of Abbreviation | Definition |
|-----------------------------|---|
| 5HIAA | 5-hydroxyindoleacetic acid |
| 5-HT | 5-hydroxytryptamine |
| 5-HTP | 5-hydroxytryptophan |
| <i>ALU</i> | Arthrobacter Lectus I |
| <i>ALU</i> cfDII | cfDNA- <i>ALU</i> integrity index |
| AUC | the area under the curve |
| bp | base pair |
| cfDNA | circulating cell-free DNA |
| cffDNA | cell-free fetal DNA |
| cfRNA | cell-free RNA |
| CgA | chromogranin A |
| CI | confidence interval |
| CSF | cerebrospinal fluid |
| Ct | cycle threshold |
| CTCs | circulating tumor cells |
| ctDNA | circulating tumor DNA |
| DII | DNA integrity index |
| DNMT | DNA methyltransferases |
| ELISA | enzyme-linked immunosorbent assay |
| EUS | endoscopic ultrasound |
| G1 | grade 1 |
| G2 | grade 2 |
| G3 | grade 3 |
| GE | number of genome equivalents |
| GEP | gastroenteropancreatic |
| GEP-NENs | gastroenteropancreatic neuroendocrine neoplasms |
| GH | Growth hormone |
| GvHD | graft-versus-host disease |
| IFN- α | interferon-alpha |
| IQR | interquartile ranges |
| <i>LINE-1</i> cfDII | cfDNA- <i>LINE-1</i> integrity index |
| <i>LINEs</i> | long interspersed nuclear elements |
| Lu-177 | Lutetium-177 |

Abbreviations

| | |
|----------|--|
| MEN1 | multiple endocrine neoplasia type 1 |
| MiNEN | mixed neuroendocrine / non-neuroendocrine neoplasm |
| miRNA | microRNA |
| mNET | metastatic neuroendocrine tumors |
| mNETs | metastatic NETs |
| MRI | magnetic resonance imaging |
| NECs | neuroendocrine carcinomas |
| NENs | neuroendocrine neoplasms |
| NETs | neuroendocrine tumors |
| NKA | neurokinin A |
| Non-mNET | non-metastatic neuroendocrine tumors |
| NSE | neuron-specific enolase |
| ORF | open reading frame |
| OS | overall survival |
| PET-CT | positron emission tomography-computed tomography |
| PFS | progression-free survival |
| PP | pancreatic polypeptide |
| PPIs | proton pump inhibitors |
| PRRT | peptide receptor radionuclide therapy |
| qPCR | quantitative polymerase chain reaction |
| ROC | receiver-operator characteristic |
| RT-PCR | real-time PCR |
| SAH | S-adenosylhomocysteine |
| SAM | S-adenosyl-methionine |
| SA72 | juxtacentromeric satellite 2 |
| SINEs | short interspersed elements |
| TEs | transposable elements |
| TSH | thyroid-stimulating hormone |
| VIP | vasoactive Intestinal Peptide |
| VIPomas | VIP secreting tumors |
| Y-90 | Yttrium-90 |

List of Figures

| | |
|---|----|
| Figure 1. Overview of light biopsy..... | 6 |
| Figure 2. A schematic of Retrotransposition assay | 9 |
| Figure 3. Schematic representation of DNA methylation..... | 11 |
| Figure 4. PCR representation with one sample | 22 |
| Figure 5. Typical melting curve graph and its temperature derivative | 23 |
| Figure 6. Illustration of unmethylated <i>ALU</i> elements measurement technique..... | 25 |
| Figure 7. Establishing qPCR to measure cfDNA fragmentation | 30 |
| Figure 8. Establishing qPCR to measure cfDNA Hypomethylation..... | 31 |
| Figure 9. Standard and efficiency curves..... | 32 |
| Figure 10. Efficiency curves of digested cfDNA for hypomethylation analysis..... | 33 |
| Figure 11. Distribution of plasma cfDNA level in the study groups..... | 36 |
| Figure 12: cfDNA level receiver operating characteristic (ROC) plots | 37 |
| Figure 13. Plasma cfDNA correlation to age..... | 38 |
| Figure 14. cfDNA Plasma concentration grouped by tumor grades..... | 39 |
| Figure 15. cfDNA level receiver operating characteristic (ROC) plots for tumor grades | 39 |
| Figure 16. cfDNA Plasma concentration grouped by tumor burden | 40 |
| Figure 17. cfDNA level receiver operating characteristic (ROC) plots for tumor burdens | 41 |
| Figure 18. cfDNA plasma concentration grouped by tumor origin | 41 |
| Figure 19. Correlation of CgA hormonal status vs. cfDNA level in the patient group..... | 42 |
| Figure 20. Distribution of <i>ALU</i> 115-bp fragment level in the study groups..... | 43 |
| Figure 21. Distribution of <i>ALU</i> 260-bp fragment level in the study groups..... | 44 |
| Figure 22. <i>ALU</i> fragmentation receiver operating characteristic (ROC) plots | 44 |
| Figure 23. Correlation of age and <i>ALU</i> fragmentation level in cfDNA..... | 46 |
| Figure 24. cfDNA <i>ALU</i> fragmentation level grouped by tumor grades..... | 47 |
| Figure 25. cfDNA <i>ALU</i> fragmentation level grouped by tumor burden..... | 47 |
| Figure 26. <i>ALU</i> 260-bp fragment level receiver operating characteristic (ROC) plots for tumor burdens | 48 |
| Figure 27. cfDNA <i>ALU</i> fragmentation level grouped by tumor origin | 49 |
| Figure 28. Correlation of CgA hormonal status and <i>ALU</i> fragmentation level in the patients | 49 |
| Figure 29. Distribution of <i>LINE-1</i> 97-bp fragment level in the study groups..... | 50 |
| Figure 30. Distribution of <i>LINE-1</i> 266-bp fragment level in the study groups..... | 51 |
| Figure 31. <i>LINE-1</i> fragmentation receiver operating characteristic (ROC) plots..... | 51 |
| Figure 32. Correlation of age and <i>LINE-1</i> fragmentation level in cfDNA | 53 |
| Figure 33. cfDNA <i>LINE-1</i> fragmentation level grouped by tumor grades..... | 54 |

| | |
|---|----|
| Figure 34.cfDNA <i>LINE</i> -1 fragmentation level grouped by tumor burden | 54 |
| Figure 35.cfDNA <i>LINE</i> -1 fragmentation level grouped by tumor origin..... | 55 |
| Figure 36.Correlation of CgA hormonal status and <i>LINE</i> -1 fragmentation level in the patients | 56 |
| Figure 37.cfDNA- <i>ALU</i> and - <i>LINE</i> -1 integrity indexes in the study groups..... | 57 |
| Figure 38. cfDNA integrity index receiver operating characteristic (ROC) plots | 58 |
| Figure 39.Correlation of age and cfDNA integrity indexes | 59 |
| Figure 40. cfDNA integrity index grouped by tumor grades..... | 60 |
| Figure 41. <i>LINE</i> -1 integrity index receiver operating characteristic (ROC) curve for tumor grades | 60 |
| Figure 42.cfDNA- <i>ALU</i> and - <i>LINE</i> -1 integrity indexes grouped by tumor burden..... | 61 |
| Figure 43.cfDNA- <i>LINE</i> -1 integrity index receiver operating characteristic (ROC) plots for tumor burdens | 62 |
| Figure 44.cfDNA integrity indexed grouped by tumor origin | 63 |
| Figure 45.Correlation of CgA hormonal status and integrity indexes in the patients..... | 63 |
| Figure 46.Percentage of hypomethylation in the study groups..... | 64 |
| Figure 47. Hypomethylation receiver operating characteristic (ROC) plots | 65 |
| Figure 48.Correlation of hypomethylation percentage to age..... | 66 |
| Figure 49. Hypomethylation percentage grouped by to tumor grade..... | 67 |
| Figure 50. Hypomethylation receiver operating characteristic (ROC) curve for tumor grade 3 | 67 |
| Figure 51. The percentage of hypomethylation grouped by tumor burden | 68 |
| Figure 52. Hypomethylation receiver operating characteristic (ROC) curve for tumor burdens | 69 |
| Figure 53. Hypomethylation percentage grouped by tumor origin..... | 69 |
| Figure 54.Correlation of CgA hormonal status and hypomethylation percentage in the patient group..... | 70 |
| Figure 55. Correlation of cfDNA level with longer fragments..... | 70 |
| Figure 56.Correlation of cfDNA level with shorter fragments | 71 |
| Figure 57.Correlation of cfDNA level with integrity indexes..... | 71 |
| Figure 58.Correlation of cfDNA level with hypomethylation percentage..... | 72 |
| Figure 59.Correlation of hypomethylation percentage with longer fragments..... | 72 |
| Figure 60.Correlation of hypomethylation percentage with shorter fragments..... | 73 |
| Figure 61.Correlation of hypomethylation percentage with integrity indexes..... | 73 |
| Figure 62. Receiver operating characteristic (ROC) curve analysis for controls vs. metastatic NET+NEC subgroups by a combination of investigated biomarkers | 74 |

Figure 63. Receiver operating characteristic (ROC) curve analysis for non-metastatic NETs vs. metastatic NET+NEC subgroups by a combination of investigated biomarkers.....75

Figure 64. Receiver operating characteristic (ROC) curve analysis of 1) individual CgA level biomarker and 2) combined with investigated biomarkers in non-metastatic NETs and metastatic NET+NEC subgroups.....76

Figure 65. Receiver operating characteristic (ROC) curve analysis for samples with no tumor burden (control+non-mNETs) from low, moderate, and high tumor burden subgroups77

Figure 66. CgA level receiver operating characteristic (ROC) curve for tumor burdens78

Figure 67. Receiver operating characteristic (ROC) curve analysis of CgA level biomarker combined with investigated biomarkers for samples with no tumor burden (non-mNETs) from low, moderate, and high tumor burden subgroups.....79

List of Tables

| | |
|--|-----|
| Table 1: WHO classification NENs (2019) ^{10,11} | 2 |
| Table 2. Classes of transposable elements in the human genome | 9 |
| Table 3. Adaptor and primer sequences | 17 |
| Table 4. The short <i>ALU</i> primers sequences used for qPCR setting up | 18 |
| Table 5. Amplicon length and qPCR assay conditions for each primer | 22 |
| Table 6. The detailed amplification efficiency for each primer | 33 |
| Table 7. Clinicopathological features of the study groups | 34 |
| Table 8. cfDNA sensitivity and the corresponding cut-off level | 37 |
| Table 9. The sensitivity and corresponding cut-off levels of cfDNA level for tumor grades.... | 40 |
| Table 10. <i>ALU</i> 115-bp fragment concentration sensitivity and the corresponding cut-off level | 45 |
| Table 11. <i>ALU</i> 260-bp fragment concentration sensitivity and the corresponding cut-off level | 45 |
| Table 12. <i>LINE-1</i> 97-bp fragment concentration sensitivity and the corresponding cut-off level | 52 |
| Table 13. <i>LINE-1</i> 266-bp fragment concentration sensitivity and the corresponding cut-off level..... | 52 |
| Table 14. The sensitivity and corresponding cut-off levels for <i>ALU</i> integrity index | 58 |
| Table 15. The sensitivity and corresponding cut-off levels of <i>LINE-1</i> integrity index | 58 |
| Table 16. The sensitivity and corresponding cut-off levels of <i>LINE-1</i> integrity index for tumor grades | 61 |
| Table 17. The sensitivity and corresponding cut-off levels of <i>ALU</i> -hypomethylation | 65 |
| Table 18. The sensitivity and corresponding cut-off levels of <i>ALU</i> -hypomethylation for G3 tumor | 67 |
| Table 19. The cfDNA concentration in the other studies..... | 113 |
| Table 20. The cfDNA integrity index in the other studies | 115 |

1. Introduction

1.1 Neuroendocrine neoplasia

Neuroendocrine neoplasms (NENs) are a heterogeneous and potentially malignant group of tumors that derive from hormonal and nervous system cells and occur in all organs. The incidence rate of NENs is about 5.6/100.000 per year ¹. NENs are divided into two groups: active and non-active. Almost half of NENs are functionally active where the endocrine cells secrete hormones, hormone-like messenger components, or neurotransmitters such as insulin, gastrin, vasoactive intestinal peptide, glucagon, or somatostatin¹⁻⁷. This functionally active group of NENs has the most common symptoms: diarrhea, stomach pain, flatulence, loss of appetite, fluctuations in blood pressure, shortness of breath and hypoglycemia, or hyperglycemia. In addition, they have specific clinical symptoms such as carcinoid or hypoglycemic or Zollinger-Ellison syndrome. Carcinoid syndrome is an effect of unmetabolized overproduced serotonin, whereas hypoglycemic syndrome and Zollinger-Ellison syndrome are caused by insulinoma and gastrin secretion, respectively⁸. Approximately 50% of NENs are non-functional and do not release hormones, hormone-like substances, or neurotransmitters. The inactive NENs are rarely associated with symptoms and are clinically clear from increasing masses, pain, or bleeding. Still, the symptoms from local growth can be seen, like stenosis of the affected part of the intestine leading to unspecific abdominal complaints or Jaundice due to compression of the common bile duct. NENs occur in the ileum, duodenum, pancreas (islet cells), stomach, appendix, colon, rectum, adrenal medulla on kidneys, pituitary adenoma, thyroid, thymus, urogenital tract, ovaries, skin, and lungs (about 25% of all NENs). Approximately 70 % of NENs appear in the gastroenteropancreatic (GEP) system; these NENs arise from the gastrointestinal tract and pancreas endocrine cells and are called gastroenteropancreatic neuroendocrine neoplasms (GEP-NENs).

The classification of the NENs is based on the spread of the tumor (staging) or tissue differentiation (grading). Cancer staging describes the disease based on the size of the tumor, localization of the primary tumor, and the spread of cancers (metastasized).

According to the World Health Organization (WHO) 2010 classification, NENs are subdivided based on histopathological grading into well to moderately differentiated G1/G2 neuroendocrine tumors (NETs) and neuroendocrine carcinomas (NECs) G3, which improves therapeutic decisions and evaluation of prognosis. Clinically and morphologically, pancreatic NECs G3 can be separated into a differentiated NET G3 subgroup and the more aggressive and undifferentiated 'classical' NEC G3 group, which has recently been incorporated into the actual WHO classification of pancreatic NENs ⁹(Table 1). Quantification of the proliferative activity of the tumor tissue is important for the staging as well and is reported as the Ki67 index.

NEN diagnosis starts with the simple biochemical quantification of general neuroendocrine markers in the plasma or serum of patients with suspected NENs. The abnormal levels of the markers are assessed further with deepening diagnostic tests¹². The histopathological

examination is used to confirm NENs diagnosis that histopathological confirmation completes with immunohistochemistry based on Ki-67 expression. Imaging diagnostics such as magnetic resonance imaging (MRI), ultrasound with endoscopic ultrasound (EUS), and positron emission tomography-computed tomography (PET-CT) are recommended for patients with biopsy-confirmed NEN and unclear primary site. PET-CT determines the somatostatin receptor density using Ga-68-labeled somatostatin analogs ¹³.

Table 1: WHO classification NENs (2019)^{10,11}

| Type (morphology) | differentiation | Grade | Ki67 Index | |
|--|---------------------|-------------------|------------------------------------|------|
| Neuroendocrine tumor (NET) | well-differentiated | G1(Low) | <3% | |
| | | G2 (Intermediate) | 3–20% | |
| | | G3 (High) | >20% | |
| Neuroendocrine carcinoma (NEC) | poor-differentiated | G3 | small-cell NECs large-cell NECs | >20% |
| Mixed neuroendocrine / non-neuroendocrine neoplasm (MiNEN) | | | | |

The high-density expression of somatostatin receptors usually characterizes NENs, and therefore, somatostatin analogs are the most widely used treatment for NEN patients. Somatostatin analogs are a synthetic version of the natural hormone somatostatin that bind specifically to different somatostatin receptors and allow the diagnostics and treatment with high sensitivity and specificity¹⁴. The somatostatin analogs, such as Octreotide and Lanreotide, have an antiproliferative effect via apoptosis induction and inhibit various growth factors. Additional to tumor growth inhibition, somatostatin analogs slow down the production of hormones and messenger substances such as gastrin, insulin, and serotonin, reducing the symptoms in functionally active NENs^{15–17}. Following the determination of somatostatin receptor expression, peptide receptor radionuclide therapy (PRRT) is a promising treatment option for NET patients. In this nuclear medical procedure, the somatostatin-like peptides are coupled to radioactive nuclides and are injected intravenously. The selective uptake via somatostatin receptors leads to a directly targeted high radiation dose to the cancer cells. Lutetium-177 (Lu-177) and Yttrium-90 (Y-90) are the most radionuclides used as radiation sources ^{14,18}.

There are different chemotherapeutic options for NEN treatment. Although the targeted agents such as everolimus¹⁹, sunitinib ²⁰, and interferon-alpha (IFN- α)²¹ are used, the most common chemotherapy drugs are alkylating agents streptozocin and temozolomide that reduce the rapid proliferation of cells in the malignancies^{22,23}.

However, the most common first-line treatment of NENs is complete surgical or endoscopic resection of the primary tumor \pm local lymph node metastases. The treatment options are used depending on the respective tumor entity or the anatomical location of GEP-NEN. The treatment should be individualized based on each patient's characteristics and require time and cost. Besides, the varied symptoms, complicated diagnostics, and frequent liver metastasis at the initial diagnosis make the therapy harder in these patients.

1.2 Circulating biomarkers for neuroendocrine neoplasms (NENs)

The biological substances that increase significantly in the body fluids due to malignant tumors are called tumor markers. Most tumor markers are proteins that are produced by

normal cells as well as by cancer cells. Many different tumor markers are used as a diagnostic tool, but they have some limitations:

- a) Some tumor markers are not unique for only one cancer type.
- b) Tumor markers are not elevated in all cancer entities alike.
- c) There is no known tumor marker for all types of cancer.
- d) Non-cancerous, pathological conditions or interactions with food can affect a tumor marker

NENs involve a heterogeneous group of tumors with different pathological and clinical statements hampers the development of NENs biomarkers. However, the classic circulating biomarkers for NENs are categorized into two main groups, namely specific and non-specific markers. The former is produced by mostly functioning NETs and varies according to hormone production. Practically all NETs²⁷ makes the latter.

1) non-specific markers

Chromogranins are released with catecholamines from chromaffin cells and nerve endings, making them a good marker for NETs²⁴. Chromogranins, particularly chromogranins A and B, are water-soluble acidic glycoproteins. Chromogranin A (CgA) has been accepted as the most common liquid biomarker for the diagnosis, follow-up, and treatment monitoring of NEN patients²⁵. Its level in the blood is associated with the size (load) of the tumor, tumor progression²⁶, presence of metastases²⁷, and response to treatment in NENs. The overall clinical sensitivity of CgA in the diagnosis of NETs is around 84%, and overall efficiency is 79 %, positive and negative predictive values are 42 % and 96 %, respectively²⁸. The sensitivity of CgA for different types of NETs is in the range of 60–100% and 70–100% for specificity²⁹. The CgA level can be influenced by several non-pathological factors, including the different backgrounds of CgA levels in populations and the food intake^{30,31}. Furthermore, pitfalls exist with measuring plasma CgA due to false-positive elevation in several non-neoplastic endocrine diseases like cardiac, inflammatory diseases³², severe hypertension¹⁸, renal insufficiency³⁶, and steroid or proton pump inhibitors (PPIs) treatment^{18,33}.

Another non-specific biomarker of NENs is neuron-specific enolase (NSE). NSE is a soluble cerebral protein, which presents in neurons and neuroendocrine cells³⁴. The sensitivity of NSE is lower than CgA (33%), but its specificity is relatively high and similar to CgA (73%)^{18,25}. NSE is a crucial enzyme of the glycolytic pathway, where NSE-overexpressing may show neuroendocrine cells that undergo oncogenic transformation³⁵. It is shown that the increase of the NSE level is correlated to the high death rate of cells with neuroendocrine differentiation³⁶. The NSE level is directly related to tumor differentiation, aggressiveness, and size^{37,38}. It correlates inversely with overall survival (OS) in ENETS TNM stage IV³⁸ and progression-free survival (PFS)¹⁹. NSE may be elevated in 38–40% of high-grade GEP-NENs, so it has a predictive value for a more aggressive period of the disease³⁸. NSE can differentiate NETs from nonendocrine tumors with low specificity and sensitivity²⁶. Also, the NSE level can be increased in other diseases, such as thyroid cancer, prostate carcinoma, neuroblastoma, and small cell lung carcinoma^{39,40}.

Pancreatic polypeptide (PP) is also used as a nonspecific NET marker. PP is a 36 amino acid linear oligopeptide produced by the pancreas and the colon and has a role in the autoregulation of secretion^{41,42}. PP is a neuroendocrine differentiation marker with 67% specificity and 31-63% sensitivity¹². Many factors can elevate the PP level, such as physical

exercise, hypoglycemia, and food intake⁴³. Somatostatin, hyperglycemia, diarrhea, laxative abuse, increased age, inflammatory processes, and chronic renal disease decrease the PP concentration⁴⁴. Despite the above limitation, the PP test is used for diagnosis and follow-up in pancreatic NET in clinical use²⁵. The decrease in PP level during patient monitoring is considered a significant prognostic marker²⁶.

2) Specific Marker

NENs specific biomarkers are bioactive peptides in the blood of functional NEN patients. The increase in these hormones is associated with symptoms that help diagnose and identify the primary site of disease⁴⁵.

Serotonin or 5-hydroxytryptamine (5-HT) is a monoamine neurotransmitter. 5-hydroxyindoleacetic acid (5HIAA) is a metabolite of serotonin that is mainly used to indicate hypersecretory activity in patients with NENs, especially in midgut NENs³⁶. The specificity and sensitivity of 5HIAA tests are 90% and 35–68%, respectively¹⁸. The elevated secretion of serotonin in NET is associated with hyperhidrosis, hypertension, tachycardia, insomnia, and hot flushes. The false-positive results occur in using some foods, e.g., pineapples, bananas, eggplant, walnut, and medications such as caffeine, paracetamol, and naproxen. In contrast, the treatment of patients by acetylsalicylic acid, adrenocorticotropin, levodopa, and phenothiazine derivatives leads to false-negative results¹⁸. However, in NETs, CgA and 5-HIAA markers are the gold standard for tumor bulk and tumor functionality, respectively. Since these gold standard tests may not apply to every type of NET, this generally accepted term is changing.

Neurokinins are neuropeptides that include mostly neurokinin A, neurokinin B, and substance P in humans. These neurotransmitters involve various processes such as smooth muscle contraction, the transmission of pain, and the control of inflammatory processes. Neurokinin A (NKA) or substance K is assumed to be valuable for identifying patients with more aggressive NETs. Plasma NKA is an accurate marker for gut-NENs that shows therapeutic responses to somatostatin analogs^{46,47}.

Gastrin is a linear peptide hormone secreted by G-cells of the pyloric antrum, duodenum, and pancreas. This specific biomarker controls chloride acid release into the stomach, gastric motility, and pancreatic secretion. The functional NENs that produce gastrin are named gastrinomas.

Insulin, another specific biomarker, is a hormone produced by pancreatic beta cells that increases glucose uptake from the blood. Insulin circulates in high levels in patients with insulin-secreting pancreatic tumors (insulinomas), resulting in hypoglycemia. Insulinomas are small neoplasms; hence local tumor mass effects are rare, unlike other NETs. Around 90% of insulinomas are benign and sporadic. About 10% of patients are found with multiple endocrine neoplasia type 1 (MEN1) syndrome. The 72-h supervised fasting test is used for insulinoma diagnosis. Serum samples are analyzed for glucose and insulin levels every six h and monitored for symptoms of hypoglycemia^{40,48}.

Glucagon is a peptide hormone that is secreted by the α -cells of the pancreatic islets. The glucagon secretion stimulates glycogenolysis and gluconeogenesis, acting as an antagonist to insulin. The functional NENs associated with increased plasma glucagon level (more than 500 pg/mL) are called glucagon-producing endocrine pancreatic tumors (glucagonomas).

However, serum insulin and plasma glucagon can also be increased in nononcologic conditions. Therefore, their concentration alone does not represent a robust marker for insulinoma or glucagonoma^{39,40}.

Somatostatin is a peptide hormone physiologically secreted by the hypothalamus, D cells of the pancreas, stomach, and intestines. Somatostatin acts as an antagonist of somatotropin on producing many other hormones, e.g., Growth hormone (GH), Thyroid-stimulating hormone (TSH), glucagon, insulin, gastrin, and histamine. The elevated level of somatostatin can result in diabetes, diarrhea, the formation of gallstones, and fat intolerance in the diet (Low, 2004). Furthermore, increased somatostatin levels are seen in somatostatinoma of the pancreas and various extra-pancreatic NENs, including medullary carcinoma of the thyroid, pheochromocytoma, and paraganglioma⁴⁹.

Vasoactive Intestinal Peptide (VIP) is a 28-residue amino acid peptide hormone released by pancreatic and brain cells. This specific biomarker is a neurotransmitter and a vasodilator that regulates smooth muscle activity, epithelial cell secretion, and blood flow in the gastrointestinal tract. VIP secreting tumors (VIPomas) are rare tumors, which most commonly develop in the pancreatic tail. The VIPomas show the symptoms such as watery diarrhea, hypokalemia, and achlorhydria²⁵.

GEP-NETs are rising worldwide while the early diagnosis is commonly delayed (a ~5-year) in these patients. At present, available biomarkers for NENs have limitations. There is a continuing need for tumor markers that can help clinicians for early diagnosis, prognosis and follow-up, classification of patients for therapy choice, and postoperative recurrence detection in NENs patients. Liquid biopsy of NEN patients may provide these next-generation biomarkers with a non-invasive procedure^{25,50,51}.

1.3 Biopsy

The process of standard biopsy includes the removal of a small amount of tissue from a living organism. With the help of pathological examinations, tissue samples can be classified as benign or malignant⁵². Phenotypic elements enable the subclassification of a tumor, its histological grading, and the determination of the extent of its spread or its pathological stage in the case of malignant samples. The using different biopsy methods depends on the organ type. The most common biopsy types are bone marrow, needle, skin (cutaneous), surgical, and endoscopic biopsy (cystoscopy collects tissue from inside the bladder, bronchoscopy from inside the lung, and colonoscopy from inside the colon). Although a tissue biopsy is a unique method to characterize the nature of the tumor (the type of cancer, gene expression of the tumor, and treatment-resistant mutations), it faces several biological and technological challenges. Tumors are heterogeneous, so different areas of the tumor may have different mutations and genetic expressions, so there is a possibility that small fragments of tissue cannot provide accurate information about the entire tumor⁵³.

In some cases, a tissue biopsy is not possible because the tumor is not accessible or possible clinical complications in connection with the invasive methods are in no relation to the information gained from a biopsy. Finally, tissue biopsies increase the time and the cost of patient care, as well as side effects such as the risk of infection, bleeding, or long recovery time⁵². However, tumors change over time, and the track of tumors is essential, but the follow-up of cancer patients and repeated biopsies are difficult because of the mentioned risks⁵⁴.

Traditional circulating biochemical biomarkers and molecular biomarkers can be analyzed by liquid biopsy. Cancer-derived material circulating in the body fluids, especially blood, has become a new way to monitor tumor genetics and dynamics. Tissue biopsy is the standard

gold method for clinical molecular investigations, cancer diagnosis, and evaluation. Still, this exciting alternative, “liquid biopsy,” promises to overcome some of the before-mentioned challenges (Fig.1). Liquid biopsy can give information about the tumor's molecular characteristics because it inherits circulating nucleic acids from all body tissue, including the malignant tissue⁵⁵⁻⁶⁰. The tumor molecular material sources, which can be evaluated by liquid biopsy, are circulating cell-free DNA (cfDNA), a subset of cfDNA representing circulating tumor DNA (ctDNA), cell-free RNA (cfRNA) including mRNA and microRNA (miRNA), and circulating tumor cells (CTCs). Up to date, there is not a standard method for isolation, analysis, and quality of processing these circulating nucleic acids. Since identifying genomic alterations within a tumor is the goal of molecular liquid biopsy, the results help choose the best treatment for cancer patients at each disease phase.

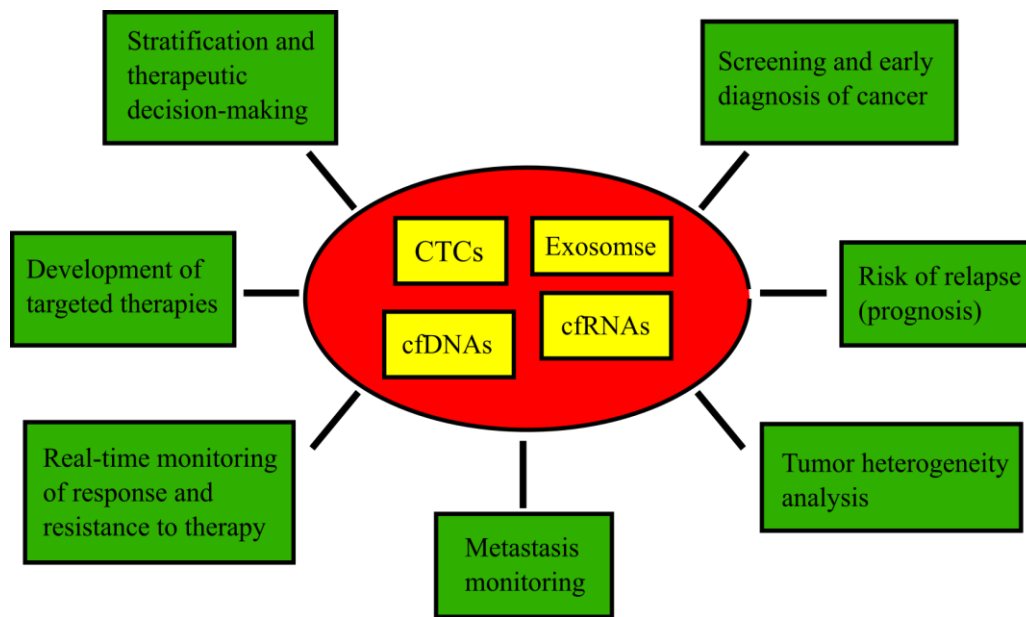


Figure 1. Overview of light biopsy

The potential clinical advantages of molecular (genetic) liquid biopsy analyses in cancer management; (circulating cell-free DNA (cfDNA), cell-free RNAs (cfRNAs), and circulating tumor cells (CTCs))

1.4 cfDNA

DNA is mainly located in the nucleus of cells, where it exists in linear form in protein complexes. For the analysis of this DNA, a cell disruption with subsequent DNA purification is necessary. Body fluids, including blood, urine, and cerebrospinal fluid (CSF) also contain DNA, which is not packaged in a cell nucleus but is available in a cell-free form as cell-free DNA (cfDNA). There are two separate mechanisms for the liberation of cfDNA: the release of newly synthesized nucleic acids by an active process and the release of the end products of necrotic or apoptotic cell death by the passive process⁶¹⁻⁶⁴. These mechanisms can be influenced by age, gender, ethnicity, diet, body-mass index, organ health, glucose levels, oxidative stress, smoking, physical activity, medication status, infections, menstruation, and pregnancy^{63,65,66}.

The cfDNA sequences are generally corresponding to the entire genome. This cfDNA can be analyzed for placental aneuploidy, cancer-specific variants, and graft-versus-host disease (GvHD) despite its small percentage in the blood^{67,68}.

Fragmented cfDNA was first discovered in the human body in 1948. cfDNA is a broad term, which describes DNA that is freely circulating in the bloodstream. Included are different forms of cfDNA, like ctDNA, a tumor-derived fragmented DNA in the bloodstream that is not associated with cells, and cell-free fetal DNA (cffDNA), fetal DNA that circulates freely in the maternal blood⁶⁹⁻⁷¹. In healthy people, the cfDNA concentration in blood is in a wide range between 2.5 to 27.0 ng/ml⁷².

Most cfDNAs are released via cleavage of genomic DNA in apoptotic cells, producing DNA fragments of less than 200 bp^{73,74}. Another DNA liberation procedure is necrosis, which by unspecific digestion releases cfDNA fragments greater than ~ 10,000 bp⁷⁵⁻⁷⁹. In contrast to the cellular destruction process, some fractions of cfDNA (ranging 1000-3000bp) are derived from active cellular secretions^{62,80-87} and carried fractions (ranging 150-6000 bp) by extracellular vesicles such as exosomes^{88,89}. In 1977 study results were published, which for the first time showed higher cfDNA levels in the serum of cancer patients compared to healthy controls. Monitored therapy showed that cfDNA level increases during metastasis but decreases during radiation therapy⁹⁰. Since then, many studies have investigated the potential uses of the cfDNA or the ctDNA as a diagnostic, prognostic, and predictive approach in cancer disease. Several subsequent studies confirmed the results: Cancer patients generally show higher cfDNA concentrations than healthy subjects⁹¹⁻⁹⁷.

Further studies have found cancer-associated mutations in the cfDNA before symptoms appear⁹⁸⁻¹⁰¹ or in the early stages of cancer¹⁰²⁻¹⁰⁷ up to 2 years before the cancer is diagnosed^{108,109}. These observations underscore the enormous potential of cfDNA as a biomarker in cancer diagnosis, especially in the early stages of cancer, where the small tumor cannot be detected using usual methods¹¹⁰. Additionally, it is known that the level of cfDNA can change in recurrence or response to treatment^{97,111}. The amount of cfDNA is affected by tumor size and stage^{105,112}. By taking all findings up to now, the cfDNA concentration seems to be a new chance for non-invasive cancer diagnosis and therapy monitoring^{113,114}.

1.5 cfDNA integrity index as a tumor marker

In addition to measuring cfDNA concentrations, the level of cfDNA fragmentation has also been considered in cancer management ⁷⁸. The DNA integrity index (DII), represented by the ratio of longer fragments to shorter fragments of DNA from the same genetic locus, can be used for tumor diagnosis. In healthy individuals, apoptotic cells are the primary source of freely circulating DNA. Apoptotic cells release DNA fragments typically 185 to 200 base pairs (bp) long; this evenly cut DNA is generated by a programmed enzymatic cleavage process during apoptosis. The cell death in tumor tissue can be traced back to necrosis, autophagy, or mitotic catastrophe, resulting in DNA fragments with different strand lengths due to the random and incomplete digestion of the genomic DNA by many deoxyribonucleases. Therefore, elevated levels of long DNA fragments can be a good marker for detecting malignant tumors^{57,115–117}. Boynton et al.2003 reported a highly significant relationship between long DNA fragments in stool and colorectal cancer. This observation may be related to disease-associated differences in the regulation of proliferation and apoptosis. Nonapoptotic cells shed from tumors may contain less degraded DNA than DNA fragments from the healthy colonic mucosa¹¹⁸.

Given the hypothesis that the normal apoptotic cells release highly fragmented DNA (about 180-200 bp lengths) due to enzymatic cleavage of nucleosome units. In contrast, the tumor cells (necrotic cells) produce longer DNA fragments by a non-specific cleavage, the relation between those has been studied^{75,119}. The induction of human tumors in mice showed that the tumor-derived cfDNA was shorter than the background mice cfDNA. The finding from this xenograft model suggests lower DNA integrity in tumor patients ¹²⁰. Since the tumors are the origin of the most cfDNA in the xenograft models, this model cannot transfer 100% to the case of the body's neoplasia ¹²¹. It is found that the ratios of short cfDNA fragments (180 bp) are associated negatively with the tumor-derived cfDNA concentration in liver cancer patients ¹²².

Real-time PCR is used to measure DII. The short and long cfDNA fragments are amplified, and the amount is determined based on a sequence in which the smaller fragments are an integral part of the larger fragments ¹²³. The non-coding genomic DNA repeat sequences such as *ALU* and *LINE-1* are the most promising genetic alterations used for calculating DII so far.

1.5.1 Non-coding genomic DNA repetitive elements: *ALU* and *LINE-1*

Mobile DNA elements, also known as jumping genes, transposons, or transposable elements (TEs), are the most repeated sequences in humans. They move from one location on the genome to another and make the genome highly dynamic. Autonomous transposons can move on their own, while nonautonomous elements require the presence of other transposable elements. Since the nonautonomous elements do not have the gene for the transposase or reverse transcriptase, they must borrow this essential protein for transposition from another element. There are four classes of transposable elements in mammals ¹²⁴ (Table 2):

- 1) Long interspersed nuclear elements (LINEs)
- 2) Short interspersed elements (SINEs)
- 3) Retrovirus-like elements
- 4) DNA transposon fossils

Table 2. Classes of transposable elements in the human genome

| Transposable elements | Classification | Length | Copy number | Genome fraction (%) |
|--------------------------|----------------|------------|-------------|---------------------|
| <i>LINEs</i> | Autonomous | 6-8kb | 850,000 | 21 |
| <i>SINEs</i> | Non-autonomous | 100-300bp | 1,500,000 | 13 |
| Retrovirus-like elements | Autonomous | 6-11kb | 450,000 | 8 |
| | Non-autonomous | 1.5-3kb | | |
| DNA transposon fossils | Autonomous | 2-3kb | 300,000 | 3 |
| | Non-Autonomous | 80-3,000bp | | |

Many mobile sequences that move by reverse transcriptase are called retrotransposons. This mechanism is called "retrotransposition." which has three steps¹²⁵⁻¹²⁷ (Fig.2):

- 1) Transcription of original retrotransposon
- 2) Reverse transcription of the RNA
- 3) Integration of the cDNA into a new genomic location

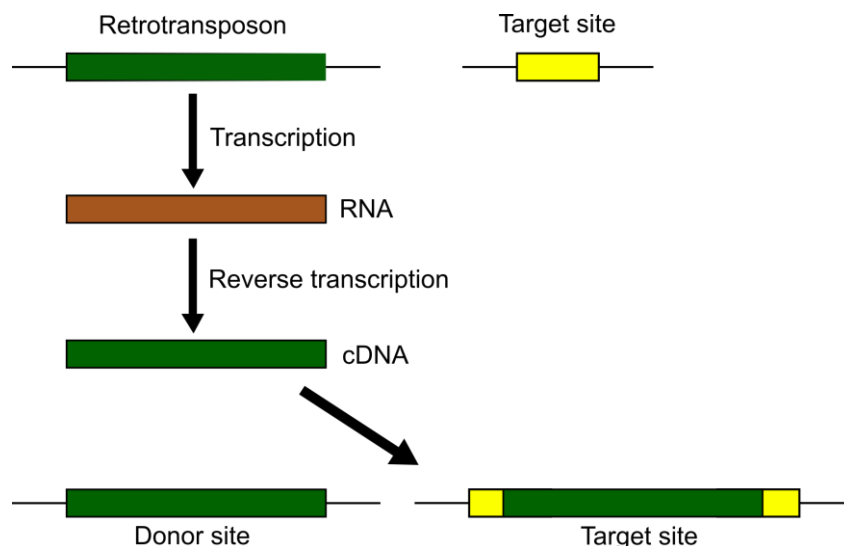


Figure 2. A schematic of Retrotransposition assay

The steps during retrotransposition event: a) Transcription of an active element to produce RNA (orange rectangle), b) Reverse transcription of RNA to produce a cDNA (green rectangle), c) Cleavage of second DNA strand of the target site to produce a break, i.e., new genomic location.

Although a large proportion (45%) of the human genome consists of transposable elements, only a tiny percentage (<0.05%) of them remain active at present. The most abundant active transposons in humans are *Arthrobacter luteus* (*ALU*) and *LINE-1* (~33%). These belong to the non-long terminal repeats (non-LTRs) retrotransposon group ¹²⁴.

LINEs are in many eukaryotic genomes. Three *LINE* families are discovered in the human genome: *LINE-1*, *LINE-2*, and *LINE-3*, but only *LINE-1* is active. *LINE-1* contains two intact open reading frames, ORF1 and ORF2, which encode proteins necessary for *LINE-1* retrotransposition. *LINEs-1* are about 6000 bp long in humans and are ~500,000 copies per human genome (equal ~to 17% of the total genome) ¹²⁴. The *LINE* machinery is used to retrotranspose the non-autonomous *SINEs* ¹²⁴.

ALU elements are the only active *SINEs* family in the human genome. They derive their name from a single recognition site for the restriction endonuclease *Arthrobacter Lectus I* (*ALU*)¹²⁸.

ALU repeats are primate-specific transposable elements with approximately 300-bp in length. They are the most abundant sequence with more than 1million copies in the human genome (equal ~11% of the total human genome) ¹²⁹. A distinction is made between different *ALU* families ^{130–132}:

ALU J (actively mobile till~55–65 million years ago)

ALU S (actively mobile till~35 million years ago)

ALU Y (remain actively mobile today)

The genome of an individual will contain many thousands of *ALU* elements from all different subfamilies.

The two repeat families (*LINE-1* and *ALU*) are considered 60% of all interspersed repeat sequences in humans. The cfDNA sequences mostly correspond uniformly to the entire genome, so *ALU* and *LINE-1* are plenty in the blood. Hence, *ALU* or *LINE-1*-based real-time PCR is a logical approach for measuring human blood cfDNA ^{124,133,134}.

1.6 cfDNA epigenetic modifications as a tumor marker (hypomethylation)

Epigenetic modifications represent epigenetic elements that control gene expression. The epigenome is a collection of all epigenetic markers that are reversible and can be passed on from one generation to the next. These epigenetic modifications change the secondary structure of DNA but not the base sequence. Therefore, epigenetic modifications influence the accessibility of DNA for transcription, leading to regulating gene expression and being involved in several cellular processes such as differentiation, development, and tumorigenesis. The destruction of epigenetic balance is correlated with various diseases such as coronary heart disease, type II diabetes, osteoporosis, cancer, autoimmune disease, neurological disorder, and metabolic diseases ¹³⁵.

Epigenetic modifications include DNA methylation, histone modification, and microRNA regulation¹³⁶. Among all studied epigenetic biomarkers, DNA methylation is the most promising biomarker for early cancer detection, monitoring the effect of applied therapies, and patient monitoring ¹³⁷. Since hypomethylation of DNA is a hallmark of cancer, thus its analysis has been suggested as a tumor marker.

The covalent addition of a methyl group to the ring system of the base cytosine in the C-5 position is called DNA methylation. DNA methylation is catalyzed by three DNA methyltransferases (DNMT 1, 3A, and 3B) by transferring the methyl groups from S-adenosyl-methionine (SAM) to the DNA (Fig.3). The DNMT1 ensures that existing methylation patterns are maintained after DNA replication; the other two methyltransferases are attributed to de novo methylation.

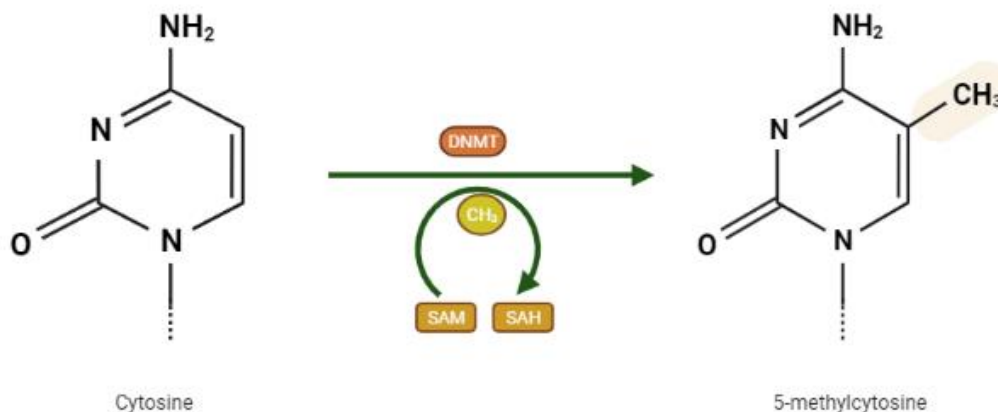


Figure 3. Schematic representation of DNA methylation

The DNA methyltransferase (DNMT) transfers a methyl residue from S-adenosyl methionine (SAM) to the C-5 position of a cytosine base in CpG dinucleotides and convert to S-adenosylhomocysteine (SAH); hence, 5-methylcytosine is produced. Created with BioRender.com

Unlike mutations, DNA methylation appears in particular regions of the DNA that can be consistently measured. The DNA methylation occurs mainly on CpG motifs, where a guanine base immediately follows a cytosine base in the 3' direction. There are over 28 million CpG dinucleotides in humans, up to 80% of which are methylated. A cluster of CpG dinucleotides that contains a large number of CpG dinucleotide repeats is called a CpG island. In mammalian genomes, CpG islands are typically 300-3,000 base pairs in length, and most of these CpG high-density regions are unmethylated¹³⁸⁻¹⁴⁰. Statistically, a small percentage (about 6%) of CpG dinucleotides are found in the human genome, but the frequency of CpG dinucleotides is much lower. In turn, they are restricted to only two locations in DNA: in a methylated form in the long repetitive sequences of non-coded DNA sections as a protective mechanism against foreign DNA (for example, viral origin) and also in the promoter area of a gene where they are often not methylated¹⁴¹.

The associated gene is “switched off” by methylation in the promoter region and is no longer expressed. This inhibition of transcription is used in the context of genetic imprinting. The female inactivated X chromosome represents a unique feature in which the fully methylated

CpG islands precede the switched-off genes and the inactivated alleles, which are also methylated in genomic imprinting ¹⁴².

It is known that the altered methylation profile results in chromosome instability and changed gene expression, and it is an event at early-stage carcinogenesis ^{64,143,144}. These findings confirm the importance of DNA methylation changes among the most promising candidates in cancer biomarker development. The methylation of promoter CpG islands (hypermethylation) and global hypomethylation are typical characteristics of tumor cells ^{143,145}. It is demonstrated that methylation of specific genes correlates with cancer risk ¹⁴⁶. Compared to the healthy cell, the malignant tumor cell shows an opposite pattern regarding its methylation status. It is identified a significant loss of methylation in the heavily methylated area of non-coded DNA sections and a considerable increase in methylation in the unmethylated promoter area of a gene section, which is also referred to as promoter hypermethylation.

In summary, methylated and unmethylated sections are essential for maintaining stable cell function. There are different methods for measuring global DNA methylation, but the most used techniques are based on the repeat elements. The methylation occurs mainly in regions where CpG density is low or at repeat DNA sites. The typically methylated repetitive elements spread in the human genome and have high copy numbers. More than half of CpG dinucleotides are located within repeat elements in the human genome. Among repeat sequences, *ALU* elements are more significant to use as a reporter of global DNA methylation. They contain the highest fraction of CpG sites in the genome (25.4%), and they are located as highly methylated gene-rich regions in somatic tissues ^{124,140}.

1.7 Aim of the work

The current study is being conducted to determine whether plasma cfDNA, cfDNA hypomethylation, cfDNA integrity index or quantitative concentrations of *ALU* 115-, *ALU* 260-, *LINE-1* 97-, *LINE-1* 266-bp fragments can be robust biomarkers for the diagnosis and prognosis of NENs. The aim is to establish a new biomarker for the diagnosis and follow-up of NEN patients on a molecular basis.

There have been investigations about cfDNA in NET patients before. Those researches focus mostly on circulating tumor cell analysis, mutation analysis, or sequencing. In contrast, my work focus on cfDNA concentration, and the corresponding analysis of cfDNA fragmentation and hypomethylation. The application of total cfDNA levels has not been widely studied in NENs. Nothing is known about the cfDNA integrity in plasma of NEN patients. In the case of *ALU* hypomethylation, research currently focuses mainly on hypermethylation, with tissue being used as the test material. We measured the hypomethylation in cell-free tissue, the cfDNA, which has not yet been published for NEN patients.

In addition, the possibility of characterizing, differentiating, and staging tumors with these parameters was evaluated in this research. cfDNA concentration, cfDNA fragmentation, cfDNA integrity, and hypomethylation are compared with the already recognized NENs biomarker CgA in order to find their specific clinical relationship.

The following questions will be addressed in the course of the experiments:

1. Is there a difference in cfDNA plasma concentration between the NEN patients and the control group? Can a difference be noted between the different tumor loads or stages of cancer?
2. Are there different concentrations of long and short cfDNA fragments, measured on *LINE-1* and *ALU*, between the control and the patient group? Is there a connection between the cfDNA fragmentation and patients with different tumor burdens or cancer stages?
3. Is there a difference in cfDNA integrity, as measured by *LINE-1* and *ALU*, between the control and patient groups? Can a different cfDNA integrity be determined between patients with different tumor burdens or cancer stages?
4. Does the measurement of hypomethylation from the cfDNA allow differentiation between NEN patients and control groups?
5. Is there a correlation between the parameters and the patients' clinical condition (age, gender, tumor grade, tumor burden, tumor origin, and CgA level)?

2. Material and Methods

2.1 Material

2.1.1 Devices

| Equipment | Manufacturer |
|---|---|
| Centrifuge, 5717R | Eppendorf, Hamburg; Germany |
| Centrifuge, 5702R | Eppendorf, Hamburg; Germany |
| CO2-Incubator | Thermo Heraeus HeraCell, Germany |
| Freezer, comfort | Liebherr, Biberach a.d. Riss; Germany |
| Inverted microscope, IX 70 | Olympus, Hamburg; Germany |
| LC Carousel Centrifuge | Roche, Germany |
| Magnetic separation rack (for 15- and 2-ml tubes) | OZ Biosciences, Marseille, France |
| Pipetting aid, Pipetboy | IBS, Integra Bioscience, Wallisellen, Switzerland |
| Qubit Fluorometer | Invitrogen, Life Technologies, CA, USA |
| Steam sterilizer, Varioclave | H+P, Oberschleißheim; Germany |
| Vacuum aspiration system | BVC Professional, Vacuubrand, Wertheim, Germany |
| Sterile bench | Hera Safe, Heraeus, Hanau, Germany |
| Thermo Cycler 480 Real-Time PCR system | Roche Diagnostics, Mannheim, Germany |
| Thermomixer compact | Eppendorf, Germany |
| Vortexer, REAX 1DR Minishaker | Heidolph, Schwabach, Germany |
| Water bath | Memmert, Germany |

2.1.2 Laboratory materials

| Materials | Manufacturer |
|---|---|
| Centrifuge tubes, Pointed bottom (15 & 50 ml) | Greiner Bio-one GmbH, Frickenhausen, Germany |
| Cell culture flask | Greiner Bio-one GmbH, Frickenhausen, Germany |
| Cell culture plates (6 & 96- Hole plates) | Nunc, Wiesbaden; Germany |
| Disposable pipettes (5, 10 & 25ml) | Greiner Bio-one GmbH, Frickenhausen, Germany |
| Powder-free Nitrile gloves | Star Guard comfort Starlab, Hamburg, Germany |
| LightCycler® Capillaries (20 µl) | Roche, Germany |
| Monovette EDTA KE/9ml | Sarstedt, Nümbrecht, Germany |
| Microcentrifuge tubes (1.5 & 2ml) | Eppendorf, Hamburg; Germany |
| Multichannel pipette (30-300µl) | Brand, Wertheim, Germany |
| Multipette tips (10 & 1 ml) | Eppendorf, Hamburg; Germany |
| Neubauer counting chamber | Marienfelda, Lauda-Königshofen Germany |
| Pipette tips with filter (5, 10, 100 & 1000 µl) | STAR LAB, Germany |
| Pasteur pipettes | Brand, Wertheim, Germany |
| Qubit assay tubes 500 tubes | Invitrogen, Thermo fisher scientific, Germany |
| Single-channel pipettes (0.1-2.5, 0.5-10, 10-100 & 100-1000 µl) | Eppendorf, Hamburg, Germany |

2.1.3 Chemicals

| Chemicals | Manufacturer |
|------------------------------|-------------------------------------|
| DMEM /F12 cell culture media | Gibco, UK |
| DNase AWAY | Molecular bioproducts, SanDiego, CA |
| RNase AWAY | Molecular bioproduct, SanDiego, CA |
| Trypan blue stain (0.4%) | Gibco, USA |
| Ethanol (96–100%) | Sigma Aldrich,Germany |
| Sera; FBS | Gibco, UK |
| Human Genomic DNA | Promega, USA |
| Isopropanol (100%) | Sigma Aldrich,Germany |
| Penicillin–streptomycin | Sigma, USA |
| PCR grade water | Invitrogen, UK |
| Terralin | Schülke, Germany |
| 10X Tango buffer | Thermo Scientific, Germany |
| 10X T4 ligase buffer | Thermo Scientific, Germany |

2.1.4 Kits with manufacturer information

| Kits | Manufacturers |
|-----------------------------------|--------------------------------------|
| FastStart DNA Master SYBR Green I | Roche Diagnostics, Mannheim, Germany |
| QIAamp MinElute ccfDNA Mini Kit | Qiagen, Hilden, Germany |
| QIAamp DNA Blood Mini Kit | Qiagen, Hilden, Germany |
| Qubit dsDNA HS Assay kit | Fisher Scientific, Germany |
| MycoBlue Mycoplasma Detector | Vazyme, Germany |

2.1.5 Enzymes with manufacturer information

| Enzyme | Manufacturers |
|------------------------------|------------------------------------|
| T4 DNA ligase (5 Weiss U/uL) | Thermo Fischer scientific, Germany |
| <i>MspI</i> (10 U/uL) | Thermo scientific, Germany |
| <i>HpaII</i> (10 U/uL) | Thermo scientific, Germany |
| Trypsine | Sigma, USA |

2.1.6 Software with manufacturer information

| Software | manufacturer |
|-------------------|-------------------------|
| MS Office 2003 | Microsoft, Seattle, USA |
| GraphPadPrism 9.1 | California, USA |
| Jamovi 1.6 (2021) | Sydney, Australia |

2.1.7 Adaptor and primer sequences

The used primer sequences were obtained in the purity from Biomers.net GmbH (Ulm, Germany). A stock solution with a concentration of 100 pmol / μ l was prepared from the initially freeze-dried material by dissolving it in an appropriate amount of PCR water. The stock solution had to be diluted 1:10 with PCR water to obtain a ready-to-use solution with a concentration of 10 pmol primer / μ l and was stored at a temperature of -20 ° C.

Table 3. Adaptor and primer sequences

| Primer | direction | sequences | Reference |
|---|-----------|-------------------------|-----------|
| <i>ALU</i> 260-bp (Long fragment) | Forward | ACGCCTGTAATCCCAGCA | 147 |
| | Reverse | CGGAGTCTCGCTCTGTCTG | |
| <i>LINE-1</i> -97-bp (Short fragment) | Forward | TGGCACATATACACCATGGAA | 147 |
| | Reverse | TGAGAATGATGGTTTCCAATTTC | |
| <i>LINE-1</i> -266 -bp (Long fragment) | Forward | ACTTGGAACCAACCCAAATG | 147 |
| | Reverse | CACCACAGTCCCCAGAGTG | |
| <i>ALU</i> 115-bp (Short fragment) | Forward | CCTGAGGTCAGGAGTTCGAG | 148 |
| | Reverse | CCCGAGTAGCTGGGATTACA | |
| Met. <i>ALU</i> | Forward | AGCTACTCGGGAGGCTGAG | 140 |
| | Reverse | ATTCGCAAAGCTCTGACGGGTT | |
| Adaptor 1 | Forward | AAAGCTCTGA | 140 |
| Adaptor 2 | Reverse | CGTCAGAGCTTTGCGAAT | |

Table 4. The short *ALU* primers sequences used for qPCR setting up

| Primer | Direction | Sequence | Reference |
|-------------------|-----------|-------------------------------|-------------|
| <i>ALU</i> 111-bp | Forward | F:5'- CTGGCCAACATGGTCAAAC -3' | 147 |
| | Reverse | 5'-AGCGATTCTCCTGCCTCAG-3' | |
| <i>ALU</i> 105-bp | Forward | 5'-GGTCAAACCCCGTCTCTACT-3 | 149 |
| | Reverse | 5'- GGTTCAGCGATTCTCCTGC-3' | |
| <i>ALU</i> 102-bp | Forward | 5'-CGGTGGCTCACGCCTGTAAT-3' | Self-design |
| | Reverse | 5'-GGGGTCTCGCTATGTTGCC-3' | |
| <i>ALU</i> 92-bp | Forward | 5'-AATTAGCCGGCGTGGTGGC-3' | Self-design |
| | Reverse | 5'-GCAGCCTCGAACTCCTGGGC-3 | |
| <i>ALU</i> 70-bp | Forward | 5'-CCCAGCACTTTGGGAGGCCG-3 | Self-design |
| | Reverse | 5'-TGTTGCCAGGCTGGTCTCG-3' | |
| <i>ALU</i> 90-bp | Probe | 5' -CGCCCGGCTAATTTTGTAT-3' | 149 |

2.1.8 Clinical sample (Human Participants)

NET patients who visited the department of endocrinology and metabolism at the university medical center, Mainz, in 2019 and 2020 were included in the study. Written informed consent was obtained from all individuals included in this study. The study was approved by the local ethics committee of the Mainz university medical center (vote number 2019-14664). Blood samples were collected following diagnosis from two patient groups:

- (a) patients with a histologically confirmed endocrine cancer disease
- (b) patients with an endocrine disorder and no malignant disease

The healthy controls had no history of cancer, autoimmune disease, tissue injury, or trauma at the time of examination and their hematological-biochemical profile was normal. The average age of control was 52 years and 64 years for patients. The included patients were 7 NECs, 47 metastatic NETs (mNETs) and 8 non-metastatic NETs (non-mNETs). Table 7 (result part) provides an overview of the patients' clinical data and the pathological parameters.

2.1.9 Media and Cell line

BON-1 Cells

BON-1 are adherent human pancreatic tumor cells. *BON-1* cells were isolated from a peripancreatic lymph node metastasis of a 28-year-old male with pancreatic neuroendocrine tumors¹⁵⁰. The *BON-1* cell line produces neurotensin, pancreastatin, CgA, 5-HT, 5-hydroxytryptophan (5-HTP), and 5-HIAA¹⁵¹.

BON-1 cell line was provided by Dr. Buchholz (University of Marburg). The cell line was confirmed as mycoplasma-free, using MycoBlue Mycoplasma Detector (Vazyme, Germany). The *BON-1* cell line was cultured in DMEM /F12 media (31331-028 Gibco, UK), supplemented with 10% heat-inactivated (v/v) FCS, 1% penicillin-streptomycin. The cell line was cultured in a humidified incubator at 5% CO₂ and 37 °C. Cells were split twice a week.

2.2 Methods

2.2.1 Sample collection

Peripheral blood was collected in 9 ml EDTA tubes (S-Monovette R, Sarstedt, Nümbrecht, Germany) and stored in a refrigerator at 4°C. The blood samples were processed within 2 hours of blood collection. Whole blood was centrifuged at 1900 x g for 10 minutes at 4°C, and the 95% of supernatant was pipetted off to the Eppendorf tube without disturbing the Buffy coat or red cell pellet. A second centrifuge was done at 16000 x g for 10 minutes at 4°C to ensure that the plasma was free of cells or cell debris. The supernatant was transferred into storage tubes. These were stored in aliquots of 4.5 ml each at a temperature of -20 °C until further use. Before extraction, only one freeze-thaw cycle was ensured for all plasma samples.

2.2.2 cfDNA purification and isolation

Using QIAamp® MinElute® ccfDNA Midi Kit

Samples were thawed on ice before the cfDNA extraction was performed. Once melted, the plasma was centrifugated at 3000x g for 3 minutes at 4°C to remove any cell debris in the supernatant. The cfDNA was isolated from the plasma samples using QIAamp® MinElute® ccfDNA Midi Kit with a protocol recommended by the manufacturer (i.e., lyse, bind, wash, and elute). The kit can provide the maximum possible concentration of cfDNA present in low concentrations in humans (typically 1–100 ng/ml plasma). The 4 ml of plasma was processed in a standard 15 ml centrifuge tube. The kit has a small magnetic bead suspension as a functional component. These beads have different binding properties for nucleic acids, depending on the ambient pH. By adding bead binding buffer in pre-concentration of circulating nucleic acids step, the pH lowers, and the surface of beads becomes positive; thus, the beads bind to negatively charged nucleic acids at low pH. Another addition to the mixture is proteinase K, which digests the contaminating proteins and enzymes, such as DNase, leading to the complete release of nucleic acids from bound proteins. For lysis of

sample and binding of magnetic beads to cfDNA, the mixture was incubated for 10 minutes at room temperature (15–25°C) while slowly rotating end-over-end.

The bounded cfDNA-magnetic beads were collected in a pellet on a magnet rack, and the supernatant was discarded. The bounded nucleic acids are released from beads if the ambient pH is elevated by bead elution buffer. Then, the no-bound cfDNA beads are separated from pre-eluate on a magnetic rack. The DNA's pre-eluate is transferred onto a QIAamp® MinElute column and centrifuged to adsorb cfDNA onto the silica membrane. In the cleanup step, buffer ACB was added to the column to change the pH value leading to optimal binding of the cfDNA to the membrane. By adding and removing buffer ACW2, proteins and other contaminations were eliminated while cfDNA remained bound to the QIAamp MinElute membrane. For removing ethanol, the membrane is dried.

In the elution step, 32 µl of ultra-clean water was used to elute extracted cfDNA in 1.5 ml Microcentrifuge tubes. The pH increase of the mixture cause separation of bound DNA on the column. QIAamp® MinElute® cfDNA columns can bind fragmented nucleic acids. The size of cfDNAs in the blood is generally as short fragments of <1000 bp. The eluate was re-applied onto the column, and the final released cfDNA solution was divided into aliquots of 8 µl each in separate tubes. Then, these eluted cfDNAs were stored at -20 ° C until further processing. The isolated cfDNA samples were stored in the low DNA adsorption tubes as recommended ⁷⁹.

2.2.3 cfDNA measurement

The cfDNA concentration was measured using the Qubit dsDNA HS Assay kit (Fisher Scientific, Germany) on a Qubit Fluorometer (Invitrogen, Life Technologies, USA) according to the manufacturer's instructions. The kit consists of a dye (fluorophore) that binds to DNA or RNA in the sample. Briefly, 2 µl of the sample was added to each tube containing Qubit® working solution for a final volume of 200µl. To each standard tube, 10µl from standards 1 or 2 and 190 µL of Qubit® working solution were mixed. The tubes were incubated at room temperature for 2min and then read by Qubit Fluorometer. The measuring range of the kit is 10pg/µl to 100 ng/µl.

2.2.4 Isolation of the genomic DNA from *BON-1* cell culture

DNA from *BON-1* (passage number 7) was isolated using a QIAamp DNA Mini Kit (Qiagen, Germany), following the manufacturer's instructions. 1×10^6 harvested cells were resuspended in PBS to a final volume of 200 µl. 20 µl proteinase K and 200 µl buffer AL are added, and the mixture is incubated at 56°C for 10 min. After adding 200 µl ethanol (96–100%) to the mix, it was applied to the QIAamp Mini spin column and centrifuged at 6000g for 1 min. Later, 500 µl Buffer AW1 was added to the column and centrifuged at 6000g for 1 min. Following discarding the collection tube with the filtrate, 500 µl buffer AW2 was added to the column. Subsequently, two steps centrifuges were applied at 20,000g for 3 min and 1 min to obliterate buffer AW2. Then, 200 µl buffer AE was added to the QIAamp Mini spin column and incubated at room temperature (15–25°C) for 1 min. In the final step, the DNA was collected by centrifuge at 6000g for 1 min.

2.2.5 Measurement of the *BON-1* genomic DNA

The concentration of the isolated DNA was quantified using a Qubit fluorometer (Invitrogen, Life Technologies, USA) with a Qubit dsDNA HS Assay kit (Fisher Scientific, Germany) according to the manufacturer's instructions.

2.2.6 Quantitative polymerase chain reaction

The concentration of different fragments under investigation was measured using the absolute quantification method. For this purpose, quantitative polymerase chain reaction (qPCR) using SYBR®Green Master Mix (Roche Diagnostics, Mannheim, Germany) and the Light Cycler 480 Real-Time PCR system (Roche Diagnostics, Mannheim, Germany) was applied. The critical enzyme is the DNA polymerase enzyme, and the cyclical changes in the reaction temperature control the total reaction in PCR. The cfDNA samples were diluted before use to achieve a 20pg/µl concentration or 100pg/reaction. LightCycler® Capillaries (Roche, Germany) are used, and a 20µl reaction mixture per capillary is applied. The reaction mixture contains 5 µl prepared template (20pg/µl), each 1µl solution with forward and reverse primer, according to 0.5 pmol/µl of each primer, as well as 4µl qPCR master mix and 9µl PCR- Water. The cfDNA double helix is denatured into two single strands at 95 ° C for 10 minutes in the first step. In the second step, the primer pairs bind complementarily to the corresponding sequences on the DNA parent strands. All primer sequences are given in table 3. In this step, which is called the annealing process, the temperature has to be lowered. The required temperature depends on the melting temperature of the primers to form a stable bond to complementary sequences and less stable connections to similar sequences. In the next step, the elongation step, the temperature is set near the optimum temperature of the DNA polymerase to sufficiently elongate the new DNA strand. The 35 cycles follow with the same sequence of denaturing, annealing and elongation. cfDNAs in blood plasma were analyzed by amplifying short and long fragments of two different loci of repetitive DNA elements: *ALU* (*ALU-115-bp*, *ALU-260-bp*) and *LINE-1* (*LINE-1-97-bp*, *LINE-1-266-bp*) during independent reactions as shown in table 5. This work uses a fluorescent dye, SYBR®Green, which binds to the DNA double-strand and transmits a fluorescence signal, which can be measured; thus, the present DNA can be measured in the reaction after each cycle. The level of the signal is correlated with the amount of DNA and can be shown graphically. At first, the fluorescent cannot be distinguished from the non-specific background because the signal is weak. As the amount of a product increases, the fluorescence signal becomes more robust, and it separates from the "background signals" in a particular threshold value for the first time. The apart takes a certain number of cycles that is called the Ct value (Cycle threshold). The exponentially increasing fluorescence signal shows the exponential growth of the amount of DNA. The consumption of some components of the reaction mixture, e.g., primer, nucleotides, leads to slow down and the end of the reaction later. For all real-time PCR reactions, the samples, a positive control made of commercial genomic DNA, and negative control of water blanks are applied in duplicate to each run. Samples with a quantification cycle value (Ct) > 35 were removed from further analysis. The sample replicates with a difference ≥of 1 Ct was re-checked.

DII was calculated according to Umetani et al. ¹⁵² as the ratio of longer fragment concentration to shorter ones for each gene: *ALU-260-/115-bp*, *LINE-1-266-/97-bp*. Since the

short sequences of each gene are represented within the annealing sites of long fragments, this ratio can range theoretically from 0 to 1. A classic process is demonstrated in Fig. 4.

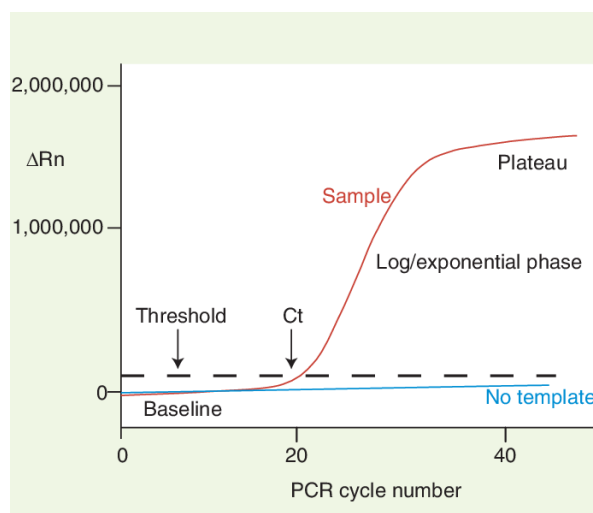


Figure 4. PCR representation with one sample

Ct = Threshold cycle, ΔRn = Fluorescence emission of the product at each time point minus fluorescence emission of the baseline ¹⁵³.

Table 5. Amplicon length and qPCR assay conditions for each primer

| Gene | Amplicon size (bp) | Real-time protocol |
|---------------|--------------------|---|
| <i>ALU</i> | 260 | Thermal cycling began with an initial denaturation step (95°C for 10 min) followed by 35 cycles of DNA denaturation (95°C for 10s), primer annealing (70°C for the 30s), and primer extension (72°C for 30s). The temperature transition rate (C/s) is set at 20 min. |
| <i>ALU</i> | 115 | Thermal cycling began with an initial denaturation step (95°C for 5min) followed by 35cycles of DNA denaturation (95°C for 5s), primer annealing (68°C for the 30s). The temperature transition rate (C/s) is set at 20 min. |
| <i>LINE-1</i> | 266 & 97 | Thermal cycling began with an initial denaturation step (95°C for 10 min) followed by 35 cycles of DNA denaturation (95°C for 10 s), primer annealing 62°C for the 30s), and primer extension (72°C for 30s). The temperature transition rate (C/s) is set at 20 min. |

*(Abbreviation: bp – base pair)

2.2.6.1 Melting curve

The crucial final point of the amplification process is the melting curve to assess the specificity of the PCR products. There are some difficulties in PCR, such as the formation of primer-dimers and nonspecific binds. The binding of complementary pieces of primer to each other is called primer dimers. The fluorescent dye recognizes these dimer forms as double-

strand DNA and binds to them, which led to a false signal. The melting curve analysis is used to realize this reaction. With continuously increasing temperature, the fluorescence signal decreases slowly. At a specific point, the melting temperature, the DNA double helix of the product is divided into its two single strands, and the signal reduces suddenly because of the release of the fluorescent dye. The melting temperature depends on the length and base composition of each strand of DNA; thus, the primer dimers have a lower melting point because they have a shorter length than the desired PCR product. A typical melting curve is shown in Fig.5. The PCR machine was programmed for the melting curve step for all qPCR reactions as one cycle: (1) 95 ° C for 0s (2) 65 ° C for the 60s with a ramping rate of 20min. This step is completed with a final stage of 95 ° C for 0s and a temperature transition rate (° C/s) 0.10s.

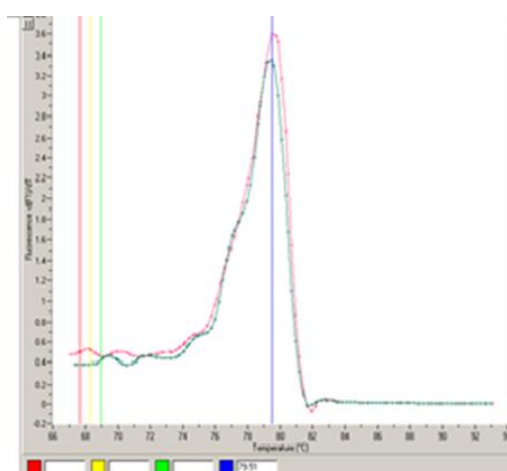


Figure 5. Typical melting curve graph and its temperature derivative

The graph illustrates a standard melting curve. A melting curve shows the relation between fluorescence and temperature for determining the melting temperature of the amplification product, which in this case is about 79.5 C.

2.2.6.2 Calculation of qPCR efficiency

A serial dilution of commercial human genomic DNA (Promega, USA) was measured for each primer set for the amplification efficiency test. DNA dilution was done by a 1:10 series, covering five dilution points (10-0.001 ng) in duplicate for *LINE-1* 97-, *LINE-1* 266-, *ALU* 115-bp series, and (1-0.00001 ng) for *ALU* 260-bp. qPCR analysis of each sample was done according to the established protocol for each primer set (see 2.2.6), followed by amplification with a standard dissociation curve analysis.

In the optimal case, which describes 100% efficient primers, DNA would be doubled in the reaction mixture within a cycle. Therefore, the amount of amplified DNA could be calculated easily as $D1 = D0 \times 2^Z$, where (D1) is the amount of amplified DNA, (D0) is the amount initially present, and (Z) is the number of cycles. In reality efficiency of primers rarely reach exact 100% and will be calculated from the slope of the standard curve of each primer as $E = 10^{-1/\text{slope}-1}$. A range between 90-110% is considered to be great.

Primer efficiency was calculated using Microsoft Excel.

2.2.6.3 Standard curve

A standard curve was applied for each primer to quantify the absolute quantitative of fragments presenting in the samples. In this study, 10-fold serial dilution of known amount commercial human genomic DNA (Promega, USA) was used in 5 dilution steps (10, 1, 0.1, 0.01, 0.001 ng/μl) for *LINE-1* 97-, *LINE-1* 266- and *ALU* 115-bp, but 6 dilution steps (1, 0.1, 0.01, 0.001, 0.0001, 0.00001 ng/μl) for *ALU* 260-bp. Additionally, a negative control was used for quality control. All measurements were done in duplicates. After RT-PCR, the Ct values of the dilutions were plotted against the concentration, and a standard line was made by linear regression. In Excel, the straight-line equation is used to calculate the concentration of an unknown sample by its Ct value.

2.2.7 cfDNA hypomethylation test

The hypomethylation test is performed according to described protocol by Buj et al., 2016¹⁴⁰. In this technique, the percentage of unmethylated *ALU* is used as a reporter of global hypomethylation. This method has three steps (Fig.6):

1. Digestion of cfDNA with isoschizomers *HpaII*/*MspI*
2. Ligation of an adaptor
3. qPCR using specific primers for the *ALU* consensus sequence

2.2.7.1 Preparation of an adaptor

A synthetic adaptor was ligated to the digested DNA fragments. For synthetic adaptor preparation, 5 μl of the adaptor 1 (100nmol/L) and 5 μl of the adaptor 2 (100nmol/L) (Table 3) were incubated at 65°C for 2 min, then cooled at room temperature for 35 minutes. The 1 ml synthetic adaptor (1nmol/L) was made by adding 990 μl PCR water to the tube. After mixing, it was aliquoted and kept at -20°C.

2.2.7.2 Treatment with restriction enzymes

The treatment of cfDNA samples with restriction enzymes is critical to distinguish between methylated and unmethylated DNA fragments. *HpaII* and *MspI* are the restriction enzymes in this process to digest cfDNA. These isoschizomers, *HpaII* and *MspI*, recognize CCGG in *ALU* consensus sequence AACCCGG, a specific base sequence present in 14.4% of *ALU* elements in CpG islands. The endonucleases break down DNA as C/CGG leading to produce fragments with specific and same sticky ends. *HpaII* is sensitive to methylation; thus, it cuts the cfDNA in unmethylated cytosine residues (no CpG methylations). *MspI* is methylation-insensitive and can cut enzymatically methylated and unmethylated cfDNA. For the reaction, 0.2 μl T4 ligase (5 Weiss U/ μl), 1 μl of tango buffer 10x (Thermo scientific, Germany), 2 μl of T4 ligase buffer 10x (Thermo scientific, Germany), 1 μl of the synthetic adaptor (1nmol/L) were transferred to two separated Eppendorf tubes. Subsequently, 0.1 μl of *HpaII* (Thermo scientific, Germany) or *MspI* (Thermo scientific, Germany), each corresponding to 1 U (unit) of the restriction enzymes, were added in each reaction tube in parallel. Additionally, two ng of cfDNA are added to each reaction tube. PCR water was added to obtain a final volume of 30 μl, mixed carefully by pipetting up and down. The tubes were incubated for 1 hour at 37 ° C and 16 ° C for 2 hours in a thermomixer. Then, incubation takes place at 65° C for 20 minutes to inactivate the enzymes.

2.2.7.3 Quantification of unmethylated *ALU* in cfDNA by qPCR

After digestion of cfDNA with enzymes, the unmethylated *ALU* was quantified in cfDNA by a qPCR assay. The used primer is shown in table 4. The primer is complementary to the AACC + synthetic adaptor. qPCR of the *MspI* digestion mixture quantified all the amplifiable *ALU* elements regardless of their methylation status. Whereas qPCR of *HpaII* digestion only amplifies unmethylated CpG ones. *LINE-1 97* is used to normalize the DNA input for both *MspI* and *HpaII* digestions. The process is performed in a final reaction volume of 10 μ l as follows: Briefly, five μ l of SYBR®Green Master Mix (Roche, Germany), 0.1 μ l of forward primer (100nmol/L), 0.1 μ l of reverse primer(100nmol/L), one μ l of the enzyme-treated cfDNA from diluted 1:20 equivalent to 0.0034 ng of cfDNA, 3.8 μ l Nuclease-free water were mixed. The thermocycler was programmed according to like 10 min 95 ° C, 40 cycles of 10 seconds at 95° C and 10 seconds at 65° C. The melting curve is analyzed to check primer-dimer formation with the program: 0s at 95°C followed by 60s at 65°C and 0s at 95°C. The cooling step was at 40 °C for the 30s. DNA normalization is performed by parallel amplification of a standard gene of *LINE-1 97*. Each sample was measured in duplicate. In addition, each assay includes water as a negative control, and the negative control should not have Ct <34.

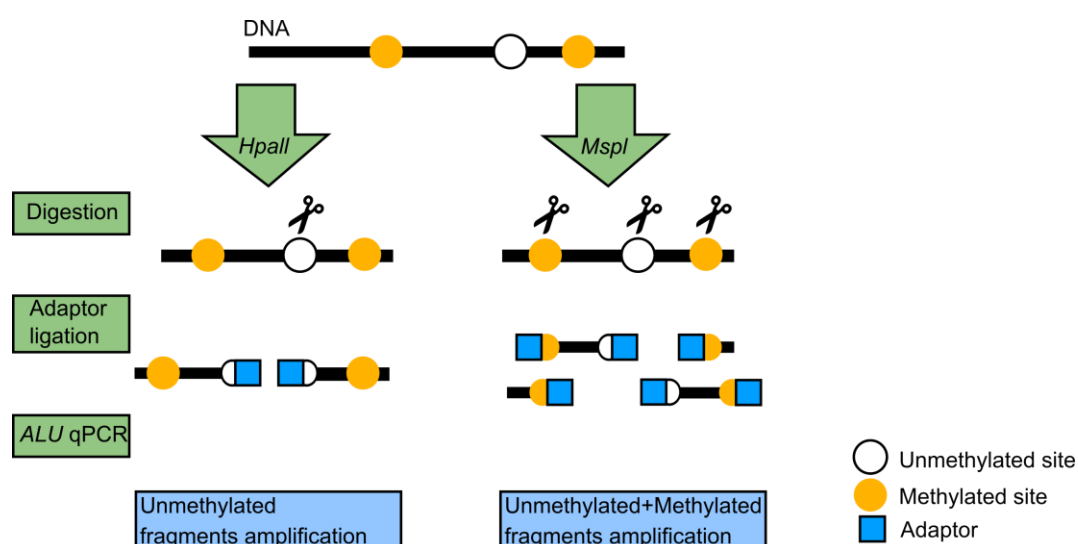


Figure 6. Illustration of unmethylated *ALU* elements measurement technique

2.2.7.4 Efficiency for methylation primer

A standard curve calculated the efficiency value for each primer pair (met. *ALU* and *LINE-1 97*-bp). Different amounts of genomic *BON-1* cell culture ranging from 1 to 100 ng are plotted against Ct values, and Microsoft Excel evaluated assay efficiency.

2.2.7.5 Calculation of percentage of hypomethylation

The relative amount of unmethylated *ALU* repeats are identified as a marker for global hypomethylation. The percentage of hypomethylation was determined using the following formula:

Percentage of unmethylated *ALU* elements =

$$\left[\frac{(E_{ALUH})^{-Ct_{ALUH}} / (E_{LINEH})^{-Ct_{LINEH}}}{(E_{ALUM})^{-Ct_{ALUM}} / (E_{LINEM})^{-Ct_{LINEM}}} \right] \times 100$$

| | |
|--------------------|--|
| E | qPCR efficiency |
| Ct | cycle threshold |
| Ct <i>ALU</i> H | Ct from qPCR using Met- <i>ALU</i> primer of <i>HpaII</i> digested cfDNA |
| Ct <i>ALU</i> M | Ct from qPCR using Met- <i>ALU</i> primer of <i>MspI</i> digested cfDNA |
| Ct <i>LINE-1</i> H | Ct from qPCR using <i>LINE-1</i> 97-bp primer of <i>HpaII</i> digested cfDNA |
| Ct <i>LINE-1</i> M | Ct from qPCR using <i>LINE-1</i> 97-bp primer of <i>MspI</i> digested cfDNA |

In this equation, the variable and base data are Ct and E, respectively. *ALU* H and *ALU* M describe unmethylated *ALU* elements and the total amplifiable *ALU* elements, while *LINE-1* H and *LINE-1* M were used for normalization.

2.2.8 Determination of established tumor marker

Cg A was measured by an enzyme-linked immunosorbent assay (ELISA) in medical labor.

2.2.9 Statistical analysis

All samples were running in the three replicates. The statistical analysis was carried out using GraphPad Prism software (version 6.1) and Jamovi (version 1.6), whereby $p \leq 0.05$ was defined as the significance level. The normality test was the Shapiro-Wilk test. The distribution is not normal, then non-parametric tests were applied further. The cfDNA concentration, cfDNA integrity, and hypomethylation play a key role here. Data in the text and graphs were presented as a median with interquartile ranges (IQR). The outliers cannot be deleted in medical data because they can show a remarkable occurrence. The outlier can seriously affect the mean, range, and standard deviation. Thus, the median is resistant to the outliers and is the midpoint of a distribution. The IQR is the distance between the 1st quartile (25th percentile) and the 3rd quartile (75th percentile). It is the middle 50% of data. IQR was used to identify the outliers to set up the minimum and maximum limits. A data is an outlier if it falls more than 1.5 IQR above the 3rd quartile or more than 1.5 IQR below the 1st quartile. The normality test was the Shapiro-Wilk test. The $p < 0.05$ means the normality test result is significant; the data is not normal.

Welch's t-test was applied for the comparison of the patients and control groups. Welch's t-test compares the means of two independent groups, and the test does not assume identical variances. Welch's t-test test also evaluated the comparison of each biomarker with gender. For comparison between three or more independent groups was applied.

Kruskal-Wallis H test. It is an extension of Mann–Whitney U test. This nonparametric test is rank-based and uses summed rank scores to determine the results. The mean rank is the average of the ranks for all observations within each sample used to calculate the test statistic (H-value). It tells if there is a significant difference between groups. It will not reveal which groups are different. If the Kruskal–Wallis test is substantial, Dwass-Steel-Critchlow-Flinger pairwise comparison test is used as a post-hoc analysis to determine which groups differ from each other group. The Kruskal–Wallis test compared the subgroups and the study groups regarding tumor grade and localization in this study.

The relationship between two variables can be compared with correlation analysis. All correlation tests, including age, tumor burden, and CgA level, were calculated by **spearman's rank correlation coefficient test**. In this nonparametric test, data are given as correlation coefficient (r). The value of (r) is a statistical measure of the strength of a relationship between paired data. The correlation between variables can be positive or negative. The strength of the correlation demonstrated using the following guide for r:

| | |
|-------------|-------------|
| 0.00 - 0.19 | very weak |
| 0.20 - 0.39 | weak |
| 0.40 - 0.59 | moderate |
| 0.60 - 0.79 | strong |
| 0.80 - 1.0 | very strong |

The discriminatory power of the biomarkers was determined with the help of **receiver operating characteristic analysis (ROC)**. All statistics were calculated with a 95% confidence interval. In a ROC curve, the sensitivity was plotted against specificity at all possible cut-off points to screen asymptomatic individuals in the tests. The sensitivity describes the proportion of true positive results (the ratio of correctly identified patients). In contrast, specificity shows the proportion of true negative (false positive or the ratio of healthy individuals who are correctly identified) results. The area under the curve (AUC) shows the discriminative potential of the biomarker, i.e., its accuracy. The AUC indicates a more precise diagnostic test if closer to 1.0, whereas values comparable to the lowest limit of 0.5 were associated with the weakest results.

The below categorizations can be used to describe the diagnostic power of the ROC curve:

AUC

| | |
|---------|-----------|
| 0.9-1.0 | very good |
| 0.8-0.9 | good |
| 0.7-0.8 | fair |
| 0.6-0.7 | poor |
| 0.5-0.6 | fail |

The cut-off value is where the sum of specificity and sensitivity is maximum and, in this point, patients and healthy differentiate with high efficiency^{154–159}. Also, other indicative parameters such as sensitivity, specificity, positive predictive value, negative predictive value were calculated to assess the discrimination power of the individual or combined biomarkers.

3. Results

3.1 Real-time PCR assay performance

RT-PCR was applied using the *ALU* and *LINE-1* genes as the amplifying target (Fig. 7). The specificity of qPCR amplification products was validated by melting curve analysis. All plasma cfDNA samples displayed a single peak corresponding to about 91 ° C, 81 ° C, 81 ° C, 79 ° C for *ALU* 260-bp, *ALU* 115-bp, *LINE-1* 266-bp, *LINE-1* 266-bp, respectively in their melting curves. This outcome supported the high specificity of the selected primers and the lack of nonspecific amplification products in qPCR assays. For *ALU* 115-bp, all plasma cfDNA samples showed a short peak before the single peak corresponding to 81 ° C. This short peak at a relatively low temperature might be because of primer dimer. More early templates may help overcome this problem, but it was impossible for some of the samples. Later, it was tried to resolve this issue by decreasing the primer concentration, increasing the annealing temperature, reducing the annealing time, and using DMSO and formamide for specific binding. In parallel, some other *ALU* primers as the short primer were tested (Table 4). The broad melting peak or two peaks in all tested short *ALU* primers was observed (melting curves are not shown), which might be because of the complexity of the *ALU* family.

In the hypomethylation test, RT-PCR was applied using the *ALU* and *LINE-1* genes as the amplifying target. Met-*ALU* and *LINE-1* 97-bp primers were applied. All the qPCRs related to a sample were applied for Met-*ALU* for *HpaII* and *MspI* and *LINE-1* 97-bp for *HpaII* and *MspI* (Fig.8). The specificity of qPCR amplification products was validated by melting curve analysis. All plasma cfDNA samples displayed a single peak corresponding to about 83.24 ° C, 83.84 ° C, 78.58° C, 78.58 ° C for Met. *ALU* H, Met.*ALU* M, *LINE-1* 97-bp H, *LINE-1* 97-bp M, respectively, in their melting curves. This observation supported the high specificity of the selected primers and the lack of nonspecific amplification products in qPCR assays.

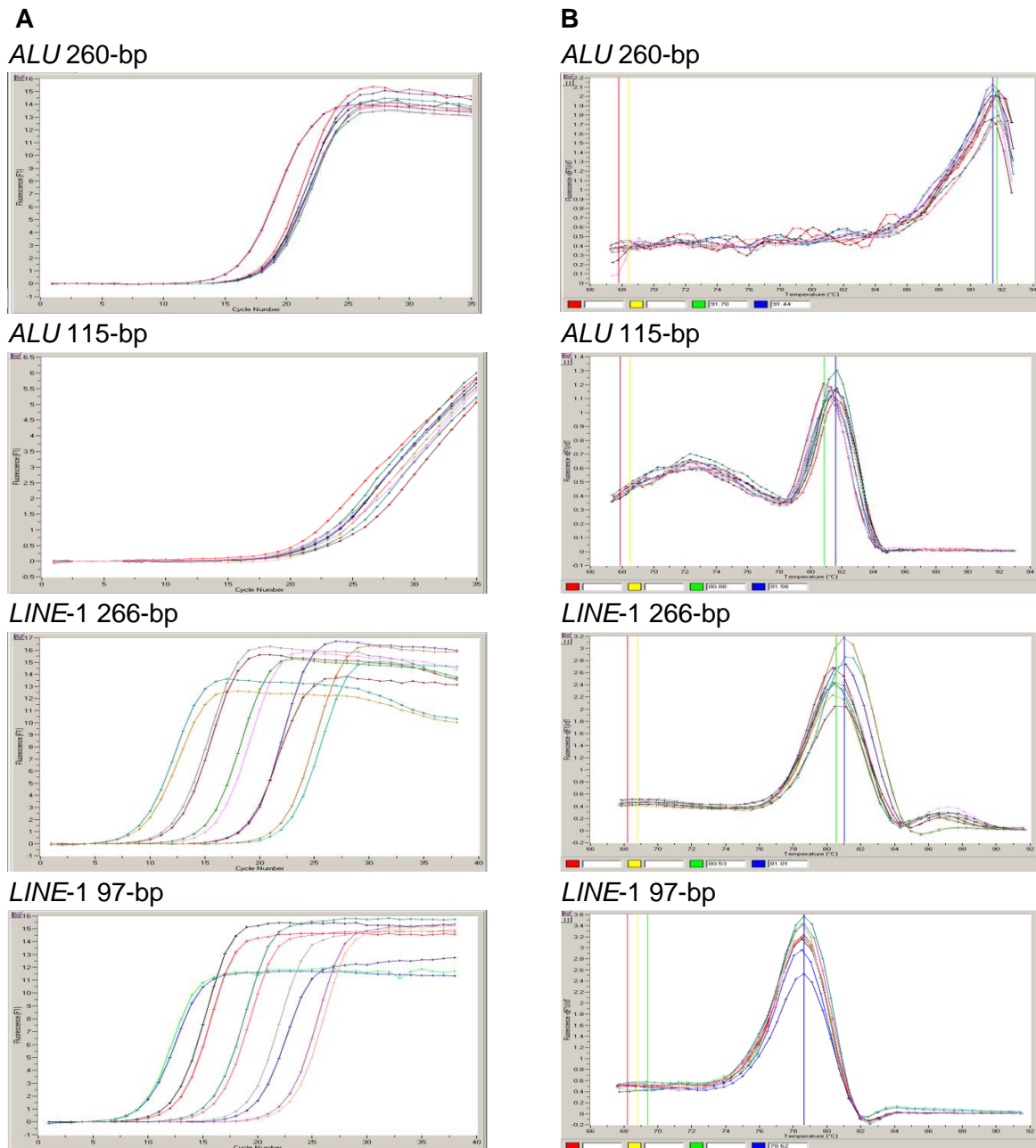


Figure 7. Establishing qPCR to measure cfDNA fragmentation

A) Amplification and B) Melting curves of *ALU* 115- and 260-, *LINE-1* 97- and 266-bp primer pairs with five different samples, each with double determination; The almost similar melting curves of the five separate determinations are shown.

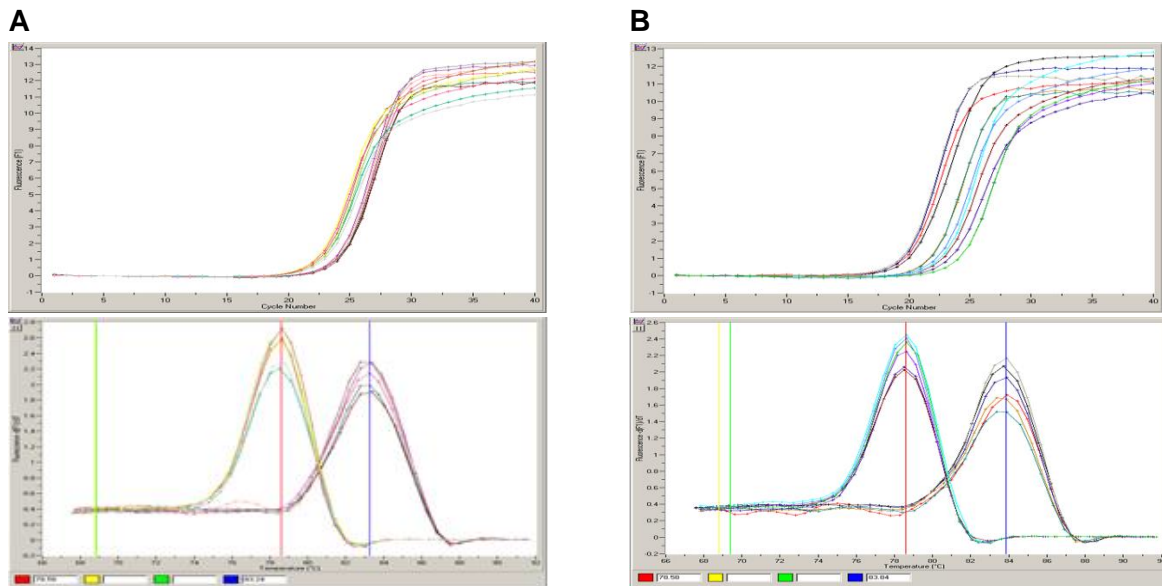


Figure 8. Establishing qPCR to measure cfDNA Hypomethylation

Representation of the PCR amplification and melting curves of A) Met.*ALU* and *LINE*-1 97-bp primers for HpaII and B) Met.*ALU* and *LINE*-1 97-bp primers for MspI for three different samples. All the qPCRs related to a sample (Met. *ALU* for HpaII and MspI and *LINE*-1 97 for HpaII and MspI) should be analyzed in the same plate. All quantitative PCRs performed in double; the almost similar melting curves of the three separate determinations are shown.

3.1.1 Efficiency and standard curves

The standard curves were applied to correct different primers' efficiencies. The standard curves were plotted by serial dilution of human genomic DNA to absolute quantification of each primer. The qPCR assay performance demonstrated a very high logarithmic of product amplification assessed. According to the Ct values, the sample concentration was concluded from the standard curves for each fragment.

An efficiency curve shows the dilution series's amplification log with a known concentration (Fig.9 and 10). The PCR primer efficiency was calculated as 2.04, 1.92, 1.98, and 2.02 for *ALU* 115-, *ALU* 260-, *LINE*-1 97- and *LINE*-1 266-bp, respectively. In the hypomethylation test, the qPCR efficiencies were 2.01, 1.89, 2.11, and 2.11 for Met. *ALU* H, Met.*ALU* M, *LINE*-1 97-bp H, *LINE*-1 97-bp M, respectively. In the hypomethylation test, the converted efficiency data were applied in a related equation described in section 2.7.5. Detailed data are shown in table 6.

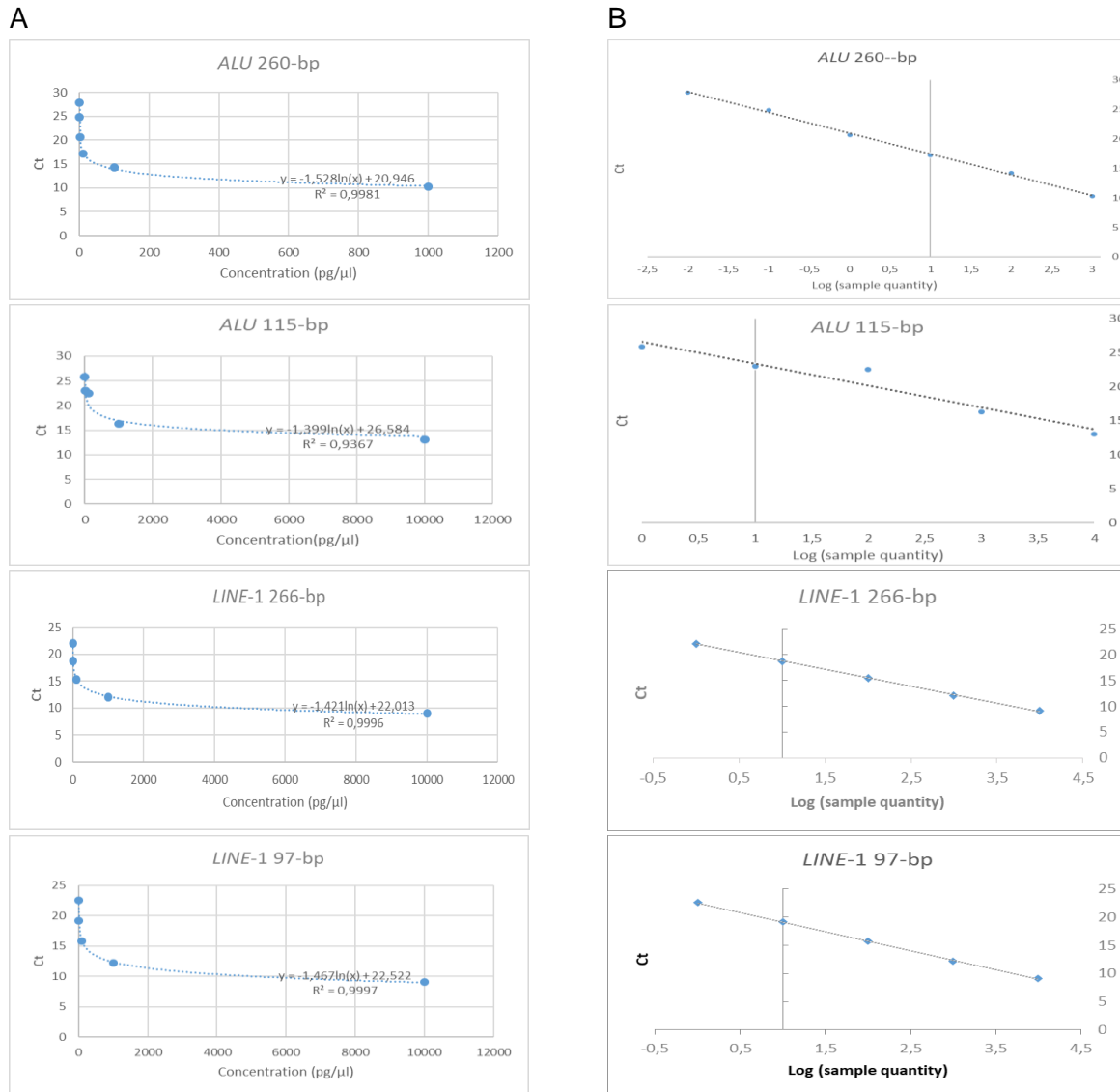


Figure 9. Standard and efficiency curves for ALU 115-bp, 260-bp, LINE-1 97-bp, and 266-bp primer pairs using a serial dilution of commercial human genomic DNA.

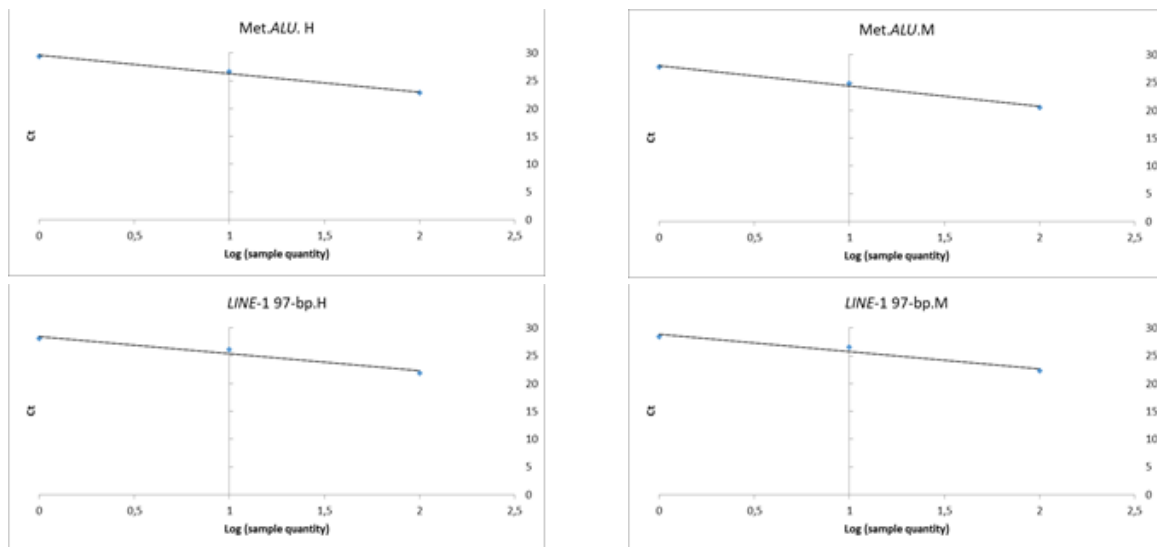


Figure 10. Efficiency curves of digested cfDNA for hypomethylation analysis
 Efficiency curves of Met.ALU H, Met.ALU M LINE-1 97-bp H and LINE-1 97-bp M primer using a serial dilution of *BON-1* genomic DNA. H for *HpaII* and M. for *MspI* digestion. Met. ALU M: qPCR using the cfDNA obtained in *MspI* digested cfDNA. Met. ALU H: qPCR using the cfDNA obtained in *HpaII* digested cfDNA.

Table 6. The detailed amplification efficiency for each primer

| Primer | R ² | Slop | Efficiency % | Converted efficiency (Efficiency /100)+ 1 |
|-----------------------------|----------------|-------|--------------|---|
| ALU 260-bp | 0.99 | -3.52 | 92.39 | 1.92 |
| ALU 115-bp | 0.94 | -3.22 | 104.37 | 2.04 |
| LINE-1 266-bp | 0.99 | -3.27 | 102.14 | 2.02 |
| LINE-1 97-bp | 0.99 | -3.38 | 97.70 | 1.98 |
| Hypomethylation test | | | | |
| Met.ALU H | 0.99 | -3.3 | 100.92 | 2.01 |
| Met.ALU M | 0.99 | -3.63 | 88.74 | 1.89 |
| LINE-1 97 H | 0.96 | -3.08 | 111.45 | 2.11 |
| LINE-1 97 M | 0.95 | -3.08 | 111.19 | 2.11 |

3.2 The study population characteristics

Sixty-two patients with confirmed NEN disease and 29 noncancerous volunteers with endocrine illness were enrolled. The clinicopathological data of controls and patients suffering from neuroendocrine cancer, including age, gender, degree of differentiation (grading), and tumor origin, are summarized in Table 7.

The mean age of controls was 52 years old, and the mean age was 52 years old, ranging from 24 to 77 years. Of 29 controls, 12 (~ 41 %) were male with a mean age of 51 years old, ranging from 25 to 77 years, and 17 (~59%) females with a mean age of 53 years old, ranging from 24 to 74 years. Of 62 NEN patients, 33 (~53%) were male with a mean age of 65 years, ranging from 33 to 87 years and 29 (~47%) females with a mean age of 63 years old, ranging from 33 to 81 years. The patients were divided into more specific subgroups: NET (n=55) and NEC (n=7). The mean age of the NEC and NET patients was 61 and 64 years old, respectively. NET patients were further separated as with mNET (n=47) and non-mNET (n=8). Most of the cases represent NETs with mNET, as can be seen in Table 5.

Concerning the appearance of the cancerous cells, the study patients' group was separated into four subgroups: Grade 1 (n=27), Grade 2 (n=21), Grade 3 (n=10), not identified (n=4). The majority was with G1 and G2 groups.

Clinical evaluation was undertaken for the determination of the tumor burden by the treating physician. The tumor burden of the patients was categorized between 0 and 3. The value zero means the patient has no known tumor in the body. Stage 3 means the patient has a very large amount of tumor tissue spread in various organs (such as e.g. lungs, liver, or bones). Regarding to tumor origin, the major tumor types included ileum NET (n=16, ~23%), small intestine NET (n=12, ~17%), pancreatic NET (n=12, ~17%), stomach NET and NEC (n=7, ~10%; n=5 and n=2, respectively), rectum NET (n=4, ~6%), lung NET and NEC (n= 3, ~4 % n=2 and n=1). There are some limitations for analysis between primary sites because of the small sample size of some subgroups.

Table 7. Clinicopathological features of the study groups

Detailed baseline clinicopathological features of the study groups including sex, age, differentiation grade (G1: Grade 1, G2: Grade 2, G3: Grade 3, NA: not identified), Tumor burden (N: no tumor, L: low, M: moderate, H: high) and location of the tumor.

| A | | | | | | | | | | | | |
|---------------------------|-------------|--------------|---------------|-------|----------------|----|----|----|---------------------|----|----|---|
| Characteristics | | | | | | | | | | | | |
| Groups / Subgroups | Nr.* | Age | Gender | | Grading | | | | Tumor burden | | | |
| | | Mean (Range) | Men | Woman | G1 | G2 | G3 | NA | N | L | M | H |
| Control | 29 | 52 (24-77) | 12 | 17 | - | - | - | - | 29 | - | - | - |
| All Patients | 62 | 64 (33-87) | 33 | 29 | 27 | 21 | 10 | 4 | 8 | 23 | 23 | 8 |
| NET | 55 | 64 (33-87) | 30 | 25 | 27 | 21 | 3 | 4 | | | | |
| mNET | 47 | 64 (33-87) | 25 | 22 | 21 | 19 | 3 | 4 | - | 22 | 20 | 5 |
| non-mNET | 8 | 65 (52-74) | 5 | 3 | 6 | 2 | - | - | 8 | - | - | - |
| NEC | 7 | 61 (41-82) | 3 | 4 | 0 | 0 | 7 | - | - | 1 | 3 | 3 |

| Primary cancer (Tumor origin) | Nr.* | Age Mean (Range) | Gender | | Grading | | | | Tumor burden | | | |
|----------------------------------|------|------------------------|--------|-------|---------|----|----|----|--------------|---|---|---|
| | | | Men | Woman | G1 | G2 | G3 | NA | N | L | M | H |
| Appendix | 1 | 33 | - | 1 | 1 | - | - | - | 1 | - | - | - |
| Cervix | 1 | 41 | - | 1 | - | - | 1 | - | - | 1 | - | - |
| Gallbladder | 1 | 61 | 1 | - | - | - | 1 | - | - | - | 1 | - |
| Ileum | 16 | 67 (52-81) | 9 | 7 | 13 | 2 | - | 1 | 5 | 4 | 6 | 1 |
| Neck | 1 | 57 | 0 | 1 | - | - | 1 | - | - | - | 1 | - |
| Lung | 3 | 72 (63-81) | 1 | 2 | 1 | 1 | 1 | - | - | 1 | 1 | 1 |
| Rectum | 4 | 64 (53-78) | 2 | 2 | - | 3 | 1 | - | - | 2 | 1 | 1 |
| Pancreas | 11 | 63 (39-87) | 5 | 6 | 2 | 6 | 1 | 2 | - | 6 | 5 | 1 |
| Pharynx | 1 | 33 | 1 | - | - | 1 | - | - | - | 1 | - | - |
| Stomach | 7 | 67 (58-82) | 4 | 3 | 2 | 3 | 2 | - | 2 | 2 | - | 3 |
| Small intestine | 12 | 66 (49-81) | 9 | 3 | 8 | 4 | - | - | 1 | 5 | 6 | - |
| Thymus | 1 | 49 | 0 | 1 | - | 1 | - | - | - | - | 1 | - |
| Unknown | 2 | 70 (63,77) | 1 | 1 | - | - | 2 | - | - | - | 1 | 1 |

*Nr. : number

3.3. Assessment of biomarkers

The biomarkers, namely cfDNA concentration, *ALU* 260-bp fragment level, *ALU* 115-bp fragment level, *LINE-1* 97-bp fragment level, *LINE-1* 266-bp fragment level, *ALU* DII, *LINE-1* DII, and hypomethylation percentage were measured and analyzed in the following study.

3.3.1 Plasma cfDNA quantification

The amount of cfDNA was determined in plasma samples from patients and healthy controls. Two commonly used kits for cfDNA isolation were tested to get the highest cfDNA population by using the same sample in this study. The spin column (QIAamp DNA Blood Mini kit) and the magnetic beads (QIAamp® MinElute® ccfDNA Midi kit) were two affinity-based methods. The spin-column method changed the parameters like the plasma and protease amount, degree and time of incubation in thermomixer, elution volume (AE buffer), and elution time. It was observed that the QIAamp® MinElute® ccfDNA Midi Kit extraction method recovered more cfDNA yield than the QIAamp DNA Blood Mini Kit method (data are not shown).

The cfDNA isolation was continued by QIAamp® MinElute® cfDNA Midi Kit. In each case, cfDNA was extracted from 4 mL of plasma. The range of cfDNA level of patients was between 0.11 and 58.20 ng/ μ L with a median of 0.92 (IQR 0.72) and 0.21 to 1.59 ng/ μ L with

a median of 0.67 (IQR 0.49) ng/ μ L for the control group (Fig. 11 A). 27 of 62 patients had cfDNA concentrations of ≥ 1 ng / μ L (~ 44%), while only 8 of 29 controls had cfDNA concentrations of ≥ 1 ng / μ L (28%).

A further division of the patient group into patients with the metastatic and non-metastatic NET disease and histologically confirmed NEC enables a more detailed examination of the biomarkers depending on the clinical picture.

The plasma cfDNA level presented the highest concentration in the mNET patient subgroup with a median of 1.04 (IQR 0.77) ng / μ L, followed by NEC patients with 0.91 (IQR 12.7) ng / μ L. The lowest concentration was found in the healthy controls with a median of 0.67 (IQR 0.49) ng / μ L. Shapiro-Wilk analysis confirmed significant deviations from a normal distribution in all subgroups. Therefore, the quantitative results were further compared using Kruskal-Wallis non-parametric ANOVA and revealed a substantial difference in the group ($X^2= 9.084$; $p=0.028$). A further pairwise comparison by Dwass-Steel-Critchlow-Flinger revealed a significant difference between the control and mNET groups ($p=0.037$) (Fig. 11 B).

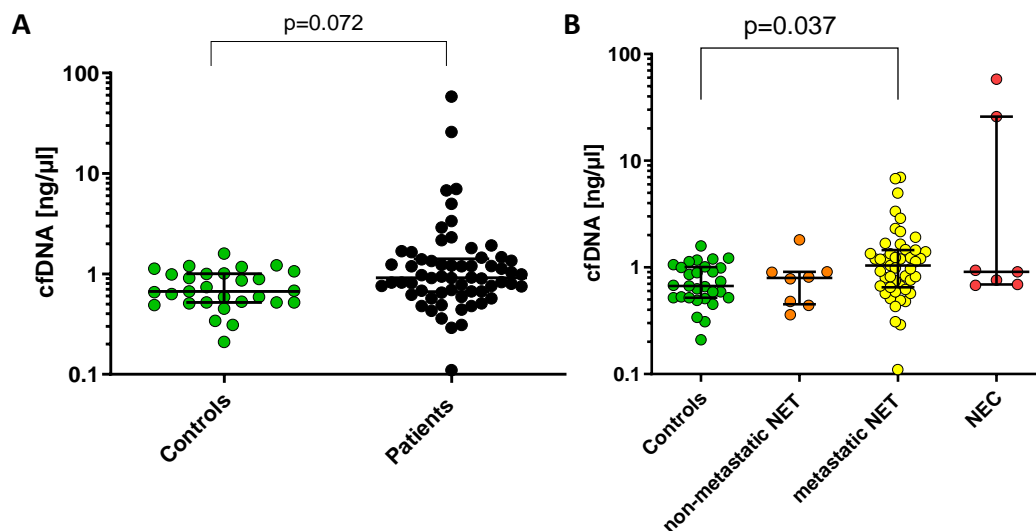


Figure 11. Distribution of plasma cfDNA level in the study groups

Plasma cfDNA levels in (A) NEN patients and the controls and (B) the patients' subgroups and the controls were measured by a fluorometric assay. Welch's t-test (A) and Kruskal-Wallis (B) analysis were performed to test the differences in plasma cfDNA levels between the study groups. Dwass-Steel-Critchlow-Flinger was applied as a post hoc test; P values ≤ 0.05 were considered significant.

The selectivity of the cfDNA level was calculated using the ROC curve.

The sensitivity of cfDNA in the patient group and mNET plus NECs subgroups were determined at several specificity levels. The corresponding sensitivities and actual cut-off points producing Fig. 12 are given in Table 8. The healthy donors and cancer patients could be differentiated with 69.4% sensitivity and 55.2% specificity based on the cfDNA concentration. A cfDNA cutoff of 0.715 ng/ μ L, with an AUC of 0.662 (95% confidence interval (CI), 0.549 to 0.775), ($P=0.013$) was established to identify NEN patients. The diagnostic power of cfDNA concentration did not change markedly when the patients were divided into the subgroups of mNET+ NEC patients (AUC= 0.689 (95% CI, 0.575 to 0.802; $P=0.004$).

Analysis of cfDNA in plasma of mNET+ NEC patients vs controls showed a 44.4 % sensitivity and 89.7 % specificity using the cut-off value of 1.18 ng/μl (Fig. 12). The subgroups of none-mNET (n=8) and NEC (n=7) were not selected for ROC Curve analysis due to the small number of cases.

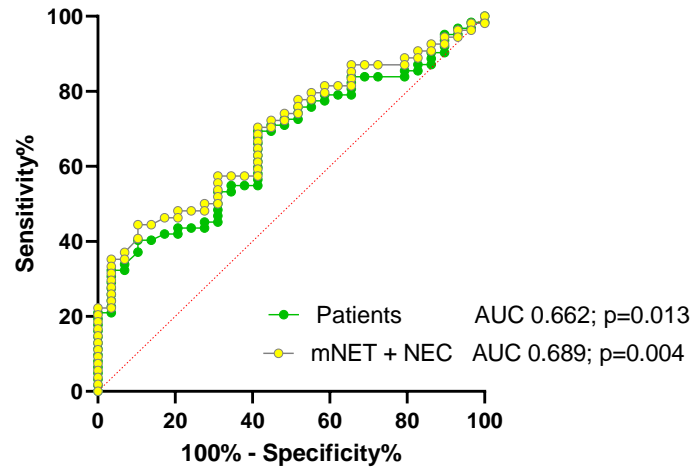


Figure 12: cfDNA level receiver operating characteristic (ROC) plots ROC from the comparison of controls vs. patients and controls vs. mNET+ NEC subgroups.

Table 8. cfDNA sensitivity and the corresponding cut-off level

From the comparison controls vs. patients and controls vs. mNET+ NEC patient’s subgroup at specificity levels between 60-95%.

| | | SPECIFICITY [%] | | | | | |
|-----------------|-----------------|-----------------|------|------|------|------|-------|
| | | 95 % | 90 % | 85 % | 80 % | 70 % | 60 % |
| SENSITIVITY [%] | Patients | 32.3 | 37 | 40.5 | 42 | 45 | 55 |
| | Cut-off [ng/μl] | 1.22 | 1.2 | 1.13 | 1.05 | 0.98 | 0.86 |
| | mNET+NEC | 35.19 | 40.4 | 44 | 46.3 | 50 | 57.41 |
| | Cut-off [ng/μl] | 1.21 | 1.19 | 1.13 | 1.06 | 0.99 | 0.85 |

3.3.1.1 Correlation of cfDNA plasma concentration with clinical characteristics

Nonparametric comparison of plasma cfDNA level with tumor grade, tumor burden, and localization tumor was evaluated by the Kruskal-Wallis test. The Spearman correlation test calculated the correlation to age, tumor burden, and CgA. Welch’s t-Test assessed the relationship to gender. A P value ≤ of 0.05 was considered statistically significant. In the patients, various clinical factors effects on biomarkers were analyzed in all plasma samples irrespective of whether they belonged to which subgroups of patients. The impact of tumor burden on cfDNA concentration was analyzed in all plasma samples regardless of whether they belonged to which group.

Correlation between cfDNA concentration and age or gender

A correlation study was carried out to rule out any influence of the cfDNA on the age of the tested people. The plasma cfDNA concentration appears to increase with age. The plasma

cfDNA concentration seems to increase with age. A significant correlation between age and cfDNA plasma concentration could be demonstrated in patients and control with $p = 0.006$. A reflection of the individual groups: control or patients showed no dependence of age on plasma cfDNA concentration (Fig.13).

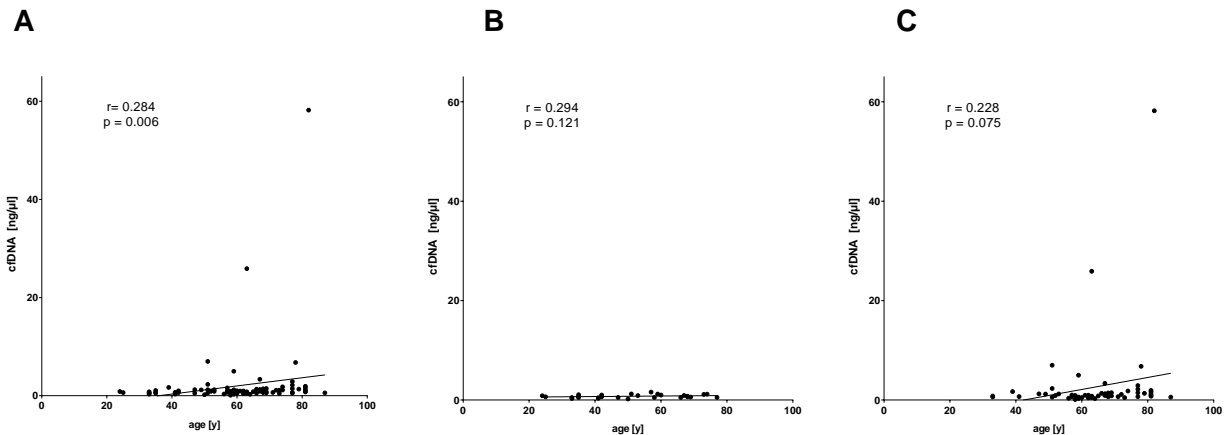


Figure 13. Plasma cfDNA correlation to age

The cfDNA level was measured by a fluorometric assay. Spearman correlation test was used to assess any differences between the age and plasma cfDNA level in A) total subjects, B) controls, and C) patients.

Differences between plasma cfDNA concentration and gender were assessed. For men, the median for the measured plasma cfDNA concentration was 0.778 (IQR 0.667), and for women, it was 0.904 (IQR 0.500). When using Welch’s t-test, men and women show no significant difference in the cfDNA concentration.

Correlation between cfDNA concentration and tumor grade

For the patients with a G1-graded tumor, cfDNA amounts between 0.29-4.98 ng/μL were measured. For the patients with a G2-confirmed tumor, 0.12-6.99 ng/μL and 0.68-58.2 ng/μL for the G3-graded tumor patients were found. Kruskal-Wallis test was used to evaluate the differences in cfDNA values between the samples from control, G1, G2, and G3 tumors and was found significant ($X^2=9.98$; $p=0.019$). With a post hoc test, Dwass-Steel-Critchlow-Flinger, the lowest p-value of 0.024 was measured between the control and G3-graded tumor groups (Fig.14).

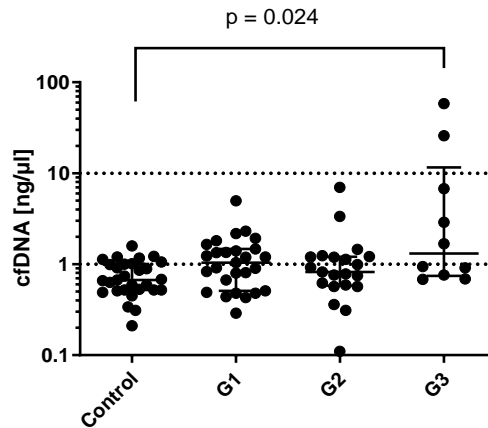


Figure 14. cfDNA Plasma concentration grouped by tumor grades

The cfDNA level was determined in the patient's plasma by a fluorometric assay. The data are divided into different groups depending on the tumor grade (controls, G1 (grade 1), G2 (grade 2), and G3 (grade 3) tumor grade). Kruskal-Wallis analysis was performed to test differences in plasma cfDNA levels between the groups. Dwass-Steel-Critchlow-Flinger was applied as a post hoc test; P values ≤ 0.05 were considered significant.

In the current ROC curve analysis, the plasma cfDNA concentration was able to distinguish between the patients with G1 (n= 27) and G2 (n=21) tumor grade from the controls with an estimated AUC of 0.66 (95% CI, 0.514 to 0.813; P=0.036) and 0.61 (95% CI, 0.451 to 0.777; P=0.172), respectively (Fig. 15). The patients with a G3 tumor grade (n=10) had a significant AUC of 0.803 (95% CI, 0.651 to 0.956; p= 0.005). cfDNA concentration had a sensitivity of 50% and a specificity of 100% at 1.64 ng/μl cutoff for the detection of patients with a G3 tumor grade. The cut-off levels at different specificity levels are given in Table 9.

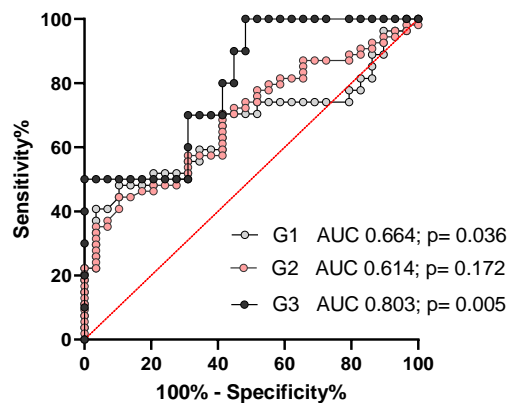


Figure 15. cfDNA level receiver operating characteristic (ROC) plots for tumor grades

ROC analysis of plasma cfDNA level for distinguishing the controls from the patients with tumor grade G1 (grey), G2 (pink), and G3 (black), along with the area under the curve (AUC).

Results

Table 9. The sensitivity and corresponding cut-off levels of cfDNA level for tumor grades
From the comparison controls vs. patients with a G1-tumor or a G2- tumor at specificity levels between 60-95%.

| | | SPECIFICITY [%] | | | | | |
|-----------------|-----------------|-----------------|-------|-------|-------|-------|-------|
| | | 95 % | 90 % | 85 % | 80 % | 70 % | 60 % |
| SENSITIVITY [%] | G1 | 40.74 | 43 | 48.15 | 48.15 | 51.85 | 59.26 |
| | Cut-off [ng/μl] | 1.25 | 1.2 | 1.10 | 1.05 | 0.97 | 0.86 |
| | G2 | 19.05 | 25.50 | 35.11 | 38.10 | 42.86 | 47.62 |
| | Cut-off [ng/μl] | 1.22 | 1.2 | 1.10 | 1.06 | 0.98 | 0.85 |
| | G3 | 50 | 50 | 50 | 50 | 50 | 70 |
| | Cut-off [ng/μl] | 1.28 | 1.19 | 1.11 | 1.07 | 0.98 | 0.85 |

Correlation between cfDNA concentration and tumor burden

cfDNA level was significantly correlated to tumor burden ($r = 0.412$; $p < 0.0001$). For the samples with no tumor, the cfDNA amount of 0.71(IQR 0.45) ng/μL was measured. cfDNA levels were 0.82(IQR 0.58) ng/μL and 1.19(IQR 0.68) ng/μL for the patients with low tumor load, i.e. 1, and moderate tumor load, i.e. 2, respectively. The patients with large tumor load, i.e. 3, showed the highest cfDNA level of 3.12(IQR 10.1)ng/μL. Kruskal-Wallis test calculated significant differences in cfDNA values between the samples from different classes of tumor burdens ($X^2= 17.36$; $p < 0.001$). With a post hoc test, Dwass-Steel-Critchlow-Flinger, the p-values of 0.007 and 0.016 were measured between samples with no tumor and moderate or large tumor burden groups, respectively. A p-value of 0.062 was obtained between patients with low and high tumor load (Fig.16).

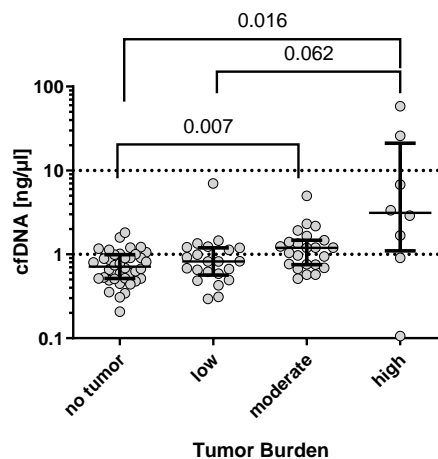


Figure 16. cfDNA Plasma concentration grouped by tumor burden

The cfDNA level was determined in the patient's plasma by a fluorometric assay. The data are divided into different groups depending on the tumor burden (no tumor, low, moderate, or high tumor burden). Kruskal-Wallis analysis was performed to test differences in plasma cfDNA levels between the groups. Dwass-Steel-Critchlow-Flinger was applied as a post hoc test; P values ≤ 0.05 were considered significant.

In the current ROC curve analysis, the plasma cfDNA concentration was able to distinguish between the patients with a different load of the tumor from the group with no tumor in the body with an estimated AUC of 0.69 (95% CI, 0.579 to 0.794; $P=0.003$). An AUC of 0.77 distinguished the patients with moderate and high tumor burden (95% CI, 0.657 to

0.885; $p= 0001$). The patients with a massive tumor load had a good AUC of 0.84 (95% CI, 0.601 to 1.00; $p= 003$) Using the cut-off value of 1.64, cfDNA level could distinguish high tumor load patients with 75% sensitivity and 97.4% specificity (Fig. 17).

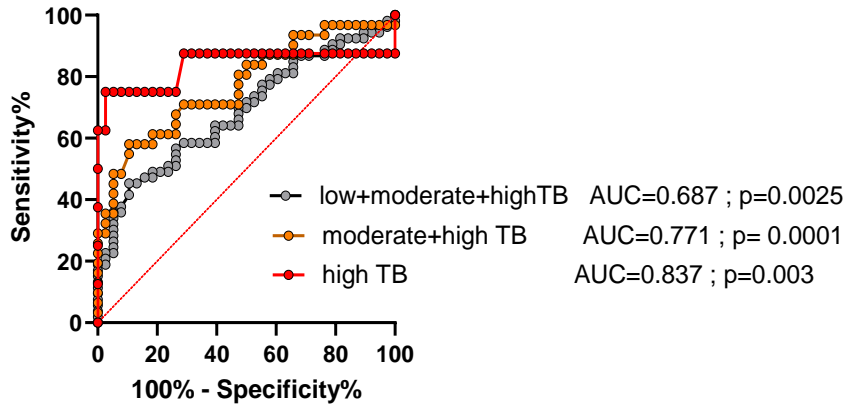


Figure 17. cfDNA level receiver operating characteristic (ROC) plots for tumor burdens
ROC analysis of plasma cfDNA level for distinguishing the group with no tumor from the patients with low, moderate, and high tumor burden (TB). Tumor burdens of low plus moderate and high (grey), moderate plus high (orange), and high (red), along with the area under the curve (AUC).

Correlation between cfDNA concentration and tumor origin

Regarding the origin of the tumor, the highest cfDNA level could be measured in the patients with a primary tumor in the small intestine, with 1.43 ng/μl (IQR 1.2). Subsequently, the patients with a primary tumor in rectum 1.21 (IQR 4.65) ng/μL and lung (1.20 (IQR 24.77) ng/μL showed higher cfDNA levels compared to other patient subgroups. The cfDNA level was 0.91 (IQR 2.92), 0.82 (IQR 0.69), 0.71(IQR 0.36) ng/μL in the patients with stomach, ileum, and pancreas tumor origin, respectively (Fig.18). A Kruskal-Wallis test compared the differences among tumor origin subgroups; a significant difference could be calculated among the groups ($X^2=12.84$; $p= 0.025$). A pairwise comparison as a post hoc test revealed significant differences between the patients with lung and ileum tumor origin ($p=0.025$).

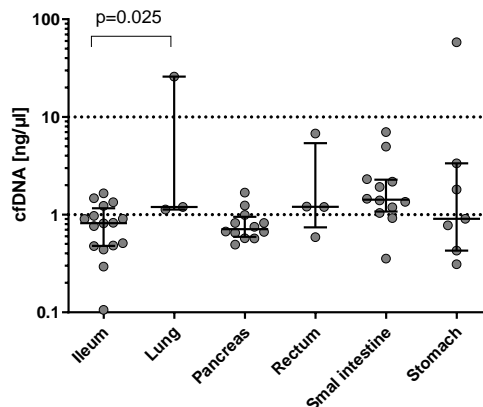


Figure 18. cfDNA plasma concentration grouped by tumor origin
The cfDNA level was determined in the patient's plasma by a fluorometric assay. The data are divided into different groups depending on the tumor origin.

Correlation between cfDNA concentration and serum-CgA level

The relationship between the increase in CgA and the cfDNA level was analyzed in the different patient groups. CgA value was not available for four patients: four NETs (three mNETs, one non-mNET). CgA level was only determined in the patients with malignant disease. The CgA value for the subgroup with mNET was 105.5 (IQR 191) ng/ml, for non-mNETs 58 (IQR 366) ng/ml, and NEC patients 125 (IQR 7861) ng/ml (Fig. 19A). No significant differences were found using the Kruskal-Wallis test. In some patients, high levels of cfDNA were found along with high levels of CgA. A substantial correlation between CgA and plasma cfDNA level could be calculated by the Spearman correlation test ($p=0.031$) with a weak positive correlation coefficient of 0.29 (Fig. 19B).

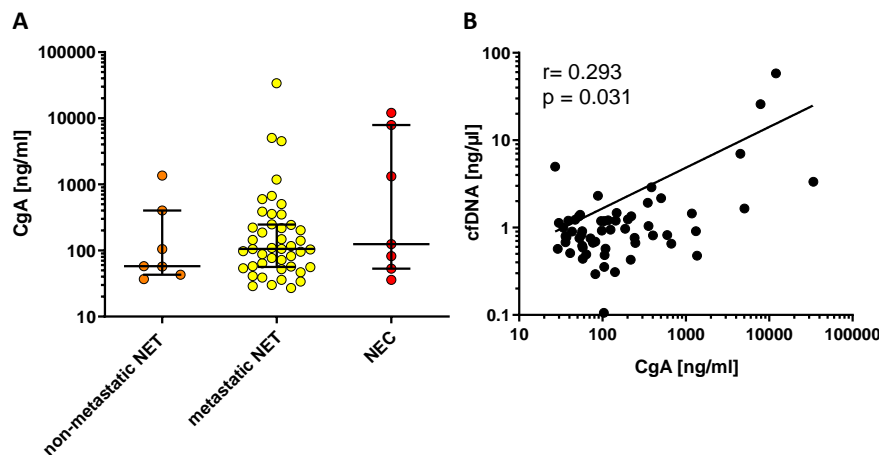


Figure 19. Correlation of CgA hormonal status vs. cfDNA level in the patient group

A: CgA level in patients' subgroups

B: Correlation of CgA and plasma cfDNA plasma in the patients. Spearman correlation revealed a weak correlation. P values ≤ 0.05 were considered significant.

3.3.2 Evaluation of cfDNA fragment size distribution

The isolated cfDNA samples were used to determine the different fragment sizes by amplifying 97-bp and 266-bp within *LINE-1*, and 115-bp and 260-bp within *ALU* target sequences, respectively.

3.3.2.1 Analysis of *ALU* fragmentation level

ALU fragmentation level of cfDNA was determined by PCR analysis.

We distinguished between two different fragmentation sizes, a short fragment of 115-bp and a longer cfDNA fragment of 260-bp length. The total amount of short fragments will always be higher than the longer fragments because *ALU* 115-bp fragments represent short and long cfDNA fragmentations.

As shown in Fig. 20A, the median of *ALU* 115-bp fragment level was similar in the patients of 29 (IQR 29.4) pg/ μ L and the controls with 29.0 (IQR 39.7) pg/ μ L. Welch's t-test showed no significant difference ($p=0.329$).

Regarding the patients' subgroups, *ALU* 115-bp fragment level in non-metastatic NETs (33.2(IQR 26.4) pg/ μ L) was higher than the controls (29 (IQR 39.7) pg/ μ L). The NEC patients revealed the highest *ALU*115 bp-fragment concentration with a median of 38.1 (IQR 25.7) pg/ μ l. The metastatic NET patients showed the lowest levels of *ALU* 115-bp fragments of 24.4 (IQR 29.6) pg/ μ L (Fig. 20B). Plasma levels of *ALU* 115-bp fragment did not discriminate significantly between the single groups ($P>0.05$). Kruskal-Wallis test was used to evaluate the differences in *ALU* 115-bp fragment values between samples from the control group and patients' subgroups; no significant differences could be measured ($p= 0.730$).

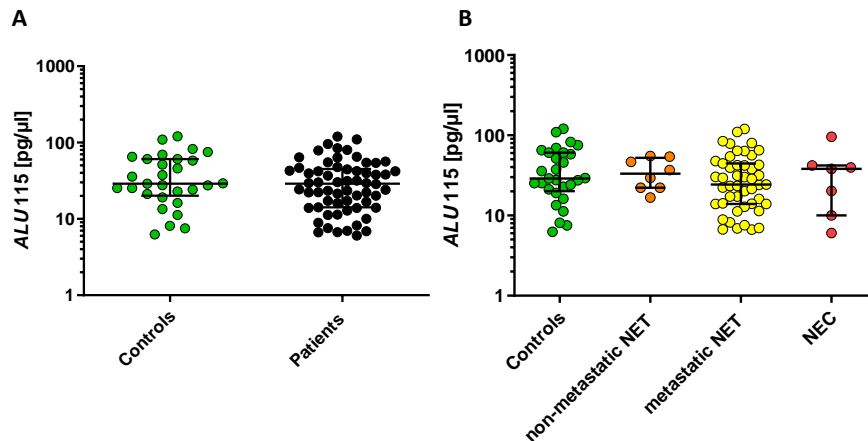


Figure 20. Distribution of *ALU* 115-bp fragment level in the study groups

ALU 115-bp fragment level in (A) NEN patients and controls and (B) patients' subgroups and controls were measured by qPCR. Welch's t-test (A) and Kruskal-Wallis (B) analysis were performed to test differences between the study groups.

The *ALU* 260- bp fragments represent the long cfDNA fragments. Measured values are illustrated in Fig. 21. The control group showed a slightly higher *ALU* 260 bp-fragment level compared to the patients (5.52 (IQR 3.02) pg/ μ L vs. 5.03 (IQR 3.37) pg/ μ L) (Fig.21A). No significant differences in *ALU* 260-bp fragment level between the samples from the control and patients were calculated by Welch's t-test ($p=0.056$).

By dividing the patients' group into subgroups, the mNET and NEC patients revealed the lowest *ALU* 260-bp fragments of 4.75 (IQR 3.6) and 5.06 (IQR 2.80) pg/ μ l, respectively. The patients with a non-mNET showed the highest amount of *ALU* 260-bp fragment with a median of 6.35 (IQR 1.99) pg/ μ l (Fig.21B). Results were further compared using the Kruskal-Wallis non-parametric ANOVA test and revealed no significant difference among patients' subgroups ($X^2=4.23$; $p=0.238$).

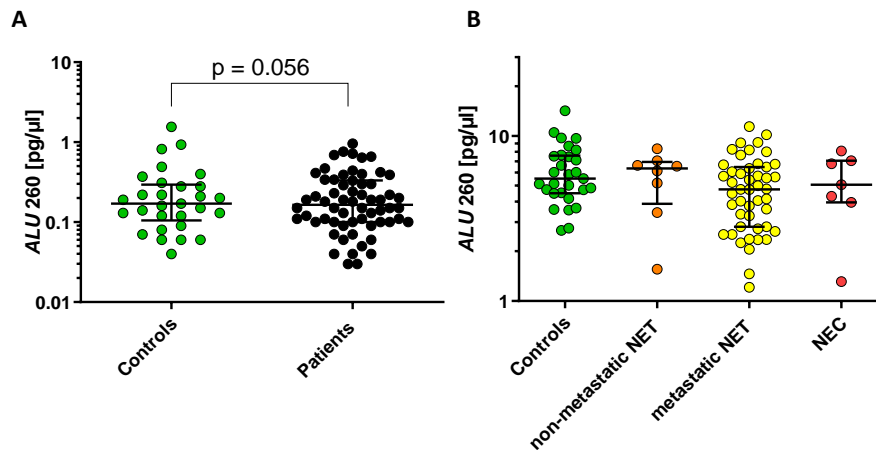


Figure 21. Distribution of *ALU* 260-bp fragment level in the study groups
ALU 260-bp fragment level in (A) NEN patients and controls and (B) patients' subgroups and controls were measured by qPCR. Welch's t-test (A) and Kruskal-Wallis (B) analysis were performed to test differences between study groups. P values ≤ 0.05 were considered significant.

The ROC curve was analyzed to test if the differences in *ALU* fragmentation level could discriminate the controls from the patients. The sensitivity of cfDNA in the patients and metastatic NET+NEC subgroups was determined at several specificity levels. The corresponding sensitivities and actual cut-off points producing Fig. 22 are given in Tables 10 and 11.

Comparison of *ALU* 115-bp fragment level between the controls and patients revealed an area under the curve of AUC = 0.56 (95% confidence interval (CI), 0.432 to 0.689; $p=0.360$) When using the subgroups of mNET +NEC, the differences could be increased slightly (AUC = 0.57, 95% confidence interval (CI), 0.437 to 0.697; $p=0.314$) (Fig 22A).

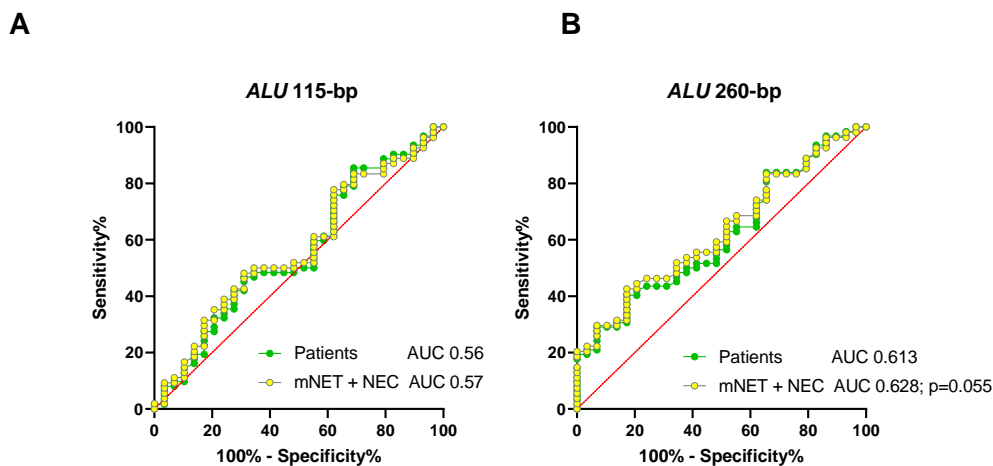


Figure 22. *ALU* fragmentation receiver operating characteristic (ROC) plots
 ROC curves from the comparison of controls vs. patients and controls vs. metastatic NET+NEC subgroups; A) *ALU* 115-bp fragment and B) *ALU* 260-bp fragment level.

The controls and cancer patients could be differentiated by *ALU* 260-bp with an AUC of 0.61 based on *ALU* 260-bp fragment level (95% confidence interval (CI), 0.494 to 0.733, $P=0.083$). The diagnostic power of *ALU* 260-bp fragment concentration could slightly be

increased when the patients have included only the subgroups of mNET+ NEC patients with a significant AUC of 0.63 (95% confidence interval (CI), 0.507 to 0.750; p=0.055) (Fig.22B).

Table 10. *ALU* 115-bp fragment concentration sensitivity and the corresponding cut-off level From the comparison control vs. patients and control vs. metastatic NET+ NEC patients' subgroups at specificity levels between 60-95%.

| | | SPECIFICITY [%] | | | | | |
|-----------------|------------------------|-----------------|-------|-------|-------|-------|-------|
| | | 95 % | 90 % | 85 % | 80 % | 70 % | 60 % |
| SENSITIVITY [%] | Patients | 8.07 | 9.68 | 19.35 | 27.42 | 41.94 | 48.39 |
| | Cut-off [pg/ μ l] | 7.35 | 8.13 | 13.30 | 16.35 | 22.80 | 25.60 |
| | Metastatic NETs + NECs | 9.26 | 11.11 | 22.22 | 31.48 | 42.59 | 50 |
| | Cut-off [pg/ μ l] | 7.37 | 7.98 | 13.40 | 16.22 | 22.95 | 25.89 |

Table 11. *ALU* 260-bp fragment concentration sensitivity and the corresponding cut-off level From the comparison control vs. patients and control vs. metastatic NET +NEC patients' subgroups at specificity levels between 60-95%.

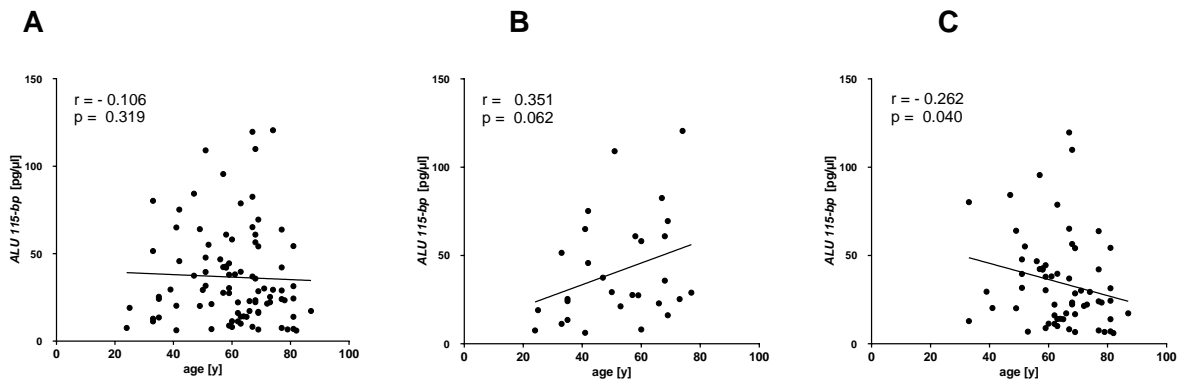
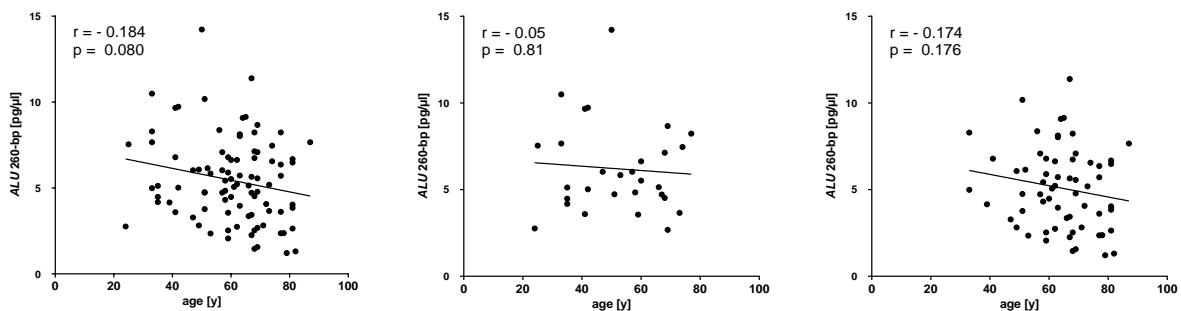
| | | SPECIFICITY [%] | | | | | |
|-----------------|-----------------------|-----------------|-------|-------|-------|-------|-------|
| | | 95 % | 90 % | 85 % | 80 % | 70 % | 60 % |
| SENSITIVITY [%] | Patients | 20.97 | 29.03 | 30.65 | 40.32 | 43.55 | 50 |
| | Cut-off [pg/ μ l] | 2.77 | 3.53 | 3.69 | 4.2 | 4.69 | 5.02 |
| | metastatic NETs +NECs | 22.22 | 29.63 | 31.48 | 42.59 | 46.30 | 53.70 |
| | Cut-off [pg/ μ l] | 2.76 | 3.50 | 3.75 | 4.19 | 4.7 | 5.01 |

3.3.2.1.1 Correlation of *ALU* fragmentation level with clinical characteristics

Nonparametric comparison of short and long *ALU* fragmentation levels with tumor grade, tumor burden, and localization was evaluated by the Kruskal-Wallis test. The Spearman correlation test calculated correlation to tumor burden, age, and CgA. Welch´s t-Test assessed the relationship to gender. A P value \leq of 0.05 was considered statistically significant. In the patients, various clinical factors effects on biomarkers were analyzed in all plasma samples irrespective of whether they belonged to which subgroups of patients. The impact of tumor burden on *ALU* fragmentation was examined in all plasma samples regardless of whether they belonged to which group.

Correlation between *ALU* fragmentation and age or gender

The Spearman correlation test calculated correlation to age. A P value \leq of 0.05 was considered statistically significant. No significant correlation could be calculated for age and *ALU* fragmentation levels in the totality of the test subjects (patients and controls) and the controls. A significant correlation between age and *ALU*-115-bp fragment concentration could be demonstrated in the patient group (p = 0.04). The correlation of short and longer *ALU* fragments to age is shown in Fig.23.

1) *ALU* 115-bp fragment level2) *ALU* 260-bp fragment levelFigure 23. Correlation of age and *ALU* fragmentation level in cfDNA

ALU fragmentation levels were measured by qPCR. Spearman correlation test was used to assess any differences between the age and *ALU* fragmentation in A) total subjects, B) controls, and C) patients.

Differences between *ALU* 115-bp fragment level and gender were assessed. For men, the median was 30.3 (IQR 34) pg/μl, and for women, 25.3 (IQR 29.1) pg/μl. Welch's t-test confirmed no gender-specific differences for short *ALU* fragments ($p = 0.485$).

Differences between *ALU* 260-bp fragment level and gender were assessed. For men, the median was 5.52 (IQR 3.93) pg/μl, and for women, 5.07 (IQR 2.88) pg/μl. Using the Welch t-test, men and women show no significant difference in long *ALU* fragments' plasma concentration ($p = 0.825$).

Correlation between ALU fragmentation and tumor grade

Regarding tumor grading, a slightly elevated *ALU* 115-bp fragment level was determined in the G2 patients with 42.30 (IQR 30.1) pg/μl compared to the controls with 29 (IQR 39.7) pg/μl. A reduced *ALU* 115-bp fragment level of 22.2 (IQR 23.4) pg/μl was observed in the G1 patients, followed by the patients with a G3 tumor with 26.4 (IQR 26.7) pg/μl. Kruskal-Wallis test revealed no significant differences between the groups ($X^2 = 5.12$; $p = 0.164$) (Fig. 24A). A decrease of *ALU* 260-bp fragment level was observed in patients' subgroups concerning the tumor grade. The patients with G1 (5.19 (IQR 3.50) pg/μl), G2 (4.75 (IQR 2.62) pg/μl) and G3 (4.68 (IQR 2.51) pg/μl) tumor showed lower *ALU* 260-bp fragment level compared to the

control with 5.52 (IQR 3.02) pg/ μ L. Kruskal-Wallis test was used to evaluate the differences in *ALU* 260-bp fragment values between samples from the controls, G1, G2, and G3 tumors ($X^2= 3.53$; $p= 0.317$)(Fig.24B).

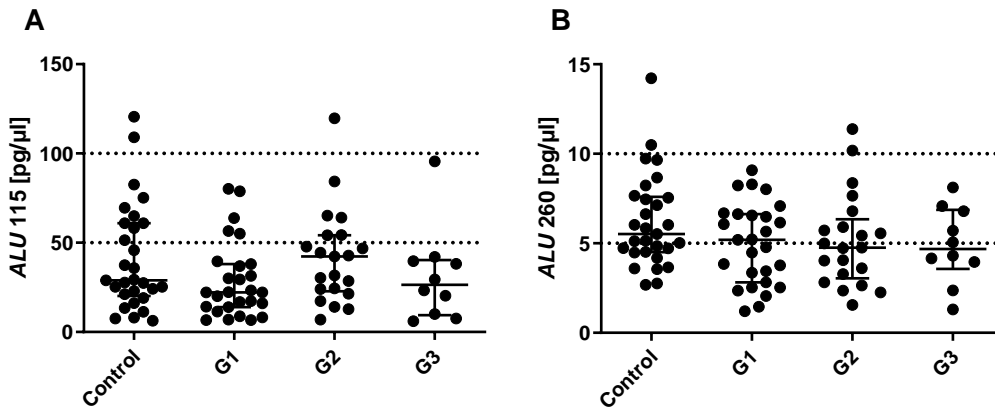


Figure 24. cfDNA *ALU* fragmentation level grouped by tumor grades

A) *ALU* 115-bp and B) *ALU* 260-bp fragment level was determined in the patients' plasma using qPCR. The data are divided into different groups depending on the tumor grade (controls, G1 (grade 1), G2 (grade 2), and G3 (grade 3) tumors).

Correlation between fragmentation and tumor burden

No correlation was found between *ALU* 115-bp fragments level and tumor burden by Spearman test ($r=-0.123$; $p=0.246$), but there was a negative correlation with *ALU* 260-bp fragments level ($r=-0.31$; $p=0.003$).

The groups with no tumor and moderate tumor load showed the highest concentration of *ALU* 115-bp fragments with 29.3 (IQR 35.2) pg/ μ and 30.1 (IQR 27.1) pg/ μ l, respectively. The level *ALU* 115-bp fragments were 26.4 (IQR 32.8) pg/ μ l in the patients with high tumor load. The patients with a low tumor load had the lowest concentration of *ALU*115-bp pieces with 22.8 (IQR 29.1) pg/ μ l (Fig. 25).

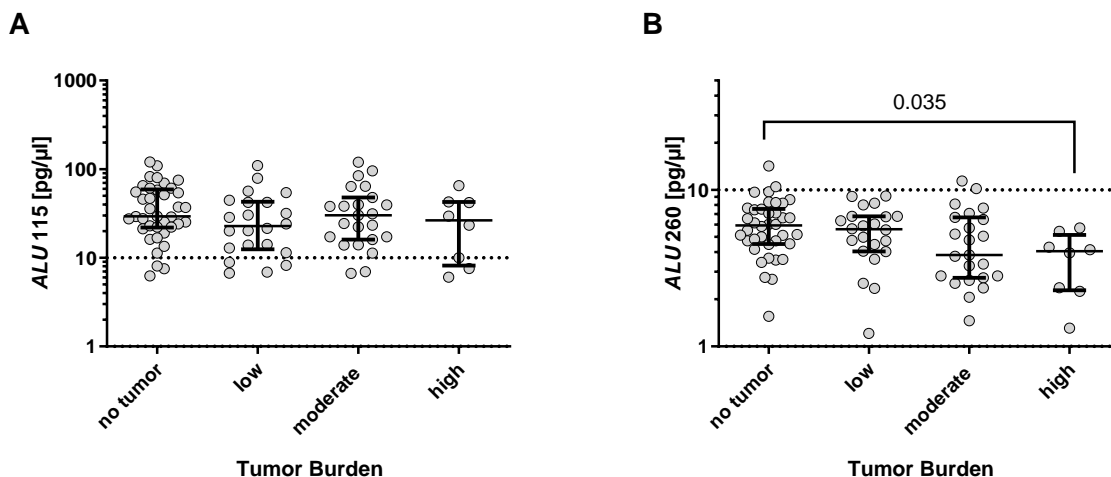


Figure 25. cfDNA *ALU* fragmentation level grouped by tumor burden

A) *ALU* 115-bp and B) *ALU* 260-bp fragment level was determined in the patients' plasma using qPCR. The data are divided into different groups depending on the tumor burden (no tumor, low, moderate, high). Kruskal-Wallis analysis was performed to test differences in plasma cfDNA levels between the groups. Dwass-Steel-Critchlow-Flinger was applied as a post hoc test; P values ≤ 0.05 were considered significant.

The highest concentration of *ALU* 260-bp fragments was obtained in the group with no tumor (5.94 (IQR 2.95)) pg/ μ l, where the lowest was in the patients with moderate tumor burden, with 3.84 (IQR 3.80) pg/ μ l. The concentration of *ALU* 260-bp fragments was higher in patients with low tumor load than high tumor burden (5.61 (IQR 2.61) vs. 4.05 (IQR 2.25) pg/ μ l.

Upon analysis of fragmentation, a significant difference was found for *ALU* 260-bp fragments between the groups by Kruskal-Wallis test ($X^2= 9.49$; $p= 0. 0.023$) but not for *ALU* 115-bp ($X^2= 2.89$; $p= 0. 0.409$). A significant difference was observed between no tumor samples and patients with high tumor load by Dwass-Steel-Critchlow-Flinger test as post hoc test ($p=0.035$) (Fig. 25).

By ROC curve analysis, the *ALU* 260-bp fragment concentration was able to distinguish between the patients with different tumor loads (low, moderate, and high) from the group with no tumor with an estimated AUC of 0.640 (95% CI, 0.526 to 0.753; $p=0.024$). An AUC of 0.70 distinguished the patients with moderate and high tumor burden (95% CI, 0.670 to 0.824; $p= 0.005$). The patients with a large tumor load had a high significant AUC of 0.81 (95% CI, 0.660 to 0.952; $p= 0.007$). The cutoff point of 5.78 pg/ μ l provided 100% sensitivity and 52.6% specificity in discriminating patients with high tumor load from individuals with no tumor (Fig. 26).

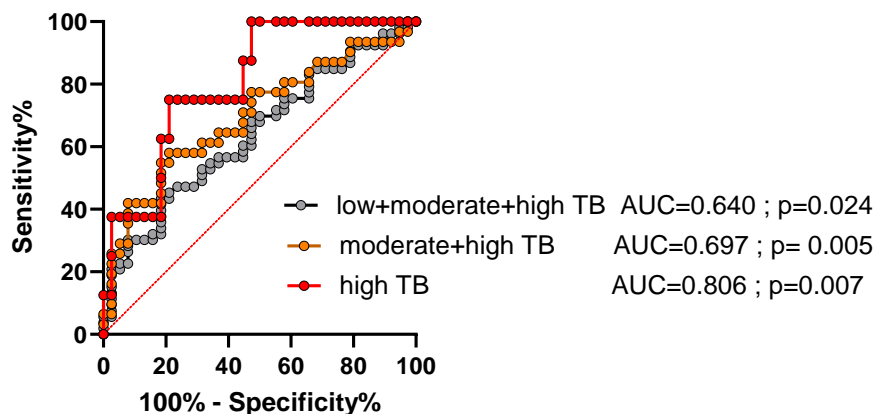


Figure 26. *ALU* 260-bp fragment level receiver operating characteristic (ROC) plots for tumor burdens. ROC analysis of *ALU* 260-bp fragment level for distinguishing the group with no tumor burden from the patients with low, moderate, and high tumor burden (TB). Tumor burdens of low plus moderate and high (grey), moderate plus high (orange), and high (red), along with the area under the curve (AUC).

Correlation between ALU fragmentation and tumor origin

The tumor origin groups with less than three members were not considered in the comparison. The highest *ALU* 115-bp fragment level was measured in the patients with a primary tumor in the rectum (33.92 (IQR 89.9) pg/ μ l), stomach (30.34 (IQR 45.26) pg/ μ l) and pancreas (29.80 (IQR 31.57) pg/ μ l) in compared to other patients' subgroups (Fig.27A). Kruskal-Wallis test was showed no correlation between *ALU* 115-bp fragment level and tumor origins ($X^2= 2.301$; $p= 0.806$).

The highest *ALU* 260-bp fragment level could be measured in patients with a primary tumor in the pancreas (5.64 (IQR 3.20) pg/μl), followed by the ileum (5.54 (IQR 3.20) pg/μl) and rectum 4.58 (IQR 7.88) pg/μl). The lowest *ALU* 260-bp fragment level was measured in the patients with stomach as tumor origin (2.53 (IQR 4.34) pg/μl (Fig.27B). The Kruskal Wallis test showed no significant differences ($X^2= 9.674$, $P= 0.085$) between the *ALU* 260-bp fragment concentration and the tumor origin.

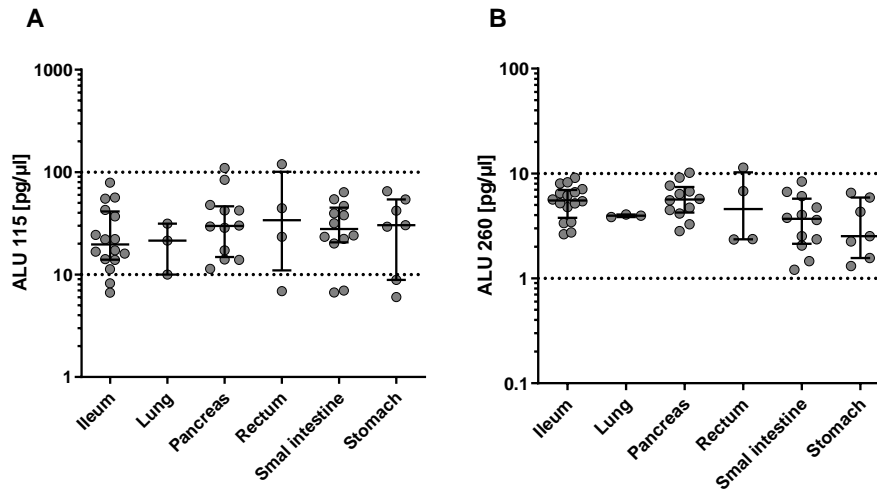


Figure 27. cfDNA *ALU* fragmentation level grouped by tumor origin
 A) *ALU* 115-bp and B) *ALU* 260-bp fragments levels were determined using quantitative PCR in the patients' plasma. The data are divided into different groups depending on the tumor origin.

Correlation between ALU fragment level and serum-CgA level

A correlation with the serum-CgA level of the patients revealed a negative relation with *ALU* fragmentation level in cfDNA (Fig.28). No significant correlation could be calculated by Spearman Correlation test for *ALU* 115-bp fragments ($p=0.126$), nor for *ALU* 260-bp ($p=0.092$) fragment concentration.

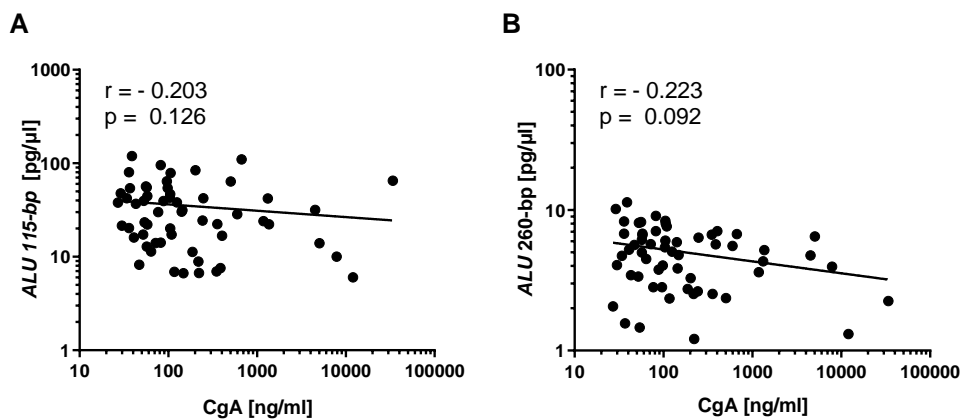


Figure 28. Correlation of CgA hormonal status and *ALU* fragmentation level in the patients
 Spearman correlation revealed a very weak, no significant correlation for A) *ALU* 115-bp and B) *ALU* 260-bp fragments levels.

3.3.2.2 Analysis of *LINE*-1 fragmentation level

LINE-1 fragmentation level of cfDNA was determined by qPCR analysis.

We distinguished between two different fragmentation sizes, a short cfDNA fragment of 97-bp and a longer fragment of 266-bp length. The total amount of short fragments will always be higher than long fragments because *LINE*-1 97-bp fragments represent short and long cfDNA fragmentations.

The amount of *LINE*-1 97-bp fragment in the controls could be measured with 16.1 (IQR 4.84) pg/ μ L. The NEN patients showed a slightly decreased *LINE*-1 97-bp fragment level of 16 (IQR 4.77) pg/ μ L. No significant differences in *LINE*-1 97-bp fragment level between the samples from control and patients were calculated by Welch's t-test ($p=0.317$) (Fig.29A).

Regarding the patients' subgroups, metastatic NET patients had a lower *LINE*-1 97-bp fragment level of 15.8 (IQR 5.11) pg/ μ L compared to the controls 16.1 (IQR 4.84). NEC patients showed a higher *LINE*-1 97-bp fragment level of 17.1 (IQR 3.47) pg μ L⁻¹ than the controls. Non-metastatic NETs showed the same *LINE*-1 97-bp fragment level concentration as the controls of 16.1 (IQR 3.7) pg/ μ L (Fig.29B). Kruskal-Wallis test was used to evaluate the differences in *LINE*-1 97-bp fragment values between samples from the control group and patients' subgroups. No significant differences could be calculated ($X^2= 0.969$; $p=0.809$).

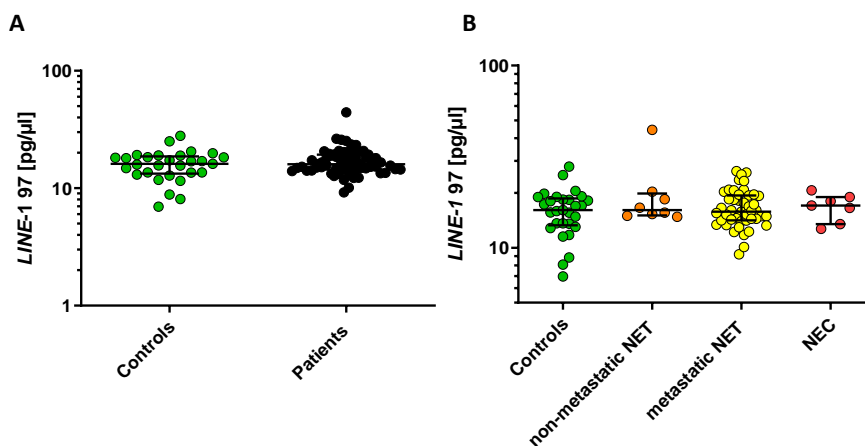


Figure 29. Distribution of *LINE*-1 97-bp fragment level in the study groups

LINE-1 97-bp fragment level in (A) NEN patients and controls and (B) patients' subgroups and controls were measured by qPCR. Welch's t-test (A) and Kruskal-Wallis (B) analysis were performed to test differences between the study groups.

The *LINE*-1 266-bp fragment level in the controls could be defined with 4.50(IQR 2.13) pg/ μ L. NEN patients showed a slightly reduced *LINE*-1 266-bp fragment of 4.10(IQR 2.12) pg/ μ L. No significant difference in *LINE*-1 266-bp fragment level between samples from the controls and patients was calculated by Welch's t-test ($p=0.144$) (Fig.30A).

Regarding patients' subgroups, the lowest concentration of *LINE*-1 266-bp fragment was observed in NECs with 3.82(IQR 1.48) pg/ μ L. A decrease of *LINE*-1 266-bp fragment level was identified in mNETs and NECs compared to the controls 4.09(IQR 2.20) and 3.82(IQR 1.48) pg/ μ L, respectively. Non-active NET demonstrated the highest *LINE*-1 266-bp fragment level of 5.22(IQR 1.01) pg/ μ L among the patients' subgroups as well as compared to the controls (Fig.30B).

Kruskal-Wallis test was used to evaluate the differences in *LINE-1* 266-bp fragment values between samples from the control group and patients' subgroups. No significant differences could be calculated ($X^2= 6.643$; $p=0.084$).

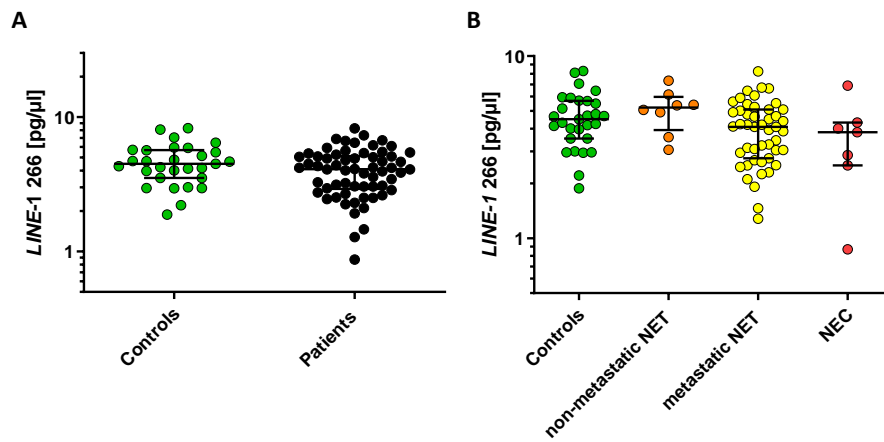


Figure 30. Distribution of *LINE-1* 266-bp fragment level in the study groups
LINE-1 266-bp fragment level in (A) NEN patients and controls and (B) patients' subgroups and controls were measured by qPCR. Welch's t-test (A) and Kruskal-Wallis (B) analysis were performed to test differences between the study groups.

The ROC curve analyzed the discriminatory power of the *LINE-1* fragmentation level. The corresponding sensitivities and actual cut-off points producing Fig. 31 are given in Tables 12 and 13. The controls and cancer patients could be differentiated by *LINE-1* 97-bp fragment levels with an AUC of 0.545 (95% confidence interval (CI), 0.413 to 0.676; $P=0.496$), and by *LINE-1* 266-bp fragment with an AUC of 0.589 (95% confidence interval (CI), 0.465 to 0.712; $p=0.174$) (Fig 31).

For *LINE-1* 97-bp fragment, the differentiation to the aggressive subgroups reduced the AUC to 0.532 (95% confidence interval (CI), 0.398 to 0.666; $P=0.733$). The diagnostic power of *LINE-1* fragmentation concentration could slightly be increased for *LINE-1*-266-bp fragment when the patients were included only to the subgroups of metastatic NETs and NECs to an AUC of 0.620 (95% confidence interval (CI), 0.495 to 0.744; $p=0.073$) (Fig 31).

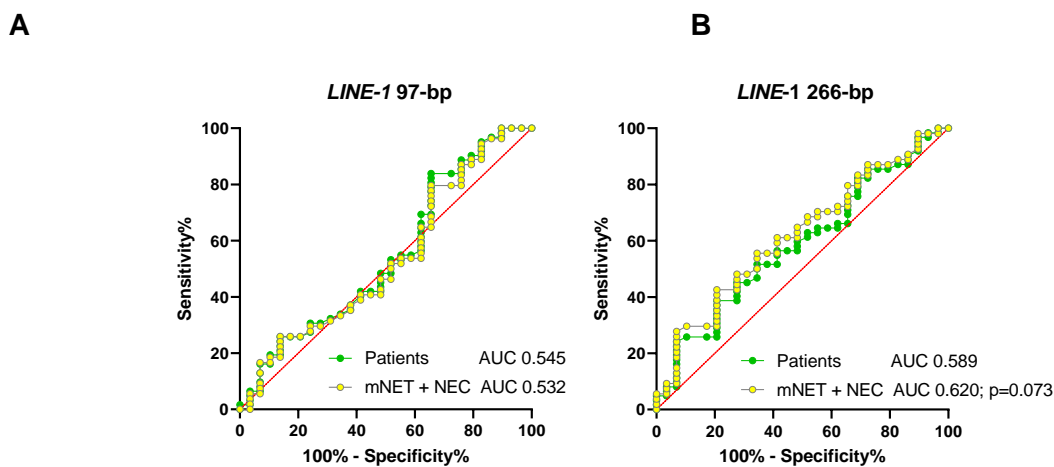


Figure 31. *LINE-1* fragmentation receiver operating characteristic (ROC) plots
 ROC curves from the comparison of controls vs. patients and controls vs. metastatic NET+NEC subgroups; A) *LINE-1* 97-bp fragment and B) *LINE-1* 266-bp fragment level.

Table 12. *LINE-1* 97-bp fragment concentration sensitivity and the corresponding cut-off level
From the comparison control vs. patients and control vs. metastatic NET+NEC patients' subgroups at specificity levels between 60-95%.

| | | SPECIFICITY [%] | | | | | |
|-----------------|--------------------------|-----------------|-------|-------|-------|-------|-------|
| | | 95 % | 90 % | 85 % | 80 % | 70 % | 60 % |
| SENSITIVITY [%] | Patients | 6.45 | 16.13 | 25.81 | 25.81 | 31.5 | 38.5 |
| | Cut-off [pg/ μ l] | 24.70 | 20.49 | 19.17 | 19.03 | 18.30 | 17.25 |
| | Metastatic NETs +NECs | 5.56 | 16.67 | 25.93 | 25.93 | 31 | 37.90 |
| | Cut-off [pg/ μ l] | 24.85 | 20.49 | 19.15 | 19.03 | 18.29 | 17.30 |

Table 13. *LINE-1* 266-bp fragment concentration sensitivity and the corresponding cut-off level
From the comparison control vs. patients and control vs. metastatic NET+NEC patients' subgroups at specificity levels between 60-95%.

| | | SPECIFICITY [%] | | | | | |
|-----------------|--------------------------|-----------------|-------|-------|-------|-------|-------|
| | | 95 % | 90 % | 85 % | 80 % | 70 % | 60 % |
| SENSITIVITY [%] | Patients | 8.07 | 24.70 | 25.81 | 25.81 | 45.16 | 51.61 |
| | Cut-off [pg/ μ l] | 2.18 | 2.91 | 2.96 | 3 | 3.96 | 4.17 |
| | Metastatic NETs +NECs | 9.26 | 28.10 | 29.63 | 29.63 | 48.15 | 55.56 |
| | Cut-off [pg/ μ l] | 2.19 | 2.92 | 2.97 | 2.99 | 3.97 | 4.18 |

3.3.2.2.1 Correlation of *LINE-1* fragmentation with clinical characteristics

Nonparametric comparison of short and longer *LINE-1* fragments levels with tumor grade, tumor burden, and localization was evaluated by the Kruskal-Wallis test. The Spearman correlation test calculated correlation to age and CgA. Welch's t-test assessed the relationship to gender. A P value \leq of 0.05 was considered statistically significant. In the patients, various clinical factors effects on biomarkers were analyzed in all plasma samples irrespective of whether they belonged to which subgroups of patients. The impact of tumor burden on *LINE-1* fragmentation was investigated in plasma samples regardless of whether they belonged to which group.

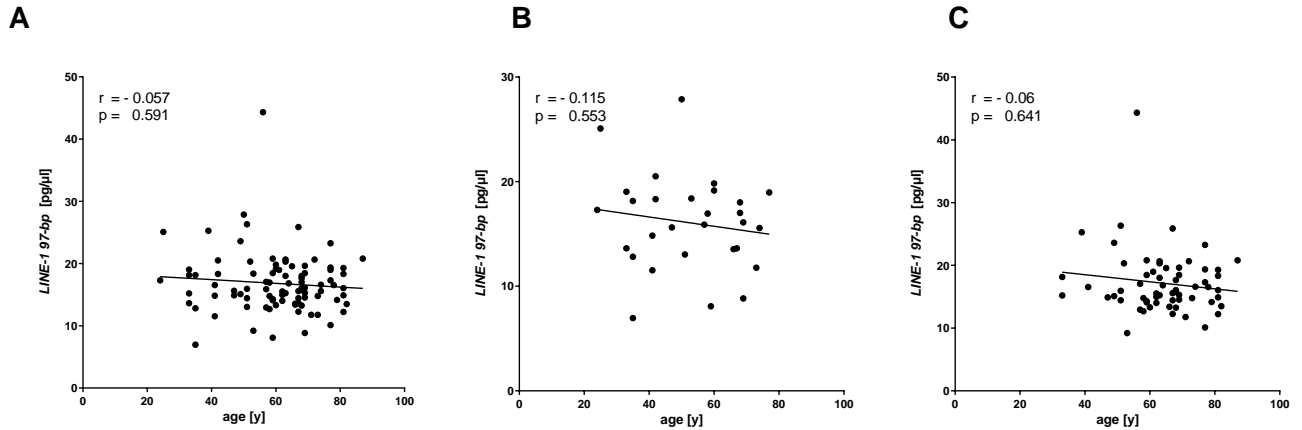
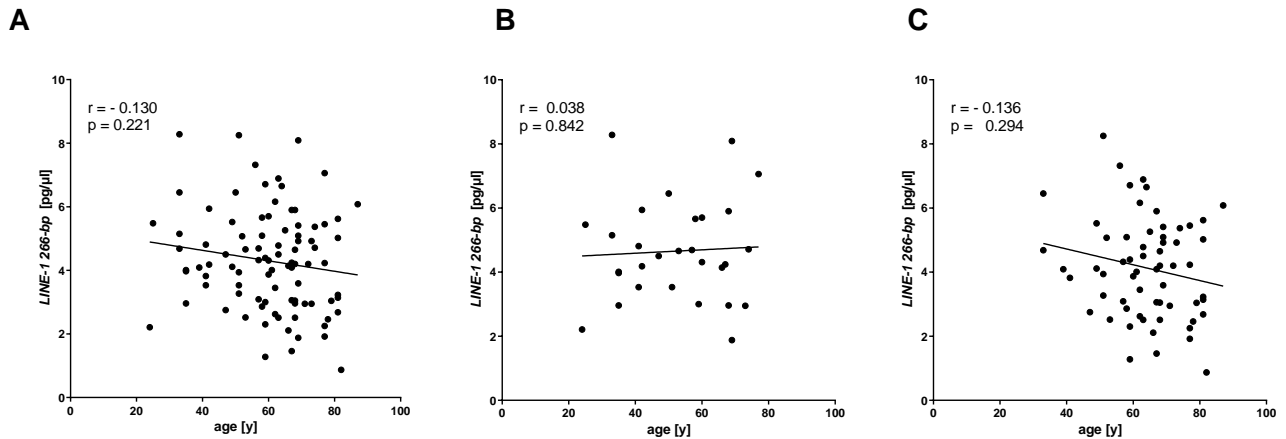
Correlation between LINE-1 fragmentation and age or gender

No significant correlation could be calculated for age and *LINE-1* fragmentation level. The correlation of short and longer *LINE-1* fragments to age is shown in Fig.32.

Differences between *LINE-1* 97-bp fragment level and gender were assessed. The median *LINE-1* 97-bp fragment level for men was 15.9 (IQR 4.68) pg/ μ l, and for women, 16.6(IQR 5.15) pg/ μ l. Welch's t-test confirmed no gender-specific differences for the amount of short *LINE-1* fragments ($p= 0.471$).

Differences between *LINE-1* 266-bp fragment level and gender were assessed. The median *LINE-1* 266-bp fragment level for men and women was 4.31 (IQR 2.39) and 4.19 (IQR 2.10) pg/ μ l, respectively.

Using Welch's t-test, men and women showed no significant difference in the plasma concentration of long *LINE-1* fragments ($p= 0.270$).

1) *LINE-1* 97-bp fragment level2) *LINE-1* 266-bp fragment levelFigure 32. Correlation of age and *LINE-1* fragmentation level in cfDNA

LINE-1 fragmentation levels were measured by qPCR for (1) *LINE-1* 97 bp cfDNA fragments or (2) *LINE-1* 266 bp fragments. Spearman correlation test was used to assess any differences between the age and *LINE-1* fragmentation in A) total subjects, B) controls, and C) patients.

Correlation between LINE-1 fragmentation and tumor grade

Regarding tumor grade, G3 patients showed a higher *LINE-1* 97-bp fragment level of 17.5 (IQR 3.68) than the controls with 16.1 (IQR 4.84) pg/ μ L. Unlike, a reduced amount of *LINE-1* 97-bp fragment was detected in earlier grades, namely G1 and G2, with 15.6 (IQR 3.61) and 15.30 (IQR 6.21) pg/ μ L, respectively compared to the control (16.11 (IQR 4.84) pg/ μ L). Among the tumor grade' subgroups, the G3 patients showed the highest level of *LINE-1* 97-bp fragment of 17.5 (IQR 3.68) pg/ μ L. Kruskal-Wallis test was used to evaluate the differences in *LINE-1* 97-bp fragment values between samples from the controls, G1, G2, and G3 tumor groups ($X^2= 2.54$, $p=0.469$). No significant differences could be identified between the control group with each subgroup concerning tumor grade as well as among the tumor grade ' subgroups ($P > 0.05$) (Fig.33A).

For the long *LINE-1* fragments, G1, G2, and G3 subgroups showed a reduced *LINE-1* 266-bp fragment level of 4.09 (IQR 2.04), 4.39 (IQR 2.43), and 3.92 (IQR 1.67) pg/ μ L compared to the controls with 4.50 (IQR 2.13) pg/ μ L. The levels of *LINE-1* 266-bp fragment were higher in G2 patients with 4.39 (IQR 2.43) pg/ μ L than G1 and G3 patients with 4.09 (IQR 2.04) pg/

μL and $3.92(\text{IQR } 1.67) \text{ pg/ } \mu\text{L}$, respectively (Fig.33B). Kruskal-Wallis test was used to evaluate the differences in *LINE-1* 266-bp fragment values between samples from the control, G1, G2, and G3 tumors ($X^2= 3.11$; $p=0.376$). No significant differences could be detected between the control group with each tumor grade subgroup and among the tumor grade' subgroups ($P > 0.05$).

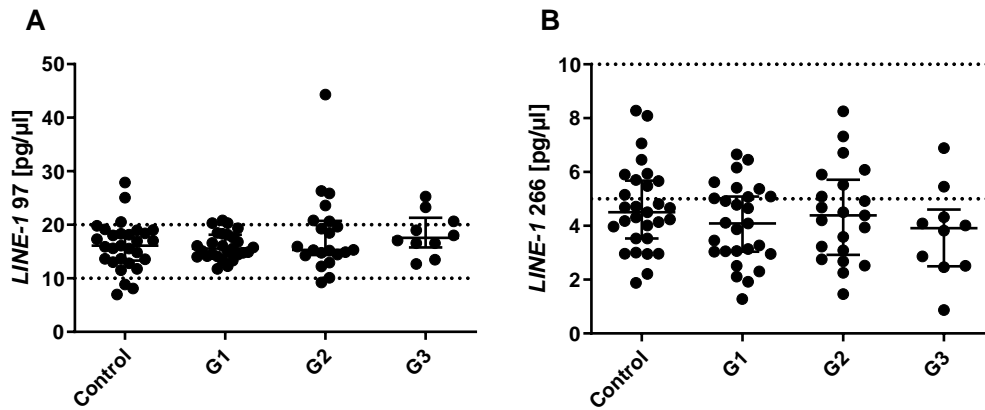


Figure 33.cfDNA *LINE-1* fragmentation level grouped by tumor grades

A) *LINE-1* 97-bp and B) *LINE-1* 266-bp fragments levels were determined in the patients' plasma using qPCR. The data are divided into different groups depending on tumor grade (controls, G1 (grade 1), G2 (grade 2), and G3 (grade 3) tumor).

Correlation between LINE-1 fragmentation and tumor burden

Tumor burden hat a negatively correlation with *LINE-1* 266-bp but not with *LINE-1* 97-bp fragments level by spearman test ($r=-0.30$; $p=0.004$ and $r=0.037$; $p=0.73$, respectively).

The highest *LINE-1* 97 and *LINE-1* 266 concentration was observed in the no tumor group with $16.4 (\text{IQR } 4.52) \text{ pg/ } \mu\text{L}$ and $4.70(\text{IQR } 2.01) \text{ pg/ } \mu\text{L}$, respectively (Fig.34).

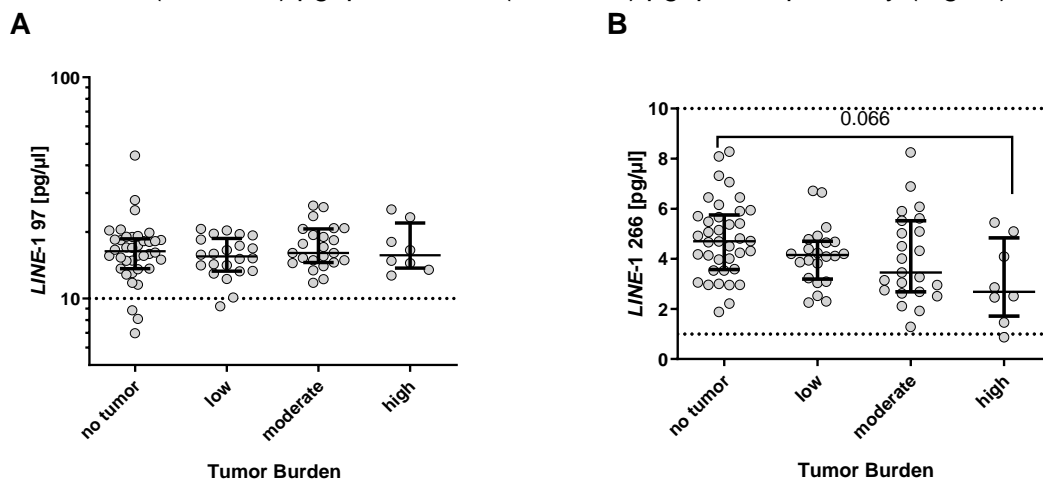


Figure 34.cfDNA *LINE-1* fragmentation level grouped by tumor burden

A) *LINE-1* 97-bp and B) *LINE-1* 266-bp fragments levels were determined in the patients' plasma using qPCR. The data are divided into different groups depending on tumor burden (no tumor, low, moderate, and high). Kruskal-Wallis analysis was performed to test differences in plasma *LINE-1* fragmentation level levels between the groups. Dwass-Steel-Critchlow-Flinger was applied as a post hoc test; P values ≤ 0.05 were considered significant.

Higher *LINE-1* 97-bp fragment concentrations were observed in the plasma samples of patients with moderate tumor load compared with low and high tumor load (16.1 (IQR 5.29) pg/ μ L vs. 15.5 (IQR 4.66) pg/ μ L and 15.7 (IQR 5.13) pg/ μ L).

A decreased tendency was found from low tumor load group to moderate and large tumor load groups for *LINE-1* 266-bp fragments level (4.16(IQR 1.29), 3.45(IQR 2.59) and 2.68(IQR 2.13) pg/ μ L, respectively). Kruskal-Wallis test was applied to evaluate the differences in *LINE-1* 97-bp fragment values between samples from different tumor burdens ($X^2= 1.63$; $p=0.652$). No significant differences could be detected between groups ($P > 0.05$).

A significant difference for *LINE-1* 266-bp was obtained between samples from different tumor burdens by the Kruskal-Wallis test ($X^2= 8.80$; $p=0.0032$). Dwass-Steel-Critchlow-Flinger was applied as a post hoc test. We did not observe any difference in *LINE-1* 266 concentration in the samples with different tumor burden classes.

Correlation between *LINE-1* fragmentation and tumor origin

No difference was observed among different tumor origins by Kruskal-Wallis test for short *LINE-1* fragments ($X^2=3.722$, $P=0.590$) and long *LINE-1* fragments ($X^2= 8.355$, $P=0.138$).

The highest concentration of *LINE-1* 97-bp fragment was observed in the patients with lung tumor origin (18.02 (IQR 5.76) pg/ μ L). The lowest *LINE-1* 97-bp fragment level of 14.44 (IQR 3.12) pg/ μ L were measured in the patients with primary stomach tumors, respectively. The patients with tumor origin of small intestine and pancreas had *LINE-1* 97-bp fragment levels of 16.86 (IQR 4.73) pg/ μ L and 16.28 (IQR 7.24) pg/ μ L, respectively. The patients with the rectum and ileum tumor origin had *LINE-1* 97-bp fragment levels of 15.42 (IQR 13.06) and 15.25 (IQR 2.5) pg/ μ L, respectively (Fig.35A).

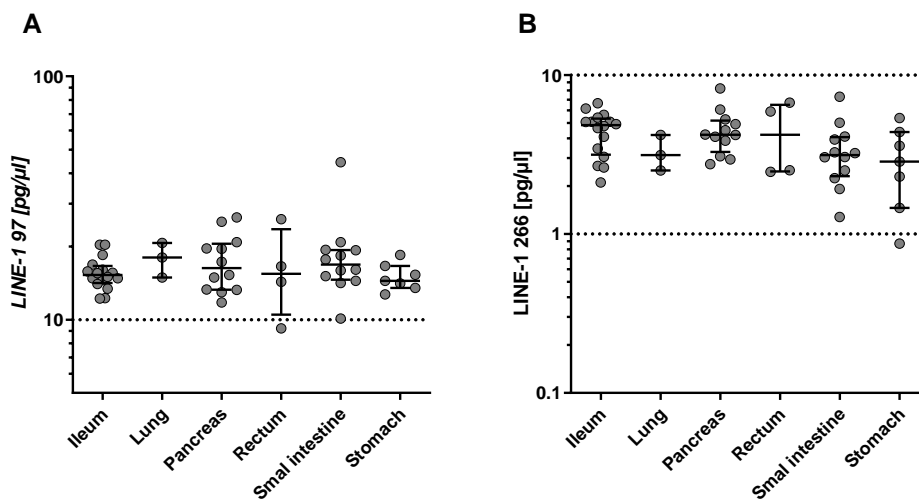


Figure 35. cfDNA *LINE-1* fragmentation level grouped by tumor origin

A) *LINE-1* 97-bp and B) *LINE-1* 266-bp fragments levels were determined in the patients' plasma using quantitative PCR. The data are divided into different groups depending on tumor origin.

The highest concentration of *LINE-1* 266-bp fragment was observed in the patients with ileum as tumor origin side (4.85 (IQR 2.17) pg/ μ L). The lowest amount was calculated for patients with a stomach tumor (2.86 (IQR 2.93) pg/ μ L). The patients with lung, pancreas and rectum tumor origin had *LINE-1* 266-bp fragment levels of 3.14(IQR 1.69), 4.22(IQR 1.89), and 4.21(IQR 4.03) pg/ μ L, respectively. The tumors with small intestine origin had lower

LINE-1 266-bp fragment concentration than those with ileum (3.14(IQR 1.75) vs. 4.85(IQR 2.17) pg/ μ L) (Fig.35B).

Correlation between *LINE-1* fragmentation level and serum-CgA level

The serum-CgA level of the patients revealed a negative relation with *LINE-1* fragments (Fig.36). No significant correlation could be calculated by Spearman correlation test for *LINE-1* 97-bp fragments ($p=0.205$), nor for *LINE-1* 266-bp ($p=0.070$) fragments concentration.

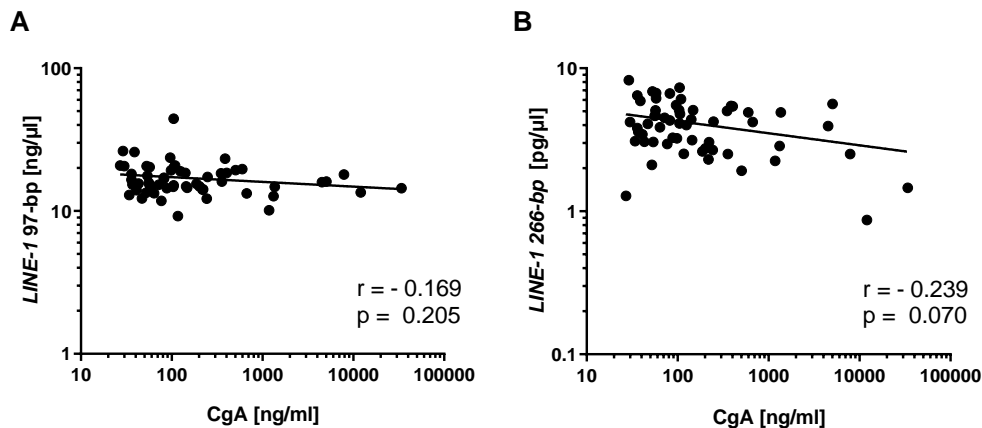


Figure 36. Correlation of CgA hormonal status and *LINE-1* fragmentation level in the patients. Spearman correlation revealed a very weak, no significant correlation for A) *LINE-1* 97-bp, and B) *LINE-1* 266-bp fragments levels.

3.3.3 Analysis of cfDNA integrity indexes

cfDNA integrity indexes were reported using: *ALU* 260-bp/115-bp ratio and *LINE-1* 266-bp/97-bp ratio.

The cfDNA-*ALU* DII (*ALU* cfDII) was slightly decreased in the patients of 0.165 (IQR 0.22) compared to the controls of 0.17 (IQR 0.16). No significant difference for *ALU* cfDII was found by Welch's t-test ($p=0.546$). Likewise, the decrease of *ALU* integrity index was observed in metastatic NETs of 0.15 (IQR 0.23). In contrast, the *ALU* cfDII came up in NECs of 0.21 (IQR 0.16) compared to the control cases. Non-metastatic NETs also showed an increase of *ALU* integrity index (0.20 (IQR 0.14) compared to the controls. The *ALU* cfDII in non-metastatic NET patients was comparable to the NEC patients (0.201(IQR 0.14) vs. 0.205 (IQR 0.16), respectively). The Kruskal-Wallis test evaluated the differences in *ALU* cfDII values between samples from the control group and patients' subgroups. The plasma *ALU* cfDII did not significantly discriminate between the different groups ($X^2=0.089$, $p=0.993$) (Fig.37A and C).

The cfDNA-*LINE-1* integrity index (*LINE-1* cfDII) in the controls could be defined with 0.30 (IQR 0.10). The NEN patients showed a reduced *LINE-1* cfDII of 0.24 (IQR 0.10). Welch's t-test reveals a significant difference for the *LINE-1* cfDII ($p=0.006$). Similarly, the decrease of *LINE-1* cfDII was detected in the subgroups of NEC patients with 0.23 (IQR 0.07) and mNET with 0.24 (IQR 0.10) compared to the controls. Among the patients' subgroups, the non-mNETs had the highest *LINE-1* cfDII with 0.27 (IQR 0.10), but lower than the control group.

mNETs had a slightly higher *LINE-1* cfDII of 0.24 (IQR 0.10) than NECs with 0.23 (IQR 0.07). Kruskal-Wallis test was used to evaluate the differences in *LINE-1* cfDII values between samples from the control group and patients' subgroups. Kruskal Wallis test showed a significant difference between *LINE-1* cfDII ($X^2=8.89$; $p=0.031$). The post hoc test revealed a significant difference between the control and mNET groups ($p=0.053$) (Fig.37B and D).

The discriminatory power of integrity indexes was calculated using the ROC curve. The sensitivity of the integrity index in the patient group and metastatic NET+NEC subgroups was determined at several specificity levels. The corresponding sensitivities and actual cut-off points producing Fig. 38 are given in Tables 14 and 15. The healthy donors and cancer patients could be differentiated with an AUC of 0.52 (95% confidence interval (CI), 0.388 to 0.643; $p=0.812$) and 0.67(95% confidence interval (CI), 0.555 to 0.79; $p=0.008$) based on the *ALU* and *LINE-1* integrity indexes, respectively (Fig. 38). The diagnostic power of *ALU* and *LINE-1* cfDIIs did not change remarkably when the patients were included only the subgroups of mNET+NEC patients (AUC= 0.517(95% CI, 0.386 to 0.648; $p=0.800$) and AUC= 0.69 (95% CI, 0.569 to 0.810; $p=0.005$), respectively. Using the cutoff value of 0.30 for *LINE-1* cfDIIs, we were able to identify mNET+NEC patients with a sensitivity of 77.8% and specificity of 55.2%.

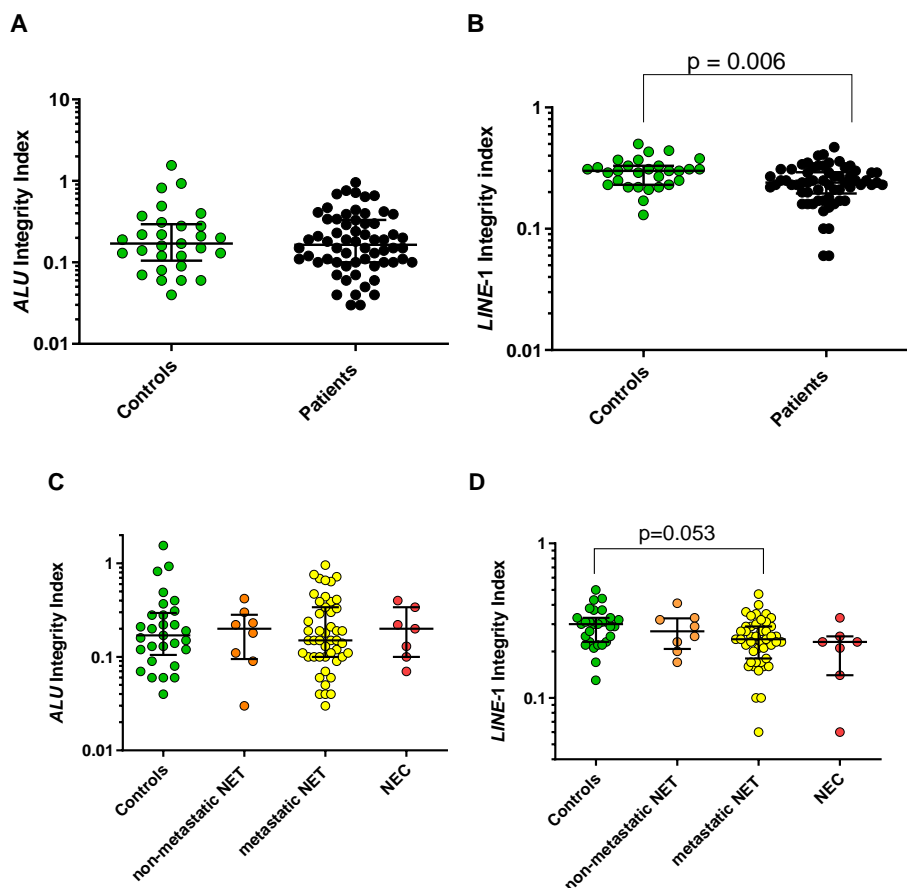


Figure 37.cfDNA- *ALU* and -*LINE-1* integrity indexes in the study groups

ALU and *LINE-1* integrity index values in (A, B) NEN patients and the controls and (C, D) patients' subgroups and the controls were determined by a ratio of *ALU* 260-bp/115-bp and *LINE-1* 266-bp/97-bp. Welch's t-test (A, B) and Kruskal-Wallis (C, D) analysis were performed to test the differences in integrity indexes between the study groups. Dwass-Steel-Critchlow-Flinger was applied as a post hoc test; P values ≤ 0.05 were considered significant.

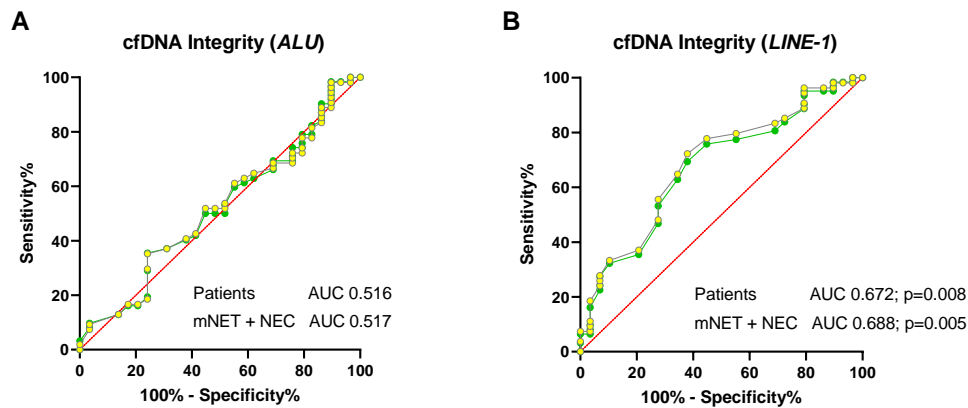


Figure 38. cfDNA integrity index receiver operating characteristic (ROC) plots
ROC curves from the comparison of controls vs. patients and controls vs. metastatic NET+NEC subgroups; A) *ALU* integrity index and B) *LINE-1* integrity index.

Table 14. The sensitivity and corresponding cut-off levels for *ALU* integrity index
From the comparison control vs. patients and control vs. metastatic NET+NEC patients' subgroups at specificity levels between 60-95%.

| | | SPECIFICITY [%] | | | | | |
|-----------------|-----------------------|-----------------|-------|-------|-------|------|-------|
| | | 95 % | 90 % | 85 % | 80 % | 70 % | 60 % |
| SENSITIVITY [%] | Patients | 10 | 10.92 | 13.10 | 16.13 | 36 | 40.90 |
| | Cut-off | 0.05 | 0.05 | 0.06 | 0.08 | 0.12 | 0.13 |
| | metastatic NET+NEC | 9.3 | 10 | 14 | 16.67 | 36 | 41 |
| | Cut-off | 0.05 | 0.06 | 0.07 | 0.08 | 0.12 | 0.14 |

Table 15. The sensitivity and corresponding cut-off levels of *LINE-1* integrity index
From the comparison control vs. patients and control vs. metastatic NET+ NEC patients' subgroups at specificity levels between 50-95%.

| | | SPECIFICITY [%] | | | | | |
|-----------------|-----------------------|-----------------|------|------|------|------|------|
| | | 95 % | 90 % | 80 % | 70 % | 60 % | 50 % |
| SENSITIVITY [%] | Patients | 17 | 32 | 35 | 54 | 70 | 76 |
| | Cut-off | 0.17 | 0.21 | 0.22 | 0.25 | 0.28 | 0.30 |
| | Metastatic NET+NEC | 19.10 | 33 | 37 | 58 | 73 | 78 |
| | Cut-off | 0.16 | 0.21 | 0.22 | 0.25 | 0.28 | 0.29 |

3.3.3.1 Correlation of cfDNA- integrity indexes with clinical characteristics

Nonparametric comparison of cfDIIs with tumor grade, burden, and localization was evaluated by the Kruskal-Wallis test. The Spearman correlation test calculated correlation to age and CgA. Welch's t-test assessed the relationship to gender. A P value \leq of 0.05 was considered statistically significant. In the patients, the effect of various clinical factors on biomarkers was analyzed in plasma samples irrespective of whether they belonged to which

subgroups of patients. The impact of tumor burden was analyzed regardless of the corresponding group.

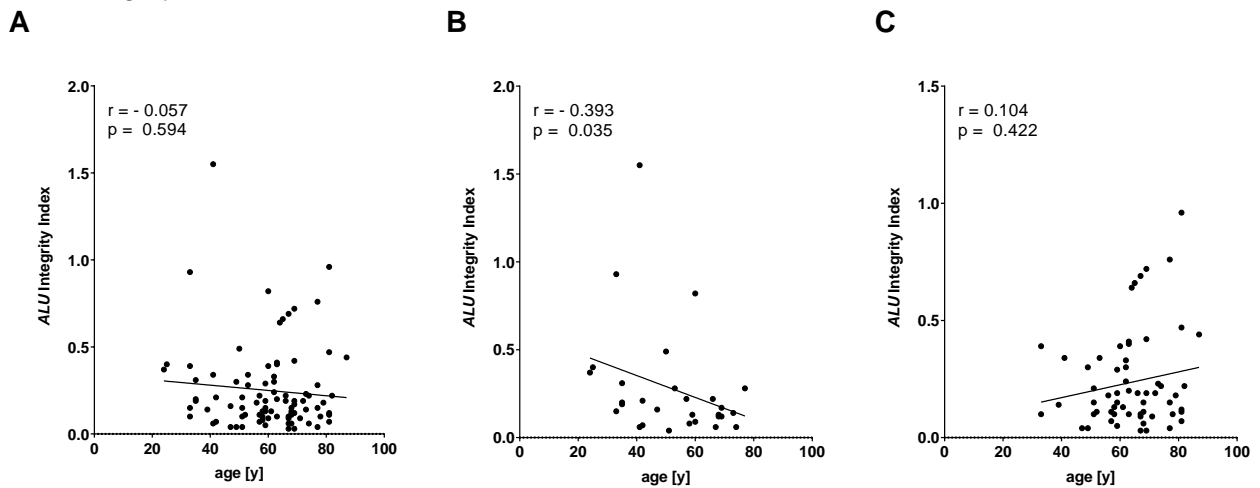
Correlation between cfDNA- integrity indexes and age or gender

The relationship age of the cohorts was evaluated with measured cfDII data. Spearman correlation did not show any significant correlation for *ALU*- or *LINE-1* cfDIIs, except for *ALU* DII in the control group. The correlation of cfDIIs to age is shown in Fig.39.

Differences between the *ALU* cfDII and gender were assessed. For men, the median of *ALU* cfDII was 0.15 (IQR 0.132), and for women, 0.192 (IQR 0.257). Welch t-test confirmed no gender-specific differences ($p=0.068$).

Differences between the *LINE-1* cfDII and gender were assessed. For men, the median of *LINE-1* cfDII was 0.251 (IQR 0.113) and 0.250 (IQR 0.085) for women. Using the Welch t-test, men and women showed no significant difference for the cfDII of *LINE-1* fragments ($p=0.515$).

1) *ALU* integrity index



2) *LINE-1* integrity index

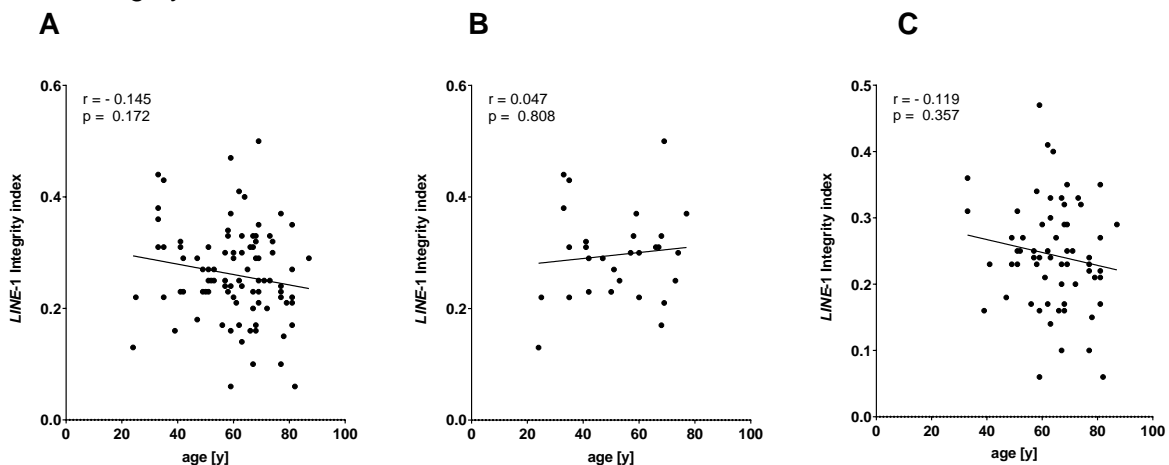


Figure 39. Correlation of age and cfDNA integrity indexes

Integrity indexes values were determined for (1) *ALU* integrity index by a ratio of *ALU* 260-bp/115-bp and (2) *LINE-1* integrity index by *LINE-1* 266-bp/97-bp. Spearman correlation test was used to assess any relationship between the age and integrity indexes in A) total subjects, B) controls, and C) patients.

Correlation between cfDNA- integrity indexes and tumor grade

Regarding tumor grade, an elevated *ALU* cfDII was demonstrated in G3 patients of 0.173 (IQR 0.2) and G1 patients of 0.195 (IQR 0.26) compared to the control with 0.17 (IQR 0.17). Unlike, G2 patients showed a reduced *ALU* integrity index of 0.15 (IQR 0.1) (Fig.40A). Kruskal-Wallis test was used to evaluate the differences in *ALU* cfDII values. No significant differences could be calculated ($X^2 = 1.86$; $p=0.602$).

For *LINE*-1 cfDII, a decreased tendency was observed from early tumor grade to late graded tumors. An increase of the *LINE*-1 cfDII was determined in the control (0.30(IQR 0.10) compared to different tumor grade' subgroups; namely G1 (0.25 (IQR 0.12), G2 (0.24 (IQR 0.07) and G3 (0.22 (IQR 0.08) (Fig.40B). Significant differences between the groups could be calculated by the Kruskal-Wallis test ($X^2 = 10.31$; $p=0.016$). A pairwise comparison with the Dwass-Steel-Critchlow post hoc test did reveal a significant difference between the controls and patients with the G3 tumor group ($p=0.024$).

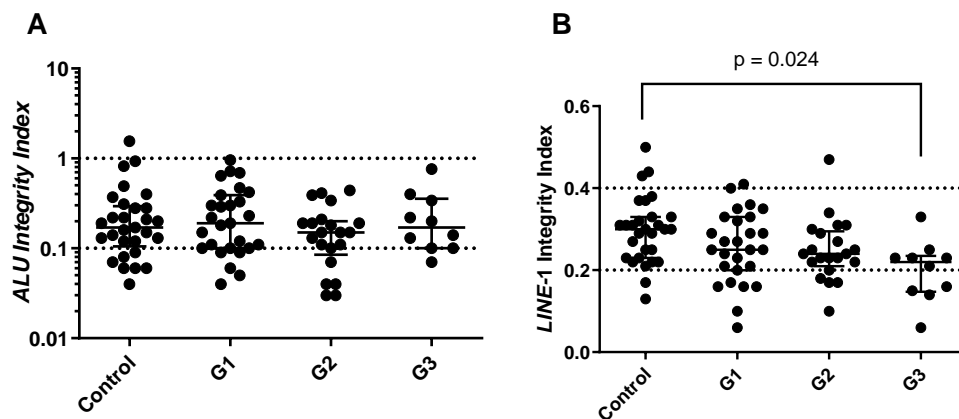


Figure 40. cfDNA integrity index grouped by tumor grades

A) *ALU* integrity index and B) *LINE*-1 integrity index was determined by the ratio of *ALU* 260-bp/115-bp and *LINE*-1 266-bp/97-bp. The data are divided into different groups depending on the tumor grade (controls, G1 (grade 1), G2 (grade 2), G3 (grade 3) tumor).

In the current ROC curve analysis, the *LINE*-1 cfDII was able to distinguish between the patients with G1 (n= 27) and G2 (n=21) tumor grade from the controls with an estimated AUC of 0.62 (95% CI, 0.472 to 0.769; $P=0.121$) and 0.67 (95% CI, 0.552 to 0.826; $P=0.037$), respectively The ROC curve distinguishing patients with a G3 tumor grade from controls indicated 90% sensitivity and 69% specificity at 0.25 cut-off (AUC=0.803, 95% CI, 0.644 to 0.963; $p= 005$) (Fig. 41). The cut-off levels at different specificity levels is given in Table 16.

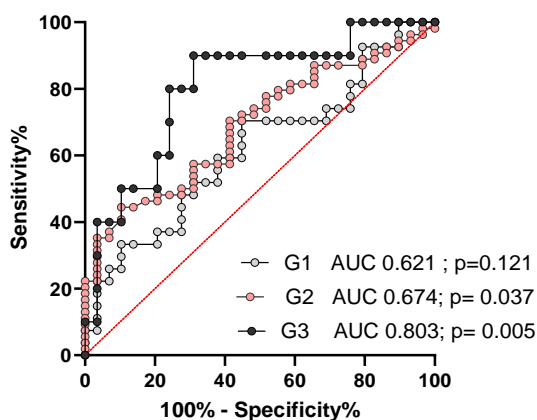


Figure 41. *LINE*-1 integrity index receiver operating characteristic (ROC) curve for tumor grades

ROC analysis of *LINE*-1 integrity index for distinguishing the controls from the patients with tumor grade G1 (grey), G2 (pink), and G3 (black), along with the area under the curve (AUC).

Table 16. The sensitivity and corresponding cut-off levels of LINE-1 integrity index for tumor grades

From the comparison controls vs. patients with a G1-grade tumor or a G2-grade tumor at specificity levels between 60-95%.

| | | SPECIFICITY [%] | | | | | |
|-----------------|---------|-----------------|-------|-------|-------|-------|-------|
| | | 95 % | 90 % | 85 % | 75 % | 70 % | 60 % |
| SENSITIVITY [%] | G1 | 22.22 | 25.93 | 33.33 | 37.04 | 48.15 | 59.26 |
| | Cut-off | 0.17 | 0.21 | 0.22 | 0.23 | 0.25 | 0.28 |
| | G2 | 14.22 | 23.88 | 28.57 | 38.10 | 60 | 71.43 |
| | Cut-off | 0.1 | 0.2 | 0.2 | 0.2 | 0.2 | 0.2 |
| | G3 | 40 | 40 | 50 | 60 | 80 | 90 |
| | Cut-off | 0.1 | 0.17 | 0.2 | 0.2 | 0.2 | 0.2 |

Correlation between integrity and tumor burden

No correlation found between ALU cfDII and tumor burden ($r=-0.061$; $p=0.56$). There was an association between LINE-1 cfDII and tumor burden ($r=-0.40$; $p<0.0001$).

The median ALU cfDII in groups with no tumor, low, moderate, and large tumor load was 0.175 (IQR 0.178), 0.190 (IQR 0.190), 0.120(IQR 0.205), and 0.135 (IQR 0.165), respectively. Kruskal-Wallis analysis showed no difference for ALU cfDII among groups ($X^2=2.44$; $p= 0.485$) (Fig.42A).

A decreased tendency was observed for LINE-1 cfDII from group with no tumor (0.3 (IQR 0.100)) to high tumor load (0.155(IQR 0.100)). Groups with low and moderate tumor load had LINE-1 cfDII of 0.25(IQR 0.058) and 0.23(IQR 0.105), respectively. A significant difference was found among groups by Kruskal-Wallis ($X^2=15.11$; $p= 0.002$).

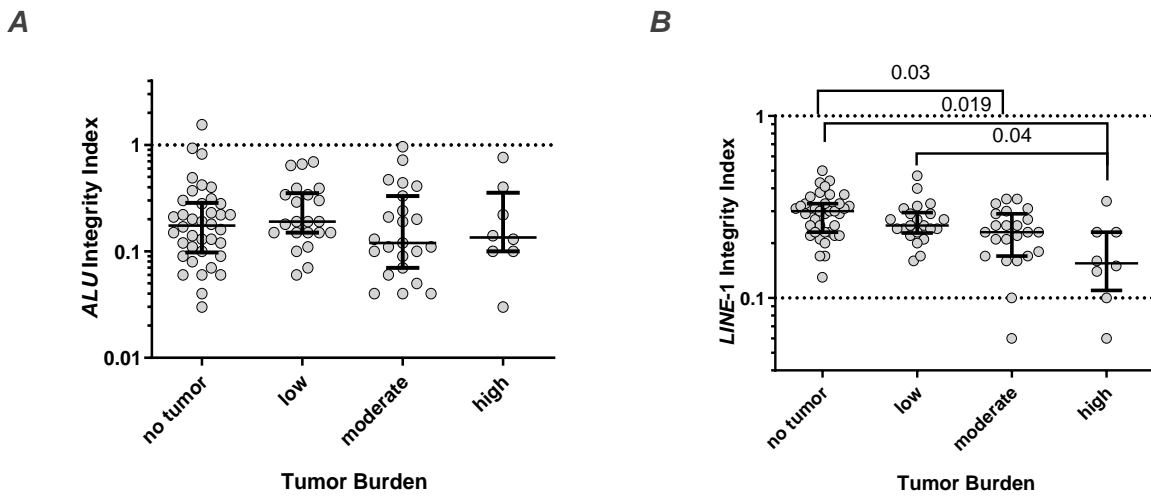


Figure 42.cfDNA- ALU and -LINE-1 integrity indexes grouped by tumor burden

A) ALU integrity index and B) LINE-1 integrity index were determined by a ratio of ALU 260-bp/115-bp and LINE-1 266-bp/97-bp. The data are divided into different groups depending on tumor burden (no tumor, low, moderate, and high). Kruskal-Wallis analysis was performed to test differences in plasma ALU and -LINE-1 integrity indexes between the groups. Dwass-Steel-Critchlow-Flinger was applied as a post hoc test; P values ≤ 0.05 were considered significant.

The pairwise analysis revealed a difference in LINE-1 cfDII between the group with no tumor with moderate and high tumor load groups ($p=0.030$ and $p=0.019$, respectively). Also, low and high tumor burden groups had a significant difference ($p=0.040$) (Fig.42B).

In the current ROC curve analysis, the *LINE-1* cfDII distinguished between the patients with different tumor loads from the group with no tumor burden with an estimated AUC of 0.69 (95% CI, 0.579 to 0.800; $P=0.002$).

An AUC of 0.74 distinguished the patients with moderate and large tumor burden (95% CI, 0.624 to 0.859; $p=0.006$). The *LINE-1* cfDII distinguished samples with different tumor burden and no tumor burden with 73.6 % sensitivity and 60.5% specificity at the cut-off of 0.28, whereas samples with moderate and large tumor burden were differentiated with 77.4% sensitivity and 60.5% specificity from samples with no tumor burden at the cut-off of 0.28. The patients with a high tumor load had a highly significant AUC of 0.83 (95% CI, 0.644 to 1.00; $p=0.004$) (Fig.43). The best sensitivity (87.5%) and specificity (71%) were obtained in the patients with a high tumor burden at a cut-off value of 0.24.

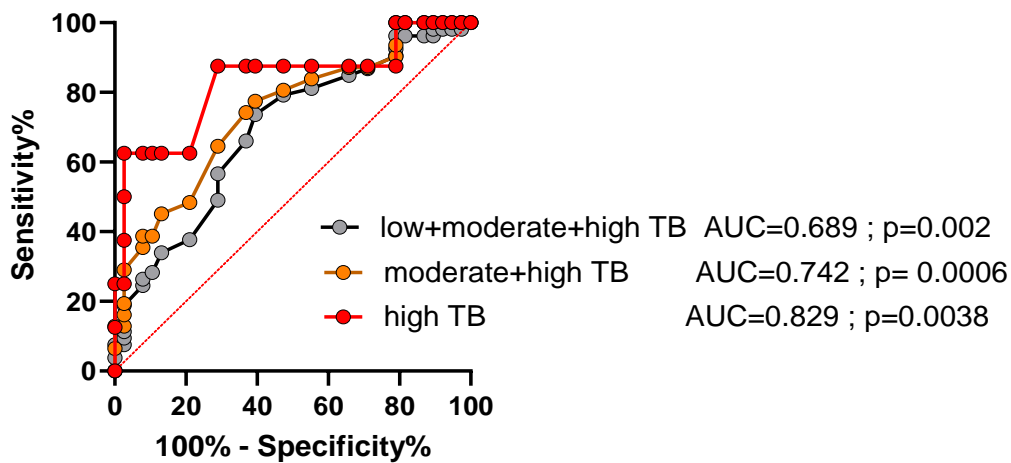


Figure 43. cfDNA-*LINE-1* integrity index receiver operating characteristic (ROC) plots for tumor burdens. ROC analysis of plasma cfDNA level for distinguishing the group with no tumor burden from the patients with low, moderate, and high tumor burden (TB). Tumor burdens of low plus moderate and high (grey), moderate plus high (orange), and high (red), along with the area under the curve (AUC).

Correlation between cfDNA- integrity indexes and tumor origin

The highest *ALU* cfDII of 0.24 (IQR 0.34) was detected in the patients with ileum tumor origin. The patients with lung and stomach tumor origin showed the *ALU* cfDII of 0.19 (IQR 0.28) and 0.19 (IQR 0.19), respectively. The lowest *ALU* integrity index was measured in the patients with the rectum (0.13(IQR 0.17) and small intestine (0.13(IQR 0.12) primary tumor (Fig.44A). Kruskal-Wallis test shows no significant differences for *ALU* cfDII related to tumor origin ($X^2 = 5.868$, $p=0.319$).

The highest *LINE-1* cfDII of 0.29 (IQR 0.12) was detected in the patients with ileum primary tumor. The patients with pancreas, rectum, and stomach tumor origin had *LINE-1* cfDII of 0.26 (IQR 0.06), 0.25 (IQR 0.25), and 0.23 (IQR 0.14). The lowest *LINE-1* cfDII was observed in the small intestine (0.19 (IQR 0.08), followed by lung (0.2 (IQR 0.07) primary tumors (Fig.44B). Kruskal-Wallis test shows a significant difference for *LINE-1* cfDII and tumor origin ($X^2=15.08$, $p=0.010$). A pairwise comparison with Dunn's multiple comparisons test reveals a significant difference between the patients with ileum and small intestine tumor origins ($p<0.05$).

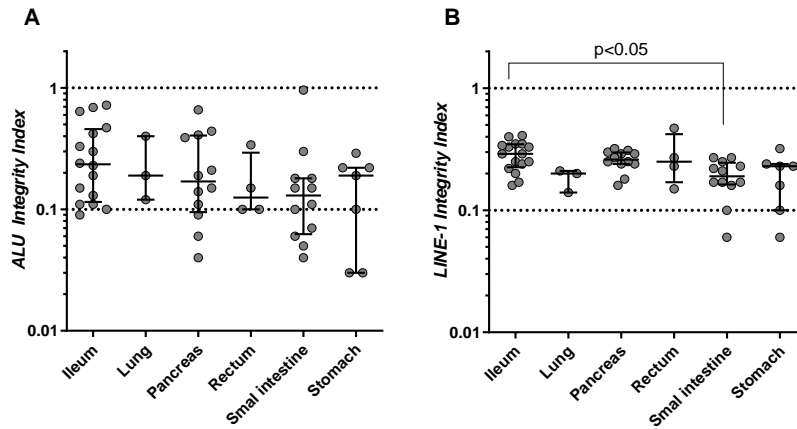


Figure 44. cfDNA integrity indexed grouped by tumor origin
 A) *ALU* integrity index and B) *LINE-1* integrity index were determined by the ratio of *ALU* 260-bp/115-bp and *LINE-1* 266-bp/97-bp. The data were divided into different groups depending on tumor origin.

Association between cfDNA- integrity indexes with serum-CgA level

For *ALU* and *LINE-1* cfDNIs, a weak negative correlation with serum-CgA level was observed in the patients, but it was not significant ($p = 0.091$ and 0.173 , respectively) (Fig.45).

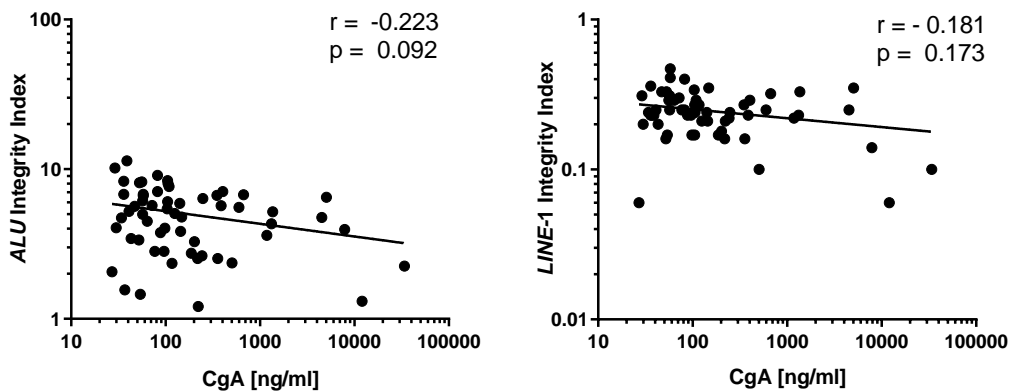


Figure 45. Correlation of CgA hormonal status and integrity indexes in the patients
 Spearman correlation revealed a very weak correlation for A) *ALU* integrity index and B) *LINE-1* integrity index.

3.3.4 Analysis of *ALU* hypomethylation percentage

Methylation levels of the major variant of *ALU* were quantified.

The NEN patients showed a slightly higher hypomethylation of 1.39 % (IQR 0.53) compared to the control with 1.23 % (IQR 0.36) (Welch's t-test $p=0.167$) (Fig. 46A).

Regarding the subgroups, the highest hypomethylation was calculated for the NEC and mNET subgroups (1.56 (IQR 1.02) and 1.45 (IQR 0.51) %, respectively). In contrast, the non-mNET subgroup showed the lowest hypomethylation rate of 1% (IQR 0.28). Shapiro-Wilk analysis confirmed significant deviations from a normal distribution. Therefore, the quantitative results were further compared using Kruskal-Wallis non-parametric ANOVA and revealed a considerable difference ($X^2=14.23$; $p=0.003$). A further pairwise comparison by Dwass-Steel-Critchlow-Flinger revealed a significant distinction between the mNET and the non-mNET subgroups ($p=0.005$) (Fig. 46B).

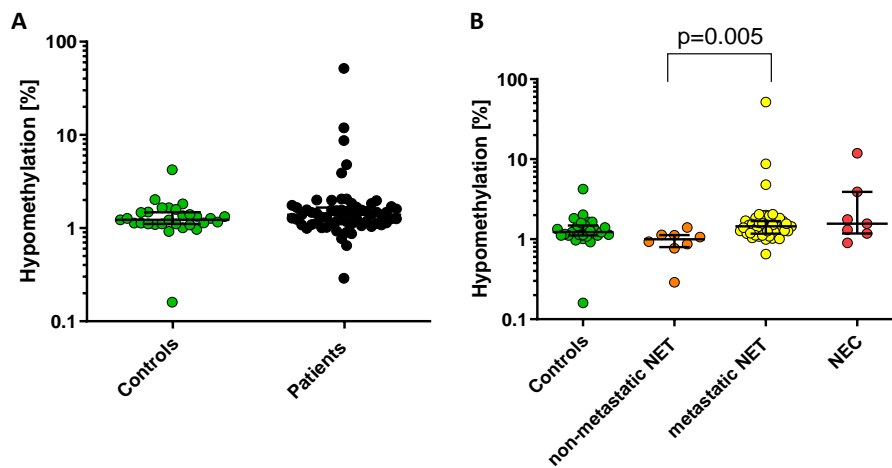


Figure 46. Percentage of hypomethylation in the study groups

The percentage of hypomethylation in (A) NEN patients and controls and (B) patients' subgroups and controls were measured by unmethylated cfDNA-*ALU* percentage. Welch's t-test (A) and Kruskal-Wallis (B) analysis were performed to test the differences in hypomethylation percentage between the study groups. Dwass-Steel-Critchlow-Flinger was applied as a post hoc test; P values ≤ 0.05 were considered significant.

The ROC curve was analyzed to discriminate the controls from the patients by hypomethylation level. Hypomethylation sensitivity in the patients and mNET plus NEC subgroups were determined at several specificity levels. The corresponding sensitivities and actual cut-off points producing Fig. 47A are given in Table 17.

The hypomethylation level could differentiate the controls and cancer patients with an AUC of 0.58 (95% confidence interval (CI), 0.460 to 0.702; $p=0.217$) (Fig.47). The diagnostic power of hypomethylation could slightly be increased when controls were compared to the mNET plus NEC subgroups, to an AUC of 0.64 (95% confidence interval, 0.513 to 0.759; $p=0.042$). The hypomethylation level at a cut-off of 1.38% yielded a specificity of 69% and sensitivity of 57.4% to differentiate mNET plus NEC subgroups from controls.

In addition, the ROC curve was analyzed to test if the differences in hypomethylation level could be useful to discriminate non-mNET from mNET patients. An AUC of 0.87 (95% confidence interval, 0.748 to 0.989; $p=0.0009$) was achieved. If all aggressive forms of the disease, namely mNETs, and NECs were included, the discriminatory power was not

changed. Comparing the subgroups of mNET and NEC to non-mNET, an AUC of 0.87 (95% confidence interval, 0.753 to 0.986, P=0.0008) could be calculated. The output data of performed ROC curves to differentiate mNET and NEC from non-mNET cases revealed that hypomethylation at a cut-off of 1.14% yielded (87.5%) sensitivity and (79.6%) specificity. The corresponding sensitivities and actual cut-off points producing Fig. 47B are given in Table 16.

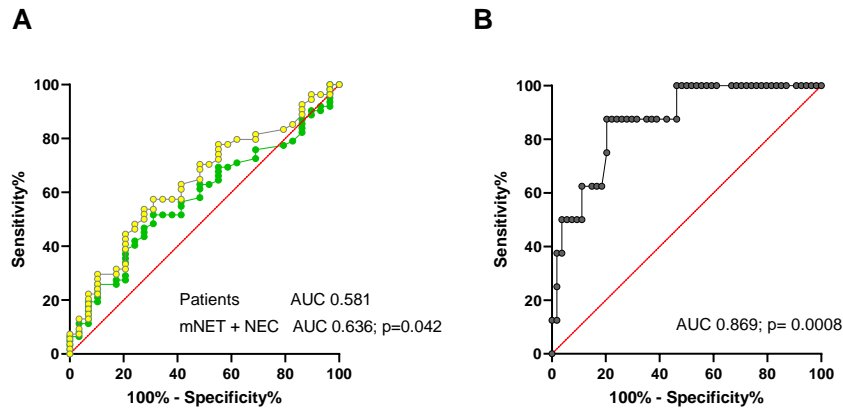


Figure 47. Hypomethylation receiver operating characteristic (ROC) plots
 A) Comparison between the controls to patients and the controls to metastatic NET+NEC subgroups.
 B) Comparison between non-metastatic NET and metastatic NETs+NECs subgroups.

Table 17. The sensitivity and corresponding cut-off levels of *ALU*-hypomethylation
 The comparison control vs. patients, control vs. metastatic NET+NEC subgroups, and metastatic NET+NEC vs. non-metastatic NET subgroup specificity levels between 60-90%.

| | | SPECIFICITY [%] | | | | |
|-----------------|-----------------------|--------------------|------|------|------|------|
| | | 90 % | 80 % | 70 % | 60 % | |
| SENSITIVITY [%] | CONTROL TO | Patients | 19.4 | 27.4 | 47 | 51.6 |
| | | Cut-off [%] | 1.80 | 1.59 | 1.41 | 1.33 |
| | Non-metastatic NET TO | Metastatic NET+NEC | 22.2 | 31.5 | 53.7 | 57.4 |
| | | Cut-off [%] | 1.8 | 1.58 | 1.40 | 1.33 |
| | | Metastatic NET+NEC | 33 | 79 | 81 | 89 |
| | | Cut-off [%] | 1.4 | 1.13 | 1.12 | 1.06 |

3.3.4.1 Correlation of hypomethylation percentage with clinical characteristics

The Kruskal-Wallis test evaluated a nonparametric comparison of hypomethylation percentage with tumor grade, tumor burden, and localization. The Spearman correlation test calculated correlation to age and CgA. Welch's t-test assessed the relationship to gender. A P value \leq of 0.05 was considered statistically significant. In the patients, various clinical factors effects on biomarkers were analyzed in all plasma samples irrespective of whether they belonged to which subgroups of patients. The impact of tumor burden on hypomethylation was examined in plasma samples regardless of whether they belonged to which group.

Association between the percentage of hypomethylation and age or gender

No significant correlation could be calculated by the Spearman correlation test for age and hypomethylation level ($p > 0.05$). The correlation of hypomethylation percentage to age is shown in Fig.48.

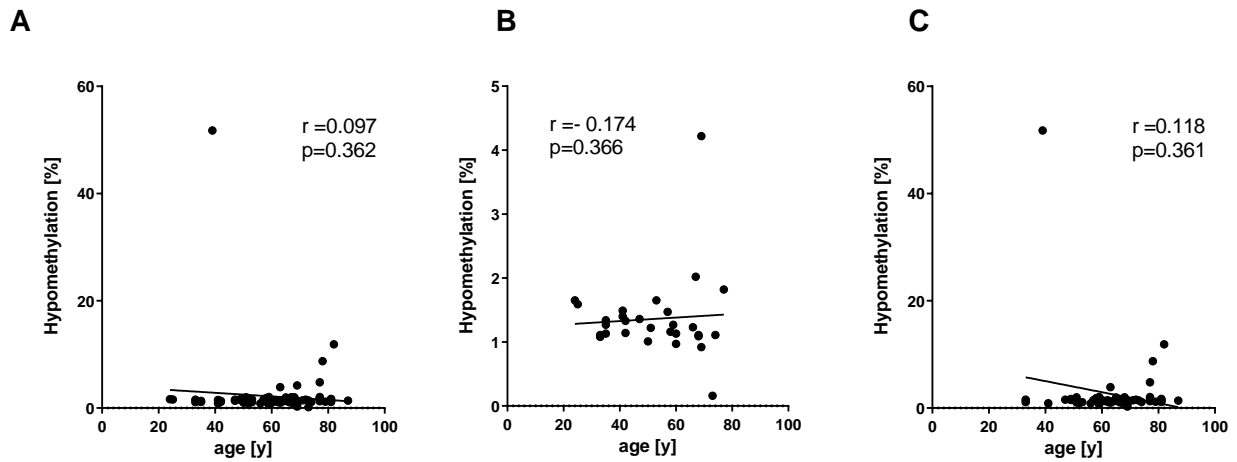


Figure 48. Correlation of hypomethylation percentage to age

The percentage of hypomethylation was measured by unmethylated cfDNA-*ALU* percentage. Spearman correlation test was used to assess any differences between the age and hypomethylation percentage in A) total subjects, B) controls, and C) patients.

Differences between hypomethylation percentage and gender were assessed. The median of hypomethylation was 1.28 (0.52 IQR) % and 1.32 (0.47 IQR) % for men and women, respectively. Welch's t-test confirmed no significant differences for gender-specific hypomethylation ($p = 0.317$).

Association between the percentage of hypomethylation and grades

Regarding tumor grade, a higher hypomethylation percentage was observed in G1 (1.27(IQR 0.36) %), G2 (1.39(IQR 0.48) %) and G3 (2.83(IQR 6.37)) tumor grade patients compared to the controls with 1.23(IQR 0.36) %. Comparison of the percentage of *ALU* unmethylation in different grades determined an elevated trend of the hypomethylation percentage from G1 to G2 and G3 (Fig.49). Kruskal-Wallis test was used to evaluate the differences in the hypomethylation percentage values between the samples from controls, G1, G2, and G3 tumors. A significant difference was found among groups ($X^2 = 7.72$, $P = 0.052$). Dwass-Steel-Critchlow-Flinger was revealed a significant difference between the controls with patients with tumor G3 ($p = 0.054$).

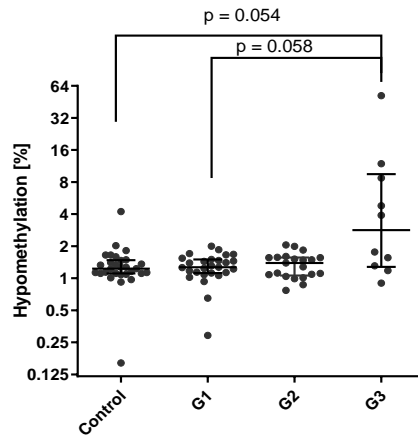


Figure 49. Hypomethylation percentage grouped by to tumor grade
Hypomethylation percentage values were determined by cfDNA-*ALU* unmethylated percentage. The data are divided into different groups depending on the tumor grade (controls, G1 (grade 1), G2 (grade 2), and G3 (grade 3) tumors).

In the current ROC curve analysis, the hypomethylation percentage was able to distinguish between the patients with G3 (n= 10) tumor grade from the controls with an estimated AUC of 0.77 (95% CI, 0.572 to 0.973; P=0.011). From the ROC curve, a cut-off of 1.53% of hypomethylation gave a sensitivity of 70% and a specificity of 79.3% for the detection of patients with G3 tumors (Fig. 50). The cut-off levels at different specificity levels are given in Table 18.

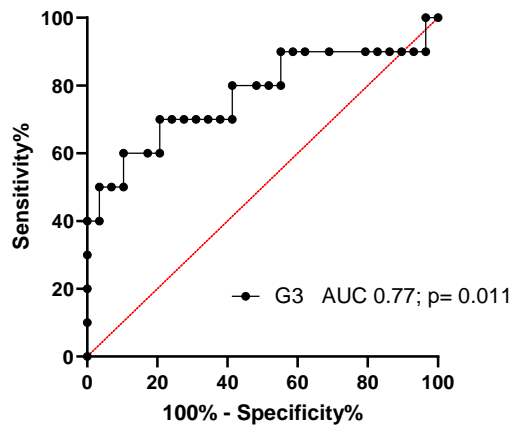


Figure 50. Hypomethylation receiver operating characteristic (ROC) curve for tumor grade 3
ROC analysis of hypomethylation level for distinguishing the controls from the patients with G3 tumor, along with the area under the curve (AUC).

Table 18. The sensitivity and corresponding cut-off levels of *ALU*-hypomethylation for G3 tumor
From the comparison controls vs. patients with a G3 tumor at specificity levels between 60-95%.

| | | SPECIFICITY [%] | | | | | |
|-----------------|-------------|-----------------|------|------|------|------|------|
| | | 95 % | 90 % | 85 % | 80 % | 70 % | 60 % |
| SENSITIVITY [%] | G3 | 50 | 50 | 60 | 60 | 70 | 70 |
| | Cut-off [%] | 2.70 | 1.8 | 1.64 | 1.59 | 1.40 | 1.33 |

Correlation between hypomethylation level and tumor burden

The Spearman test showed a positive correlation between hypomethylation percentage and tumor burden ($r=0.424$, $p < 0.0001$).

An increasing tendency was observed from the no tumor group (1.13 (IQR 0.31))% to the group with high tumor load (4.34 (IQR 7.69) %). The hypomethylation percentage was in patients with low and moderate tumor burdens as (1.27 (IQR 0.540) and (1.39 (IQR 0.3), respectively.

Kruskal Wallis test showed a significant difference among groups ($\chi^2=22.62$; $p < 0.001$). The patients with high tumor load were significantly different from groups with no tumor, with low and moderate tumor burdens ($p < .001$, $p=0.004$, and $p < .001$, respectively)(Fig.51).

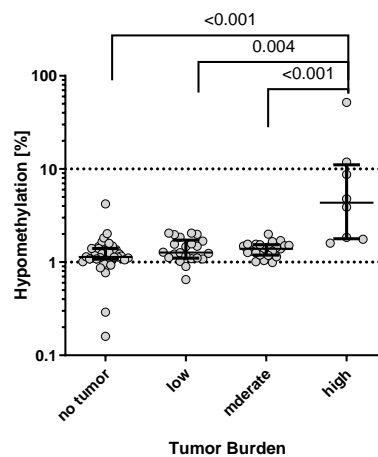


Figure 51. The percentage of hypomethylation grouped by tumor burden

The percentage of hypomethylation was measured by unmethylated cfDNA-*ALU* percentage. The data are divided into different groups depending on tumor burden (no tumor, low, moderate, and high). Kruskal-Wallis analysis was performed to test the differences in hypomethylation percentage between the groups. Dwass-Steel-Critchlow-Flinger was applied as a post hoc test; P values ≤ 0.05 were considered significant.

In the current ROC curve analysis, the percentage of hypomethylation was able to distinguish between the patients with different tumor loads (low, moderate, and high) from the group with no tumor burden with an AUC of 0.70 (95% CI, 0.590 to 0.808; $P=0.001$). At a cutoff of 1.18%, patients with different tumor burdens could be detected at a sensitivity of 77.4% and a specificity of 55.3%. An AUC of 0.75 distinguished the patients with moderate and high tumor burden (95% CI, 0.638 to 0.869; $p= 0.003$). The sensitivity and specificity for the patients with moderate and high tumor burden were 87.1 and 55.3% at the cut-off value of 1.17.

At a cutoff of 1.60%, patients with a high tumor load could be detected at a sensitivity of 100% and a specificity of 86.8%. The AUC of the ROC curve was 0.96 (95% CI, 0.915 to 1.00; $p < 0.0001$) (Fig.52).

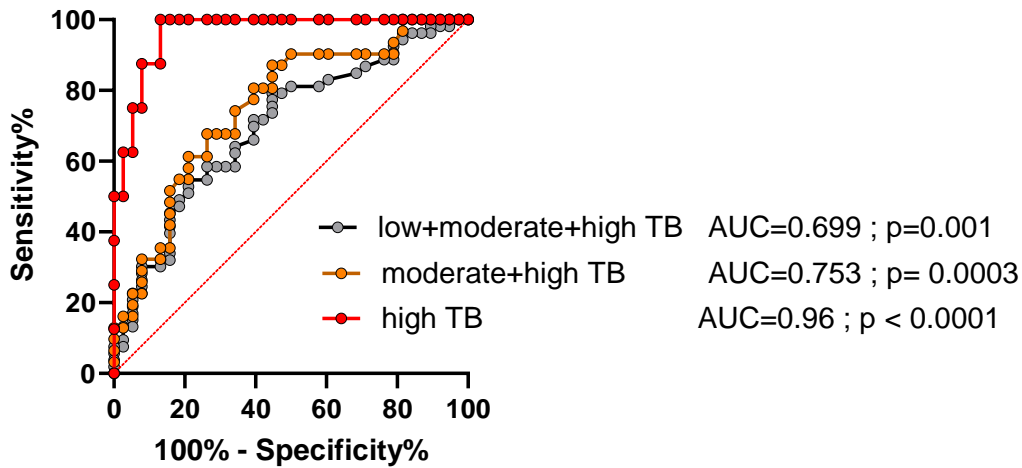


Figure 52. Hypomethylation receiver operating characteristic (ROC) curve for tumor burdens
 ROC analysis of hypomethylation percentage for distinguishing the group with no tumor from the patients with low, moderate, and high tumor burden (TB). Tumor burdens of low plus moderate and high (grey), moderate plus high (orange), and high (red), along with the area under the curve (AUC).

Association between the percentage of hypomethylation and tumor origin

Regarding tumor origin, the hypomethylation percentage was higher in the patients with lung (1.57(IQR 2.36) %), rectum (1.57(IQR 6.04) %), and pancreas (1.46(IQR 0.72) %) tumor origin compared to other groups. The patients with stomach, small intestine, and ileum tumor origin had the hypomethylation percentage of (1.13(IQR 0.99) %), (1.34(IQR 0.48) %) and (1.23(IQR 0.40) %). Kruskal Wallis test shows no significant difference between the tumor origin groups corresponding to hypomethylation percentage ($X^2= 4.680$; $P = 0.456$) (Fig.53).

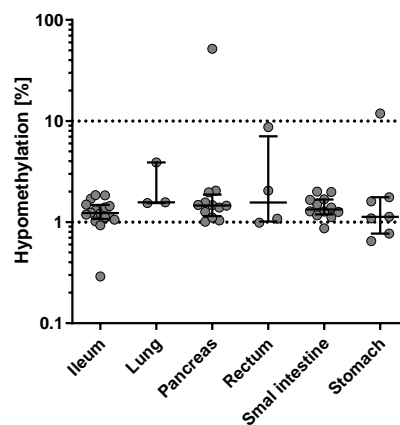


Figure 53. Hypomethylation percentage grouped by tumor origin
 Hypomethylation percentage was determined by cfDNA-ALU unmethylated percentage. The data are divided into different groups depending on tumor origin.

Association between the percentage of hypomethylation with serum-CgA level

A correlation with the serum-CgA level of the patients revealed a significant positive relation with hypomethylation percentage in the total patient group ($p = 0.009$) (Fig.54).

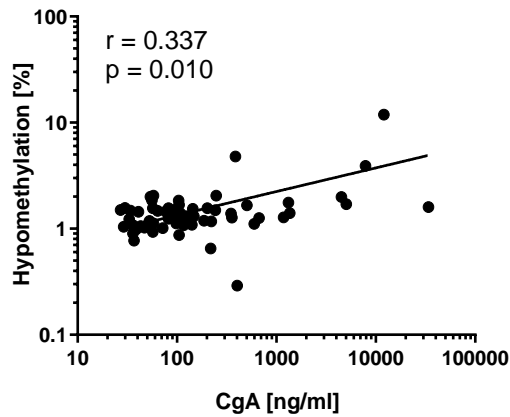


Figure 54. Correlation of CgA hormonal status and hypomethylation percentage in the patient group. Spearman correlation revealed a weak and significant correlation for hypomethylation levels. The correlation was considered significant at \leq the 0.05 level.

3.3.5 Biomarkers correlation analysis

The Spearman-Rank-correlation test performed the correlation of measured biomarkers in the control and patients. No correlation between biomarkers in the control group was observed; thus, the graphs and data were not shown. The correlation was considered significant at \leq the 0.05 level.

3.3.5.1 Correlation of cfDNA level with longer fragments concentration

Comparing cfDNA with *ALU* 260-bp or *LINE-1* 266-bp fragments level showed that they characterized two dependent biomarkers. In the patient group, total cfDNA had a moderate negative correlation with *ALU* 260-bp fragments level ($r = -0.49$, $P < 0.0001$), as well as with *LINE-1* 266-bp fragments level ($r = -0.46$, $P = 0.0002$) (Fig.55).

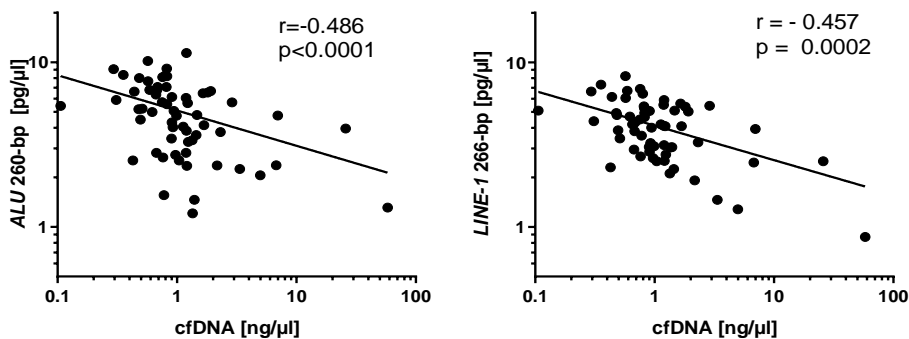


Figure 55. Correlation of cfDNA level with larger fragments. The correlation of cfDNA level with *ALU* 260-bp and *LINE-1* 266-bp fragments was analyzed by the Spearman-Rank-correlation test. The data was illustrated in the patients. The correlation was considered significant at \leq the 0.05 level.

3.3.5.2 Correlation of cfDNA level with shorter fragments concentration

The comparison of cfDNA and short fragments level showed that they characterized two independent biomarkers. The interaction between cfDNA level and *ALU* 115 fragments level was very weak negative correlation ($r = -0.159$, $p = 0.217$). There was a very weak correlation between cfDNA with *LINE-1* 97-bp fragments level ($r = 0.008$, $p = 0.952$). The correlation was not significant for both fragments (Fig.56).

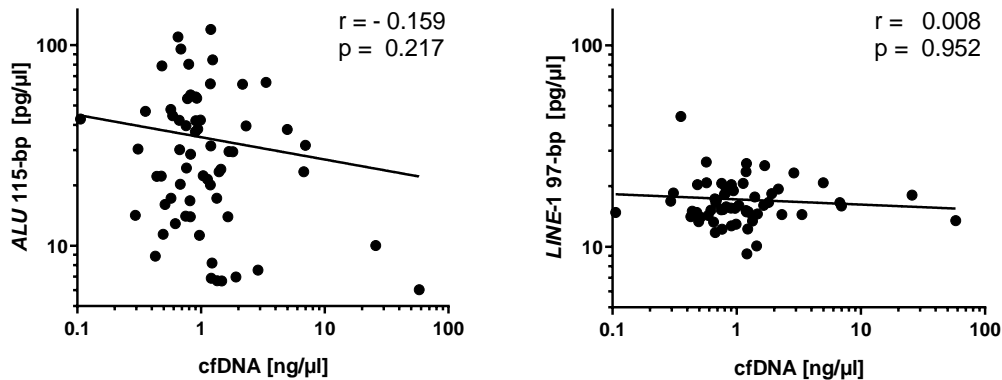


Figure 56. Correlation of cfDNA level with shorter fragments

The correlation of cfDNA level with *ALU* 115-bp and *LINE-1* 97-bp fragments was analyzed by the Spearman-Rank-correlation test. The data was illustrated in the patients. The correlation was considered significant at \leq the 0.05 level.

3.3.5.3 Correlation of cfDNA level with integrity indexes

The results of cfDNA concentration and cfDNA integrity for *LINE-1* had a moderate negative correlation ($r = -0.479$, $p < 0.0001$). The cfDNA concentration and cfDNA integrity for *ALU* showed a weak negative correlation ($r = -0.122$, $p = 0.344$). According to a significant relationship between cfDNA level and *LINE-1* cfDII, it was apparent that the cfDNA level and *LINE-1* cfDII represent two dependent biomarkers (Fig.57).

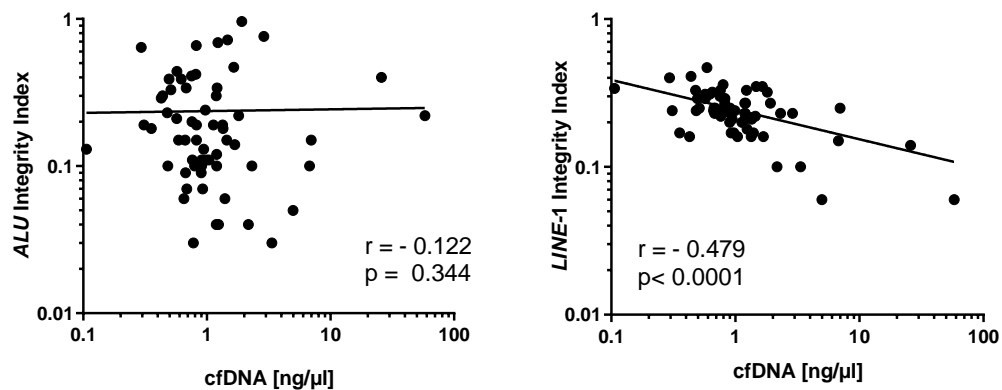


Figure 57. Correlation of cfDNA level with integrity indexes

The correlation of cfDNA level with the integrity indexes was analyzed by the Spearman-Rank-correlation test. The data was illustrated in the patients. The correlation was considered significant at \leq the 0.05 level.

3.3.5.4 Correlation of cfDNA level with hypomethylation percentage

The comparison of cfDNA and hypomethylation percentage showed that they characterized two dependent biomarkers in the patient group but with weak correlation ($r = 0.375$, $p = 0.003$) (Fig. 58).

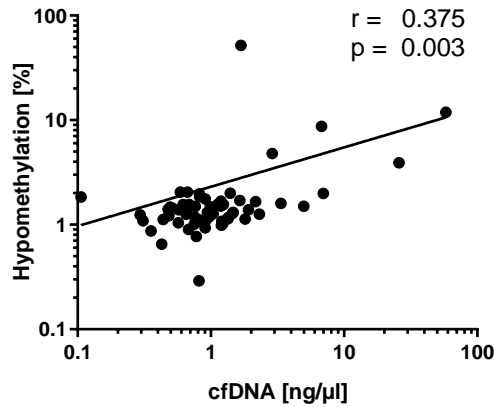


Figure 58. Correlation of cfDNA level with hypomethylation percentage

The correlation of cfDNA level with hypomethylation percentage was analyzed by the Spearman-Rank-correlation test. The data was illustrated in the patients. The correlation was considered significant at ≤ 0.05 level.

3.3.5.5 Correlation of hypomethylation percentage with longer fragments concentration

The comparison of cfDNA and longer fragments level showed that they characterized two independent biomarkers. The interaction between cfDNA level and *ALU* 260-bp fragments level was very weak negative correlation ($r = -0.211$, $p = 0.099$). There was a very weak negative correlation between cfDNA and *LINE-1* 266-bp fragments level ($r = -0.198$, $p = 0.123$). The correlation was not significant for both fragments (Fig.59).

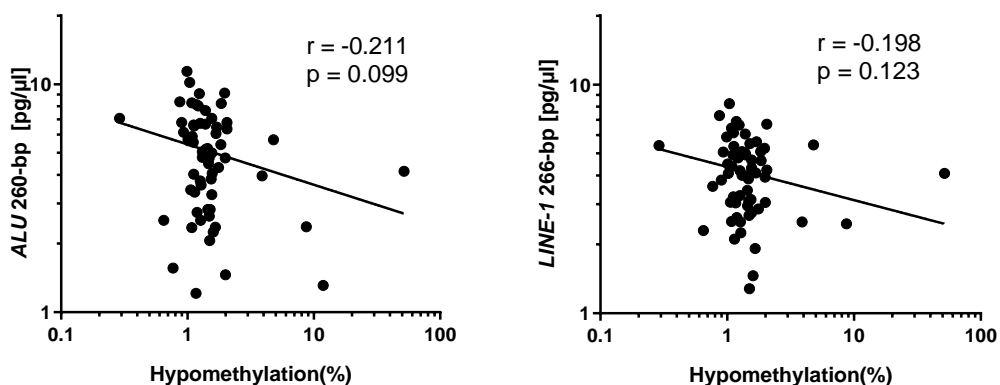


Figure 59. Correlation of hypomethylation percentage with longer fragments

The Spearman-Rank-correlation test analyzed the correlation of hypomethylation percentage with longer fragments. The data was illustrated in the patients. The correlation was considered significant at ≤ 0.05 level.

3.3.5.6 Correlation of hypomethylation percentage with shorter fragments concentration

The comparison of cfDNA and shorter fragments levels showed that they characterized two independent biomarkers. The interaction between cfDNA level and *ALU* 115-bp fragment levels was very weak negative correlation ($r = -0.030$, $p = 0.814$). There was a very weak correlation between cfDNA with *LINE-1* 97-bp fragment levels ($r = 0.046$, $p = 0.721$). The correlation was not significant for both fragments (Fig.60).

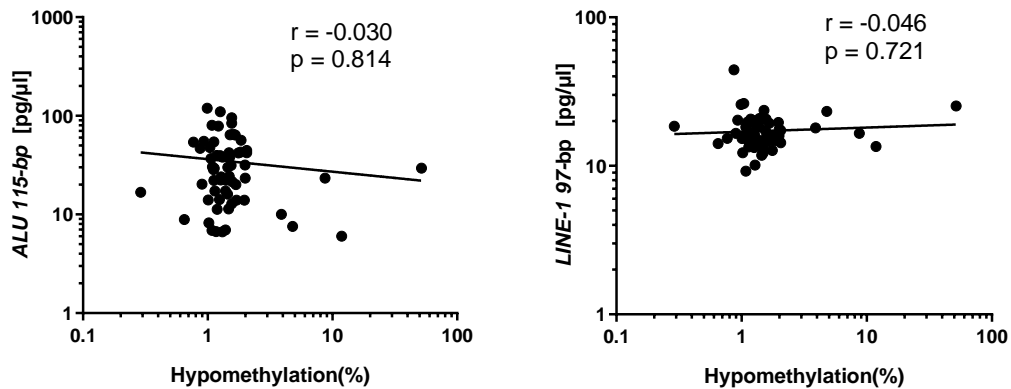


Figure 60. Correlation of hypomethylation percentage with shorter fragments

The Spearman-Rank-correlation test analyzed the correlation of hypomethylation percentage with shorter fragments. The data was illustrated in the patients. The correlation was considered significant at \leq the 0.05 level.

3.3.5.7 Correlation of hypomethylation percentage with integrity indexes

Hypomethylation percentage and *ALU* cfDII represent a very weak negative correlation in ($r = -0.091$, $p = 0.482$). There was a weak negative interaction between hypomethylation percentage and *LINE-1* cfDII ($r = -0.175$, $p = 0.174$). A significant relationship was not observed between the hypomethylation percentage and both cfDIIs. It was apparent that the hypomethylation percentage and both cfDIIs represent two independent biomarkers (Fig.61).

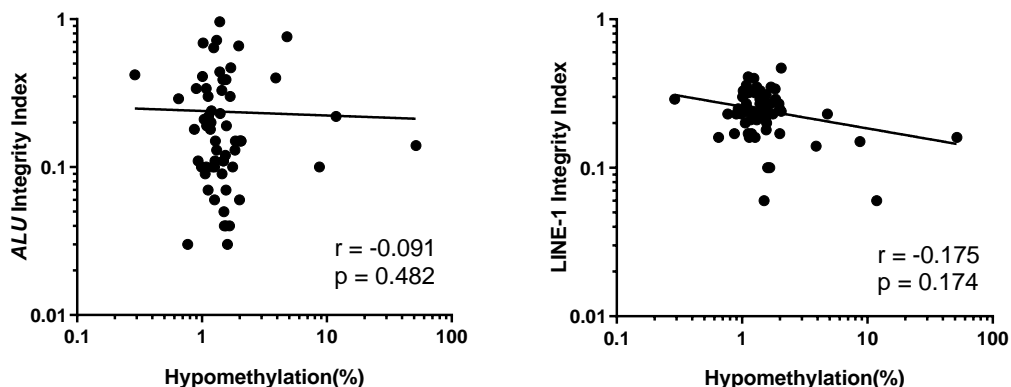


Figure 61. Correlation of hypomethylation percentage with integrity indexes

The Spearman-Rank-correlation test analyzed the correlation of hypomethylation percentage with integrity indexes. The data was illustrated in the patients. The correlation was considered significant at \leq the 0.05 level.

3.3.6 Prognostic value evaluation

The multiple logistic regression of measured potential biomarkers was performed to assess the ability to differentiate the cancer patients from the controls by the measured value. The control group was compared to the mNET patients plus NEC patients to predict a prognostic potential. The different combinations of biomarkers showed different AUCs for ROC curve analysis (Fig.62).

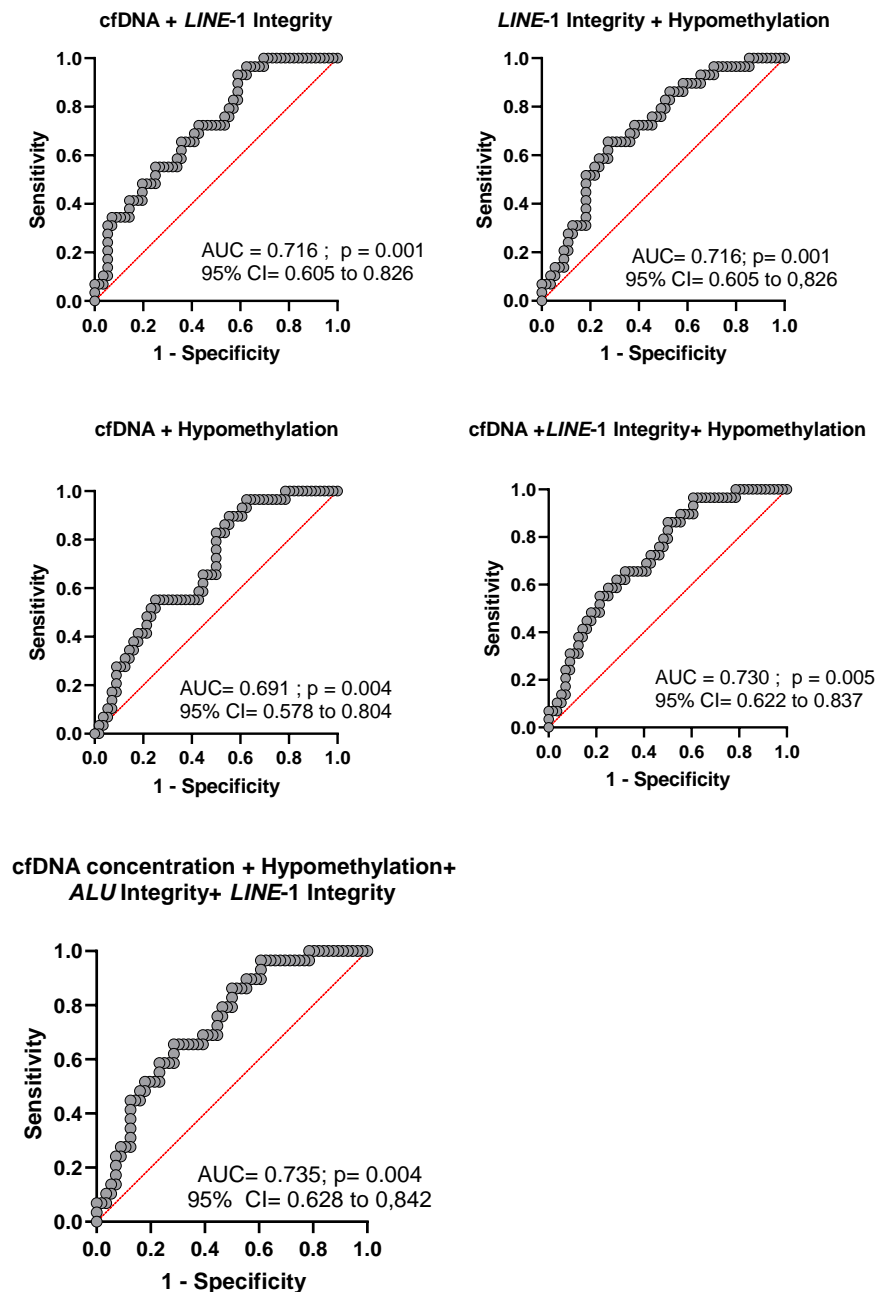


Figure 62. Receiver operating characteristic (ROC) curve analysis for controls vs. metastatic NET+NEC subgroups by a combination of investigated biomarkers

Receiver operating characteristic (ROC) curves of the biomarkers for distinguishing controls from metastatic NET+NEC subgroups were analyzed combined, a logistic regression model was used for the combination of these biomarkers. Biomarkers included cfDNA level, hypomethylation, *LINE-1*, and *ALU* integrity indexes.

If we compared the non-mNETs to mNETs plus NEC, more discriminatory power would be achieved for the combination of cfDNA+hypomethylation level and cfDNA+hypomethylation+*LINE-1* cfDII (Fig.63).

The calculated ROC AUC was 0.87 (95% CI, 0.756–0.984; $P=0.001$), which was suggestive of a good discrimination power for cfDNA+hypomethylation biomarkers. A positive predictive value of 66.7% and a negative predictive value of 89.8% were demonstrated.

The combination of cfDNA+hypomethylation+*LINE-1* cfDII in the plasma for the identification of non-metastatic NETs from mNET+NEC presented an AUC of 0.887(95% CI, 0.793–0.980; $P=0.001$), with positive and negative predictive values of 66.7%, and 89.8%, respectively.

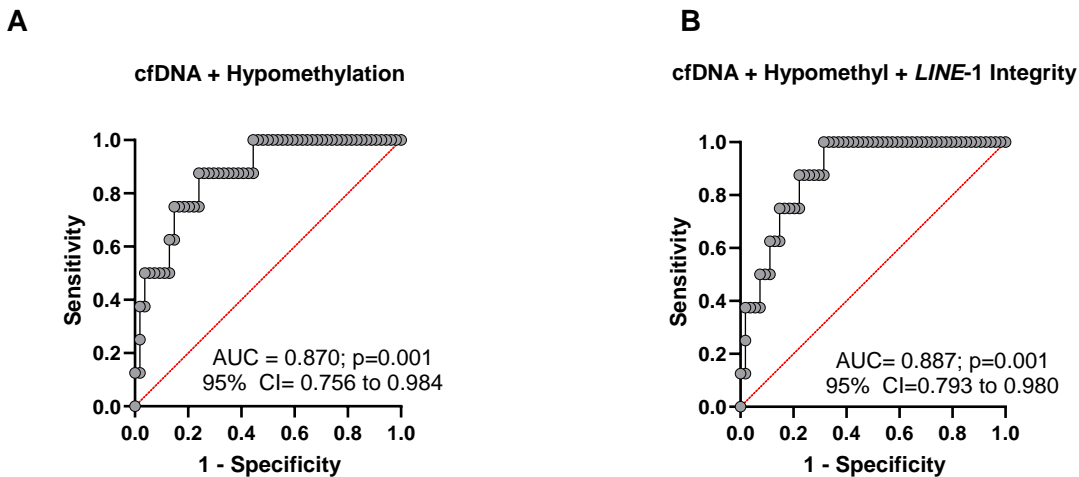


Figure 63. Receiver operating characteristic (ROC) curve analysis for non-metastatic NETs vs. metastatic NET+NEC subgroups by a combination of investigated biomarkers

Receiver operating characteristic (ROC) curves of the biomarkers for distinguishing non-metastatic NETs from metastatic NET+NEC subgroups were analyzed combined, a logistic regression model was used for the combination of these biomarkers. Biomarkers included in each plot are (A) cfDNA level+ hypomethylation; (B) cfDNA level+ hypomethylation +*LINE-1* integrity index.

The serum-CgA level was not determined in the control group; thus, the non-mNETs were compared to mNETs plus NEC. An AUC of 0.57 (95% CI=0.339 to 0.801; $p=0.551$) for serum-CgA level between non-mNET and mNET+ NEC patients was achieved.

If we combined the serum-CgA level with other biomarkers, the AUC was increased. A good AUC was calculated with combination of serum-CgA and hypomethylation level (AUC= 0.87, 95% CI=0.738 to 1.00; $p=0.002$). The negative and positive predictive powers were 90.91 and 66.67%, respectively. The combination of the serum-CgA level with cfDNA and hypomethylation showed a great AUC of 0.91(95% confidence interval 0.825 to 0.995; $p=0.001$) and negative and positive predictive powers of 90.91 and 66.67%, respectively. Also, a very good AUC was achieved when the serum-CgA level was combined with cfDNA, *LINE-1* cfDII, and hypomethylation levels (AUC= 0.91, 95% confidence interval 0.813 to 0.996; $p=0.001$), with negative predictive and positive predictive powers of 89.29 and 50.00, respectively (Fig.64).

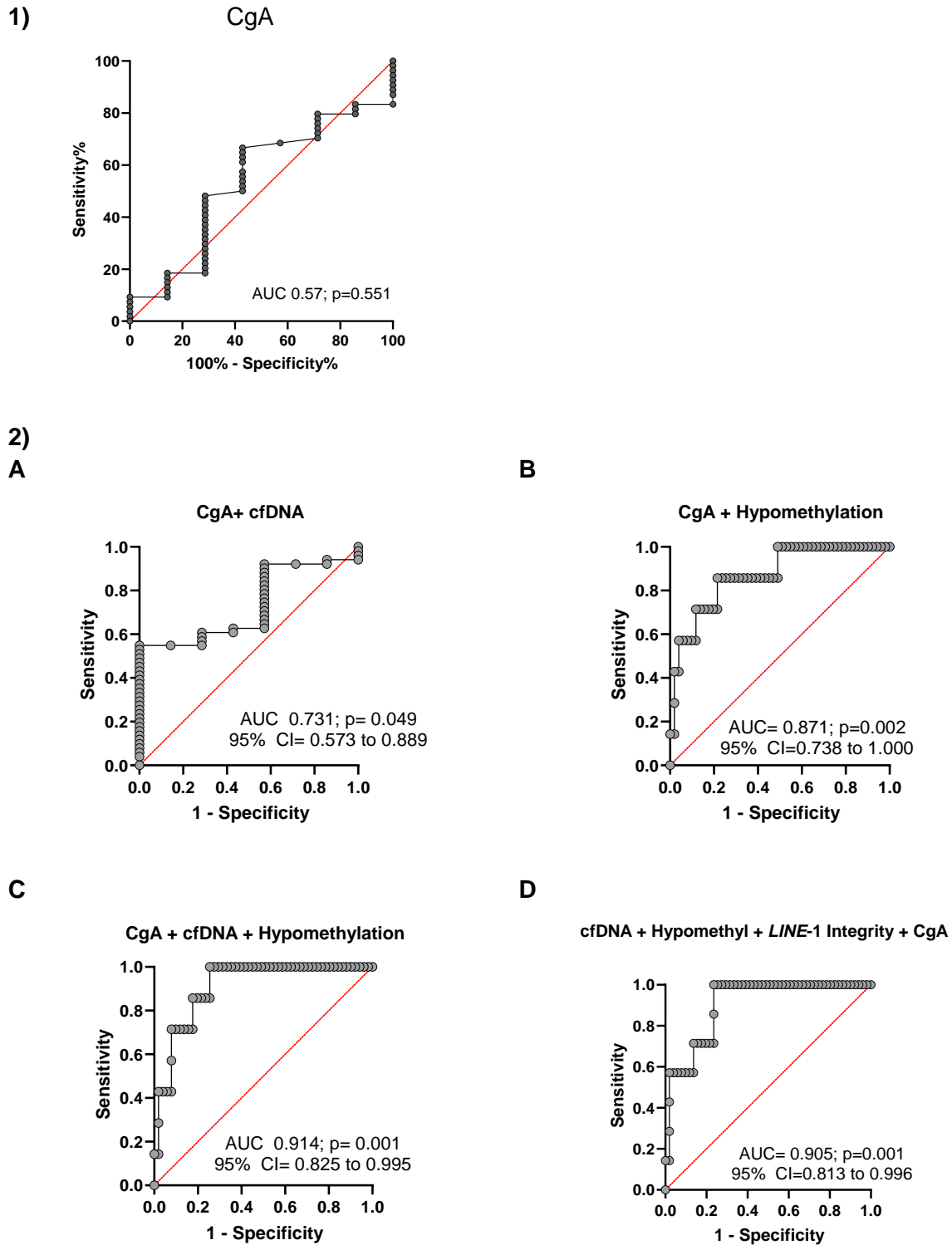


Figure 64. Receiver operating characteristic (ROC) curve analysis of 1) individual CgA level biomarker and 2) combined with investigated biomarkers in non-metastatic NETs and metastatic NET+NEC subgroups Receiver operating characteristic (ROC) curves of the biomarkers for distinguishing non-metastatic NETs from metastatic NET+NEC subgroups were analyzed combined, a logistic regression model was used for the combination of CgA level with investigated biomarkers. Biomarkers included in each plot are (A)CgA +cfDNA level; (B) CgA level+ hypomethylation; (C) CgA level+ cfDNA+ hypomethylation;(D) CgA level+ cfDNA+hypomthylation + LINE-1 integrity index.

The group with no tumor (control+non-mNETs) was compared to the patients categorized in different tumor burden groups to predict a prognostic potential. The different combinations of biomarkers showed different AUCs for ROC curve analysis (Fig.65). The ROC analysis indicated that a combination of cfDNA levels with hypomethylation or *LINE-1* DII showed moderate accuracy to distinguish samples with no tumor load from patients with low, moderate, and high tumor loads (AUC =0.724 and 0.716, respectively). cfDNA concentrations added little information to a combination of *LINE-1* DII and hypomethylation to differentiate samples with no tumor load from patients with low, moderate, and high tumor loads as it increased the AUC from 0.743 to 0.758.

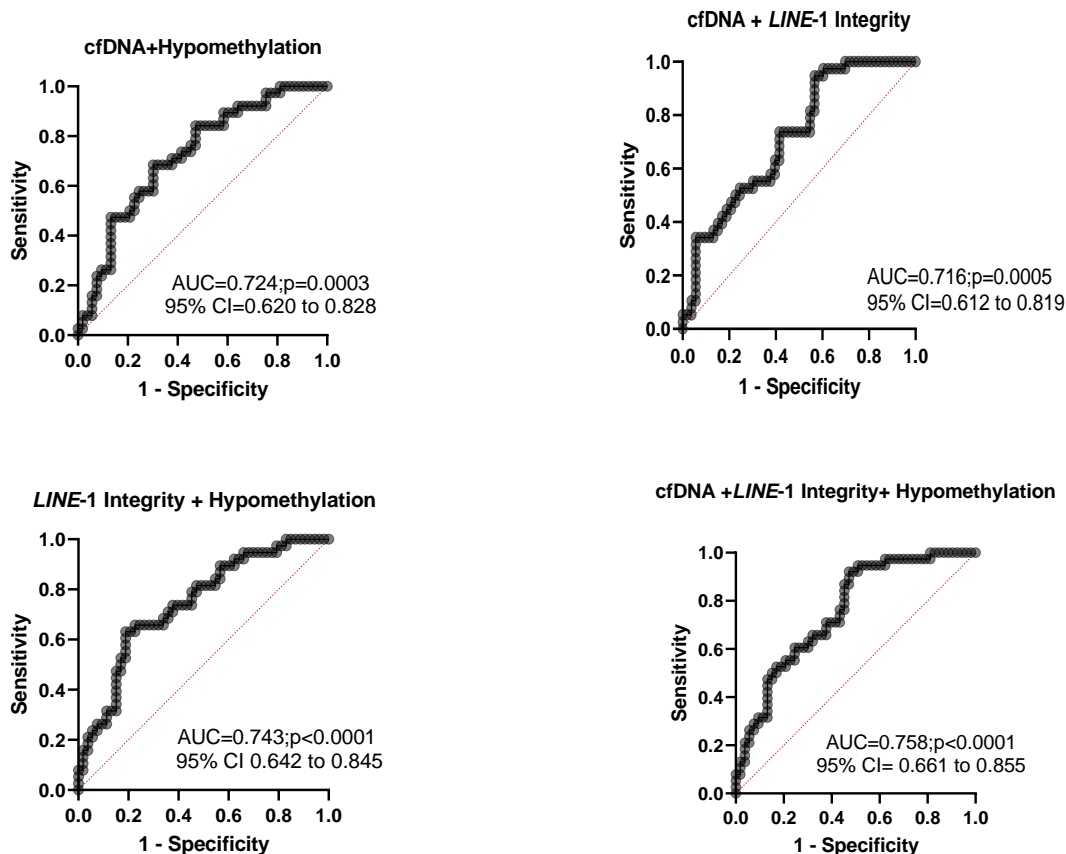


Figure 65. Receiver operating characteristic (ROC) curve analysis for samples with no tumor burden (control+non-mNETs) from low, moderate, and high tumor burden subgroups
Receiver operating characteristic (ROC) curves of the biomarkers for a distinguishing group with no tumor burden (control+non-mNETs) from low, moderate, and high tumor burden subgroups were analyzed combined, a logistic regression model was used for the combination of these biomarkers. Biomarkers included cfDNA level, hypomethylation, and *LINE-1* integrity index.

To include the CgA level of the patients for Multiple logistic regression analysis the healthy controls were excluded from the reference group. The serum-CgA level was not determined in the control group; thus, the group with no tumor included only non-mNETs that were compared to patients with different tumor burdens.

An AUC of 0.62 (95% CI=0.402 to 0.843; $p=0.269$) for a serum-CgA level between patients with no tumor and patients with different tumor loads was calculated. CgA showed an AUC of 0.64 (95% CI=0.413 to 0.871; $p=0.223$) for the distinction of patients with moderate and higher tumor burden. The highest discriminatory power was found for the group with a large tumor load (AUC=0.875 (95% CI=0.692 to 1.00; $p=0.020$)) (Fig.66).

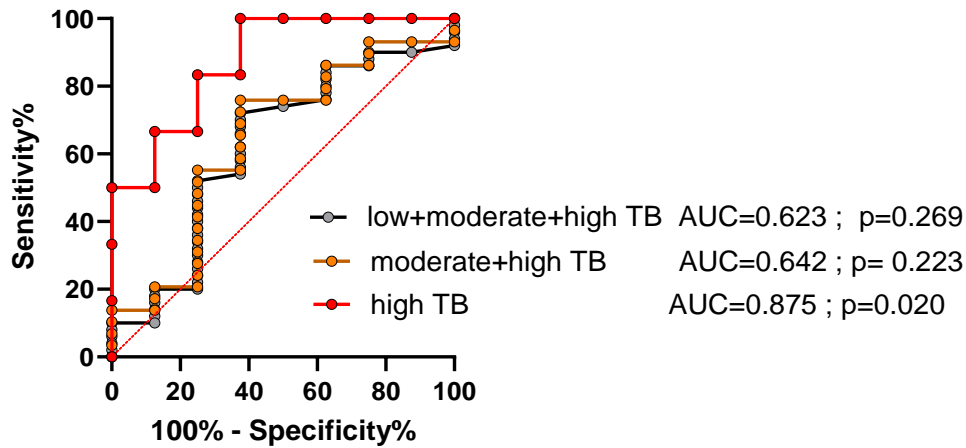


Figure 66. CgA level receiver operating characteristic (ROC) curve for tumor burdens
ROC analysis of CgA level for distinguishing the patients with no tumor from the patients with low, moderate, and high tumor burden (TB). Tumor burdens of low plus moderate and high (grey), moderate plus high (orange), and high (red), along with the area under the curve (AUC).

If we combined the serum-CgA level with other biomarkers, the AUC was increased (Fig. 67). The AUC of 0.871 was achieved to distinguish patients with different tumor loads from patients with no tumor when the serum-CgA level was combined with hypomethylation levels (95% CI=0.738 to 1.00; $p=0.002$). The negative and positive predictive powers were 90.91 and 66.67, respectively. The combination of serum-CgA and cfDNA +*LINE-1* cfDII+ hypomethylation levels showed a greater AUC (0.924) than other combinations (95% CI=0.847 to 1.00; $p<0.0001$). Interestingly, the AUC of the combination of serum-CgA and hypomethylation+ cfDNA was somehow similar to that of the combination of all four biomarkers (AUC=0.910) (95% CI=0.825 to 0.995; $p=0.001$), with a positive and negative predictive power of 90.91 and 66.67, respectively.

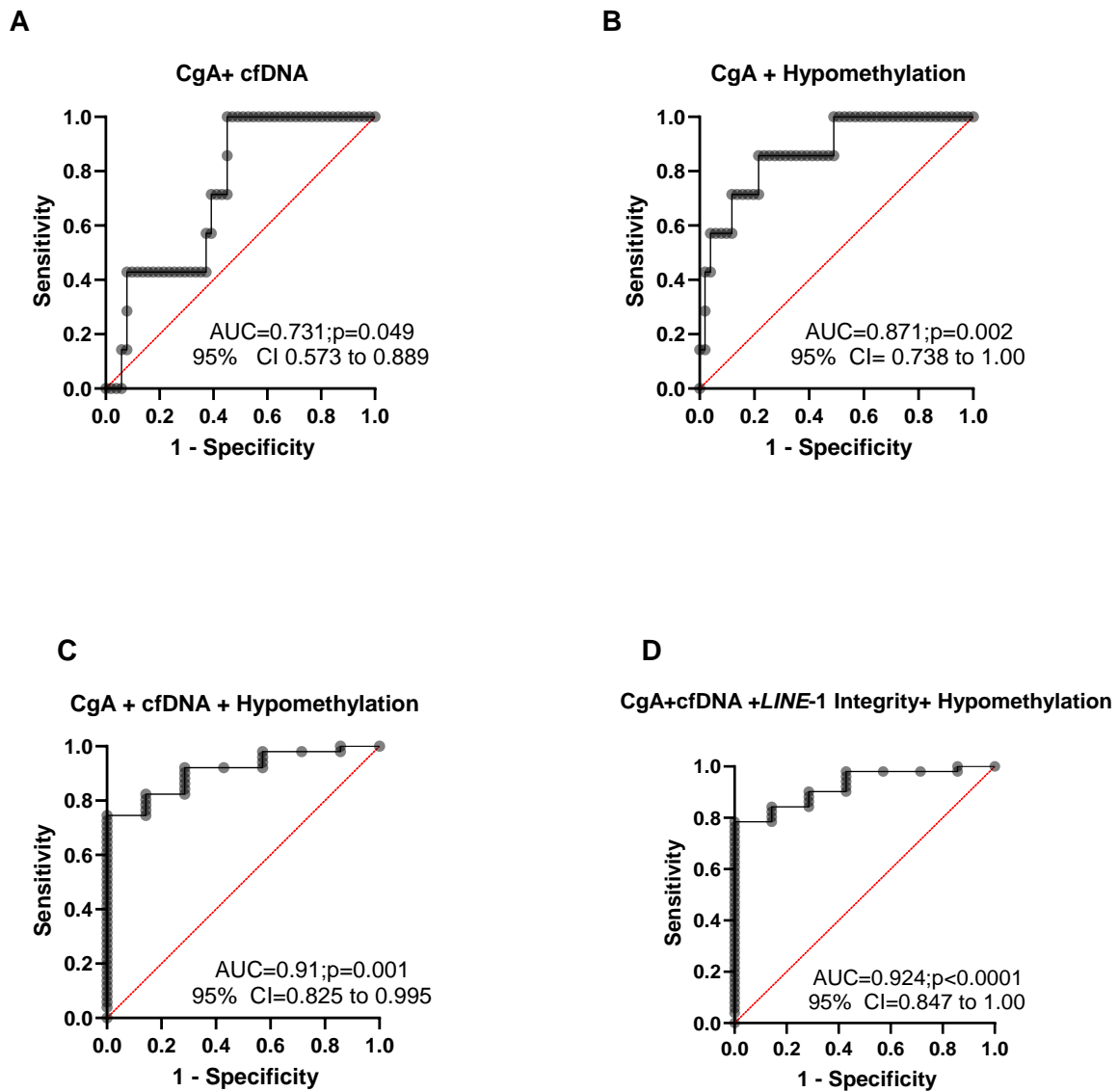


Figure 67. Receiver operating characteristic (ROC) curve analysis of CgA level biomarker combined with investigated biomarkers for samples with no tumor burden (non-mNETs) from low, moderate, and high tumor burden subgroups

Receiver operating characteristic (ROC) curves of the biomarkers for distinguishing groups with no tumor burden(non-mNETs) from low, moderate, and high tumor burden subgroups were analyzed combined, a logistic regression model was used for the combination of CgA level with investigated biomarkers. Biomarkers included in each plot are (A)CgA +cfDNA level; (B) CgA level+ hypomethylation; (C) CgA level+ cfDNA+ hypomethylation;(D)CgA level+ cfDNA+hypomthylation + *LINE-1* integrity index.

4. Discussion

Some studies focus on liquid biopsy, especially blood analysis at a molecular level as a non-invasive method for diagnosing, prognosis, and monitoring NEN cancers. There is a need to introduce sensitive and specific novel circulating biomarkers for NENs. For this purpose, four cfDNA-based biomarkers were examined in this study:

- a) cfDNA concentration
- b) cfDNA fragmentation
- c) cfDNA integrity
- d) cfDNA hypomethylation

4.1. cfDNA Isolation

The small overall amount of cfDNA in plasma, serum, and other body fluids is the main problem of biomarkers based on cfDNA. To establish biomarker-based cfDNA analysis, the extraction of the cfDNA must be valid and, above all, reproducible in the laboratory. The most critical points of the isolation process, which are decisive for reliable comparison, are discussed. This standardization ensures that patient-related differences cannot be traced back to incorrect or different processing.

The evaluation of new biomarkers from cfDNA starts with the isolation of the cfDNA. Usually, the cfDNA is obtained from blood serum or plasma. During method establishment, plasma and serum were tested as a source for cfDNA (data was not shown). A higher amount of cfDNA could be isolated from the serum compared to the plasma from the same person. It might be because extraneous DNA released from leukocytes lyse during the coagulation process^{160–169}. For this reason, the plasma was chosen for this study to avoid contamination with genomic DNA, which would cloud the results. EDTA-containing tubes (EDTA-K3) were used for the blood collection to prevent the blood coagulation instead of the heparin and citrate: Heparin and citrate can inhibit PCR by an interaction with DNA and DNA polymerase^{170,171}. The samples need to process within four h after the blood draw to prevent the release of germline DNA from the lysis of peripheral blood cells¹⁷². Since cfDNA has a half-life between 16 min and 2.5 h in blood, the samples were processed within 2 hours of blood collection in this study^{173–176}.

The high-speed centrifugation (<20,000 g) can fully obtain the low concentration of cfDNA in plasma. For optimal purification of plasma, two-step of cooled centrifugation, i.e., first at a slow speed to remove the blood cells followed by a high-speed to remove the cell debris, was applied as validated in the literature.

The thawing temperature of the plasma for optimal cfDNA extraction has not yet been described in the literature. Plasma thawing was applied at room temperature in this study. However, the effect of the thawing procedure (duration, i.e., fast vs. slow, temperature) on cfDNA quantity/quality must be studied further. Care was taken to ensure that the samples were not subjected to repeated freeze-thaw cycles. The samples with only one thawing cycle were used for the analysis.

The cfDNA isolation methods can affect cfDNA yield and recover shorter and longer cfDNA fragments¹⁷⁷. The most common method for cfDNA extraction is a spin column extraction kit.

Other used methods of extraction include magnetic beads, phenol/chloroform extraction, and alkaline salting. It was indicated that the extraction efficiency of the QIAamp® circulating nucleic acid kit (Qiagen, Hilden, Germany) and QIAamp DNA blood mini kit (Qiagen, Hilden, Germany) was better than FitAmp™ plasma/serum DNA isolation kit (Epigentek, Hopkinton, MA)¹⁷⁸. QIAamp circulating nucleic acid kit (Qiagen, Valencia, CA, USA) extracted less cfDNA (1.08 ng/μL) compared to Maxwell® RSC (MR) ccfDNA Plasma Kit (1.25 ng/μL)¹⁷⁷. The QIAamp® circulating nucleic acid can extract smaller DNA fragments (115-bp) than the QIAamp DNA blood mini kit, significantly affecting cfDNA integrity¹⁷⁸. The MagNA Pure Compact Nucleic Acid Isolation Kit I can isolate more cfDNA fragments ranging in size from 150-200-bp compared to Maxwell® RSC ccfDNA Plasma Kit method¹⁷⁷.

According to the present study, the QIAamp® MinElute® ccfDNA Midi Kit extraction method recovered more cfDNA yield than the QIAamp DNA Blood Mini Kit method. It was shown that the use of different extraction methods led to significant differences in the yield of cfDNA.

4.2 cfDNA concentration as a biomarker for NEN patients

High cfDNA levels in the blood have already been published in various cancers, such as breast cancer^{57,95,152,179,180}, malignant gastrointestinal¹⁸¹, colorectal^{96,123,182}, lung¹¹¹, ovarian¹⁸³, prostate^{184,185}, testicular germ cell cancer¹⁸⁶. In agreement with these studies, we demonstrated a trend towards a higher cfDNA level in the plasma for patients with NEN disease.

A cfDNA amount between 0 and 100 ng/ml of blood can be detected in healthy people. (average of 30 ng/ml)¹⁸⁷. A wide scatter of cfDNA values was reported according to the cfDNA source, the isolation technique, and the type, location, and stage of cancer in healthy individuals and cancer patients (App. Table 19). Up to now, a threshold value as a reference amount was not determined because of these possible variations¹⁸⁸.

So far only one study has been published that examines cfDNA levels in NEN patients. The study focuses on the relationship between plasma cfDNA levels and clinical features of low-grade patients with small bowel or pancreatic NETs. In contrast to the present study, the localization of the primaries has already been defined, i.e. H. small intestine or pancreas were included in the study and only patients with low-grade tumors. Higher cfDNA levels were reported in NET patients than in healthy controls, but there was no association with disease progression¹⁸⁹.

We have specifically examined the differences between the patients with a none metastatic NET disease (non-mNET), a metastatic NET disease (mNET), and very aggressive NEC disease. Patients with mNETs showed accuracy in the elevated cfDNA level compared to the healthy individuals. Interestingly, non-mNET patients showed the same low cfDNA concentration as healthy controls, most likely due to the no tumor burden. It seems to be the case that the more aggressive the tumor disease, the higher the cfDNA level of the patient (mNET and NEC > non-mNET), which has been reported before: the increased cfDNA level correlated with aggressive cancers¹⁹⁰. It has been shown that the cfDNA concentration increases with the duration of the disease and is particularly high in dying patients¹⁷⁷. A previous study reported that colon cancer patients with a high cfDNA value greater than 1000 ng/ml blood at the time of initial diagnosis had a shorter life expectancy than patients with a cfDNA value less than 1000 ng/ml blood. After 19 months, about 27% of patients with cfDNA concentrations more than 1000 ng/mL survived, and 73% were dead¹⁸². In the present study, thirteen patients showed a cfDNA level of more than 1500 ng/ml plasma. Four patients

died after less than six months, namely patients with the measured cfDNA concentrations of 58 200, 25 900, 2170, and 1680 ng/ml. One patient in the NEC subgroup died with only a measured cfDNA concentration of 688 ng/ml.

In another study, continuous measurement of the progression will provide information as to whether an increase in cfDNA correlates directly with progressive disease.

The accurate staging or grading in treating cancer patients is of primary importance. Treatment will be planned and recommended based on the stage of cancer. Knowing the stage gives an educated estimate of life expectancy and the chance of a cure. No significant differences between the healthy control group and the patients could be found for the tumor grade. However, if one looks at the cfDNA as a function of tumor differentiation, a significant difference to patients with highly differentiated tumors could be determined. It appears that, due to a higher cfDNA level over patients with G3 tumors, the cfDNA can represent a robust marker for differentiating healthy people (AUC = 0.803). Presumably, due to the small number of cases, we were only able to demonstrate a low sensitivity of 50% with a specificity of 100%.

Many studies have confirmed the correlation of high cfDNA level with tumor stage^{105,106,191–194} and tumor size^{94,112,121,195–198}. Finding a correlation between cfDNA level and tumor burden was another area of investigation. Tumor burden is a clinical factor associated with treatment response that can evaluate the efficacy of new cancer therapeutics. There is no uniform assessment method to determine the tumor burden. Radiologic assessment is widely used to measure anatomical tumor burden that has limitations, such as trouble measuring bone lesions and enhanced radiation load for the patient¹⁹⁹. In addition, circulating biomarkers, such as include carcinoembryonic antigen (CEA), carbohydrate antigen 199 (CA199), carbohydrate antigen 125 (CA125), neuron-specific enolase (NSE), lactate dehydrogenase (LDH), are used to monitor the tumor burden²⁰⁰.

Currently, there is no molecular blood biomarker to routinely evaluate tumor burden and treatment response for NEN patients. In this study, the increase of cfDNA level was correlated with tumor load, where patients with a high tumor load had the highest cfDNA concentration with a good discriminator power of AUC =0.84.

The data are conflicting about the association between cfDNA and tumor burden. The utility of cfDNA in the evaluation of tumor burden was reported in some published studies^{200–202}, while a study reported no correlation between cfDNA and tumor burden in lung cancer patients²⁰³. The relationship between cfDNA level and tumor burden was also found in human xenograft models, in which the cfDNA was increased with increasing tumor burden^{121,204}. Others reported that tumor-derived cfDNA load analysis could be more sensitive than using imaging techniques to monitor tumor burden in the lung, breast, and colorectal cancer^{205–208}.

In the current study, the cfDNA concentration was positively correlated with tumor load in NEN patients ($r= 417$; $p<0.0001$). It should be noted that the correlation obtained might not be tumor-specific because cfDNAs involve both healthy and tumor DNA. Hence, although the current study suggests cfDNA concentration as a quantitative biomarker of tumor burden in NEN patients, it will be important to assess the test performance with a strict process to isolate tumor-derived cfDNA in prospective cohort studies. The combination of cfDNA concentration and mutational frequency by analysis of tumor-derived cfDNA to assess tumor burden has been supported by other studies^{200,209–211}.

To the best of our knowledge, our study is the first to compare the cfDNA level with tumor burden in NENs. Comparison of the data with primary tumor size was not considered in the

current study, but the entire tumor mass, evaluated by the treating oncologist. A follow-up study with more patients with G3 tumors and a high tumor burden and strict monitoring could clarify the correlation of tumor grade, tumor size, tumor burden, and cfDNA level.

Since a NET primary can develop in the whole body, a correlation between the increase in biomarker and tumor location would be desirable. A higher cfDNA level could be detected in patients with a small intestine tumor as tumor origin in the present study. In comparison, a lower level could be identified in patients with pancreas cancer. We could only detect tendencies. No significant differences in cfDNA concentration depending on the location of the primary tumor could be determined.

Studies that observe the cfDNA level of the patients over a more extended time have observed an increased cfDNA level in the case of progressive disease or relapses.

In contrast, it decreased in tumor-free patients after surgery or after responding to anti-tumor therapy^{57,90,97,111,177,184,188,190,212–216}.

The cfDNA level and CgA were significantly correlated ($p=0.031$). CgA revealed a discriminatory power of 0.57 to differentiate between mNET+ NEC and non-mNET disease. Combining CgA to cfDNA level, the AUC could be increased to 0.73. This sensitivity and specificity are considered to be insufficient for the detection of mNET+NEC.

Undoubtedly, there is a significant lack of knowledge about the origin of cfDNA. Although it has already been proven that a large part of the cfDNA originates from apoptosis, it is clear that cfDNA is released into circulation by multiple mechanisms. Each of these mechanisms is modulated by a wide range of biological and environmental factors virtually unique to each individual. Variables include age, gender, ethnicity, body mass index, organ health, smoking, physical activity, diet, glucose levels, oxidative stress, drug status, infections, menstruation, and pregnancy⁷⁹. We determined a significant correlation between the cfDNA level and the age of all tested people. A publication like our observation did not find a clear correlation between the cfDNA status and age for only healthy individuals or patients²¹⁷.

Initial studies deal with the degradation of cfDNA in vitro and estimate the half-life of circulating cfDNA between 16 min and 2.5 h, but this requires further confirmation¹⁷⁵. The balance between releasing and clearance of cfDNA determines the amount of cfDNA within the bloodstream. The patient's physiological condition, such as asthma, glaucoma, diabetes, or any malfunction in various filtration organs, namely renal, spleen and liver, or circulating enzymes, may influence tumor DNA clearance after cancer recovery^{218,219}. The absolute cfDNA level could be directly affected by the cfDNA clearance rate, but cfDNA integrity would not be affected because the effect of cfDNA clearance on the amounts of longer and shorter DNA fragments would be similar¹⁵².

Unfortunately, cfDNA is so versatile but also very unstable and prone to outliers that we only recommend to a limited extent or in combination with other markers to establish the measurement of the absolute cfDNA plasma concentration as a biomarker for the identification of a NEN disease. Continuous cfDNA measurement should be considered in follow-up studies to better illustrate the course of the disease and to what extent a worsening of cancer can be mapped through cfDNA analysis.

4.3 cfDNA Fragmentation as a biomarker for NEN patients

In healthy individuals, the primary source of cfDNA is apoptotic cells, which release tiny fragments of cfDNA with ~185–200 base pairs in length. In contrast, cfDNA from cancer patients contains DNA fragments of two different sizes. Short fragments come from

hematopoietic cells and longer fragments from necrosis, autophagy, or mitotic catastrophe^{188,220}. CfDNA fragmentation was measured by amplifying short or long DNA fragments using the qPCR method. The primers were selected according to the mononucleosome average size¹²⁰, i.e., amplicon size of longer and shorter than 180-bp represent long and short fragments, respectively.

Inconsistent results were presented in earlier studies on the size of circulating DNA in cancer patients. Some amplicon-based studies have shown the increase in shorter fragments in some cancers, assuming that the short DNA fragments are due to tumor-derived cfDNA. Underhill et al. found the most common fragment lengths in patients with melanoma and lung cancer were 134 bp and 144 bp that was shorter than the most common fragment length in the healthy controls (167 bp)²²¹. They observed the highest proportion of mutant allele in 110-140-bp fragment lengths. Most of the previous reports examined tumor-derived fragments larger than 105 bp in size^{152,222-225}. The number of fragments carrying cancer-associated mutation would increase when shorter amplicons are selected^{120,226}. Diel et al., found that along with decreasing fragment sizes from 1,296 to 100 bp, the fraction of mutant molecules would increase by 5- to 20-fold in colorectal cancer patients²²⁶. Another study reported the varying presence of fragments in relation to their size (many of <100 bp, most with the size of 150-400 bp and low levels of > 400 bp fragments).in metastatic colon cancer compared to samples from healthy volunteers¹²⁰. Their findings confirmed greater fragmentation of the tumoral cfDNA (at a size <100 bp), while most previous amplicon-based studies estimated tumor-derived cfDNA from a size of 150 bp.¹²⁰ The size of tumor-derived cfDNA fragments for patients with renal, bladder, pancreatic, glioma, breast, melanoma, ovarian, lung, colorectal, cholangiocarcinoma was reported between 90–150 bp²²⁷.

The fragment lengths distribution identified for cfDNA in the present study was consistent with cellular apoptosis rather than necrosis. Concerning short fragments, no substantial difference for *ALU* 115-bp and *LINE-1* 97-bp was observed in any groups. The highest *ALU* 115-bp fragments levels in the subgroups were found in NEC > non-mNET > control > mNET. Likewise, the highest level of *LINE-1* 97-bp fragments in NEC patients and lowest in mNET was observed. Interestingly, patients with G3 tumors had higher levels of short pieces than G1 tumor patients. Meaning, the short fragment levels were specific for the late-phase disease in this study.

Umetani et al. previously reported similar findings from the serum of patients with advanced colorectal or periampullary cancer with regards to the higher level of *ALU* 115-bp fragment¹²³. Also, an increasing trend of *ALU*115-bp fragment value with tumor stage was found in breast cancer¹⁵². Contrary to our results, Thakur et al. detected a higher level of *ALU* 115-bp fragments in the benign patients characterized by the larger tumor size than thyroid cancer patients characterized by smaller tumor size²²⁸. No correlation was found between short fragments levels, i.e., *ALU* 115- and *LINE-1* 97-bp with tumor classes. It might show that shorter fragment releasing is affected more by the tumor's intrinsic biological characteristics than tumor burden. No correlation of tumor-derived cfDNA release was reported in a published study²⁰⁹. This result is supported by reports that showed tumor-derived cfDNAs are more likely in short length.

The mechanisms underlying the shorter fragment size of cfDNA originating from non-hematopoietic cells are unclear. The cause of the shorter fragment length connected to tumor-derived cfDNA is still unclear, but the difference between hematopoietically derived cfDNA and cfDNA fragments derived from non-hematopoietic cells, including tumor cells, has been confirmed in different studies^{122,162,221,222,227,229,230}. Hematopoietic cells are the major

source of cfDNA in plasma. Zheng et al. found that cfDNA derived from other tissue of origin is shorter than hematopoietically derived cfDNA in organ transplant patients²²⁹. Tissue-specific differences in nucleosome wrapping²³¹ may result in this difference. Another explanation may be the slight digestion of cancer cells containing mutant DNA by macrophage leading to higher short fragments in cancer patients²²⁶. The presence of mitochondria-derived cfDNA is also another possibility for shorter fragments in cancer patients. The increasing concentration of mitochondrial DNA in hepatocellular carcinoma patients compared with the healthy subjects was reported. The mitochondrial DNAs are shorter (<150bp) than the nuclear DNAs in plasma¹²². Maybe the major source of cfDNA is mitochondria in some cancers like hepatocellular carcinoma because there are a higher number of mitochondria in liver cells in general compared with hematopoietic cells¹²². Later it was shown that this mitochondria DNA in plasma is much shorter than previously reported (30~60 bp)²³².

There is also contradictory evidence that tumor-derived cfDNA might be longer than those derived from nonmalignant cells⁷⁵. Inconsistent with our result some investigations reported more level longer fragments in gynecological⁷⁸, pancreatic¹¹⁹, breast¹⁵² cancers compared to healthy individuals. We expected a higher concentration of long cfDNA fragments in the patients with a malignant tumor. A smaller amount of *ALU* 260-bp fragments were found in the patients compared to the control (borderline significance 0.056). The subgroups' highest *ALU* 260-bp fragment levels were in order: non-mNET > control > NEC > mNET. Likewise, fewer *LINE-1* 266-bp fragments in the patients compared to the control were observed (not significant) in order of highest *LINE-1* 266-bp fragment levels in non-mNET > control > mNET > NEC.

Interestingly, the patients with G3 tumors had the lowest long and the highest short *LINE-1* fragment levels. The patients with G1 tumors showed the highest long and lowest short fragment levels considering the *ALU* gene. However, the concentration of longer fragments could not be correlated to tumor grade or metastatic- state of the cancer disease.

The longer fragments showed a significant relationship with increasing cfDNA levels in the patients. *ALU* 260-bp and *LINE-1* 266-bp fragments levels revealed a discriminatory power of 0.628 and 0.620, respectively, to differentiate between mNET plus NEC and non-mNET disease. This sensitivity and specificity are considered to be insufficient for the detection of mNET plus NEC disease.

Regarding tumor burden, a significant difference in the cfDNA fragmentation was not observed in this study except for *ALU* 260-bp. Patients with a high tumor burden showed a significantly lesser amount of long *ALU*-fragments, with an AUC of 0.81 leading to moderate discriminatory power.

In patients with inactive tumor disease or tumor-free patients, tumor-derived cfDNAs can be expected to come from apoptotic cells. There have been reports of an increase in the shorter and longer fragments after surgery. Iqbal et al. observed longer pieces of cfDNA after removing the tumor in patients with breast cancer²³⁴. This report agrees with the high presence of *LINE-1* 266-bp and *ALU* 260-bp fragments in the non-mNET patients compared to aggressiveness disease in our study. A higher level of *ALU* 115-bp fragment has been reported in post-surgery patients with breast cancer²³⁴. A higher level of short fragments was observed in the non-mNET patients. Cancer isn't always the reason for necrosis; many causes, including injury, trauma, infection, infarction, toxins, chemicals, radiation, cold, and inflammation, can induce necrosis^{228,235,236}.

In addition to apoptosis and necrosis in the primary tumor, cfDNA can be derived from circulating tumor cells (CTC)²³⁷. This fact might suggest that circulating tumor cell dissemination involves cfDNA production at one point, the same as a metastatic outgrowth. Even if we assume that our NEC patients show the highest level of CTC in the blood, which contributes to an increase in the short fragments, we cannot explain why we could detect the lowest level of short fragments for metastatic NET disease.

There was limited information about the therapy (type and duration) and time of blood draw after a possible treatment. This lack of information hinders the study of the treatment effect on fragmentation. It has been published that necrosis increase after chemotherapy^{238,239}. In addition, the source of cfDNA and tumor DNA levels could change over time during treatment²¹⁸. A published study reported that the principal sources of cfDNA are apoptotic and non-apoptotic cell death in the patients with prostate cancer before and three months after diagnosis, whereas the patients after six months showed cfDNA released at non-apoptotic cells⁷⁶.

No correlation was found for any fragmentation markers with gender and tumor origin. A published study has reported the independence of *ALU* 115-bp fragment level and gender in thyroid cancer²²⁸.

Interestingly, our study revealed that the *ALU* 115-bp fragment level is affected by age in the patient group ($p= 0.04$), which was also shown by Thakur et al. for thyroid cancer²²⁸. In contrast, the independence of *ALU* 115-bp fragment level and age was observed by Fawzy and colleagues for prostate cancer²³⁷. It is known that the rate of apoptosis is elevated in aging and age-associated disease. The increased apoptosis may be a protective mechanism against age-related tumorigenesis^{240,241}. No correlation to CgA was found.

4.4 cfDNA Integrity as a biomarker for NEN patients

The *ALU* and *LINE-1* repeat sequences have a high prevalence in the DNA; hence they are optimal sequences for cfDII testing²²⁸. The association between NEN cancer and two different cfDIIs, namely *ALU* cfDII or *LINE-1* cfDII, was examined in the plasma samples.

Measuring two genes to determine cfDII has two advantages; first, it could reflect a global status of the cfDNA, and, second, independent cfDII measurements of these two repetitive elements reduce the likelihood of false positives.

We used *ALU* primer pairs for this study, namely *ALU* 260- and 115-bp, which were previously not used in other cfDII research. Both cfDIIs are decreased in the patient group. The calculated cfDII, determined via *ALU* fragmentation, showed an increase for patients with NEC disease. The cfDII for *LINE-1* fragmentation decreased for patients with mNET and NEC compared to the controls and the patients with non-mNET.

So far, almost nothing is known about the cfDNA integrity in NEN patients.

At first, it seems contradictory that we can prove different results for *ALU* and *LINE-1* cfDII in the same patient group. Various locus genes can be used to assess the cfDNA integrity.

It is described that, depending on which primer pair are used for amplification, either higher cfDII^{123,152,234,242,243} or lower cfDII^{57,244} were determined, even if similar cancer were examined¹¹⁷.

Unfortunately, we could not confirm the significant results between the *ALU* cfDII in the plasma of NEN patients and the controls, nor was there a substantial difference in *ALU* cfDII in the plasma of patients' subgroups. The *LINE-1* cfDII was less in the patients. The lowest

cfDII was found in NECs, mNETs, and patients with G3 tumors. Thus, low *LINE-1* cfDII was associated with tumor aggressiveness. These findings could be explained in different ways:

- 1) Some cell death rate factors such as inflammation and autoimmune diseases could be the source of released cfDNA accompanied by the apoptotic cells in the non-cancerous cases ^{75,245}.
- 2) More necrotic cfDNA fragments may be produced only at a certain point by the tumor cells ²⁴⁶.
- 3) Necrosis is only responsible for a few amounts of cfDNA in cancer patients ^{62,90}.
- 4) Recent studies have shown that tumor-derived cfDNA are more likely to be shorter fragments (<100 bp)²⁴⁷. The increase in shorter fragments in patients leads to a decrease in integrity.
- 5) Most of the cancer patients in our cohort had a low tumor burden; therefore, necrosis is unlikely to affect cfDII. A good correlation coefficient value of *LINE-1* cfDII with tumor burden ($r = -0.40$; $p < 0.0001$) also represents its prognostic benefit for NEN cancer progression.

A decreased cfDII was reported in other cancers such as colorectal ^{120,248}, testicular germ cell ¹⁸⁶, breast ^{57,244,249}, hepatocellular ¹⁴⁸, and ovarian ²⁵⁰.

Contrary to our results, namely an elevated of cfDII, was reported in some cancers such as gynecological ⁷⁸, colorectal^{123,251}, breast ^{57,115,234,243,252}, ovarian ²⁵³, head and neck ⁷⁷, acute leukemia²⁵⁴, renal cell ²⁵⁵, melanoma ^{256,257}, periampullary¹²³, hepatocellular ^{258,259}, bladder ²⁶⁰, glioma ²⁶¹, and prostate ^{237,262,263}.

However, the current results revealed that *LINE*-cfDII was lower the more aggressive the NEN disease (non-mNET < mNET < NEC). A meaningful difference was observed between metastatic NETs and healthy individuals. In line with these findings, the lower cfDII than the healthy controls was reported in the metastatic breast patients ^{57,243}, while non-metastatic patients showed higher cfDII than the healthy controls ^{152,234,242}. It seems that *LINE-1* cfDII increases at the initial stages of cancer and decreases in the metastatic step. Unlike the *ALU* cfDII, *LINE-1* cfDII was tumor origin and grade-dependence. Some published studies showed that elevated cfDII was tumor stage-dependent in breast cancer ^{115,152}. For NEN patients we could detect a significant decrease for patients with a highly differentiated tumor (G3) or patients with a high tumor burden.

In addition, *LINE-1* cfDII showed a low ability to differentiate patients from the control cases (AUC: 0.67). The AUC could be increased slightly by excluding the non-mNET from patient groups (AUC: 0.69), with a low sensitivity and specificity and the chosen cut off point with 77.8 and 55.2%, respectively. Comparing the ROC curves of *LINE-1* cfDII and cfDNA was shown a similar AUC of 0.67 vs. 0.66 and 0.69 vs. 0.69 for total patients and mNETs plus NECs, respectively. A multiple logistic regression model of cfDNA level and *LINE-1* cfDII was applied to improve the discriminatory power. There was a rise in sensitivity for detecting NEN disease when NECs and mNETs were used as patient groups.

Necrosis correlated with tumor burden (volume) and the growth of invasive tumors ^{174,238,265}. The increasing tumor volume and growth are associated with a shortage of blood vessels, leading to more extensive necrotic regions. Contrary to our expectations *LINE-1* integrity index was remarkably decreased along with the rising tumor burden in cohorts with moderate and high tumor burdens compared to no tumor. The high discriminatory power of *LINE-1* cfDII for the detection of the patients with a high tumor load (87.5% sensitivity, 71%

specificity; AUC: 0.83) showed that this biomarker can be a good candidate for disease progression.

We could not find any connection with other clinical characteristics such as age, gender, and CgA value in our setting. Unrelated cfDII to age was reported in previously published studies^{228,264}. Other groups, however, postulated a gender dependency. Higher (0.40 vs. 0.15) and lower (0.46 vs. 0.56) *ALU*-cfDII in women than in men were reported^{228,264}. These inconsistent data of the effect of gender on cfDII suggest that it is one of several other factors affecting cfDII. However, cfDII results are affected by the sources of cfDNA, different sample preparation protocols, the PCR assays and primers used, and the various investigated patient groups^{72,245,266}. These may cause the heterogeneity of cfDII results reported in several studies (App. Table 20).

In conclusion, the high diagnostic capacity of cfDII for cancer detection was not shown by our data. A reason for the results could be the low patient number in each subgroup and the patient heterogeneity related to the pre – or post-therapy in our setting. Maybe a specific division of the cancer patient group would allow more explicit discrimination.

4.5 cf DNA Hypomethylation as a biomarker for NEN patients

There is currently conflicting publication on the correlation between hypomethylation and gender and age. A study with only healthy people found gender-dependent differences with a higher methylation level in males²⁶⁷. An association of hypomethylation of *ALU* elements with age has been proven²⁶⁸, where 718 healthy individuals have been measured for eight years, and a progressive decrease in the mean *ALU* methylation could be observed over time. Jintaridth group found that age was negatively associated with *ALU* methylation levels in healthy individuals. Wherever the population consisted of aged 20 –90 years, hypomethylation of *ALU* happened during ages 34-68 years²⁶⁹.

Regarding cancer diseases, it has been published for different cancers such as prostate, non-small cell lung cancer, lung cancer, glioma, hepatocellular, breast, and esophageal squamous cell carcinoma, pancreatic cancer toward the *ALU* hypomethylation^{270–278} that sex or age does not affect the methylation of *ALU* repeats. In the present study, hypomethylation of *ALU* elements was not associated with age and gender. In contrast, the association between gastric cancer risk and *ALU* methylation was found to be modified by age⁽²⁵³⁾. The heterogeneity of the NEN disease and a small number of samples in our groups based on age or gender make it difficult to trust the current results.

Increased rates of global hypomethylation have been reported in tissue^{272,279–289} and blood^{278,290–292} of many cancer patients, whereas not much is known about global hypomethylation of cfDNA in cancer patients^{273,293,294}.

Little is known about global hypomethylation during NEN carcinogenesis, not just at what point in time it takes place, nor at what genome location. The *ALU* gene's methylation level of the major variant was investigated in the present work in cfDNA to introduce an epigenetic biomarker for cancerization, namely a potentially predictive or diagnostic marker in NEN patients. It was illuminated whether or not hypomethylation is present in NENs and, if present, whether *ALU* elements were affected. To our knowledge, this is the first study to assess the association between the cfDNA-hypomethylated *ALU* gene and NEN patients. Other studies investigated hypomethylation in tissue samples of neuroendocrine tumors by analyzing *LINE-1* and *ALU* methylation, where hypomethylation was found to be more

common in carcinoid tumors than in pancreatic endocrine tumors. The hypomethylation was correlated to lymph node metastases²⁸⁵. Also, they reported that hypomethylation was more common in ileal NETs than in non-ileal NETs²⁸⁵. Another study determined the higher *LINE-1* hypomethylation in small intestinal-neuroendocrine tumors than normal references²⁸⁹. The increase of hypomethylation was demonstrated in distant metastasis compared with primary tumors or regional metastasis²⁸⁹.

The current study revealed slightly higher cfDNA *ALU*-hypomethylation in NEN patients compared to the controls (1.39 vs. 1.23%). In line with our finding, the higher *ALU* hypomethylation levels had been reported in various carcinomas such as colon²⁹⁵, liver²⁷⁴, gastric⁽²⁶³²⁹⁷⁾, esophageal squamous cell carcinomas²⁷⁶, ovarian²⁹⁸, thyroid¹⁴⁰, breast¹⁴⁰, colon¹⁴⁰, and lung⁽¹⁴⁴⁾ than their corresponding healthy samples. Similarly, increasing *ALU* hypomethylation in the blood of pancreatic²⁷⁸ and glioma patients compared to healthy controls was indicated⁽²⁵⁸⁾.

With 70% specificity and sensitivity of 47%, 1.41 % was taken as a cut-off value to consider a tumor as hypomethylated. In this cut-off, the analysis revealed that 47% of NEN tumors were hypomethylated, while in mNETs and NECs, this amount was 53% and 57%, respectively. Otherwise, all non-mNETs had *ALU* hypomethylation percentages below the reference value. A poor discriminatory power was obtained for mNETs plus NECs (AUC:0.64). Combining *ALU* hypomethylation percentage with cfDNA level somehow increases the distinguishing power between the controls and mNET plus NECs (AUC: 0.69). This increasing power was demonstrated more if the hypomethylation combined with *LINE-1* cfDII (AUC: 0.72). On condition that the hypomethylation combined with both cfDNA level and *LINE-1* cfDII, an AUC of 0.73 was obtained.

The key finding of this study is the significantly elevated hypomethylation of cfDNA in the patients with mNET compared to non-mNETs (1.45 vs. 0.995 %, P= 0.005). The hypomethylation percentage can distinguish between patients with advanced NEN disease (mNETs plus NECs) from patients with non-mNETs with a negative and positive predictive powers of 90.91 and 66.67%, respectively (AUC: 87) and be more informative than the common tumor biomarker of NENs, namely CgA (AUC: 0.57).

Given 80% specificity, the highest sensitivity achieved in detecting the non-mNET group from mNET plus NEC groups was 75% at the percentage cut-off of 1.12. About eighty and one percent of mNET patients had an *ALU* hypomethylation above this cut-off. This amount is nearly eighty and six, and twenty and five percentage for NECs and non-mNETs, respectively.

Methylation prevents chromosomal rearrangements and chromosome translocation by silencing repetitive elements^{299–302}. There is an association between hypomethylation and genomic instability^{299,303–305}, particularly hypomethylated *ALU*²⁹⁵. Thus, hypomethylation may increase the potential of NENs by inducing genomic instability. In agreement with our initial expectation, the highest *ALU* hypomethylation was observed in NECs, which might be related to chromosomal instability of this subgroup of NENs^{306,307}. NECs showed elevated *ALU* hypomethylation compared to non-mNETs (1.56 vs. 0.995 %) with a close to the significant difference (p=0.072).

Multiple combination biomarkers were applied to improve the diagnostic accuracy. Combining *ALU* hypomethylation percentage with cfDNA level and *LINE-1* cfDII slightly increases the distinguishing power between mNET plus NEC and non-mNET groups with a positive and negative predictive value of 66.7%, and 89.8%, respectively (AUC: 0.89). By combining hypomethylation with cfDNA concentration and CgA levels, the analysis revealed

a high discriminatory potential, with an AUC of 0.91, and a negative and positive predictive power of 90.91 and 66.67%, respectively.

Global hypomethylation seems to be an early event for some cancers, e.g., colon, chronic lymphocytic leukemia, and breast cancer^{275,308–310}. While for other cancers such as hepatocellular carcinoma, cervical and ovarian, the hypomethylation degree increase with stage or histological grade^{311–314}. In the current study, the tendency to increase *ALU* hypomethylation varied from the controls and the patients with early grade tumors (i.e., G1 and G2 tumors) to the advanced patients (i.e., with G3 tumor). This increased *ALU* hypomethylation dependent on tumor grade showed a meaningful difference between the controls and the G3 tumor patients ($p= 0.024$). Reduced *ALU* methylation correlated with tumor grade has also been reported in hepatocellular carcinoma (Grade 1 and 2 tumors showed 13.2% hypomethylation, compared to G3 and G4 tumors with 13.2%²⁷⁴, and in high-grade gliomas (grade IIIIV) compared to low-grade gliomas (I-II) (52.01 vs. 64.86%, respectively)²⁷³.

In contrast, no association between *ALU* hypomethylation and tumor grade has been reported for pancreatic cancer²⁷⁸. The good discriminatory power of *ALU* hypomethylation in detecting patients with G3 suggests a diagnostic role for the late phase of the disease (AUC: 0.77). Thus, our outcomes indicate that the *ALU* hypomethylation may occur more meaningfully in the disease progression but not at the early onset of carcinogenesis and tumor initiation. *ALU* hypomethylation was found to have significant discriminatory ability in detecting NEN patients with G3 tumors. The model presented an AUC of 0.77, a sensitivity of 70%, and a specificity of 79.3% for detecting G3 tumor samples at the chosen cut off level.

Upon analysis of *ALU* hypomethylation, the highest significant correlation coefficient was found between *ALU* hypomethylation level and tumor burden ($r=0.424$, $p= <0.0001$) compared to other present biomarkers, thus it was more representative of tumor progression. Interestingly, higher hypomethylation was observed in patients with large tumor burden compared with other patients as NEC patients with higher hypomethylation were characterized by higher tumor burden. As a result, the cfDNA hypomethylation difference could be attributed to tumor burden.

The *ALU* hypomethylation was associated with high progressive accuracy with an estimated AUC of 0.96 for the patient with high tumor loads, with a sensitivity of 100% and a specificity of 86.8%.

Combined detection of serum-CgA, cfDNA, *LINE-1* cfDII, and hypomethylation levels could improve the diagnostic efficiency for patients with no tumor from other patients (AUC= 0.924; $p< 0.0001$) with a positive and negative predictive power of 90.91 and 66.67, respectively, suggesting this combination as a candidate for NENs underlying therapy. It seems this combination has more power than the common indicator of NENs, i.e CgA, to monitor the treatment efficiency or detect the residual tumor after surgery.

Moreover, our study cannot be compared directly with other studies because we could not find the relationship between *ALU* hypomethylation and tumor burden in other cancers.

In addition to *ALU*, other repetitive DNA segments were examined to study the hypomethylation, such as *SAT2* (juxtacentromeric satellite 2) and *LINE-1*. Here, discrepancies about the time of hypomethylation could be observed in various types of cancer. Kwon et al. reported that morphological progression from adenoma to carcinoma did not go along with increases in *ALU* and *LINE-1* hypomethylation. *ALU* and *LINE-1*

hypomethylation are early events in multistep colorectal carcinogenesis. They observed that hypomethylation levels of *ALU* and *LINE-1* elements erase from the normal tissue to the adenoma. This decrease in methylation could not be found in the progression from the adenoma to cancer.

On the other hand, *SAT2* showed a stepwise decrease in methylation level from normal tissue to adenoma and then to cancer³¹⁵. The *SAT2* hypomethylation happened earlier than *LINE-1* or *ALU* hypomethylation in multistep hepatocarcinogenesis. Whereas *LINE-1* or *ALU* hypomethylation was not found in the normal liver compared to the chronic liver disease, it only occurred in hepatocellular carcinoma²⁷⁴. For gastric and breast cancer progression, an earlier hypomethylation of *LINE-1* compared to *ALU* hypomethylation was confirmed^{275,279}. Future studies would be interesting to identify the hypomethylation timing of repetitive elements, namely *SAT2*, *LINE-1*, and *ALU* sequences, during NEN progression. Their prognostic value seems promising.

Regarding the tumor site, it has been published that the degree of hypomethylation is variable among different cancer types, where thyroid, prostate, and breast cancer exhibited low hypomethylation levels, while cancers of colon and lung displayed the highest levels¹⁴⁰. A study using methylation references out of 25 human cancer cell types demonstrated that methylation patterns of cfDNA could represent the tissue origins of cfDNA³¹⁶. The methylation profile of primaries and metastases can be similar. In confirmation of this report, the resemblance of *ALU* hypomethylation between distant metastases and matched primary tumors was indicated in thyroid cancer³¹⁷. It was demonstrated that the hyper/hypomethylation of 21 genes in small intestinal neuroendocrine tumor liver metastases is in concordance with the pattern seen in small intestinal neuroendocrine tumor primaries³¹⁸. In 12-22% of patients with NEN, the primary location of the tumor cannot be identified by routine imaging or histopathology, which worsens the prognosis. Some novel molecular techniques are currently under investigation to recognize the primary tumor site. An inquiry with *ALU* methylation was carried out in the current study to find a correlation to the tissue origin of the NEN. No significant difference could be observed between the *ALU* methylation level and the origin of the tumor. The highest percentage of *ALU* hypomethylation was observed in lung and rectum tumor origin with 1.57%. The stomach tumor origin showed less *ALU* hypomethylation percentage with 1.13%. Interestingly, the higher *ALU* hypomethylation percentage of lung and colon tumor origins was also reported compared to the primary thyroid tumor by Buj et al. (14.6, 14.6, and 8.2%)¹⁴⁰. The different hypomethylation rates might be related to drugs, chemicals, pollutants, and the different dynamics of the tumor progression in various tumor types^(144,287,288).

We demonstrated a positive correlation between the degree of hypomethylation and the cfDNA concentration in NEN patients. In published studies has been shown that the higher the tumor burden, the higher the detectable cfDNA concentration in the plasma¹⁹⁸. The increased cfDNA is, therefore, most likely from the tumor. Any uncontrolled cfDNA, i.e., unmethylated cfDNA, is also due to tumor tissue. Moreover, a weak significant positive association between *ALU* hypomethylation and CgA expression level was observed in the patients ($r=0.337$, $p=0.01$). Global DNA hypomethylation and its correlation to the circulating biomarkers had been observed in some disorders, but we could not find a study showing *ALU* hypomethylation's correlation to the already established biomarkers in cancer.

To conclude, there is little information about the methylation landscape for NENs and the relationship between detection of methylation abnormalities in NENs in the plasma or serum. The current evidence demonstrated that aberrant epigenetic regulation, namely hypomethylation of *ALU*, was present in NENs and *ALU* hypomethylation was present even in the non-metastatic patients. The *ALU* hypomethylation could be influenced by the disease condition and correlates with the aggressiveness of NENs. Since hypomethylation is potentially reversible, chromosomal instability may be due to the early incidence of *ALU* hypomethylation. However, the role of DNA methylation in resistance to cancer therapy was proved³¹⁹. Global hypomethylation is an active process in most cancers³²⁰. This genome-wide hypomethylation leads to cellular phenotypic changes due to alteration in gene expression. Hence, new prevention and treatment cancer investigations focus on this epigenetic change as a promising candidate for new cancer drug design^{319–321}. The suppression of hypomethylation induction might be applied as a new target of NEN cancer inhibition.

As a fundamental basis to understand NEN carcinogenesis, it was illuminated that hypomethylation of the major variant of *ALU* in blood for the first time. In this study, the tendencies and the connection between *ALU* hypomethylation and NEN disease are accepted. In addition, *ALU* hypomethylation may have a value for the NEN risk assessment; it is, therefore, worthwhile to find the change in the hypomethylation pattern of other repetitive elements in cfDNA from NEN patients. However, it is still unclear which DNA hypomethylation changes are tumor-driving events and how these changes are initiated. Further genome-wide studies to measure the hypomethylation level of each *ALU* locus may improve PCR-based methylation analysis to allow for more specific and sensitive detection of cancer DNA or calculation of particular cancer phenotypes.

5. Challenges and future perspectives

Many liquid biopsy tools to improve the management of cancer patients have been deployed in the last years. The early diagnosis, early detection of recurrence, and personalized treatment are challenges in cancers including NEN patients.

Only new biomarkers accompanying high standards can be used in clinical. The liquid biopsy-based molecular biomarkers have not achieved the high sensitivity and specificity with current methods, but the encouraging results obtained in different investigations. These results support the potential prognostic, diagnostic and predictive role of the molecular new biomarkers which suggest considering them in numerous prospective trials.

Among liquid biopsy-based molecular parameters, cfDNA and CTCs detection and characterization have presented a fundamental role. In this context, ctDNA characterization might act as a noninvasive biomarker that assists tissue biopsy to manage cancer in the future.

Some open questions must be addressed, such as the relative contribution of different sources of cfDNA such as apoptosis, necrosis, other cell death mechanisms, and active secretion. Which underlying mechanisms or factors change the releasing and clearance of cfDNA, and are there the consequences for more cfDNA fragments production from each source. In the future, it will be essential to understand the relationship between tumor DNA release with tumor biology to accept the cfDNA as a clinical biomarker in cancer patients. The biology of cfDNA and the correlation between cfDNA characteristics and the clinical manifestations of disease must be studied more in extensive clinical studies.

The study population must be chosen more specifically. It seems that tested biomarkers are more promising for the different courses of disease and have a less discriminatory diagnosis for healthy individuals. Hence, it is better to focus on patients' particular subgroups with different phases of the disease in future studies though, it is challenging to assemble a large cohort of patients, as many NENs are rare diseases. Additionally, the factors such as ethnicity, small sample size, unbalanced number, and age of the participants among groups may influence the results. The clinical impact of novel biomarkers needs to be further confirmed in larger-scale studies stratified by different ethnic and age NEN patients.

It may be valuable that the control group includes two subgroups: healthy individuals with no cancer history and people with benign diseases of the corresponding organ systems. Benign and malignant diseases have clinical similarities. Consequently, the diagnosis can be difficult and the high rate of patients with benign conditions go on to tissue biopsy. A new biomarker with high sensitivity to discriminate benign from malignant disease prevents this invasive, costly, and risky procedure and all patients receive proper treatment. Thus, the detection of benign disease is most important for discriminatory diagnosis in further evaluations.

To avoid confounders of the underlying disease, it would therefore be important for future studies to characterize the control group not only with respect to lifestyle factors, age, and sex but also for inflammatory or autoimmune disease e.g. by including additional markers like C-reactive protein. Furthermore, traditional neuroendocrine tumor markers like chromogranin A should also be included in a future confirmatory study and could potentially increase the diagnostic sensitivity in combination with cfDNA integrity and hypomethylation.

Furthermore, this study only included patients one time and unfortunately, continuous monitoring was not performed. The long time monitoring (follow-up time) of subjects and investigating the patients with no symptoms or onset of symptoms should be considered.

There is always the risk of different errors in measurement that lead to different measured values from the true value. The one-time measuring can not be a mirror for the process of disease. Accordingly, continuous measuring may decrease this error analysis and also give a complete difference and new insight in disease development compared to one-time measuring. Thus, clinical monitoring should be added to assess whether the biomarkers can detect changing conditions.

The future of tumor biomarkers might be a combination of traditional specific circulating biochemical and new-generation biomarkers, especially molecular (genetic) markers in non-solid biological tissues. For the detection of metastatic, cfDNA, *LIEN-1* cfDII and hypomethylation biomarkers in combination with CgA had the overall best diagnostic profile in our study suggesting the hope of a simple blood test as a possible secondary screen for NEN cancers. Future studies should investigate these biomarkers with each other or in combination with other circulating biomarkers such as miRNAs, mRNA transcripts, proteins, exosomes, metabolites, CTCs, or mitochondrial DNA as a novel biomarker in NEN patients. It looks that a combination of biomarkers and multianalyte analysis is more sensitive than monoanalytes especially for NEN, and might give new insight and improve clinical value. However, validation is still needed.

To conclude, liquid biopsy analyzing cfDNA, cfDII and *ALU* hypomethylation had limited utility as a diagnostic marker in the evaluation of NEN patients. A liquid biopsy might be a useful prognostic and risk stratifying tool in patients with more aggressive NEN cancers.

6. Conclusion

Cancer management through a non-invasive method like cfDNA analysis remains one of the most exciting goals. Improving the NEN cancer screening is crucial for timely discovery, prognosis, and monitoring for early relapse detection or treatment response.

Plasma blood samples from NEN patients were examined to introduce a new biomarker via a noninvasive method.

Collectively, the assessed biomarkers were informative for patients with disease different courses, but not the healthy individuals from patients, hence they are not suitable for the early diagnosis of NEN cancer. Also, the biomarkers did not show good efficiency to discriminate the patients with an early phase of the disease. The three tested biomarkers, i.e. cfDNA level, *LINE-1* cfDII, and hypomethylation had acceptable results to differentiate patients with tumor G3. The best outcomes were obtained for the biomarkers when the different tumor loads were considered. Although, it seems that these biomarkers could not be helpful to detect tumor origin the potential value of cfDNA level or *LINE-1* cfDII as a biomarker for tumor localization suggests being investigated with more patients in each subgroup.

In detail, analysis of cfDNA level indicated that it might be a good marker for predicting survival and classification of risk for advanced NENs undergoing treatment. Although the cfDNA level was higher in mNETs than in healthy individuals, the discriminatory power was not satisfactory for clinical use. Since this biomarker was able to differentiate well between the patients with a G3 tumor or a high tumor burden, the inclusion of the cfDNA level would certainly be helpful in screening high-risk patients or during therapy to control progression.

The fragmentation of the cfDNA, with the exception of the longer *ALU* fragments, will not be included in routine diagnostics due to the insignificant results.

cfDNA integrity, measured on *LINE-1*, could significantly differentiate patients from healthy controls, and a significant reduction in integrity in relation to tumor differentiation and tumor burden could be demonstrated. In order to function as a singular biomarker, the potential to differentiate between healthy and patient is insufficient to be of clinical use. As a progression parameter and in combination with other biomarkers, however, cfDNA integrity is a promising biomarker for NEN diseases.

ALU hypomethylation was not able to distinguish between patients and healthy controls. But, *ALU* hypomethylation was the most promising candidate for assessing the clinical course and therapy monitoring of NENs. We were able to demonstrate the highest significance and potential for discrimination between the patients with the highest tumor burden, which unfortunately also accounts for the lowest number of patients. Therefore the results should be verified with a higher number of cases so that they can be recommended for clinical use. Therefore, *ALU* hypomethylation can be an interesting progression and therapy monitoring parameter, as well as a relapse predictor during follow-up care for NEN cancer.

Interestingly, cfDNA and hypomethylation were correlated with each other and also with CgA levels. This relationship may support the benefit of these two biomarkers along with CgA.

The combination of the tested, individual biomarkers increased the distinctive character necessary for clinical application. Combined detection of serum-CgA, cfDNA, *LINE-1* cfDII, and hypomethylation levels could improve the diagnostic efficiency for patients with no tumor from other patients (AUC= 0.924; $p < 0.0001$) with a positive and negative predictive power of

90.91 and 66.67, respectively, suggesting this combination as a candidate for NENs underlying therapy. It seems this combination has more power than the common indicator of NENs, i.e CgA, to monitor the treatment efficiency or detect the residual tumor after surgery. This study's finding may open a perspective for NEN screening strategy combining molecular liquid biopsy and tissue biopsy. The combination of tissue biomarkers and cfDNA-based liquid biopsy test may complete the tissue biopsy and improve the sensitivity and specificity in an assessment in the future.

7. Summary

7.1 Summary

The current study is being conducted to determine whether plasma cfDNA, cfDNA hypomethylation, cfDNA integrity index or quantitative concentrations of *ALU* 115-, *ALU* 260-, *LINE-1* 97-, *LINE-1* 266-bp fragments can be robust biomarkers for the diagnosis and prognosis of NENs. The aim is to establish a new biomarker for the diagnosis and follow-up of NEN patients on a molecular basis. This study evaluates the efficiency of these suggested biomarkers in different phases of NEN cancer and the association between each biomarker and clinicopathological tumor characteristics.

Methods: The cfDNA plasma samples originated from 62 patients, aged (33-87), with pathologically confirmed NEN, and 29 control, aged (24-77) years, from neuroendocrine patients without neoplastic diseases were evaluated. Depending on the disease, the patients were categorized into different groups to 47 patients with the metastatic NET disease (mNET), 8 nonmetastatic NET disease (non-mNET), and 7 NEC disease. Here, we examined the cfDNA plasma concentration, concentration of long and short cfDNA fragments measured via *ALU* and *LINE-1* repetitive DNA elements, cfDNA integrity, and cfDNA hypomethylation. The integrity index was calculated using: the *ALU* 266/115 ratio and the *LINE-1* 266/97 ratio, based on the data obtained by real-time PCR. The cfDNA hypomethylation was assessed based on the methylation status of *ALU* and was considered representative of the global hypomethylation status. The discriminatory power of each logistic model was investigated using the area under the ROC curve (AUC).

Results: cfDNA biomarker: NEN Patients, showed a higher, but not significant increase of cfDNA concentration in comparison to healthy controls. Dividing the study patients' group to non-metastatic NET (non-mNET), metastatic NET (mNET) and NEC patients, a significant increase for mNET could be detected. Further analysis revealed, the more advanced the NEN disease, the higher the cfDNA level, leading to significant differences for controls to patients with a G3 tumor or a significant increase for patients with a moderate or high tumor burden. ROC curve for discriminating patients with grade 3(G3) NENs from healthy subjects had an AUC of 0.80 (at 50% sensitivity and 100% specificity). The ROC curve for discriminating patients with moderate and high tumor burden displayed an AUC of 0.77 and for patients with high tumor burdens an AUC of 0.84 (at 75% sensitivity and 97.4% specificity). The analysis confirmed higher cfDNA levels in patients were associated with an increased risk of death. The patients with lung tumor origin had a higher quantity of cfDNA than patients with a primary tumor of the ileum. **Fragment sizes biomarker:** No significant difference was observed in levels of short and longer fragments between groups, but a significant decrease in *ALU* 260-bp fragment level was detected in samples with no tumor compared to large tumor burdens. ROC curve analysis showed a good distinguish accuracy between these two groups (AUC: 0.81, 100% sensitivity, and 52.6% specificity). **cfDNA integrity index (cfDII) biomarker:** We did not find any significant differences regarding *ALU* cfDII between the groups. In contrast, the *LINE-1* cfDII was significantly decreased in plasma of NEN patients compared to healthy control, but it showed a low accuracy in ROC analysis (AUC=0.67). For *LINE-1* cfDII, we could see in the more advanced the NEN disease, the lower the *LINE-1* cfDII, leading to a good discriminatory AUC of 0.80 (at 90% sensitivity and 69% specificity) for G3 classified tumors or an AUC of 0.83 (at 87.5% sensitivity and 71%

specificity) for patients with a high tumor burden to healthy controls. In addition, a lower *LINE-1* cfDII was observed in patients with primary tumors in the small intestine than in patients with the primary tumor in the ileum. **ALU hypomethylation biomarker:** Significant higher hypomethylation was observed in patients with mNETs than patients with non-mNETs, with a sensitivity of 87.5% at 79.6% specificity and an AUC of 0.87. Regarding tumor grade and tumor burden, the more advanced the disease, the higher was the measured hypomethylation level. A great discriminatory accuracy was calculated between patients with a high tumor burden and healthy or cured patients (AUC: 0.96; at 100% sensitivity and 86.8% specificity). A positive correlation between hypomethylation and CgA levels was detected. **Combined biomarkers:** With the multiparametric ROC curve analysis including cfDNA, hypomethylation, and CgA level as a biomarker, a great diagnostic accuracy between patients with mNET and NEC to patients with non-mNET could be calculated with 66.67% positive predictive and 90.91% negative predictive values (AUC:0.91).

Conclusion: Current findings support the role of the tested biomarkers for prognosis, progressive and predictive, but not a diagnostic. The combination of tested biomarkers contributes to better efficiency relative to the single-use them. The novel biomarkers can be valuable biomarkers for the management of patients, optimal treatment, and open new therapy views correlated with sickness course. *ALU* hypomethylation was the most promising molecular marker that would be useful in monitoring patients for disease progression. However, these potential molecular biomarkers need clinical confirmation and more validation to use as a non-invasive tool for routine monitoring in a clinical setting.

7.2 Zusammenfassung

In der aktuellen Studie wurde die Eignung von Plasma-cfDNA, cfDNA-Hypomethylierung, cfDNA-Integritätsindex oder quantitative Konzentrationen von *ALU* 115-, *ALU* 260-, *LINE-1* 97- und *LINE-1* 266-bp-Fragmenten, als robuste Biomarker für die Diagnose und Prognose von Neuroendokrinen Neoplasien (NEN) untersucht. Die Studie bewertet die Effizienz dieser möglichen Biomarker-Kandidaten in verschiedenen Tumorstadien und den Zusammenhang zu den klinisch-pathologischen Eigenschaften der Patienten. Ziel ist die Etablierung eines neuen Biomarkers für die Diagnostik und Nachsorge von NEN-Patienten auf molekularer Basis.

Methoden: Plasmaproben von 62 Patienten im Alter (33-87) mit pathologisch bestätigter NEN und 29 Kontrollproben im Alter (24-77) Jahre von neuroendokrinen Patienten ohne neoplastische Erkrankungen wurden entnommen. Die Einteilung der Patienten erfolgt anhand ihres Krankheitsbildes in folgende Gruppen: 47 Patienten mit metastasierter NET-Erkrankung (mNET), 8 nicht metastasierte NET-Erkrankung (non-mNET) und 7 NEC-Erkrankung. Untersucht wurden die cfDNA-Plasmakonzentration, die Konzentration von langen und kurzen cfDNA-Fragmenten, gemessen über *ALU*- und *LINE-1*-repetitiven DNA-Elementen, die cfDNA-Integrität und die cfDNA-Hypomethylierung. Basierend auf den erhaltenen PCR-Daten wurde der Integritätsindex jeweils anhand dem Verhältnis von *ALU* 266 zu *ALU* 115 und dem Verhältnis von *LINE-1* 266 zu *LINE-1* 97 berechnet. Die cfDNA-Hypomethylierung wurde anhand des Methylierungsstatus von *ALU* bewertet und als repräsentativ für den globalen Hypomethylierungsstatus angesehen. Die Trennschärfe jedes logistischen Modells wurde anhand einer ROC-Kurve, über die AUC (Area under the curve) ausgewertet.

Ergebnisse: cfDNA-Konzentration: NEN Patienten zeigten eine Erhöhung der cfDNA-Konzentration im Vergleich zu gesunden Kontrollen (nicht signifikant). Unterteilt man die Studienpatienten in nicht metastasierte NET (kein-mNET), metastasierte NET (mNET) und NEC-Patienten, konnte ein signifikanter Anstieg für mNET festgestellt werden. Weitere Analysen ergaben, dass der cfDNA-Spiegel mit dem Fortschreiten der NEN-Krankheit steigt. Es konnten signifikante Unterschiede zwischen Kontrollen und Patienten mit NEN Tumor Grad 3 (G3) bzw. ein signifikanter Anstieg bei Patienten mit mittlerer oder hoher Tumorlast gezeigt werden. Patienten mit NEN G3 konnten von gesunden Probanden in der ROC-Analyse mit einem AUC von 0,80 unterschieden werden (bei 50% Sensitivität und 100% Spezifität). Für Patienten mit mittlerer und hoher Tumorlast konnte ein AUC von 0,77 und für Patienten mit hoher Tumorlast eine AUC von 0,84 ermittelt werden (bei 75% Sensitivität und 97,4% Spezifität). Die Analyse bestätigte, dass höhere cfDNA-Spiegel mit einem erhöhten Sterberisiko bei NEN Patienten verbunden sind. Patienten mit Primärtumor der Lunge hatten eine höhere cfDNA Konzentration, als Patienten mit einem Primärtumor des Ileums. cfDNA Fragmentenlänge: Zwischen den Gruppen wurde kein signifikanter Unterschied in der Menge kurzer und langer *LINE-1* Fragmente beobachtet. Patienten zeigten eine signifikant niedrigere *ALU*-260-bp-Fragmentmenge im Vergleich zur Kontrollgruppe, mit einer Trennschärfe von AUC 0,81 (bei 100% Sensitivität und 52,6% Spezifität). cfDNA-Integritätsindex (cfDII): Wir fanden keine signifikanten Unterschiede bezüglich *ALU* cfDII zwischen den Gruppen. Im Gegensatz dazu war *LINE-1* cfDII im Plasma von NEN-Patienten, verglichen zur gesunden Kontrollgruppe, signifikant erniedrigt, zeigte jedoch eine geringe Genauigkeit in der ROC-Analyse (AUC:0,67). Je weiter fortgeschritten die NEN-Krankheit, desto niedriger ist die *LINE-1* cfDII, was zu einer guten Trennschärfe in der ROC-Kurve führt

(AUC:0,80 für Tumorgrad G3 - Kontrollen bei 90% Sensitivität und 69% Spezifität / AUC:0,83 bei 87,5% Sensitivität und 71% Spezifität für hohe Tumorlast – Kontrollen). Darüber hinaus wurde bei Patienten mit Primärtumor im Dünndarm ein niedrigerer *LINE-1* cfDI beobachtet, als bei Patienten mit Primärtumor im Ileum. ALU-Hypomethylierung: Bei Patienten mit mNETs wurde eine signifikant höhere Hypomethylierung beobachtet als bei Patienten mit Nicht-mNETs, mit einer Sensitivität von 87,5% bei einer Spezifität von 79,6%% und einer gemessenen AUC von 0,87. Bezüglich Tumorgrad und Tumorlast war die gemessene Hypomethylierung umso höher, je weiter die Erkrankung fortgeschritten war. Es wurde eine hohe Trennschärfe zwischen Patienten mit hoher Tumorlast und gesunden bzw. geheilten Patienten berechnet (AUC: 0,96 bei 100% Sensitivität und 86,8% Spezifität). Es wurde eine positive Korrelation zwischen Hypomethylierung und CgA-Spiegeln festgestellt. Kombinierte Biomarker: Anhand multiparametrischer ROC-Kurvenanalyse, mit cfDNA, Hypomethylierung und CgA-Spiegel als Biomarker, konnte eine hohe diagnostische Genauigkeit zwischen Patienten mit mNET und NEC zu Patienten mit Nicht-mNETs mit 66,67 % positiven prädiktiven und 90,91 % negativen prädiktiven Werten berechnet werden (AUC:0,91).

Schlussfolgerung: Aktuelle Erkenntnisse unterstützen die Rolle der getesteten Biomarker für die Prognose, Progredienz und Prädiktion, aber nicht für die Diagnose. Die Kombination der getesteten Biomarker trägt zu einer besseren Effizienz im Vergleich zu den Einwegmarkern bei. Die neuartigen Biomarker können wertvolle Biomarker für das Patientenmanagement und die optimale Behandlung sein und neue, mit dem Krankheitsverlauf korrelierte Therapieperspektiven eröffnen. *ALU*-Hypomethylierung war der vielversprechendste molekulare Marker, der sich zur Überwachung der Patienten hinsichtlich einer Progression der Erkrankung eignen würde. Weitere klinische Bestätigung und genauere Validierung sind nötig, um diese potenziellen molekularen Biomarker als nicht-invasives Werkzeug für die routinemäßige Überwachung in einer klinischen Umgebung anwenden zu können.

8. References

1. Rindi, G. & Wiedenmann, B. Neuroendocrine neoplasms of the gut and pancreas: new insights. *Nat Rev Endocrinol* **8**, 54–64 (2011).
2. Oberg, K., Hellman, P., Kwekkeboom, D., Jelic, S., & ESMO Guidelines Working Group. Neuroendocrine bronchial and thymic tumours: ESMO Clinical Practice Guidelines for diagnosis, treatment and follow-up. *Ann Oncol* **21 Suppl 5**, v220-222 (2010).
3. Klöppel, G. Neuroendocrine Neoplasms: Dichotomy, Origin and Classifications. *Visc Med* **33**, 324–330 (2017).
4. Taal, B. G. & Visser, O. Epidemiology of neuroendocrine tumours. *Neuroendocrinology* **80 Suppl 1**, 3–7 (2004).
5. Meeker, A. & Heaphy, C. Gastroenteropancreatic endocrine tumors. *Mol Cell Endocrinol* **386**, 101–120 (2014).
6. Srirajakanthan, R. *et al.* ENETS TNM Staging Predicts Prognosis in Small Bowel Neuroendocrine Tumours. *ISRN Oncol* **2013**, 420795 (2013).
7. Scherübl, H. & Cadiot, G. Early Gastroenteropancreatic Neuroendocrine Tumors: Endoscopic Therapy and Surveillance. *Visc Med* **33**, 332–338 (2017).
8. Pobłocki, J., Jasińska, A., Syrenicz, A., Andrysiak-Mamos, E. & Szczuko, M. The Neuroendocrine Neoplasms of the Digestive Tract: Diagnosis, Treatment and Nutrition. *Nutrients* **12**, E1437 (2020).
9. Scoazec, J.-Y. & Couvelard, A. Classification des tumeurs neuroendocrines pancréatiques : nouveautés introduites par la classification OMS 2017 des tumeurs des organes endocrines et perspectives. *Annales de Pathologie* **37**, 444–456 (2017).
10. Nagtegaal, I. D. *et al.* The 2019 WHO classification of tumours of the digestive system. *Histopathology* **76**, 182–188 (2020).
11. Siebenhüner, A. *et al.* Neuroendokrine Tumoren. *Swiss Med Forum* **19(2324)**, 378–384 (2019).
12. Walter, T. *et al.* Is the combination of chromogranin A and pancreatic polypeptide serum determinations of interest in the diagnosis and follow-up of gastro-entero-pancreatic neuroendocrine tumours? *Eur J Cancer* **48**, 1766–1773 (2012).
13. Berner, A. M. *et al.* Diagnostic Approaches to Neuroendocrine Neoplasms of Unknown Primary Site. *Neuroendocrinology* **110**, 563–573 (2020).
14. Lee, S. T., Kulkarni, H. R., Singh, A. & Baum, R. P. Theranostics of Neuroendocrine Tumors. *Visc Med* **33**, 358–366 (2017).
15. Rinke, A. *et al.* Placebo-controlled, double-blind, prospective, randomized study on the effect of octreotide LAR in the control of tumor growth in patients with metastatic neuroendocrine midgut tumors: a report from the PROMID Study Group. *J Clin Oncol* **27**, 4656–4663 (2009).
16. Caplin, M. E. *et al.* Lanreotide in metastatic enteropancreatic neuroendocrine tumors. *N Engl J Med* **371**, 224–233 (2014).
17. Pavel, M. *et al.* ENETS Consensus Guidelines Update for the Management of Distant Metastatic Disease of Intestinal, Pancreatic, Bronchial Neuroendocrine Neoplasms (NEN) and NEN of Unknown Primary Site. *Neuroendocrinology* **103**, 172–185 (2016).
18. Herrera-Martínez, A. D. *et al.* Neuroendocrine neoplasms: current and potential diagnostic, predictive and prognostic markers. *Endocr Relat Cancer* **26**, R157–R179 (2019).
19. Yao, J. C. *et al.* Everolimus for advanced pancreatic neuroendocrine tumors. *N Engl J Med* **364**, 514–523 (2011).
20. Raymond, E. *et al.* Sunitinib Malate for the Treatment of Pancreatic Neuroendocrine Tumors. *New England Journal of Medicine* **364**, 501–513 (2011).
21. Oberg, K. Interferons in the management of neuroendocrine tumors and their possible mechanism of action. *Yale J Biol Med* **65**, 519–529; discussion 531-536 (1992).
22. Kulke, M. H. *et al.* Phase II study of temozolomide and thalidomide in patients with metastatic neuroendocrine tumors. *J Clin Oncol* **24**, 401–406 (2006).
23. Kerr, C. Oral regimen for metastatic neuroendocrine tumours. *Lancet Oncol* **7**, 197 (2006).
24. Di Giacinto, P. *et al.* Chromogranin A: From Laboratory to Clinical Aspects of Patients with Neuroendocrine Tumors. *Int J Endocrinol* **2018**, 8126087 (2018).
25. Bocchini, M. *et al.* Biomarkers for Pancreatic Neuroendocrine Neoplasms (PanNENs) Management-An Updated Review. *Front Oncol* **10**, 831 (2020).
26. Hofland, J., Zandee, W. T. & de Herder, W. W. Role of biomarker tests for diagnosis of neuroendocrine tumours. *Nat Rev Endocrinol* **14**, 656–669 (2018).

27. Modlin, I. M., Bodei, L. & Kidd, M. Neuroendocrine tumor biomarkers: From monoanalytes to transcripts and algorithms. *Best Pract Res Clin Endocrinol Metab* **30**, 59–77 (2016).
28. Al-Risi, E. S., Al-Essry, F. S. & Mula-Abed, W.-A. S. Chromogranin A as a Biochemical Marker for Neuroendocrine Tumors: A Single Center Experience at Royal Hospital, Oman. *Oman Med J* **32**, 365–370 (2017).
29. Gut, P. *et al.* Chromogranin A - unspecific neuroendocrine marker. Clinical utility and potential diagnostic pitfalls. *Arch Med Sci* **12**, 1–9 (2016).
30. Modlin, I. M. *et al.* Chromogranin A--biological function and clinical utility in neuro endocrine tumor disease. *Ann Surg Oncol* **17**, 2427–2443 (2010).
31. Jianu, C. S., Fossmark, R., Syversen, U., Hauso, Ø. & Waldum, H. L. A meal test improves the specificity of chromogranin A as a marker of neuroendocrine neoplasia. *Tumour Biol* **31**, 373–380 (2010).
32. Sciarra, A. *et al.* Chromogranin A expression in familial versus sporadic prostate cancer. *Urology* **66**, 1010–1014 (2005).
33. Lawrence, B. *et al.* The clinical relevance of chromogranin A as a biomarker for gastroenteropancreatic neuroendocrine tumors. *Endocrinol Metab Clin North Am* **40**, 111–134, viii (2011).
34. Jørgensen, L. G., Løber, J., Carlsen, N. L., Momsen, G. & Hirsch, F. R. Serum neuron specific enolase (S-NSE) reference interval evaluation by time-resolved immunofluorometry compared with a radioimmunoassay. *Clin Chim Acta* **249**, 77–91 (1996).
35. Park, T. *et al.* Overexpression of Neuron-Specific Enolase as a Prognostic Factor in Patients with Gastric Cancer. *J Gastric Cancer* **17**, 228–236 (2017).
36. Bajetta, E. *et al.* Chromogranin A, neuron specific enolase, carcinoembryonic antigen, and hydroxyindole acetic acid evaluation in patients with neuroendocrine tumors. *Cancer* **86**, 858–865 (1999).
37. Baudin, E. *et al.* Neuron-specific enolase and chromogranin A as markers of neuroendocrine tumours. *Br J Cancer* **78**, 1102–1107 (1998).
38. van Adrichem, R. C. S. *et al.* Serum neuron-specific enolase level is an independent predictor of overall survival in patients with gastroenteropancreatic neuroendocrine tumors. *Ann Oncol* **27**, 746–747 (2016).
39. Appetecchia, M., Lauretta, R., Rota, F. & Carlini, M. Neuroendocrine Tumors Biomarkers. in *Abdominal Neuroendocrine Tumors* (ed. Carlini, M.) 65–78 (Springer Milan, 2018). doi:10.1007/978-88-470-3955-1_5.
40. Sansone, A. *et al.* Specific and Non-Specific Biomarkers in Neuroendocrine Gastroenteropancreatic Tumors. *Cancers (Basel)* **11**, E1113 (2019).
41. Eriksson, B., Oberg, K. & Stridsberg, M. Tumor markers in neuroendocrine tumors. *Digestion* **62 Suppl 1**, 33–38 (2000).
42. Panzuto, F. *et al.* Utility of combined use of plasma levels of chromogranin A and pancreatic polypeptide in the diagnosis of gastrointestinal and pancreatic endocrine tumors. *J Endocrinol Invest* **27**, 6–11 (2004).
43. Kanakis, G. & Kaltsas, G. Biochemical markers for gastroenteropancreatic neuroendocrine tumours (GEP-NETs). *Best Pract Res Clin Gastroenterol* **26**, 791–802 (2012).
44. Yu, R. Radiotherapy: Radioactive somatostatin analog therapy against carcinoids. *Nat Rev Endocrinol* **6**, 428–430 (2010).
45. Kyriakopoulos, G., Mavroei, V., Chatzellis, E., Kaltsas, G. A. & Alexandraki, K. I. Histopathological, immunohistochemical, genetic and molecular markers of neuroendocrine neoplasms. *Ann Transl Med* **6**, 252 (2018).
46. Turner, G. B. *et al.* Circulating markers of prognosis and response to treatment in patients with midgut carcinoid tumours. *Gut* **55**, 1586–1591 (2006).
47. Patel, P. & Galoian, K. Molecular challenges of neuroendocrine tumors. *Oncol Lett* **15**, 2715–2725 (2018).
48. Al Jadir, S. Insulinoma: Literature's Review (Part 1). *Endocrinology&Metabolism International Journal* **2**, (2015).
49. Perry, R. R. & Vinik, A. I. Clinical review 72: diagnosis and management of functioning islet cell tumors. *J Clin Endocrinol Metab* **80**, 2273–2278 (1995).
50. Huang, P.-Y. *et al.* Prognostic factors of patients with gastroenteropancreatic neuroendocrine neoplasms. *Kaohsiung J Med Sci* **34**, 650–656 (2018).
51. Malczewska, A., Bodei, L., Kidd, M. & Modlin, I. M. Blood mRNA Measurement (NETest) for Neuroendocrine Tumor Diagnosis of Image-Negative Liver Metastatic Disease. *J Clin Endocrinol Metab* **104**, 867–872 (2019).
52. Yeh, S.-C. A. *et al.* 5-aminolevulinic acid induced protoporphyrin IX as a fluorescence marker for quantitative image analysis of high-grade dysplasia in Barrett's esophagus cellular models. *JBO* **20**, 036010 (2015).
53. Shtivelman, E. Testing for Tumor Mutations: Liquid Biopsy Versus Traditional Biopsy. *Cancer Commons* <https://cancercommons.org/latest-insights/testing-for-tumor-mutations-liquid-biopsy-versus-solid-tumor-biopsy/> (2017).
54. Criscitiello, C. *et al.* Biopsy confirmation of metastatic sites in breast cancer patients: clinical impact and future perspectives. *Breast Cancer Res* **16**, 205 (2014).

55. Shen, J., Stass, S. A. & Jiang, F. MicroRNAs as potential biomarkers in human solid tumors. *Cancer Lett* **329**, 125–136 (2013).
56. Paterlini-Brechot, P. & Benali, N. L. Circulating tumor cells (CTC) detection: clinical impact and future directions. *Cancer Lett* **253**, 180–204 (2007).
57. Madhavan, D. *et al.* Plasma DNA integrity as a biomarker for primary and metastatic breast cancer and potential marker for early diagnosis. *Breast Cancer Res Treat* **146**, 163–174 (2014).
58. Madhavan, D. *et al.* Circulating miRNAs as surrogate markers for circulating tumor cells and prognostic markers in metastatic breast cancer. *Clin Cancer Res* **18**, 5972–5982 (2012).
59. Cuk, K. *et al.* Circulating microRNAs in plasma as early detection markers for breast cancer. *International Journal of Cancer* **132**, 1602–1612 (2013).
60. Cuk, K. *et al.* Plasma MicroRNA Panel for Minimally Invasive Detection of Breast Cancer. *PLOS ONE* **8**, e76729 (2013).
61. Stroun, M. *et al.* The origin and mechanism of circulating DNA. *Ann N Y Acad Sci* **906**, 161–168 (2000).
62. Stroun, M., Lyautey, J., Lederrey, C., Olson-Sand, A. & Anker, P. About the possible origin and mechanism of circulating DNA apoptosis and active DNA release. *Clin Chim Acta* **313**, 139–142 (2001).
63. van der Vaart, M. & Pretorius, P. J. Circulating DNA. Its origin and fluctuation. *Ann N Y Acad Sci* **1137**, 18–26 (2008).
64. Diaz, L. A. & Bardelli, A. Liquid biopsies: genotyping circulating tumor DNA. *J Clin Oncol* **32**, 579–586 (2014).
65. Thierry, A. R., El Messaoudi, S., Gahan, P. B., Anker, P. & Stroun, M. Origins, structures, and functions of circulating DNA in oncology. *Cancer Metastasis Rev* **35**, 347–376 (2016).
66. Aucamp, J., Bronkhorst, A. J., Badenhorst, C. P. S. & Pretorius, P. J. The diverse origins of circulating cell-free DNA in the human body: a critical re-evaluation of the literature. *Biol Rev Camb Philos Soc* **93**, 1649–1683 (2018).
67. Beck, J., Urnovitz, H. B., Riggert, J., Clerici, M. & Schütz, E. Profile of the circulating DNA in apparently healthy individuals. *Clin Chem* **55**, 730–738 (2009).
68. Holdenrieder, S. & Stieber, P. Apoptotic markers in cancer. *Clin Biochem* **37**, 605–617 (2004).
69. Mandel, P. & Metais, P. Nuclear Acids In Human Blood Plasma. *C R Seances Soc Biol Fil* **142**, 241–243 (1948).
70. Tan, E. M., Schur, P. H., Carr, R. I. & Kunkel, H. G. Deoxybonucleic acid (DNA) and antibodies to DNA in the serum of patients with systemic lupus erythematosus. *J Clin Invest* **45**, 1732–1740 (1966).
71. Koffler, D., Agnello, V., Winchester, R. & Kunkel, H. G. The occurrence of single-stranded DNA in the serum of patients with systemic lupus erythematosus and other diseases. *J Clin Invest* **52**, 198–204 (1973).
72. Jung, K., Fleischhacker, M. & Rabien, A. Cell-free DNA in the blood as a solid tumor biomarker--a critical appraisal of the literature. *Clin Chim Acta* **411**, 1611–1624 (2010).
73. Chan, K. C. A., Yeung, S.-W., Lui, W.-B., Rainer, T. H. & Lo, Y. M. D. Effects of preanalytical factors on the molecular size of cell-free DNA in blood. *Clin Chem* **51**, 781–784 (2005).
74. Bortner, C. D., Oldenburg, N. B. & Cidlowski, J. A. The role of DNA fragmentation in apoptosis. *Trends Cell Biol* **5**, 21–26 (1995).
75. Jahr, S. *et al.* DNA fragments in the blood plasma of cancer patients: quantitations and evidence for their origin from apoptotic and necrotic cells. *Cancer Res* **61**, 1659–1665 (2001).
76. Delgado, P. O. *et al.* Characterization of cell-free circulating DNA in plasma in patients with prostate cancer. *Tumour Biol* **34**, 983–986 (2013).
77. Jiang, W.-W. *et al.* Increased plasma DNA integrity index in head and neck cancer patients. *Int J Cancer* **119**, 2673–2676 (2006).
78. Wang, B. G. *et al.* Increased plasma DNA integrity in cancer patients. *Cancer Res* **63**, 3966–3968 (2003).
79. Bronkhorst, A. J., Ungerer, V. & Holdenrieder, S. The emerging role of cell-free DNA as a molecular marker for cancer management. *Biomol Detect Quantif* **17**, 100087 (2019).
80. Gahan, P. B. & Stroun, M. The virtosome-a novel cytosolic informative entity and intercellular messenger. *Cell Biochem Funct* **28**, 529–538 (2010).
81. Stroun, M. *et al.* Presence of RNA in the nucleoprotein complex spontaneously released by human lymphocytes and frog auricles in culture. *Cancer Res* **38**, 3546–3554 (1978).
82. Anker, P., Stroun, M. & Maurice, P. A. Spontaneous release of DNA by human blood lymphocytes as shown in an in vitro system. *Cancer Res* **35**, 2375–2382 (1975).
83. Stroun, M. & Anker, P. Nucleic acids spontaneously released by living frog auricles. *Biochem J* **128**, 100P-101P (1972).
84. Borenstein, S. & Ephrati-Elizur, E. Spontaneous release of DNA in sequential genetic order by *Bacillus subtilis*. *J Mol Biol* **45**, 137–152 (1969).

85. Wang, W. *et al.* Characterization of the release and biological significance of cell-free DNA from breast cancer cell lines. *Oncotarget* **8**, 43180–43191 (2017).
86. Aucamp, J. *et al.* Kinetic analysis, size profiling, and bioenergetic association of DNA released by selected cell lines in vitro. *Cell Mol Life Sci* **74**, 2689–2707 (2017).
87. Bronkhorst, A. J. *et al.* Characterization of the cell-free DNA released by cultured cancer cells. *Biochim Biophys Acta* **1863**, 157–165 (2016).
88. Fernando, M. R., Jiang, C., Krzyzanowski, G. D. & Ryan, W. L. New evidence that a large proportion of human blood plasma cell-free DNA is localized in exosomes. *PLoS One* **12**, e0183915 (2017).
89. Thakur, B. K. *et al.* Double-stranded DNA in exosomes: a novel biomarker in cancer detection. *Cell Res* **24**, 766–769 (2014).
90. Leon, S. A., Shapiro, B., Sklaroff, D. M. & Yaros, M. J. Free DNA in the serum of cancer patients and the effect of therapy. *Cancer Res* **37**, 646–650 (1977).
91. Gormally, E., Caboux, E., Vineis, P. & Hainaut, P. Circulating free DNA in plasma or serum as biomarker of carcinogenesis: practical aspects and biological significance. *Mutat Res* **635**, 105–117 (2007).
92. Zanetti-Dällenbach, R. *et al.* Positive correlation of cell-free DNA in plasma/serum in patients with malignant and benign breast disease. *Anticancer Res* **28**, 921–925 (2008).
93. Zhong, X. Y. *et al.* Elevated level of cell-free plasma DNA is associated with breast cancer. *Arch Gynecol Obstet* **276**, 327–331 (2007).
94. Fleischhacker, M. & Schmidt, B. Circulating nucleic acids (CNAs) and cancer—a survey. *Biochim Biophys Acta* **1775**, 181–232 (2007).
95. Gal, S. *et al.* Quantitation of circulating DNA in the serum of breast cancer patients by real-time PCR. *Br J Cancer* **90**, 1211–1215 (2004).
96. Danese, E. *et al.* Real-time polymerase chain reaction quantification of free DNA in serum of patients with polyps and colorectal cancers. *Clinical Chemistry and Laboratory Medicine* **48**, 1665–1668 (2010).
97. Faria, G., Silva, E., Da Fonseca, C. & Quirico-Santos, T. Circulating Cell-Free DNA as a Prognostic and Molecular Marker for Patients with Brain Tumors under Perillyl Alcohol-Based Therapy. *Int J Mol Sci* **19**, E1610 (2018).
98. Chan, K. C. A. *et al.* Analysis of Plasma Epstein-Barr Virus DNA to Screen for Nasopharyngeal Cancer. *N Engl J Med* **377**, 513–522 (2017).
99. Bianchi, D. W. *et al.* Noninvasive Prenatal Testing and Incidental Detection of Occult Maternal Malignancies. *JAMA* **314**, 162–169 (2015).
100. Amant, F. *et al.* Presymptomatic Identification of Cancers in Pregnant Women During Noninvasive Prenatal Testing. *JAMA Oncol* **1**, 814–819 (2015).
101. Sun, K. *et al.* Plasma DNA tissue mapping by genome-wide methylation sequencing for noninvasive prenatal, cancer, and transplantation assessments. *Proc Natl Acad Sci U S A* **112**, E5503–5512 (2015).
102. Cohen, J. D. *et al.* Detection and localization of surgically resectable cancers with a multi-analyte blood test. *Science* **359**, 926–930 (2018).
103. Tian, G. *et al.* *The Early Diagnosis in Lung Cancer by the Detection of Circulating Tumor DNA*. 189340 <https://www.biorxiv.org/content/10.1101/189340v2> (2017) doi:10.1101/189340.
104. Cohen, P. A. *et al.* Abnormal plasma DNA profiles in early ovarian cancer using a non-invasive prenatal testing platform: implications for cancer screening. *BMC Med* **14**, 126 (2016).
105. Bettegowda, C. *et al.* Detection of Circulating Tumor DNA in Early- and Late-Stage Human Malignancies. *Science Translational Medicine* (2014).
106. Newman, A. M. *et al.* An ultrasensitive method for quantitating circulating tumor DNA with broad patient coverage. *Nat Med* **20**, 548–554 (2014).
107. Kinde, I. *et al.* Evaluation of DNA from the Papanicolaou test to detect ovarian and endometrial cancers. *Sci Transl Med* **5**, 167ra4 (2013).
108. Gormally, E. *et al.* TP53 and KRAS2 mutations in plasma DNA of healthy subjects and subsequent cancer occurrence: a prospective study. *Cancer Res* **66**, 6871–6876 (2006).
109. Mao, L., Hruban, R. H., Boyle, J. O., Tockman, M. & Sidransky, D. Detection of oncogene mutations in sputum precedes diagnosis of lung cancer. *Cancer Res* **54**, 1634–1637 (1994).
110. Aravanis, A. M., Lee, M. & Klausner, R. D. Next-Generation Sequencing of Circulating Tumor DNA for Early Cancer Detection. *Cell* **168**, 571–574 (2017).
111. Holdenrieder, S. *et al.* Circulating nucleosomes predict the response to chemotherapy in patients with advanced non-small cell lung cancer. *Clin Cancer Res* **10**, 5981–5987 (2004).
112. Abbosh, C. *et al.* Phylogenetic ctDNA analysis depicts early-stage lung cancer evolution. *Nature* **545**, 446–451 (2017).

113. Siravegna, G., Marsoni, S., Siena, S. & Bardelli, A. Integrating liquid biopsies into the management of cancer. *Nat Rev Clin Oncol* **14**, 531–548 (2017).
114. Wan, J. C. M. *et al.* Liquid biopsies come of age: towards implementation of circulating tumour DNA. *Nat Rev Cancer* **17**, 223–238 (2017).
115. Kamel, A. M., Teama, S., Fawzy, A. & El Deftar, M. Plasma DNA integrity index as a potential molecular diagnostic marker for breast cancer. *Tumour Biol* **37**, 7565–7572 (2016).
116. Zonta, E., Nizard, P. & Taly, V. Assessment of DNA Integrity, Applications for Cancer Research. *Adv Clin Chem* **70**, 197–246 (2015).
117. Sobhani, N., Generali, D., Zanconati, F., Bortul, M. & Scaggiante, B. Cell-free DNA integrity for the monitoring of breast cancer: Future perspectives? *World J Clin Oncol* **9**, 26–32 (2018).
118. Boynton, K. A., Summerhayes, I. C., Ahlquist, D. A. & Shuber, A. P. DNA integrity as a potential marker for stool-based detection of colorectal cancer. *Clin Chem* **49**, 1058–1065 (2003).
119. Giacona, M. B. *et al.* Cell-free DNA in human blood plasma: length measurements in patients with pancreatic cancer and healthy controls. *Pancreas* **17**, 89–97 (1998).
120. Mouliere, F. *et al.* High fragmentation characterizes tumour-derived circulating DNA. *PLoS One* **6**, e23418 (2011).
121. Thierry, A. R. *et al.* Origin and quantification of circulating DNA in mice with human colorectal cancer xenografts. *Nucleic Acids Res* **38**, 6159–6175 (2010).
122. Jiang, P. *et al.* Lengthening and shortening of plasma DNA in hepatocellular carcinoma patients. *Proc Natl Acad Sci U S A* **112**, E1317–1325 (2015).
123. Umetani, N. *et al.* Increased integrity of free circulating DNA in sera of patients with colorectal or periampullary cancer: direct quantitative PCR for ALU repeats. *Clin Chem* **52**, 1062–1069 (2006).
124. Lander, E. S. *et al.* Initial sequencing and analysis of the human genome. *Nature* **409**, 860–921 (2001).
125. Andreassen, R. [Alu elements in the human genome]. *Tidsskr Nor Laegeforen* **124**, 2345–2349 (2004).
126. Ostertag, E. M. & Kazazian, H. H. Biology of mammalian L1 retrotransposons. *Annu Rev Genet* **35**, 501–538 (2001a).
127. Ostertag, E. M. & Kazazian, H. H. Twin priming: a proposed mechanism for the creation of inversions in L1 retrotransposition. *Genome Res* **11**, 2059–2065 (2001b).
128. Schmid, C. W. & Deininger, P. L. Sequence organization of the human genome. *Cell* **6**, 345–358 (1975).
129. Batzer, M. A. & Deininger, P. L. Alu repeats and human genomic diversity. *Nat Rev Genet* **3**, 370–379 (2002).
130. Deininger, P. Alu elements: know the SINEs. *Genome Biol* **12**, 236 (2011).
131. Walker, J. A. *et al.* Human DNA quantitation using Alu element-based polymerase chain reaction. *Anal Biochem* **315**, 122–128 (2003).
132. Price, A. L., Eskin, E. & Pevzner, P. A. Whole-genome analysis of Alu repeat elements reveals complex evolutionary history. *Genome Res* **14**, 2245–2252 (2004).
133. Zheng, Z., Luo, Y. & McMaster, G. K. Sensitive and quantitative measurement of gene expression directly from a small amount of whole blood. *Clin Chem* **52**, 1294–1302 (2006).
134. Hwu, H. R., Roberts, J. W., Davidson, E. H. & Britten, R. J. Insertion and/or deletion of many repeated DNA sequences in human and higher ape evolution. *Proc Natl Acad Sci U S A* **83**, 3875–3879 (1986).
135. Moosavi, A. & Motevalizadeh Ardekani, A. Role of Epigenetics in Biology and Human Diseases. *Iran Biomed J* **20**, 246–258 (2016).
136. Guo, M., Peng, Y., Gao, A., Du, C. & Herman, J. G. Epigenetic heterogeneity in cancer. *Biomark Res* **7**, 23 (2019).
137. Santini, V., Kantarjian, H. M. & Issa, J. P. Changes in DNA methylation in neoplasia: pathophysiology and therapeutic implications. *Ann Intern Med* **134**, 573–586 (2001).
138. Peinado, M. A. Hypomethylation of DNA. In *Encyclopedia of Cancer*, M. Schwab, ed. (Berlin, Heidelberg: Springer Berlin Heidelberg),. (2011).
139. Janitz, K. & Janitz, M. Chapter 12 - Assessing Epigenetic Information. in *Handbook of Epigenetics* (ed. Tollefsbol, T.) 173–181 (Academic Press, 2011). doi:10.1016/B978-0-12-375709-8.00012-5.
140. Buj, R. *et al.* Quantification of Unmethylated Alu (QUALu): a tool to assess global hypomethylation in routine clinical samples. *Oncotarget* **7**, 10536–10546 (2016).
141. Robertson, K. D. & Wolffe, A. P. DNA methylation in health and disease. *Nat Rev Genet* **1**, 11–19 (2000).
142. Herman, J. G. & Baylin, S. B. Gene silencing in cancer in association with promoter hypermethylation. *N Engl J Med* **349**, 2042–2054 (2003).
143. Feinberg, A. P. & Vogelstein, B. Hypomethylation distinguishes genes of some human cancers from their normal counterparts. *Nature* **301**, 89–92 (1983).
144. Ting, A. H., McGarvey, K. M. & Baylin, S. B. The cancer epigenome--components and functional correlates. *Genes Dev* **20**, 3215–3231 (2006).

145. Jones, P. A. & Baylin, S. B. The epigenomics of cancer. *Cell* **128**, 683–692 (2007).
146. Lee, Y.-C. *et al.* Revisit of field cancerization in squamous cell carcinoma of upper aerodigestive tract: better risk assessment with epigenetic markers. *Cancer Prev Res (Phila)* **4**, 1982–1992 (2011).
147. Cheng, J. *et al.* Cell-free circulating DNA integrity is an independent predictor of impending breast cancer recurrence. *Oncotarget* **8**, 54537–54547 (2017).
148. Huang, A. *et al.* Plasma Circulating Cell-free DNA Integrity as a Promising Biomarker for Diagnosis and Surveillance in Patients with Hepatocellular Carcinoma. *J Cancer* **7**, 1798–1803 (2016).
149. Funakoshi, K. *et al.* Highly sensitive and specific Alu-based quantification of human cells among rodent cells. *Sci Rep* **7**, 13202 (2017).
150. Townsend, C. M., Ishizuka, J. & Thompson, J. C. Studies of growth regulation in a neuroendocrine cell line. *Acta Oncol* **32**, 125–130 (1993).
151. Parekh, D. *et al.* Characterization of a human pancreatic carcinoid in vitro: morphology, amine and peptide storage, and secretion. *Pancreas* **9**, 83–90 (1994).
152. Umetani, N. *et al.* Prediction of breast tumor progression by integrity of free circulating DNA in serum. *J Clin Oncol* **24**, 4270–4276 (2006).
153. Arya, M. *et al.* Basic principles of real-time quantitative PCR. *Expert Rev Mol Diagn* **5**, 209–219 (2005).
154. Bossuyt, P. M. *et al.* Towards complete and accurate reporting of studies of diagnostic accuracy: the STARD initiative. Standards for Reporting of Diagnostic Accuracy. *Clin Chem* **49**, 1–6 (2003).
155. Weiß, C. *Basiswissen Medizinische Statistik*. (Springer Berlin Heidelberg, 2019). doi:10.1007/978-3-662-56588-9.
156. Obuchowski, N. A., Lieber, M. L. & Wians, F. H. ROC curves in clinical chemistry: uses, misuses, and possible solutions. *Clin Chem* **50**, 1118–1125 (2004).
157. Carter, J. V., Pan, J., Rai, S. N. & Galandiuk, S. ROC-ing along: Evaluation and interpretation of receiver operating characteristic curves. *Surgery* **159**, 1638–1645 (2016).
158. García-Giménez, J. L. *et al.* Epigenetic biomarkers: Current strategies and future challenges for their use in the clinical laboratory. *Crit Rev Clin Lab Sci* **54**, 529–550 (2017).
159. Ekelund, S. ROC Curves—What are They and How are They Used? *Point of Care* **11**, 16–21 (2012).
160. Lo, Y. M. *et al.* Quantitative analysis of fetal DNA in maternal plasma and serum: implications for noninvasive prenatal diagnosis. *Am J Hum Genet* **62**, 768–775 (1998).
161. Lee, T. H., Montalvo, L., Chrebtow, V. & Busch, M. P. Quantitation of genomic DNA in plasma and serum samples: higher concentrations of genomic DNA found in serum than in plasma. *Transfusion* **41**, 276–282 (2001).
162. Lui, Y. Y. N. *et al.* Predominant hematopoietic origin of cell-free DNA in plasma and serum after sex-mismatched bone marrow transplantation. *Clin Chem* **48**, 421–427 (2002).
163. Jung, M., Klotzek, S., Lewandowski, M., Fleischhacker, M. & Jung, K. Changes in concentration of DNA in serum and plasma during storage of blood samples. *Clin Chem* **49**, 1028–1029 (2003).
164. Umetani, N., Hiramatsu, S. & Hoon, D. S. B. Higher amount of free circulating DNA in serum than in plasma is not mainly caused by contaminated extraneous DNA during separation. *Ann N Y Acad Sci* **1075**, 299–307 (2006).
165. Wang, K. *et al.* Comparing the MicroRNA spectrum between serum and plasma. *PLoS One* **7**, e41561 (2012).
166. Vallée, A. *et al.* Plasma is a better source of tumor-derived circulating cell-free DNA than serum for the detection of EGFR alterations in lung tumor patients. *Lung Cancer* **82**, 373–374 (2013).
167. Warton, K. *et al.* Methylation-capture and Next-Generation Sequencing of free circulating DNA from human plasma. *BMC Genomics* **15**, 476 (2014).
168. Nie, K., Jia, Y. & Zhang, X. Cell-free circulating tumor DNA in plasma/serum of non-small cell lung cancer. *Tumour Biol* **36**, 7–19 (2015).
169. Keller, L., Belloum, Y., Wikman, H. & Pantel, K. Clinical relevance of blood-based ctDNA analysis: mutation detection and beyond. *Br J Cancer* **124**, 345–358 (2021).
170. Yokota, M., Tatsumi, N., Nathalang, O., Yamada, T. & Tsuda, I. Effects of heparin on polymerase chain reaction for blood white cells. *J Clin Lab Anal* **13**, 133–140 (1999).
171. Cai, D., Behrmann, O., Hufert, F., Dame, G. & Urban, G. Capacity of rTth polymerase to detect RNA in the presence of various inhibitors. *PLoS One* **13**, e0190041 (2018).
172. Normanno, N., Denis, M. G., Thress, K. S., Ratcliffe, M. & Reck, M. Guide to detecting epidermal growth factor receptor (EGFR) mutations in ctDNA of patients with advanced non-small-cell lung cancer. *Oncotarget* **8**, 12501–12516 (2017).
173. Diehl, F. *et al.* Circulating mutant DNA to assess tumor dynamics. *Nat Med* **14**, 985–990 (2008).
174. Roth, C. *et al.* Apoptosis-related deregulation of proteolytic activities and high serum levels of circulating nucleosomes and DNA in blood correlate with breast cancer progression. *BMC Cancer* **11**, 4 (2011).
175. Yao, W., Mei, C., Nan, X. & Hui, L. Evaluation and comparison of in vitro degradation kinetics of DNA in serum, urine and saliva: A qualitative study. *Gene* **590**, 142–148 (2016).

176. Bhangu, J. S., Taghizadeh, H., Braunschmid, T., Bachleitner-Hofmann, T. & Mannhalter, C. Circulating cell-free DNA in plasma of colorectal cancer patients - A potential biomarker for tumor burden. *Surg Oncol* **26**, 395–401 (2017).
177. Pérez-Barrios, C. *et al.* Comparison of methods for circulating cell-free DNA isolation using blood from cancer patients: impact on biomarker testing. *Transl Lung Cancer Res* **5**, 665–672 (2016).
178. Devonshire, A. S. *et al.* Towards standardisation of cell-free DNA measurement in plasma: controls for extraction efficiency, fragment size bias and quantification. *Anal Bioanal Chem* **406**, 6499–6512 (2014).
179. Kohler, C. *et al.* Levels of plasma circulating cell free nuclear and mitochondrial DNA as potential biomarkers for breast tumors. *Mol Cancer* **8**, 105 (2009).
180. Catarino, R. *et al.* Quantification of free circulating tumor DNA as a diagnostic marker for breast cancer. *DNA Cell Biol* **27**, 415–421 (2008).
181. Shapiro, B., Chakrabarty, M., Cohn, E. M. & Leon, S. A. Determination of circulating DNA levels in patients with benign or malignant gastrointestinal disease. *Cancer* **51**, 2116–2120 (1983).
182. Schwarzenbach, H., Stoehlmacher, J., Pantel, K. & Goekkurt, E. Detection and monitoring of cell-free DNA in blood of patients with colorectal cancer. *Ann N Y Acad Sci* **1137**, 190–196 (2008).
183. Zachariah, R. R. *et al.* Levels of circulating cell-free nuclear and mitochondrial DNA in benign and malignant ovarian tumors. *Obstet Gynecol* **112**, 843–850 (2008).
184. Jung, K. *et al.* Increased cell-free DNA in plasma of patients with metastatic spread in prostate cancer. *Cancer Lett* **205**, 173–180 (2004).
185. Allen, D. *et al.* Role of Cell-Free Plasma DNA as a Diagnostic Marker for Prostate Cancer. *Annals of the New York Academy of Sciences* **1022**, 76–80 (2004).
186. Ellinger, J. *et al.* Cell-free circulating DNA: diagnostic value in patients with testicular germ cell cancer. *J Urol* **181**, 363–371 (2009).
187. Haselmann, V. *et al.* Results of the first external quality assessment scheme (EQA) for isolation and analysis of circulating tumour DNA (ctDNA). *Clin Chem Lab Med* **56**, 220–228 (2018).
188. Schwarzenbach, H., Hoon, D. S. B. & Pantel, K. Cell-free nucleic acids as biomarkers in cancer patients. *Nat Rev Cancer* **11**, 426–437 (2011).
189. Oversoe, S. K., Sorensen, B. S., Tabaksblat, E. M., Gronbaek, H. & Kelsen, J. CELL-FREE DNA AND CLINICAL CHARACTERISTICS IN PATIENTS WITH SMALL INTESTINAL OR PANCREATIC NEUROENDOCRINE TUMORS. *Neuroendocrinology* (2021) doi:10.1159/000514457.
190. Alix-Panabières, C., Schwarzenbach, H. & Pantel, K. Circulating Tumor Cells and Circulating Tumor DNA. *Annual Review of Medicine* **63**, 199–215 (2012).
191. Agassi, R. *et al.* Measurement of circulating cell-free DNA levels by a simple fluorescent test in patients with breast cancer. *Am J Clin Pathol* **143**, 18–24 (2015).
192. Mouliere, F. *et al.* Circulating Cell-Free DNA from Colorectal Cancer Patients May Reveal High KRAS or BRAF Mutation Load. *Transl Oncol* **6**, 319–328 (2013).
193. Esposito, A. *et al.* Monitoring tumor-derived cell-free DNA in patients with solid tumors: clinical perspectives and research opportunities. *Cancer Treat Rev* **40**, 648–655 (2014).
194. Wang, Y. *et al.* Detection of tumor-derived DNA in cerebrospinal fluid of patients with primary tumors of the brain and spinal cord. *Proc Natl Acad Sci U S A* **112**, 9704–9709 (2015).
195. Parkinson, C. A. *et al.* Exploratory Analysis of TP53 Mutations in Circulating Tumour DNA as Biomarkers of Treatment Response for Patients with Relapsed High-Grade Serous Ovarian Carcinoma: A Retrospective Study. *PLoS Med* **13**, e1002198 (2016).
196. Gorges, T. M. *et al.* Cancer therapy monitoring in xenografts by quantitative analysis of circulating tumor DNA. *Biomarkers* **17**, 498–506 (2012).
197. Kamat, A. A. *et al.* Circulating cell-free DNA: a novel biomarker for response to therapy in ovarian carcinoma. *Cancer Biol Ther* **5**, 1369–1374 (2006).
198. Peled, M. *et al.* Cell-free DNA concentration in patients with clinical or mammographic suspicion of breast cancer. *Sci Rep* **10**, 14601 (2020).
199. Eisenhauer, E. A. *et al.* New response evaluation criteria in solid tumours: revised RECIST guideline (version 1.1). *Eur J Cancer* **45**, 228–247 (2009).
200. Xu, X. *et al.* Role of circulating free DNA in evaluating clinical tumor burden and predicting survival in Chinese metastatic colorectal cancer patients. *BMC Cancer* **20**, 1006 (2020).
201. Hamfjord, J. *et al.* Total circulating cell-free DNA as a prognostic biomarker in metastatic colorectal cancer before first-line oxaliplatin-based chemotherapy. *Ann Oncol* **30**, 1088–1095 (2019).
202. Berger, A. W. *et al.* Treatment monitoring in metastatic colorectal cancer patients by quantification and KRAS genotyping of circulating cell-free DNA. *PLoS One* **12**, e0174308 (2017).

203. Nygaard, A. D., Holdgaard, P. C., Spindler, K.-L. G., Pallisgaard, N. & Jakobsen, A. The correlation between cell-free DNA and tumour burden was estimated by PET/CT in patients with advanced NSCLC. *Br J Cancer* **110**, 363–368 (2014).
204. Rago, C. *et al.* Serial assessment of human tumor burdens in mice by the analysis of circulating DNA. *Cancer Res* **67**, 9364–9370 (2007).
205. Phallen, J. *et al.* Early Noninvasive Detection of Response to Targeted Therapy in Non-Small Cell Lung Cancer. *Cancer Res* **79**, 1204–1213 (2019).
206. Dawson, S.-J. *et al.* Analysis of circulating tumor DNA to monitor metastatic breast cancer. *N Engl J Med* **368**, 1199–1209 (2013).
207. Goldberg, S. B. *et al.* Early Assessment of Lung Cancer Immunotherapy Response via Circulating Tumor DNA. *Clin Cancer Res* **24**, 1872–1880 (2018).
208. Allegretti, M. *et al.* Cross-sectional analysis of circulating tumor DNA in primary colorectal cancer at surgery and during post-surgery follow-up by liquid biopsy. *J Exp Clin Cancer Res* **39**, 69 (2020).
209. Vidal, J. *et al.* Plasma ctDNA RAS mutation analysis for the diagnosis and treatment monitoring of metastatic colorectal cancer patients. *Ann Oncol* **28**, 1325–1332 (2017).
210. Cao, H. *et al.* Circulating Tumor DNA Is Capable of Monitoring the Therapeutic Response and Resistance in Advanced Colorectal Cancer Patients Undergoing Combined Target and Chemotherapy. *Front Oncol* **10**, 466 (2020).
211. Ma, F. *et al.* Assessing tumor heterogeneity using ctDNA to predict and monitor therapeutic response in metastatic breast cancer. *Int J Cancer* **146**, 1359–1368 (2020).
212. Tuma, R. S. *et al.* Characterization of SYBR Gold nucleic acid gel stain: a dye optimized for use with 300-nm ultraviolet transilluminators. *Anal Biochem* **268**, 278–288 (1999).
213. Frattini, M. *et al.* Quantitative analysis of plasma DNA in colorectal cancer patients: a novel prognostic tool. *Ann N Y Acad Sci* **1075**, 185–190 (2006).
214. Shaw, J. A. *et al.* Circulating tumor cells and plasma DNA analysis in patients with indeterminate early or metastatic breast cancer. *Biomark Med* **5**, 87–91 (2011).
215. Forshew, T. *et al.* Noninvasive identification and monitoring of cancer mutations by targeted deep sequencing of plasma DNA. *Sci Transl Med* **4**, 136ra68 (2012).
216. Agassi, R. *et al.* Measurement of circulating cell-free DNA levels by a simple fluorescent test in patients with breast cancer. *Am J Clin Pathol* **143**, 18–24 (2015).
217. Chen, E. *et al.* Cell-free DNA concentration and fragment size as a biomarker for prostate cancer. *Sci Rep* **11**, 5040 (2021).
218. Leung, F. *et al.* Circulating Tumor DNA as a Cancer Biomarker: Fact or Fiction? *Clinical Chemistry* **62**, 1054–1060 (2016).
219. Adashek, J. J., Janku, F. & Kurzrock, R. Signed in Blood: Circulating Tumor DNA in Cancer Diagnosis, Treatment and Screening, *Cancers*. **13**, 3600, (2021).
220. Schwarzenbach, H., Müller, V., Milde-Langosch, K., Steinbach, B. & Pantel, K. Evaluation of cell-free tumour DNA and RNA in patients with breast cancer and benign breast disease. *Mol Biosyst* **7**, 2848–2854 (2011).
221. Underhill, H. R. *et al.* Fragment Length of Circulating Tumor DNA. *PLoS Genet* **12**, e1006162 (2016).
222. Chan, K. C. A. *et al.* Size distributions of maternal and fetal DNA in maternal plasma. *Clin Chem* **50**, 88–92 (2004).
223. Mamon, H. *et al.* Preferential amplification of apoptotic DNA from plasma: potential for enhancing detection of minor DNA alterations in circulating DNA. *Clin Chem* **54**, 1582–1584 (2008).
224. Mori, S. *et al.* The possibility of a valuable resource of circulating DNA for single nucleotide polymorphisms genotyping: the application of a rapid and simple polymerase chain reaction with melting curve analysis for methyltetrahydrofolate reductase polymorphisms. *Lab Hematol* **13**, 1–5 (2007).
225. Liu, K. J., Brock, M. V., Shih, I.-M. & Wang, T.-H. Decoding circulating nucleic acids in human serum using microfluidic single molecule spectroscopy. *J Am Chem Soc* **132**, 5793–5798 (2010).
226. Diehl, F. *et al.* Detection and quantification of mutations in the plasma of patients with colorectal tumors. *Proc Natl Acad Sci U S A* **102**, 16368–16373 (2005).
227. Mouliere, F. *et al.* Enhanced detection of circulating tumor DNA by fragment size analysis. *Sci Transl Med* **10**, eaat4921 (2018).
228. Thakur, S. *et al.* Limited Utility of Circulating Cell-Free DNA Integrity as a Diagnostic Tool for Differentiating Between Malignant and Benign Thyroid Nodules With Indeterminate Cytology (Bethesda Category III). *Front Oncol* **9**, 905 (2019).
229. Zheng, Y. W. L. *et al.* Nonhematopoietically derived DNA is shorter than hematopoietically derived DNA in plasma: a transplantation model. *Clin Chem* **58**, 549–558 (2012).

230. Lapin, M. *et al.* Fragment size and level of cell-free DNA provide prognostic information in patients with advanced pancreatic cancer. *J Transl Med* **16**, 300 (2018).
231. Widom, J. A relationship between the helical twist of DNA and the ordered positioning of nucleosomes in all eukaryotic cells. *Proc Natl Acad Sci U S A* **89**, 1095–1099 (1992).
232. Zhang, R., Nakahira, K., Guo, X., Choi, A. M. K. & Gu, Z. Very Short Mitochondrial DNA Fragments and Heteroplasmy in Human Plasma. *Sci Rep* **6**, 36097 (2016).
233. Cristiano, S. *et al.* Genome-wide cell-free DNA fragmentation in patients with cancer. *Nature* **570**, 385–389 (2019).
234. Iqbal, S. *et al.* Circulating cell-free DNA and its integrity as a prognostic marker for breast cancer. *Springerplus* **4**, 265 (2015).
235. Adigun, R., Basit, H. & Murray, J. Cell Liquefactive Necrosis. in *StatPearls* (StatPearls Publishing, 2021).
236. Whitlock, J. Overview of Necrosis in the Human Body. (2020).
237. Fawzy, A., Sweify, K. M., El-Fayoumy, H. M. & Nofal, N. Quantitative analysis of plasma cell-free DNA and its DNA integrity in patients with metastatic prostate cancer using ALU sequence. *Journal of the Egyptian National Cancer Institute* **28**, 235–242 (2016).
238. Lee, S. Y. *et al.* Regulation of Tumor Progression by Programmed Necrosis. *Oxid Med Cell Longev* **2018**, 3537471 (2018).
239. Song, W. S. *et al.* Spontaneous necrosis and additional tumor necrosis induced by preoperative chemotherapy for osteosarcoma: a case-control study. *J Orthop Sci* **20**, 174–179 (2015).
240. Tower, J. Programmed cell death in aging. *Ageing Res Rev* **23**, 90–100 (2015).
241. Lu, B., Chen, H.-D. & Hong-Guang, H.-G. The relationship between apoptosis and aging. *Advances in Bioscience and Biotechnology* **03**, 705 (2012).
242. Agostini, M. *et al.* Circulating cell-free DNA: a promising marker of regional lymphonode metastasis in breast cancer patients. *Cancer Biomark* **11**, 89–98 (2012).
243. Stötzer, O. J., Lehner, J., Fersching-Gierlich, D., Nagel, D. & Holdenrieder, S. Diagnostic relevance of plasma DNA and DNA integrity for breast cancer. *Tumour Biol* **35**, 1183–1191 (2014).
244. Cheng, J., Tang, Q., Cao, X. & Burwinkel, B. Cell-Free Circulating DNA Integrity Based on Peripheral Blood as a Biomarker for Diagnosis of Cancer: A Systematic Review. *Cancer Epidemiol Biomarkers Prev* **26**, 1595–1602 (2017).
245. Holdenrieder, S., Burges, A., Reich, O., Spelsberg, F. W. & Stieber, P. DNA integrity in plasma and serum of patients with malignant and benign diseases. *Ann N Y Acad Sci* **1137**, 162–170 (2008).
246. Tuchalska-Czuroń, J., Lenart, J., Augustyniak, J. & Durlik, M. Clinical value of tissue DNA integrity index in pancreatic cancer. *Surgeon* **18**, 269–279 (2020).
247. Mouliere, F. *et al.* Selecting short DNA fragments in plasma improves detection of circulating tumour DNA. 134437 <https://www.biorxiv.org/content/10.1101/134437v1> (2017) doi:10.1101/134437.
248. Mead, R., Duku, M., Bhandari, P. & Cree, I. A. Circulating tumour markers can define patients with normal colons, benign polyps, and cancers. *Br J Cancer* **105**, 239–245 (2011).
249. Maltoni, R. *et al.* Cell-free DNA detected by ‘liquid biopsy’ as a potential prognostic biomarker in early breast cancer. *Oncotarget* **8**, 16642–16649 (2017).
250. Yu, Z., Qin, S. & Wang, H. Alter circulating cell-free DNA variables in plasma of ovarian cancer patients. *J Obstet Gynaecol Res* **45**, 2237–2242 (2019).
251. Hao, T. B. *et al.* Circulating cell-free DNA in serum as a biomarker for diagnosis and prognostic prediction of colorectal cancer. *Br J Cancer* **111**, 1482–1489 (2014).
252. Lehner, J., Stötzer, O. J., Fersching, D., Nagel, D. & Holdenrieder, S. Circulating plasma DNA and DNA integrity in breast cancer patients undergoing neoadjuvant chemotherapy. *Clin Chim Acta* **425**, 206–211 (2013).
253. Zhang, R. *et al.* Clinical value of ALU concentration and integrity index for the early diagnosis of ovarian cancer: A retrospective cohort trial. *PLoS One* **13**, e0191756 (2018).
254. Gao, Y.-J. *et al.* Increased integrity of circulating cell-free DNA in plasma of patients with acute leukemia. *Clin Chem Lab Med* **48**, 1651–1656 (2010).
255. Hauser, S. *et al.* Cell-free circulating DNA: Diagnostic value in patients with renal cell cancer. *Anticancer Res* **30**, 2785–2789 (2010).
256. Pinzani, P. *et al.* Circulating cell-free DNA in plasma of melanoma patients: qualitative and quantitative considerations. *Clin Chim Acta* **412**, 2141–2145 (2011).
257. Salvianti, F. *et al.* Multiparametric analysis of cell-free DNA in melanoma patients. *PLoS One* **7**, e49843 (2012).
258. El-Shazly, S. F., Eid, M. A., El-Souroy, H. A., Attia, G. F. & Ezzat, S. A. Evaluation of serum DNA integrity as a screening and prognostic tool in patients with hepatitis C virus-related hepatocellular carcinoma. *Int J Biol Markers* **25**, 79–86 (2010).

259. Chen, H., Sun, L., Zheng, H., Zhang, Q. & Jin, X. Total serum DNA and DNA integrity: diagnostic value in patients with hepatitis B virus-related hepatocellular carcinoma. *Pathology* **44**, 318–324 (2012).
260. Hauser, S. *et al.* Cell-free serum DNA in patients with bladder cancer: results of a prospective multicenter study. *Anticancer Res* **32**, 3119–3124 (2012).
261. Shi, W. *et al.* Prognostic value of free DNA quantification in serum and cerebrospinal fluid in glioma patients. *J Mol Neurosci* **46**, 470–475 (2012).
262. Hanley, R. *et al.* DNA integrity assay: a plasma-based screening tool for the detection of prostate cancer. *Clin Cancer Res* **12**, 4569–4574 (2006).
263. Feng, J. *et al.* Plasma cell-free DNA and its DNA integrity as biomarker to distinguish prostate cancer from benign prostatic hyperplasia in patients with increased serum prostate-specific antigen. *Int Urol Nephrol* **45**, 1023–1028 (2013).
264. Chudasama, D. Y. *et al.* Prognostic value of the DNA integrity index in patients with malignant lung tumors. *Oncotarget* **9**, 21281–21288 (2018).
265. Kim, M. S. *et al.* Tumor necrosis rate adjusted by tumor volume change is a better predictor of survival of localized osteosarcoma patients. *Ann Surg Oncol* **15**, 906–914 (2008).
266. Sikora, K. *et al.* Evaluation of cell-free DNA as a biomarker for pancreatic malignancies. *Int J Biol Markers* **30**, e136-141 (2015).
267. El-Maarri, O. *et al.* Gender specific differences in levels of DNA methylation at selected loci from human total blood: a tendency toward higher methylation levels in males. *Hum Genet* **122**, 505–514 (2007).
268. Bollati, V. *et al.* Decline in genomic DNA methylation through aging in a cohort of elderly subjects. *Mech Ageing Dev* **130**, 234–239 (2009).
269. Jintaridh, P. & Mutirangura, A. Distinctive patterns of age-dependent hypomethylation in interspersed repetitive sequences. *Physiol Genomics* **41**, 194–200 (2010).
270. Cho, N.-Y. *et al.* Hypermethylation of CpG island loci and hypomethylation of LINE-1 and Alu repeats in prostate adenocarcinoma and their relationship to clinicopathological features. *J Pathol* **211**, 269–277 (2007).
271. Barry, K. H. *et al.* Prospective study of DNA methylation at LINE-1 and Alu in peripheral blood and the risk of prostate cancer. *Prostate* **75**, 1718–1725 (2015).
272. Daskalos, A. *et al.* Hypomethylation of retrotransposable elements correlates with genomic instability in non-small cell lung cancer. *Int J Cancer* **124**, 81–87 (2009).
273. Chen, J. *et al.* Alu methylation serves as a biomarker for non-invasive diagnosis of glioma. *Oncotarget* **7**, 26099–26106 (2016).
274. Lee, H. S. *et al.* Prognostic implications of and relationship between CpG island hypermethylation and repetitive DNA hypomethylation in hepatocellular carcinoma. *Clin Cancer Res* **15**, 812–820 (2009).
275. Park, S. Y. *et al.* Alu and LINE-1 hypomethylation is associated with HER2 enriched subtype of breast cancer. *PLoS One* **9**, e100429 (2014).
276. Matsuda, Y. *et al.* Hypomethylation of Alu repetitive elements in esophageal mucosa, and its potential contribution to the epigenetic field for cancerization. *Cancer Causes Control* **23**, 865–873 (2012).
277. Rhee, Y.-Y. *et al.* Prognostic significance of promoter CpG island hypermethylation and repetitive DNA hypomethylation in stage I lung adenocarcinoma. *Virchows Arch* **466**, 675–683 (2015).
278. Dauksa, A. *et al.* Whole Blood DNA Aberrant Methylation in Pancreatic Adenocarcinoma Shows Association with the Course of the Disease: A Pilot Study. *PLOS ONE* **7**, e37509 (2012).
279. Bae, J. M. *et al.* ALU and LINE-1 hypomethylations in multistep gastric carcinogenesis and their prognostic implications. *Int J Cancer* **131**, 1323–1331 (2012).
280. Yegnasubramanian, S. *et al.* DNA hypomethylation arises later in prostate cancer progression than CpG island hypermethylation and contributes to metastatic tumor heterogeneity. *Cancer Res* **68**, 8954–8967 (2008).
281. Dammann, R. H. *et al.* Frequent aberrant methylation of the imprinted IGF2/H19 locus and LINE1 hypomethylation in ovarian carcinoma. *Int J Oncol* **36**, 171–179 (2010).
282. Kreimer, U., Schulz, W. A., Koch, A., Niegisch, G. & Goering, W. HERV-K and LINE-1 DNA Methylation and Reexpression in Urothelial Carcinoma. *Front Oncol* **3**, 255 (2013).
283. Saito, K. *et al.* Long interspersed nuclear element 1 hypomethylation is a marker of poor prognosis in stage IA non-small cell lung cancer. *Clin Cancer Res* **16**, 2418–2426 (2010).
284. Ogino, S. *et al.* A cohort study of tumoral LINE-1 hypomethylation and prognosis in colon cancer. *J Natl Cancer Inst* **100**, 1734–1738 (2008).
285. Choi, I.-S. *et al.* Hypomethylation of LINE-1 and Alu in well-differentiated neuroendocrine tumors (pancreatic endocrine tumors and carcinoid tumors). *Mod Pathol* **20**, 802–810 (2007).
286. Hur, K. *et al.* Hypomethylation of long interspersed nuclear element-1 (LINE-1) leads to activation of proto-oncogenes in human colorectal cancer metastasis. *Gut* **63**, 635–646 (2014).

287. Iwagami, S. *et al.* LINE-1 hypomethylation is associated with a poor prognosis among patients with curatively resected esophageal squamous cell carcinoma. *Ann Surg* **257**, 449–455 (2013).
288. Lee, J. R. *et al.* Differential LINE-1 Hypomethylation of Gastric Low-Grade Dysplasia from High Grade Dysplasia and Intramucosal Cancer. *Gut Liver* **5**, 149–153 (2011).
289. Fotouhi, O. *et al.* Global hypomethylation and promoter methylation in small intestinal neuroendocrine tumors: an in vivo and in vitro study. *Epigenetics* **9**, 987–997 (2014).
290. Dauksa, A., Gulbinas, A., Endzinas, Z., Oldenburg, J. & El-Maarri, O. DNA methylation at selected CpG sites in peripheral blood leukocytes is predictive of gastric cancer. *Anticancer Res* **34**, 5381–5388 (2014).
291. Gao, Y. *et al.* Blood leukocyte Alu and LINE-1 methylation and gastric cancer risk in the Shanghai Women's Health Study. *Br J Cancer* **106**, 585–591 (2012).
292. Fabris, S. *et al.* Biological and clinical relevance of quantitative global methylation of repetitive DNA sequences in chronic lymphocytic leukemia. *Epigenetics* **6**, 188–194 (2011).
293. Tiwawech, D. *et al.* Alu methylation in serum from patients with nasopharyngeal carcinoma. *Asian Pac J Cancer Prev* **15**, 9797–9800 (2014).
294. Wedge, E. *et al.* Global hypomethylation is an independent prognostic factor in diffuse large B cell lymphoma. *Am J Hematol* **92**, 689–694 (2017).
295. Jordà, M. *et al.* The epigenetic landscape of Alu repeats delineates the structural and functional genomic architecture of colon cancer cells. *Genome Res* **27**, 118–132 (2017).
296. Yoshida, T. *et al.* Alu and Sata hypomethylation in Helicobacter pylori-infected gastric mucosae. *Int J Cancer* **128**, 33–39 (2011).
297. Xiang, S. *et al.* Methylation status of individual CpG sites within Alu elements in the human genome and Alu hypomethylation in gastric carcinomas. *BMC Cancer* **10**, 44 (2010).
298. Akers, S. N. *et al.* LINE1 and Alu repetitive element DNA methylation in tumors and white blood cells from epithelial ovarian cancer patients. *Gynecol Oncol* **132**, 462–467 (2014).
299. Gaudet, F. *et al.* Induction of tumors in mice by genomic hypomethylation. *Science* **300**, 489–492 (2003).
300. Sheaffer, K. L., Elliott, E. N. & Kaestner, K. H. DNA Hypomethylation Contributes to Genomic Instability and Intestinal Cancer Initiation. *Cancer Prev Res (Phila)* **9**, 534–546 (2016).
301. Belancio, V. P., Deininger, P. L. & Roy-Engel, A. M. LINE dancing in the human genome: transposable elements and disease. *Genome Med* **1**, 97 (2009).
302. Bollati, V. & Baccarelli, A. Environmental epigenetics. *Heredity (Edinb)* **105**, 105–112 (2010).
303. Eden, A., Gaudet, F., Waghmare, A. & Jaenisch, R. Chromosomal instability and tumors promoted by DNA hypomethylation. *Science* **300**, 455 (2003).
304. Kawano, H. *et al.* Chromosomal instability associated with global DNA hypomethylation is associated with the initiation and progression of esophageal squamous cell carcinoma. *Ann Surg Oncol* **21 Suppl 4**, S696-702 (2014).
305. Zhang, W. *et al.* Global DNA Hypomethylation in Epithelial Ovarian Cancer: Passive Demethylation and Association with Genomic Instability. *Cancers (Basel)* **12**, E764 (2020).
306. Dijkstra, K. K. *et al.* Patient-Derived Organoid Models of Human Neuroendocrine Carcinoma. *Front Endocrinol (Lausanne)* **12**, 627819 (2021).
307. Wang, H. *et al.* Genomic dissection of gastrointestinal and lung neuroendocrine neoplasm. *Chin J Cancer Res* **31**, 918–929 (2019).
308. Wilson, A. S., Power, B. E. & Molloy, P. L. DNA hypomethylation and human diseases. *Biochimica et Biophysica Acta (BBA) - Reviews on Cancer* **1775**, 138–162 (2007).
309. Kondo, Y. & Issa, J.-P. J. Epigenetic changes in colorectal cancer. *Cancer Metastasis Rev* **23**, 29–39 (2004).
310. Jackson, K. *et al.* DNA hypomethylation is prevalent even in low-grade breast cancers. *Cancer Biol Ther* **3**, 1225–1231 (2004).
311. Ehrlich, M. DNA hypomethylation in cancer cells. *Epigenomics* **1**, 239–259 (2009).
312. Kim, Y.-I. *et al.* Global DNA hypomethylation increases progressively in cervical dysplasia and carcinoma. *Cancer* **74**, 893–899 (1994).
313. Widschwendter, A. *et al.* DNA Methylation in Serum and Tumors of Cervical Cancer Patients. *Clin Cancer Res* **10**, 565–571 (2004).
314. Lin, C.-H. *et al.* Genome-wide Hypomethylation in Hepatocellular Carcinogenesis. *Cancer Res* **61**, 4238–4243 (2001).
315. Kwon, H.-J. *et al.* DNA methylation changes in ex-adenoma carcinoma of the large intestine. *Virchows Arch* **457**, 433–441 (2010).
316. Moss, J. *et al.* Comprehensive human cell-type methylation atlas reveals origins of circulating cell-free DNA in health and disease. *Nat Commun* **9**, 5068 (2018).

317. Klein Hesselink, E. N. *et al.* Increased Global DNA Hypomethylation in Distant Metastatic and Dedifferentiated Thyroid Cancer. *J Clin Endocrinol Metab* **103**, 397–406 (2018).
318. Karpathakis, A. *et al.* Progressive epigenetic dysregulation in neuroendocrine tumour liver metastases. *Endocrine-Related Cancer* **24**, L21–L25 (2017).
319. Romero-Garcia, S., Prado-Garcia, H. & Carlos-Reyes, A. Role of DNA Methylation in the Resistance to Therapy in Solid Tumors. *Front Oncol* **10**, 1152 (2020).
320. Kitkumthorn, N. & Mutirangura, A. Long interspersed nuclear element-1 hypomethylation in cancer: biology and clinical applications. *Clin Epigenetics* **2**, 315–330 (2011).
321. Gerhauser, C. Cancer chemoprevention and nutriepigenetics: state of the art and future challenges. *Top Curr Chem* **329**, 73–132 (2013).
322. Kamm, R. C. & Smith, A. G. Nucleic acid concentrations in normal human plasma. *Clin Chem* **18**, 519–522 (1972).
323. Chang, H.-W. *et al.* Assessment of plasma DNA levels, allelic imbalance, and CA 125 as diagnostic tests for cancer. *J Natl Cancer Inst* **94**, 1697–1703 (2002).
324. Maire, F. *et al.* Differential diagnosis between chronic pancreatitis and pancreatic cancer: value of the detection of KRAS2 mutations in circulating DNA. *Br J Cancer* **87**, 551–554 (2002).
325. Moriyama, H. *et al.* Allelic imbalance and microsatellite instability in plasma DNA released from polyclonal pancreatic adenocarcinoma. *Int J Oncol* **21**, 949–956 (2002).
326. Deligezer, U., Yaman, F., Erten, N. & Dalay, N. Frequent copresence of methylated DNA and fragmented nucleosomal DNA in plasma of lymphoma patients. *Clin Chim Acta* **335**, 89–94 (2003).
327. Di, G., Liu, G., Wu, J., Shen, Z. & Shao, Z. [Peripheral blood mutated p53 DNA and its clinical value in human breast cancer]. *Zhonghua Zhong Liu Za Zhi* **25**, 137–140 (2003).
328. Ito, T. *et al.* Clinical significance in molecular detection of p53 mutation in serum of patients with colorectal carcinoma. *Oncol Rep* **10**, 1937–1942 (2003).
329. Kamat, A. A. *et al.* Plasma cell-free DNA in ovarian cancer: an independent prognostic biomarker. *Cancer* **116**, 1918–1925 (2010).
330. SHAO, X. *et al.* Quantitative analysis of cell-free DNA in ovarian cancer. *Oncol Lett* **10**, 3478–3482 (2015).
331. Leszinski, G., Lehner, J., Gezer, U. & Holdenrieder, S. Increased DNA integrity in colorectal cancer. *In Vivo* **28**, 299–303 (2014).
332. El-Gayar, D., El-Abd, N., Hassan, N. & Ali, R. Increased Free Circulating DNA Integrity Index as a Serum Biomarker in Patients with Colorectal Carcinoma. *Asian Pac J Cancer Prev* **17**, 939–944 (2016).

9. Appendix

Table 19. The cfDNA concentration in the other studies

| Reference | Groups | cfDNA Source | cfDNA concentration (median) |
|-----------|-----------------------------|--------------|------------------------------|
| 322 | healthy subjects | Plasma | 14 ng/mL |
| 75 | unselected cancer | Plasma | 219 ng/mL |
| | healthy subjects | | 3.7 ng/mL |
| 323 | healthy subjects | Plasma | 7ng/ml |
| | non-malignant diseases | | 16ng/ml |
| | unselected cancer | | 59ng/ml |
| 324 | pancreatic cancer | Serum | 730 ng/mL |
| | chronic pancreatitis | | 560 ng/mL |
| 325 | pancreas adenocarcinoma | Plasma | 568 ng/mL |
| | other pancreato-biliary | | 462 ng/mL |
| | malignant tumors | | |
| | chronic pancreatitis | | 343 ng/mL |
| 326 | lymphoma patients | Plasma | 256 ng/mL |
| | healthy subjects | | 44 ng/mL |
| 327 | breast cancer | Plasma | 211 ng/mL |
| | healthy women | | 21 ng/mL |
| 328 | colorectal cancer | Serum | 560 ng/mL stage I |
| | | | 720 ng/mL stage II |
| | | | 609 ng/mL stage III |
| | | | 769 ng/mL stage IV |
| | healthy subjects | 320 ng/mL | |
| 184 | healthy subjects | Plasma | 20 ng/mL |
| | benign prostate hyperplasia | | 28 ng/mL |
| | prostate cancer, pN0M0 | | 20 ng/mL |
| | prostate cancer, pN1M0 | | 26 ng/mL |
| | prostate cancer, M1 | | 41 ng/mL |

Appendix

| | | | |
|-----|-------------------------|--------|-------------|
| 182 | colorectal cancer | Serum | 868 ng/mL |
| | healthy subjects | | 7 ng/mL |
| 329 | ovarian cancer | Plasma | 10113 GE/mL |
| | Healthy subjects | | 1912 GE/mL |
| | benign ovarian neoplasm | | 2365 GE/mL |
| 330 | ovarian cancer | Serum | 811.4 ng/mL |
| | healthy subjects | | 197.2 ng/mL |
| | benign tumor | | 199.9 ng/mL |
| 97 | brain metastasis | Serum | 588 ng/mL |
| | glioblastoma | | 286 ng/mL |
| | healthy subjects | | 40 ng/mL |

#(GE/mL genome equivalents/milliliter)

Table 20. The cfDNA integrity index in the other studies

| Reference | Case | Control | Gene (bp) | Cancer type | cfDNA Source | Case value | Control value | P |
|-----------|------|---------|------------------------|-----------------------------|-----------------|--------------------------------|---------------------------|---------|
| 78 | 61 | 65* | <i>ACTB</i> 400/100 | Mixed | Plasma | 0.66 (0.42– 0.90) | 0.14 (0.06– 0.28) | <0.0001 |
| 123 | 32 | 51 | <i>ALU</i> 247/115 | Colorectal Periampullary | Serum | 0.22 ± | 0.13± | <0.05 |
| | 19 | | | | | 0.02 | 0.01 | |
| 123 | 19 | 51 | <i>ALU</i> 247/115 | Colorectal Periampullary | Serum | 0.25 ± | 0.13± | <0.05 |
| | 51 | | | | | 0.03 | 0.01 | |
| 152 | 51 | 51 | <i>ALU</i> 247/115 | Breast | Serum | 0.25 ± 0.03 | 0.13 ± 0.01 | <0.05 |
| 77 | 58 | 47 | <i>ACTB</i> 400/100 | Head and neck | Plasma | 0.24 (0.11– 0.38) | –2.24 (–2.92–1. 56) | <0.0001 |
| 245 | 40 | 17* | Gene 347/137 | Mixed | Plasma | 0.46 (0.15– | 0.56 (0.15– | 0.53 |
| | 40 | 15* | | | | 1.44) | 2.07) | |
| 245 | 40 | 15* | Gene 347/137 | Mixed | Serum | 0.43 (0.06– 1.28) | 0.33 (0.10– 0.75) | 0.1 |
| | 40 | 15* | | | | 0.43 | 0.33 | 0.1 |
| 186 | 74 | 35 | <i>ACTB</i> 384/106 | Testicular germ cell | Serum | 0.41 (0.43– 0.48) | 0.98 (0.57– 1.40) | <0.001 |
| 258 | 25 | 25* | <i>ALU</i> 247/115 | Hepatocellula r | Serum | 0.34 ± 0.07 | 0.20 ± 0.02 | 0.001 |
| 254 | 60 | 30 | <i>ACTB</i> 384/106 | Acute leukemia | Plasma | 0.51 (0.11– 0.92) | 0.18 (0.07– 0.37) | <0.001 |
| 255 | 35 | 54 | <i>ACTB</i> 384/106 | Renal cell | Serum | 1.074 | 0.716 | 0.04 |

Appendix

| | | | | | | | | |
|-----|-----|-----|--|--------------------------|--------|----------------------------|-------------------------|----------------|
| | | | <i>APP</i> 180/67 | | | 0.8 ± 0.05 | 0.5 ± 0.04 | <0.001 |
| 256 | 57 | 34 | <i>APP</i> 306/67 | Melanoma | Plasma | 0.3 ± 0.03 | 0.2 ± 0.02 | 0.008 |
| | | | <i>APP</i> 476/67 | | | 0.2 ± 0.03 | 0.1 ± 0.01 | 0.002 |
| | 24 | 35 | <i>ALU</i> | | | 14.02 | 10.01 | <0.001 |
| 248 | 24 | 26* | 115/247 | Colorectal | Plasma | 11.89 | 10.01 | 0.043 |
| | 24 | 35 | <i>LINE-1</i> | | | 9.11 | 6.67 | 0.001 |
| | 24 | 26* | 79/300 | | | 7.76 | 6.67 | 0.033 |
| | | | <i>ACTB</i> 400/100 | Hepatocellular carcinoma | Serum | 0.41 ± 0.18 | 0.15 ± 0.12 | <0.001 |
| 259 | 80 | 50 | | | | | | |
| | 80 | 80* | <i>ACTB</i> 400/100 | | | 0.41 ± 0.18 | 0.23 ± 0.12 | <0.001 |
| 260 | 143 | 84 | <i>ACTB</i> 384/106 | Bladder | Serum | 0.69 | 0.36 | <0.001 |
| 242 | 39 | 49 | <i>ALU</i> 247/115 | Breast | Plasma | 0.62 | 0.33 | 0.0002 |
| 257 | 76 | 63 | <i>APP</i> 180/67 | Melanoma | Plasma | 0.75 (0.07– 2.57) | 0.46 (0.09– 1.81) | <0.0001 |
| 261 | 70 | 22 | <i>ALU</i> 247/115 | Glioma | Serum | 0.64 ± 0.14 | 0.59 ± 0.21 | 0.067 |
| 263 | 71 | 33* | <i>ALU</i> 247/115 | Prostate | Plasma | 0.34 ± 0.12 | 0.23 ± 0.09 | <0.001 |
| 251 | 104 | 110 | <i>ALU</i> 247/115 | Colorectal | Serum | 0.62 (0.51– 0.65) | 0.38 (0.29– 0.49) | <0.0001 |
| 57 | 82 | 100 | <i>ALU</i> 260/111 <i>LINE-1</i> 266/97 | Breast | Plasma | 0.62 0.48 | 0.65 0.50 | 0.046 0.041 |
| 331 | 24 | 24 | <i>ALU</i> 247/115 | Colorectal | Serum | 1.31 | 1.07 | 0.005 |

Appendix

| | | | | | | | | |
|-----|-----|-----------|------------------------------|----------------|--------|--------------------------------|--|------------------|
| 243 | 65 | 28 12* | <i>ALU</i> 247/115 | Breast | Plasma | 1.1 (0.6– 1.7) | 1.2 (0.5– 9.3) 0.9 (0.5– 1.1) | <0.0001 |
| 234 | 148 | 51 | <i>ALU</i> 247/115 | Breast | Serum | 0.56 ± 0.24 | 0.35 ± 0.27 | < 0.001 |
| 115 | 95 | 70 95* | <i>Beta-actin</i> 400/100 | Breast | Plasma | 0.72 ± 0.23 | 0.15 ± 0.11 0.28 ± 0.18 | <0.001 |
| 332 | 50 | 20 10* | <i>ALU</i> 247/115 | Colorectal | Serum | 1.54 (0.7– 3.1) | 0.3 (0.2– 1.9) 0.17 (0.1– 1.35) | <0.001 |
| 237 | 50 | 25* 30 | <i>ALU</i> 247/115 | Prostate | Plasma | 0.29 (0.16– 0.43) | 0.10 (0.06– 0.15) 0.03 (0.01– 0.05) | <0.001 <0.001 |
| 148 | 53 | 22 15* | <i>ALU</i> 247/115 | Hepatocellular | Plasma | 0.55 (0.20– 1.20) | 0.69 (0.49– 0.99) 0.68 (0.41– 1.03) | 0.003 0.017 |

Appendix

| | | | | | | |
|-----|----|----|-----------------|-------------|-------|--------------|
| | | | <i>HER2,</i> | | | |
| | | | <i>295/ 126</i> | | | |
| | | | BCAS1 | 0.23 | 0.35 | 0.33 |
| | | | <i>266/129</i> | 0.29 | 0.52 | 0.002 |
| 249 | 79 | 10 | <i>MYC</i> | Breast | Serum | 0.03 |
| | | | <i>264/128</i> | | | 0.66 |
| | | | <i>PIK3CA</i> | | | 0.36 |
| | | | <i>274/129</i> | | | 0.092 |

* The controls have benign disease.

Lower cfDII in cancer patients is shown in bold.

10. Acknowledge

My special thanks go to Prof. Matthias M. Weber; he gave me the opportunity to carry out this work in the research laboratory of the university medicine with a focus on endocrinology and metabolic diseases. His valuable guidance and interest in the topic and his trust in me have contributed greatly to the success of this work.

I would like to thank Dr. Christian Fottner for his willingness to help, constant guidance, patient support, and suggestions.

I am extremely grateful to Dr. Esther Mettler for her cooperation, commitment, and valuable advice on the practical implementation of many experiments throughout the project work. Her creative discussions pushed me to sharpen my thinking and brought my work to a higher level.

I would like to acknowledge Anja Trenkler for her support and collaboration.

Finally, I would like to give special thanks to God for providing me with support, good health, and strength to perform this work.

11. Curriculum Vitae

Personal Information

Name: **Neda Bakhshandeh**

E-Mail: nedabakhshandeh2012@yahoo.com

Education

Ph.D. student

Jul. 2017-Jan.2023

Department of Endocrinology and Metabolic diseases, Mainz University of Medical Sciences, Mainz, Germany

Thesis Title: Investigation of blood-based biomarkers as prognostic and predictive factors in patients with neuroendocrine neoplasms

Master (Biochemistry)

Aug. 2004-Jun. 2006

Department of Biochemistry, University of Mysore, Mysore, India

Thesis Title: Inhibition of PLA2 enzyme by pomegranate fruit extract

Bachelor (Biology, Animal Science)

Sep. 1999-Jul. 2003

Department of Science, University of Shahid Chamran, Ahvaz, Iran

Employment

Research Assistant

Jul. 2020-present

Mainz University of Medical Sciences, Mainz, Germany

Researcher

Jan. 2015-Jun. 2017

Department of Biochemistry, Semnan University of Medical Sciences, Semnan, Iran

Lecturer

Jan. 2012-Jun. 2017

Centre of Agriculture and Applied science, Semnan, Iran

Lecturer

Jan. 2011-Jan. 2012

Institute of applied science technology Jahad Daneshgahi, Semnan, Iran

Lecturer

Jan. 2008-Mar. 2010

Department of Biology, Faculty of Science, Islamic Azad University, Izeh, Iran

Researcher

Jan. 2007-Nov. 2009

Razi Vaccine and Serum Research Institute, Ahvaz, Iran